PROBING PRESYNAPTIC REGULATION OF DOPAMINE RELEASE IN HEALTH AND DISEASE

Rishi Anand

Department of Physiology, Anatomy and Genetics

Oxford-MRC DTP iCASE

Wadham College

University of Oxford

Thesis submitted for the degree of

Doctor of Philosophy

Hilary Term 2023

Table of Contents

Statement of Authorship

This thesis does not contain any material that has been accepted for the award of any other degree at any University or other institution. All data included in this thesis is my own work, except where contributed by others and their contribution is stated below and in the main text.

The FSCV data included in **Chapter 3, Section 3.3.15** were collected and analysed by Mr Elliot Yates, a Part II Biochemistry undergraduate student in the laboratory of Professor Stephanie Cragg, supervised by Dr Katherine Brimblecombe. These data are included with Mr Yates' full permission and are identified in the corresponding figure legends

The electrophysiology data included in **Chapter 4, Section 4.3.12** were collected and analysed by Dr Jeffrey Stedehouder, a former postdoctoral researcher in the laboratory of Professor Stephanie Cragg. These data are included with Dr Stedehouder's full permission and are identified in the corresponding figure legend.

The electrophysiology data included in **Chapter 4, Section 4.3.15** were collected and analysed by Dr Simon Bossi, a current postdoctoral researcher in the laboratory of Professor Stephanie Cragg. These data are included with Dr Bossi's full permission and are identified in the corresponding figure legend.

The RNAscope data included in **Chapter 4, Section 4.3.2** and **Chapter 4.3.15** were collected and analysed by Dr Ioannis Mantas and Ms Vasiliki Skara, a postdoctoral researcher and PhD student respectively in the laboratory of Professor Dinos Meletis, a collaborator of our lab via the Aligning Science Across Parksinon's (ASAP): Team Cragg. These data are included with their full permission and are identified within the corresponding figure legend.

The FSCV data included in **Chapter 5** were part of a collaboration with Professor Rosario Moratalla and Professor Mario Vallejo, and collected and analysed by myself and Dr Stefania Vietti-Michelina together, previously a PhD student in our lab. These data are included with her full permission and indicated in the corresponding figure legends. These data formed part of a wider study, resulting in a publication: Pérez-Taboada I, Alberquilla S, Martìn ED, **Anand R**, Vietti-Michelina S, Tebeka NN, Cantley J, Cragg SJ, Moratalla R, Vallejo M. Diabetes causes dysfunctional dopamine neurotransmission favoring nigrostriatal degeneration in mice. Movement Disorders. 35:1636-1648 (2020)

Conference Abstracts and Manuscripts

Conference Abstracts

Anand R, Brimblecombe KR, Cragg SJ. Glycine reduces evoked striatal dopamine release in a region-dependent manner. British Neuroscience Association: Festival of Neuroscience (2021, Virtual; Poster).

Anand R, Vietti-Michelina S, Brimblecombe KR, Cragg SJ. Striatal glycine inhibits axonal dopamine release in a region-specific manner and partly via regulation of striatal ACh. Virtual Dopamine Conference, ViDA (2021, Virtual; Poster).

Anand R, Vietti-Michelina S, Brimblecombe KR, Cragg SJ. Striatal glycine inhibits axonal dopamine release in a region-specific manner and partly via regulation of striatal ACh. Dopamine 2022 (Montréal, Canada; Poster).

Manuscripts

Pérez-Taboada I, Alberquilla S, Martìn ED, **Anand R**, Vietti-Michelina S, Tebeka NN, Cantley J, Cragg SJ, Moratalla R, Vallejo M. Diabetes causes dysfunctional dopamine neurotransmission favoring nigrostriatal degeneration in mice. Movement Disorders. 35:1636-1648 (2020)

Threlfell S, Mohammadi AS, Ryan BJ, Connor-Robson N, Platt NJ, **Anand R**, Serres F, Sharp T, Bengoa-Vergniory N, Wade-Martins R, Ewing A, Cragg SJ, Brimblecombe KR. Striatal dopamine transporter function is facilitated by converging biology of alpha-synuclein and cholesterol. Frontiers in Cellular Neuroscience. 15:658244 (2021)

Burli R, Christie L, Brice N, Rowland A, Dickson L, **Anand R**, Teall M, Doyle K, Lakshmi N, Mitchell C, Harvey J, Mulligan V, Dawson L, Cragg S, Carlton M. Discovery of CVN417, a novel brain-penetrant α6 nicotinic receptor antagonist for the modulation of motor dysfunction. Submitted for Review. (2023)

Acknowledgements

There are many people who I would like to thank for their contributions and support over the course of my DPhil project. This has been an incredibly rewarding experience for me and would not have been possible without their help.

First and foremost, I would like to thank my supervisors Professor Stephanie Cragg and Dr Katherine Brimblecombe. I am grateful to Professor Cragg for giving me the opportunity to pursue a project in her lab, and to both Professor Cragg and Dr Brimblecombe for their guidance, mentorship, and support throughout. This project has been filled with twists and turns, and I cannot thank them enough for their expertise and help to drive this project through, whether developing hypotheses or troubleshooting problems on the rig! I would also like to thank all the Cragg lab members for being such fantastic friends and colleagues, creating an open and collaborative environment that has been an absolute pleasure to work in. In particular, I would like to thank Dr Emanuel Lopes, Dr Bradley Roberts, and Dr Stefania Vietti-Michelina for their help teaching me new techniques and being role-models to me throughout my DPhil. I would also like to thank my colleagues and collaborators who have contributed to this project, including Elliot Yates, Dr Jeffrey Stedehouder, Dr Simon Bossi, Dr Stefania Vietti-Michelina from our lab, and Dr Ioanis Mantas and Ms Vasiliki Skara from the lab of Professor Dinos Meletis as part of the ASAP collaboration.

This project would not have been possible without the financial support of the Oxford MRC-DTP iCASE programme, who I would like to thank for awarding me a studentship to conduct my research. I would also like to thank my industrial sponsor Cerevance, and in particular Dr Louisa Christie for her input on my project in Oxford and supervising my internship with Cerevance in Cambridge. The experience of pharmaceutical R&D in industry was incredibly valuable and will be in future as I continue my professional development.

Away from the lab, I would like to thank all my friends from DPAG and the OXION programme, the Wadham College MCR and Boat Club, and from back home in London for making life in Oxford for the past four years so much fun and giving plenty of opportunities to take a much-needed break! And a huge thank you to my girlfriend Elise, for her immense support whether venting together after a long day of failed experiments or shared weekend trips to the BSB, I'm so grateful to have her by my side.

Finally, I would like to thank my parents, Praveen and Uma. Over-hearing conversations at the dinner table about calcium-imaging, cannabinoids and TRPV1 modulation was always going to pique some interest in neuroscience for me while growing-up! I want to thank them for their love and support throughout my childhood and academic studies, without which none of this would have been possible. And thank you to my sister Pia for ensuring that we talk about something other than neuroscience!

Abstract

Dopamine (DA) plays a key role in regulating behaviours controlled within the basal ganglia, including movement, action selection, and motivation. Consequently, dysfunction of dopaminergic neurotransmission can result in psychomotor disorders, including Parkinson's disease and addiction disorders. Striatal DA release is not only regulated by somatodendritic activity in the midbrain, but also local circuits acting on the extensive axonal arbour of DA neurons that can modulate and drive DA release. It is important that we understand the mechanisms that control the release and re-uptake of dopamine within the striatum to identify new targets that may be exploited for the treatment of diseases with dysfunctional dopaminergic neurotransmission.

Glycine is classically considered as an inhibitory neurotransmitter acting in caudal regions of the CNS, but there is evidence for the expression and function of glycine receptors and transporters within the striatum. Previous studies investigating how glycine may regulate DA release have discrepancies, and any underlying mechanism remains unclear. These studies may not have accounted for recent developments identifying excitatory glycine receptors (eGlyRs), or our understanding of the indirect regulation of DA release via striatal cholinergic interneurons (ChIs) and astrocytes. In this thesis, I revisit the question of how glycine and glycine receptors regulate striatal DA release within mouse striatum.

In the first chapter of this thesis, I investigate how the components of glycinergic signalling within the striatum alter DA release, recorded using fast-scan cyclic voltammetry in mouse striatal slices. I find that classical inhibitory glycine receptors (cGlyRs) are tonically active and inhibit DA release under the control of an ambient glycine tone, at least in part regulated by astrocytic glycine transporter 1 (GlyT1). I also find that glycine itself reduces DA release, with a greater effect in dorsal than ventral striatum. This effect is multiphasic, with components mediated via nicotinic acetylcholine receptors (nAChRs) and adenosine receptors. I then show that eGlyRs also control DA release via nAChRs.

In the second chapter of this thesis, I investigate how glycine receptors control the release of ACh from ChIs in the striatum, recorded using the recently developed $GRAB_{ACh3.0}$ sensor expressed in mouse striatal slices. With our collaborators, I show that both cGlyRs and eGlyRs are expressed and functional on ChIs and modulate evoked ACh release. Glycine itself is also able to trigger spontaneous ACh release, showing that glycine is able to regulate ChI activity via multiple mechanisms. These data suggest a complex interplay on DA release, via indirect mechanisms where eGlyRs regulate the activity of ChIs and the release of ACh acting at nAChRs on DA axons, and a putative direct effect mediated by cGlyRs on DA axons.

In the final chapter of my thesis, I investigate whether dopaminergic transmission is altered in two mouse models of diabetes as part of a collaboration, given previous evidence of co-morbidity

between diabetes and PD. I show that the profile of DA release is altered in both diabetes models, but without evidence of a deficit in release. This is likely due at least in part to altered dopamine transporter expression observed by our collaborators in both diabetes models, and slower uptake kinetics we observed in one model.

Overall, these results identify glycine receptors as overlooked but powerful regulators of DA and ACh release within the striatum, including the first functional identification of eGlyRs within the striatum. They also show that dopaminergic neurotransmission is altered in diabetes and may contribute to the co-morbidity observed between PD and diabetes.

Abbreviations

1p	single pulse
4p	4 pulse train
6-OHDA	6-hydroxydopamine
AAV	Adeno-associated virus
ACh	Acetylcholine
AChE	Acetylcholinesterase
aCSF	Artificial cerebrospinal fluid
AP	Action potential
α-syn	α-synuclein
ATP	Adenosine triphosphate
AUC	Area under curve
CFM	Carbon fibre microelectrode
cGlyR	Classical (inhibitory) glycine receptor
ChOx	Choline oxidase
ChR2	Channelrhodopsin-2
CNS	Central nervous system
cpGFP	Circularly permutated green fluorescence protein
CPu	Caudate putamen
D2-R	Dopamine D2-receptor
D-AP5	D-(2R)-amino-5-phosphonopentanoate
DA	Dopamine
$[DA]_o$	Extracellular concentration of dopamine
DAT	Dopamine transporter
DCKA	5,7-dichlorokynurenic acid
DHβE	Dihydro-β-erythroidine
dlCPu	Dorsolateral caudate putamen
eGlyR	Excitatory glycine receptor
eYFP	Enhanced yellow fluorescent protein
FSCV	Fast-scan cyclic voltammetry
FSI	Fast spiking interneuron
GABA	γ-amino butyric acid
$GABA_AR$	GABA type-A receptor
$GABA_BR$	GABA type-B receptor
GAT	GABA transporter
GPCR	G-protein coupled receptor
GPe	Globus Pallidus external segment

GPi	Globus Pallidus internal segment
HPLC	High-performance liquid chromatography
hSyn	Human synapsin gene promoter
IHC	Immunohistochemistry
IPSC	Inhibitory postsynaptic current
IRES-Cre	Internal ribosome entry site-linked Cre-recombinase
ISH	*in situ* hybridisation
L-DOPA	Levodopa
LED	Light-emitting diode
LTSI	Low-threshold spiking interneuron
mAChR	Muscarinic acetylcholine receptor
mGlyR	Muscarinic glycine receptor
MPTP	1-methyl-4-phenyl-1,2,3,6-tetreahydropyridine
MSN	Medium spiny neuron
NAc	Nucleus accumbens
NAcC	Nucleus accumbens core
NAcS	Nucleus accumbens shell
nAChR	Nicotinic acetylcholine receptor
NBQX	2,3-dihydroxy-6-nitro-7-sulfamoyl-benzo[f]quinoxaline-2,3-dione
NMDG	N-Methyl-D-glucamine diatrizoate
NPY	Neuropeptide Y
PD	Parkinson's disease
PTX	Picrotoxin
ROI	Region of interest
SNc	Substantia nigra pars compacta
SNr	Substantia nigra pars reticulata
SNCA	Human α-synuclein gene
Snca	Mouse α-synuclein gene
SNCA-OVX	Human α-synuclein overexpressing mouse model of PD
SST	Somatostatin
STN	Subthalamic nucleus
TH	Tyrosine hydroxylase
TTX	Tetrodotoxin
VGAT	Vesicular GABA transporter
VTA	Ventral Tegmental Area
WT	Wild-type

Chapter 1: Introduction

1.1. Thesis Overview

Dopamine (DA) is a neuromodulator with a critical role in mediating many fundamental behaviours, including movement, motivation, and reward. Disruption of dopaminergic neurotransmission often results in pathology related to behaviour or movement, including Parkinson's disease (PD). Given improvements in healthcare and lifestyle resulting in longer life-expectancies, incidence of PD is projected to grow rapidly over the coming decades. However, there is no cure for PD, and symptomatic treatment using Levodopa (L-DOPA) can result in undesirable side-effects. Therefore, it is important that research is undertaken to understand how dopaminergic neurotransmission is regulated, both under normal conditions and in PD, to find novel targets for treatment.

Although neurotransmitter release is classically regulated at the level of the cell body, typically via neuron firing rate, striatal DA release is heavily regulated locally at the level of the axon. DA neurons have an extensive axonal arbour, that are influenced directly by receptors expressed on DA axons, and indirectly via astrocytes and the large variety of interneurons present in striatum. Acetylcholine (ACh) and γ-aminobutyric acid (GABA) are both examples of neurotransmitters with powerful regulatory effects at DA axons. The striatum contains many neurotransmitters and neuromodulators that may also regulate DA release. Understanding their role in regulating DA release under normal conditions may allow identification of novel targets for the treatment of PD.

In **Chapter 3**, I investigate the role of glycine as a regulator of dopamine release, via classical glycine receptors (cGlyRs) and relatively recently identified excitatory glycine receptors (eGlyRs). In **Chapter 4**, I investigate glycinergic regulation of ACh in more depth, as an indirect mechanism regulating DA release. Finally in **Chapter 5**, I investigate whether dopaminergic neurotransmission is altered in diabetes models, as part of a collaboration.

1.2. Organisation and Function of the Striatum

1.2.1. Structure and function of the striatum

The striatum is a nucleus of the basal ganglia, a group of subcortical nuclei that are associated with a wide range of behavioural processes, including behaviour selection, learning, cognition, and reward processing (Graybiel 1998, Lanciego, Luquin et al. 2012). The basal ganglia consist of the striatum, globus pallidus (GP), subthalamic nucleus (STN), and the substantia nigra (SN) and ventral tegmental area (VTA) in the midbrain (Obeso, Rodriguez-Oroz et al. 2014). The substantia nigra itself can be divided into the pars reticulata (SNr) and pars compacta (SNc). The globus pallidus can also be divided into the external segment (GPe) and internal segment (GPi). The striatum is the main input nucleus of the basal ganglia, with the GPe, STN and SNc/VTA lying below in a series of parallel connections making up the "direct" and "indirect" pathways. The GPi and SNr are the main output nuclei of the basal ganglia, back to thalamus and brainstem (Crittenden and Graybiel 2011) (Foster, Barry et al. 2021) (**Fig. 1.1**). Dysfunction of any component of the basal ganglia can result in a diverse range of psychomotor diseases, including movement disorders such as Parkinson's disease and Huntington's disease, addiction disorders, and cognitive disorders (Ring and Serra-Mestres 2002, Wichmann and Dostrovsky 2011).

As the main input nucleus of the basal ganglia, the striatum receives inputs from many regions of the brain including cortex, thalamus, midbrain, and brainstem (Matsuda, Furuta et al. 2009, Reiner, Hart et al. 2010, Lanciego, Luquin et al. 2012, Hunnicutt, Jongbloets et al. 2016). It integrates these inputs with local modulation and provides outputs primarily via the direct and indirect pathways to downstream nuclei of the basal ganglia. The functional processing of inputs and subsequent outputs associated with specific behaviours is spatially organised within the striatum from a dorsolateral to ventromedial axis, and histochemically defined "striosome-matrix" compartments within this axis. The striatum is divided into distinct structures in humans and non-human primates, but forms a continuous structure in rodents (**Fig.1.2**). The caudate and putamen are distinct nuclei in primates, divided by the white matter of the internal capsule, but are analogous to the combined caudate-putamen (CPu) in rodents. The Nucleus Accumbens (NAc) is located relatively ventromedial to the internal capsule in

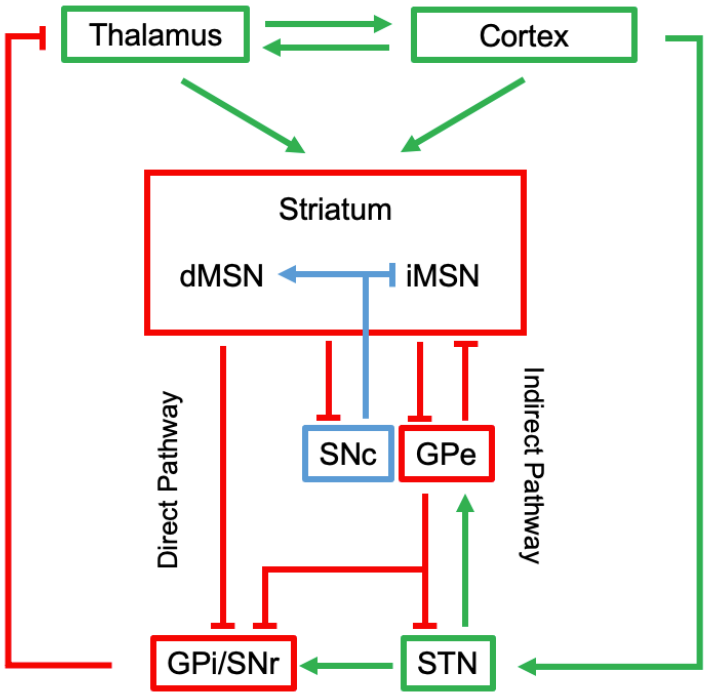

Figure 1.1. The classical model of basal ganglia connectivity

A simplified schematic showing functional connectivity of nuclei of the basal ganglia and afferent inputs from cortex and thalamus. Dopamine regulates the activity of the direct and indirect pathways. Dopaminergic input to the striatum activates the direct pathway and inhibits the indirect pathway, increasing inhibition of GPi, relieving inhibition of thalamus and cortex. In addition to the direct and indirect pathways, there are other interconnected loops between basal ganglia nuclei. Excitatory glutamatergic projections are shown in green, inhibitory GABAergic projections are shown in red, dopaminergic projections are shown in blue. SNc = substantia nigra pars compacta, SNr = substantia nigra pars reticulata, STN = subthalamic nucleus, GPe = globus pallidus (external segment), GPi = globus pallidus (internal segment). dMSN = direct pathway (D1-R) MSN, iMSN = indirect pathway (D2-R) MSN

primates but is located ventrally in the striatum of rodents. Whilst more clearly delineated in primates by the internal capsule, anatomical separation between these functional regions is less clear in rodents.

The striatum is functionally segregated along a dorsolateral to ventromedial axis (Voorn, Vanderschuren et al. 2004). The dorsal striatum is associated with motor and habit-forming behaviour, distributed with motor behaviour with the dorsolateral striatum and habit behaviour associated with the ventromedial striatum. The NAc is more associated with reward-based behaviours, motivation and learning, and is further sub-divided into the NAc core (NAcC), and NAc shell (NAcS) that is relatively more ventromedial. These regions have subtly different roles in addiction (Rossi, Reverte et al. 2020) and limbic information processing (Ito and Hayen 2011).

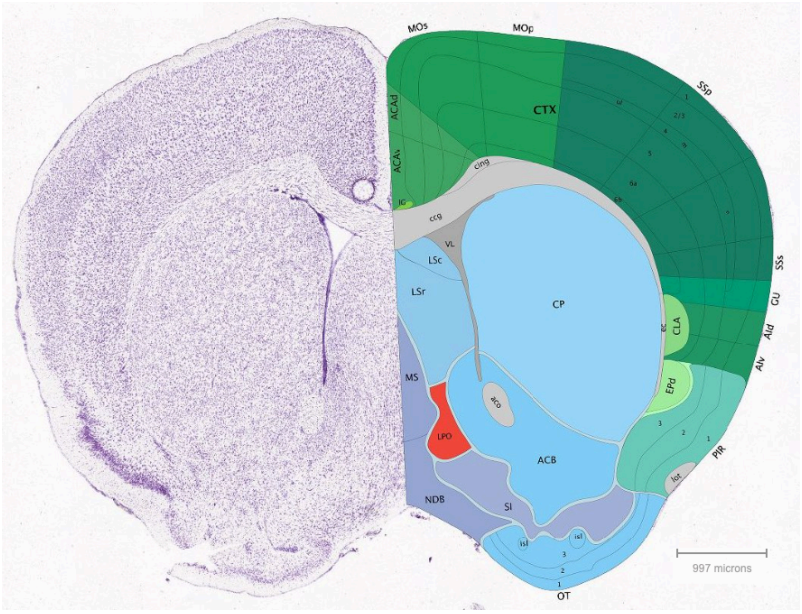

Figure 1.2. Coronal section of adult mouse brain including striatum

Image showing a Nissl-stained coronal section of adult mouse brain with anatomical annotations. The dorsal striatum is labelled as the caudate-putamen (CP), and the ventral striatum labelled as the nucleus accumbens (ACB). From the Allen Mouse Brain Atlas and Allen Reference Atlas – Mouse Brain, mouse.brain-map.org and atlas.brain-map.org

The striatum is also divided into histochemically distinct striosome and matrix compartments (Gerfen, Herkenham et al. 1987, Crittenden and Graybiel 2011). Striosomes constitute roughly 15% of overall striatal volume with the remaining 85% being the surrounding matrix (Brimblecombe and Cragg 2017). The proportion of striosome to matrix decreases along an anterior to posterior axis, and from medial to lateral axis. Striosomes have a "patchy" distribution within the surrounding matrix, with no clear physical delineation. Striosomes are defined by their enrichment in μ-opioid receptor (MOR), substance P, met-enkephalin, and D1 receptors, whilst the matrix is enriched is calbindin, somatostatin, and D2 receptors (Brimblecombe and Cragg 2017). Striosomes and matrix also both have different functional connectivity. Striosomes receive greater input from limbic cortices, while matrix typically receives inputs from sensorimotor and associative cortices. Within the striatum, the distribution of some interneurons varies between striosome and matrix compartments, and we are only starting to understand their roles in regulating neurotransmitter release and associated compartmentalisation in health and disease (Crittenden, Cantuti-Castelvetri et al. 2009, Crittenden and Graybiel 2011, Brimblecombe and Cragg 2015).

1.2.2. Medium spiny neurons

Medium Spiny Neurons (MSNs) make up 95% of neurons in the striatum. These receive the majority of striatal inputs, including glutamatergic afferents from cortex and thalamus, and dopaminergic afferents from midbrain (Tepper, Abercrombie et al. 2007). These also receive inputs from local striatal interneurons (**Section 1.2.3**), which modulate their own activity following afferent input. MSNs are also the predominant output neuronal type of the striatum, and project to downstream basal ganglia nuclei either down the direct pathway (to GPi and SNr) or the indirect pathway (GPe and STN) (**Fig. 1.1**). MSN axon collaterals also project to other MSNs, resulting in a network effect of recurrent inhibition (Taverna, Ilijic et al. 2008).

MSNs can be divided into two, equally distributed sub-populations: D1-R expressing MSNs that project via the direct pathway, and D2-R expressing MSNs that project via the indirect pathway. Activation of direct pathway MSNs inhibits activation of the SNr/GPi basal ganglia output, which is itself inhibitory, resulting overall in disinhibition. In contrast, activation of indirect pathway MSNs results in inhibition of the GPe and disinhibition of the subthalamic nucleus, which ultimately increases SNr/GPi basal ganglia output, resulting overall in inhibition. Thus, the direct and indirect pathways oppose each other, with the direct pathway important for the initiation of movement and other behaviours associated with striatum (e.g. habit-formation, reward) but opposed by the indirect pathway (Gerfen and Surmeier 2011). The classical direct-indirect pathway model of the basal ganglia is well-established but over-simplified, with new research identifying different projection targets and associated functions (Chuhma, Tanaka et al. 2011, Mallet, Micklem et al. 2012, Crittenden, Tillberg et al. 2016).

1.2.3. Striatal interneurons

The remaining c. 5% of neurons in the striatum are local interneurons. There is a large variety of interneurons, defined by their expression of specific biochemical markers. Aside from cholinergic interneurons (ChIs) (**Section 1.4**), striatal interneurons are GABAergic. Although the number of subtypes of striatal interneuron is expanding based on sub-classifications, there are 3 main categories:

low threshold spiking interneurons (LTSIs), fast-spiking interneurons (FSIs), and calretinin-expressing (CR) interneurons (Tepper, Tecuapetla et al. 2010, Tepper, Koos et al. 2018).

LTSIs are defined by their expression of somatostatin (SST), neuropeptide Y (NPY), and nitric oxide synthase (NOS) (Chesselet and Graybiel 1986). Their name arises from their characteristic low threshold to action potential firing, and they also have a long duration action potential and prolonged plateau after depolarisation. These receive inputs from ChIs, DA axons, and glutamatergic afferents from cortex. They project predominantly to MSNs, with some reciprocal connections to adjacent ChIs (Elghaba, Vautrelle et al. 2016). They have been shown to regulate striatal DA release via GABAergic neurotransmission and are associated with goal-directed learning (Holly, Davatolhagh et al. 2019, Holly, Davatolhagh et al. 2021). However, the potential of SST and NPY to modulate striatal neurotransmission warrants further investigation, particularly given the localisation of LTSIs to the boundary of striosomes and matrix, possibly allowing communication between these compartments or discretely altering neurotransmission (Brimblecombe and Cragg 2017).

FSIs are characterised by their expression of the calcium binding protein parvalbumin (Gerfen, Baimbridge et al. 1985). They have a distinct electrophysiological profile, in particular their firing at frequencies up to 400 Hz upon depolarisation (Kawaguchi, Wilson et al. 1995). FSIs receive afferent input primarily from cortex, but also inhibitory input from GPe (Bevan, Booth et al. 1998) (Ramanathan, Hanley et al. 2002). Their activation powerfully inhibits neighbouring MSNs via feed-forward inhibition, and they are thought to be involved in action selection (Koos, Tepper et al. 2004, Gittis, Leventhal et al. 2011).

CR interneurons have been the least investigated, composing only 0.5% of neurons in striatum in rodents (Tepper, Tecuapetla et al. 2010). However, the proportion of CR interneurons versus FSIs or LTSIs is much greater in primates than rodents, and may have a greater role in these species (Wu and Parent 2000). Despite being one of the first striatal interneuron types identified based on immunohistochemistry, the lack of a reliable Cre-reporter line has made it difficult to investigate (Bennett and Bolam 1993, Tepper, Koos et al. 2018). However, recent studies have identified 3 sub-populations of CR interneurons, with variable tonic firing between differing brain activation states

(Garas, Kormann et al. 2018). Their contribution to striatal processing and ultimately behaviour warrants further investigation.

1.2.4. Astrocytes

Astrocytes are a type of glial cell found across the brain. Originally thought to only mediate a structurally supportive role of neurons, over time they have been identified as important regulators of the extracellular environment, source of lactate for neurons, and regulators of synaptic and extrasynaptic neurotransmission (Walz and Allen 1987, Perea, Navarrete et al. 2009, Suzuki, Stern et al. 2011, Chung, Allen et al. 2015). Astrocytes themselves are able to signal to other cell types via gliotransmission, with transmitters such as glutamate and ATP (Savtchouk and Volterra 2018, Pittolo, Yokoyama et al. 2022). Astrocytes also set and regulate basal levels of transmitters within the striatum via expression of transporters, such as GABA via GABA transporters types 1 and 3 (GAT-1 and GAT-3), and adenosine via the Equilibrative Nucleoside Transporter 1 (ENT-1) (Roberts, Doig et al. 2020, Roberts, Lambert et al. 2022). Some transporters expressed by astrocytes exhibit promiscuous transport of multiple substrates. These include the Organic Cation Transporter (OCT) family that can transport monovalent cations including catecholamines and methamphetamine (Cuia, Arasa et al. 2009), the l-amino acid transporters (LATs) that can transport essential amino acids such as leucine and methionine (Errasti-Murugarren, Fort et al. 2019), and the neutral amino acid transporter Asc-1 that can transport amino acids including glycine and L-serine (Ehmsen, Liu et al. 2016). There is also a growing understanding that astrocytes can contribute to disease pathology, such as Parkinson's disease where GAT downregulation results in the augmentation of extracellular GABA that enhances tonic inhibition of DA release in dorsal striatum (Yun, Kam et al. 2018, Roberts, Doig et al. 2020).

1.3. Mesostriatal Dopaminergic System

1.3.1. Mesostriatal dopaminergic projections

Dopaminergic neurons are predominantly located in two discrete nuclei of the midbrain: the SNc (A9 group) and VTA (A10 group) (Gantz, Ford et al. 2018). These have extensively distributed projections across the brain to areas including the striatum, the subthalamic nucleus (STN), hippocampus, cortical regions, and the amygdala. The projections from SNc and VTA to the striatum are defined as the mesostriatal dopaminergic system, with the projection from SNc to CPu further classified as the nigrostriatal pathway and the projection from VTA to NAc classified as the mesolimbic pathway. Within the striatum, although there is broad topological organisation across a dorsolateral to ventromedial axis, there is also overlap between terminal axon fields arising from DA neurons of SNc and VTA (Bjorklund and Dunnett 2007).

DA neurons have a distinct morphology. From their cell body in the SNc or VTA, they have a single unmyelinated axon projecting to the striatum, where it undergoes extensive arborisation to cover nearly 6% of the total striatal volume (Matsuda, Furuta et al. 2009). In rat, this corresponds to a length of approximately 50 cm and approximated with 14 branch levels providing an estimate of over 16,000 branches (Pissadaki and Bolam 2013). Given this size and number of branch points across this axonal arbour, DA neurons require a large amount of energy to maintain this structure and facilitate action potential propagation. The DA axon also expresses receptors for locally released neurotransmitters and neuromodulators, suggesting that this is a potential site for the local control of action potential propagation and DA release across the terminal field (Sulzer, Cragg et al. 2016).

DA neurons are tonically active *in vivo*, firing either at low frequencies between 1-10 Hz or at higher frequencies between 20-40 Hz within discrete burst spike activity (Hyland, Reynolds et al. 2002). The transition from tonic to burst firing is thought to signal salient stimuli, to be used for reward prediction (Cragg 2006). Dopamine is released from axonal varicosities, and acts as a volume transmitter, with most dopamine receptors located extrasynaptically (Cragg and Rice 2004, Rice, Patel et al. 2011). Dopamine is subsequently taken-up by the dopamine transporter (DAT), expressed on DA

axons and not associated with synaptic expression (Pittolo, Yokoyama et al. 2022). Beyond re-uptake of DA, DATs also regulate axonal excitability due to their electrogenic coupling, and regulate the short-term plasticity of DA release (Storch, Ludolph et al. 2004, Condon, Platt et al. 2019).

1.3.2. Local striatal modulation of dopamine release

The release of neurotransmitters by a neuron is classically governed by the firing rate of the neuron that is determined within the somatodendritic compartment. However, DA release is also subject to gating at the level of the axon, regulated by different neurotransmitters and neuromodulators within the striatum that act on receptors directly on DA axons, or indirectly via other local circuits (Sulzer, Cragg et al. 2016). Some of these include: acetylcholine, GABA, glutamate, adenosine, substance P, nitric oxide, and orexin (Hartung, Threlfell et al. 2011, Patyal, Woo et al. 2012, Brimblecombe and Cragg 2015, Kosillo, Zhang et al. 2016, Lopes, Roberts et al. 2019, Roberts, Doig et al. 2020, Roberts, Lambert et al. 2022).

The predominant local regulatory mechanism is via ACh, which will be described in more detail below (**Section 1.4.2**). However, an example mechanism highlights our increased understanding of the role of astrocytes in regulating dopaminergic neurotransmission. Lopes, Roberts et al. showed that extracellular GABA levels regulate dopamine release via tonic inhibition, and this is in turn regulated via GABA transporters (GATs) expressed on astrocytes (Lopes, Roberts et al. 2019, Roberts, Doig et al. 2020). Subsequent work has shown that GABA directly inhibits DA release via $GABA_A$ receptors ($GABA_ARs$) on DA axons (Kramer, Twedell et al. 2020). The striatum is rich in a large number of neurotransmitters and neuropeptides, from afferent inputs and from the extensive variety of local interneurons (Brimblecombe and Cragg 2017, Castro and Bruchas 2019). Many of these have been under investigated for any regulation of DA release and represent opportunities to understand the complexity surrounding the axonal regulation of dopamine release.

1.3.3. Dopamine modulation of striatal signalling

Dopamine released from mesostriatal dopaminergic inputs acts on DA receptors expressed across the striatum on different cell types. DA receptors are all G-protein coupled receptors, split into Gs coupled receptors (D1-Rs and D5-Rs) and Gi/o coupled receptors (D2-, D3-, and D4-Rs). In the striatum, D1-Rs and D2-Rs are expressed on different cell types. D1-Rs are expressed on direct pathway projecting MSNs, while D2-Rs are expressed on indirect pathway projecting MSNs. Thus, striatal DA will activate the direct pathway and reduce activation of the indirect pathway, overall promoting motor behaviour. D2-Rs are also expressed on ChIs and DA axons. These act as inhibitory autoreceptors, whereby the release of dopamine reduces activation of the cholinergic interneurons and subsequent dopamine release. When D2-Rs are inhibited, the activity of the cholinergic interneurons increases. Although DA release will activate D2 autoreceptors, the time scale for activation of the D2-Rs plus the diffusion distance required for dopamine to reach them after being released, is long enough that D2-Rs will not alter dopamine release from a single evoked pulse (Cragg and Rice 2004). However, D2-Rs do modulate and suppress DA release from prolonged train stimulation. Recent research has identified D5-Rs expressed on astrocytes, however more research is still required to understand how DA affects astrocytic signalling (Shibasaki, Hosoi et al. 2017).

1.3.4. Behavioural roles of mesostriatal dopamine release

As described above, DA is important for regulating a wide range of behaviours that are processed within the striatum, including movement and reward behaviour. For movement, DA preferentially activates the direct pathway but suppresses the indirect pathway, resulting in the promotion of movement. In Parkinson's disease where there is a loss of striatal DA, activation of the direct pathway is reduced and inhibition of the indirect pathway is also reduced, resulting in difficulty initiating movement (McGregor and Nelson 2019). DA is also important for signalling reward prediction errors. The reward prediction error is a process whereby the salience of a stimulus is used to predict the anticipated reward which corresponds to an amount of dopamine being released (Schultz

2016). As will be discussed below, this has a close relationship to acetylcholine release (**Section 1.4.2**). Dysfunction of dopaminergic neurotransmission can result in psychomotor disorders including Parkinson's disease and addiction type diseases.

1.4. Striatal Cholinergic System

1.4.1. Striatal cholinergic interneurons and connectivity

Cholinergic interneurons (ChIs) in the striatum, defined by their expression of choline acetyltransferase (ChAT), have been extensively studied and constitute approximately 1% of all neurons in the striatum. They are the main source of striatal ACh, and can account for all the effects of ACh regulation of DA release via nicotinic ACh receptors (nAChRs) (Brimblecombe, Threlfell et al. 2018). They are distributed across the striatum but with greater proportions in rostral and dorsal striatum than ventral and medial striatum (Matamales, Gotz et al. 2016). They are also preferentially located in the boundary region between striosomes and matrix (Brimblecombe and Cragg 2017). Morphologically, they have historically also been known as Giant Aspiny Neurons (GANs) due to their large cell bodies and relatively few somatic and dendritic spines, and Tonically Active Neurons (TANs) *in vivo* based on their tonic activity recorded using electrophysiology (Aosaki, Tsubokawa et al. 1994, Gonzales and Smith 2015). Similar to DA neurons, they have an extensive axonal arbour with an estimate of c. 500,000 axonal varicosities per ChI (Contant, Umbriaco et al. 1996). ChIs also have a distinctive electrophysiological profile, and are tonically active at a frequency of c. 2-10 Hz, facilitated by their relatively depolarised resting membrane potential (c. -60 mV) (Bennett and Wilson 1999). They can also be identified by their depolarising sag after application of a hyperpolarising current injection (Sullivan, Chen et al. 2008). Released ACh is broken down by acetylcholinesterase (AChE), which is expressed on cell membranes (Asri, O'Neill et al. 2016). AChE is part of the feedback loop that regulates extracellular ACh concentration. Given that ChIs are tonically active, this results in an ambient ACh tone that is present across the striatum, using ACh as a volume transmitter (Descarries, Gisiger et al.

1997). This is supported by ultrastructural evidence that only 10% of ChI axonal varicosities show synaptic specialisation (Contant, Umbriaco et al. 1996).

ChIs express receptors for many different neurotransmitters and neuropeptides, including GABA, glutamate, DA and ACh itself. ChIs receive GABAergic input from MSNs, LTSIs, and GPe, where GABA reduces the activity of ChIs, ultimately reducing ACh release (Gonzales and Smith 2015). A polysynaptic recurrent inhibitory circuit has been identified, where activation of ChIs causes excitation of local GABAergic interneurons, in turn inhibiting ChIs (Sullivan, Chen et al. 2008). ChIs also express D2-Rs, D5-Rs, and a small proportion of D1-Rs. Activation of D2-Rs reduces ChI firing rate via reduction in pacemaking Na^+ currents (Maurice, Mercer et al. 2004), whilst co-transmission of glutamate from different populations of DA neurons has also been shown to differentially regulate ChI activity in dorsolateral versus ventromedial striatum (Cai and Ford 2018). ChIs also express both muscarinic and nicotinic acetylcholine receptors (mAChRs & nAChRs). Expression of M_2- and M_4-mAChRs act as autoreceptors, reducing ChI firing rate in response to ACh release to prevent excess excitation and ACh release (Lim, Kang et al. 2014). Release of ACh can alter the activity of many striatal cell types, including DA neurons (**Section 1.4.2**), MSNs, and striatal GABAergic interneurons (Oldenburg and Ding 2011, Kocaturk, Guven et al. 2022).

1.4.2. Modulation of striatal dopamine release by acetylcholine

DA release is powerfully regulated by ACh via the expression of nAChRs, which express the β2-subunit, directly on striatal DA axons. Via nAChRs expressed on DA axons and independent of DA neuron somatodendritic activity, synchronised stimulation of a small population of ChIs can generate action potentials in DA axons and evoke DA release (Threlfell, Lalic et al. 2012, Liu, Cai et al. 2022). Activation of nAChRs results in a powerful short-term depression of DA release, whereby release is almost completely insensitive to its neuronal firing rate at low or high frequencies (Rice and Cragg 2004). However, when nAChRs are either not active or desensitised, this short-term depression is lost, and DA release more faithfully reflects the frequency of firing from the cell body, restoring frequency-dependence. This is observed *in vivo*, where the firing activity of ChIs briefly pauses and then bursts

upon presentation of a salient stimulus, and is hypothesised to allow the greatest modulation of DA release to encode the reward prediction error (Cragg 2006). The ability of ACh to modulate the frequency-sensitivity of DA release, and even evoke DA release demonstrates how powerfully ACh regulates DA release at the axonal level. Therefore, ChIs represent an important target for indirect mechanisms regulating DA release, via changes in the activity of ChIs and in turn the activation of nAChRs on DA axons.

1.4.3. Monitoring ACh release

Until recently with the advent of the $GRAB_{ACh}$ sensors, it has been difficult to measure ACh release with a high level of spatial and temporal resolution. The family of GRAB (GPCR-activation based) sensors are based on the GPCR for a neurotransmitter of interest, linked to a circular permutated fluorescent protein (**Section 2.3** for further detail) (Jing, Zhang et al. 2018). Upon ligand binding, the sensor undergoes a conformational change, allowing fluorescence of the fluorophore. This approach is useful for neurotransmitters that are not electroactive and cannot be detected using fast-scan cyclic voltammetry (FSCV,) such as ACh, and has been used *ex vivo* and *in vivo* (Jing, Li et al. 2020, Sabatini and Tian 2020). However, other approaches have previously been used for the detection of ACh.

Microdialysis with analyte detection using high-performance liquid chromatography (HPLC) coupled to mass spectrometry allows direct measurement of ACh content in a sample, including an absolute baseline concentration of neurotransmitter which is not possible using FSCV. However, temporal resolution typically ranges from 1-10 minute sampling due to the quantity of dialysate required to perform HPLC, and is unsuitable for monitoring the sub-second dynamics of ACh release (Chefer, Thompson et al. 2009).

An electrochemical approach is to detect ACh indirectly from the detection of H_2O_2 at the surface of a carbon fibre electrode that has been treated with AChE and choline oxidase (ChOX) (Asri, O'Neill et al. 2016). ACh in contact with the electrode is degraded by AChE (or by AChE in the striatal environment). This produces choline that then undergoes oxidation by ChOX, producing H_2O_2. This has previously been performed in striatal coronal mouse brain sections, and as with DA detection with

FSCV allows direct measurement of ACh concentration by calibrating the electrode with a known concentration of ACh after the experiment. However, detecting the breakdown product of ACh or choline reduces temporal resolution, and FSCV also detects other electroactive species present in higher concentrations e.g. DA. A Pt-based microelectrode chemical biosensor was previously tested by our lab for the detection of choline, but due to non-specific detection of DA we did not continue to use it (Baker, Bolger et al. 2017).

Cholinergic signalling within the striatum can also be measured by the electrophysiological activity of ChIs, and particularly the effect of neurotransmitters and neuromodulators. The activity of ChIs can be used as a proxy for the release of ACh, although we do not know if there is a direct relationship between ChI activity and ACh release, or if there are other regulatory mechanisms (as for DA release) (Lemos, Shin et al. 2019). An alternative approach is to measure the effect of ACh on downstream cells, by using electrophysiology to record postsynaptic currents mediated by ACh (Saunders, Granger et al. 2015). However, this is an indirect approach subject to additional factors such as the desensitisation of nAChRs, the relatively slow activity of mAChRs, and any mechanisms that may alter the relationship between ACh release and a postsynaptic ACh-mediated response (Dani and Bertrand 2007).

1.5. Glycine receptor signalling in striatum

Until recently, there has been relatively little investigation of glycinergic regulation of DA release in striatum. The main focus has been on glycine-gated Cl^- permeable ligand-gated ion channels, known as glycine receptors. However, recent studies have identified other receptors that are gated by glycine, including excitatory glycine receptors (eGlyRs) and the recently re-assigned metabotropic glycine receptors (mGlyRs) (Bossi, Dhanasobhon et al. 2022, Laboute, Zucca et al. 2023). I will describe the Cl^- permeable glycine receptors as classical glycine receptors (cGlyRs) over the course of this thesis to distinguish between them.

cGlyRs have been identified on multiple cell-types in striatum, including ChIs that are known to regulate DA release (Darstein, Landwehrmeyer et al. 2000). There is also previous ISH evidence that

eGlyRs are expressed in striatum but has not been localised to specific cell-types (Allen Institute for Brain Science, 2011, Experiment: 73907499). Functional glycine transporter 1 (GlyT1) has been identified in striatum (McCracken, Lowes et al. 2017); given recent work by our lab showing that astrocytes are powerful regulators of striatal DA release via GABA and adenosine signalling, it is possible that glycinergic signalling may alter DA release via astrocytes (Roberts, Doig et al. 2020, Roberts, Lambert et al. 2022). I will describe the known function of these components of glycinergic signalling in striatum, and previous studies investigating glycinergic regulation of DA release.

1.5.1. Classical glycine receptors (cGlyRs) in striatum

1.5.1.1. Structure and subunit composition

cGlyRs are a member of the pentameric ligand-gated ion channels (LGICs) family. They are composed of a combination of α1, α2, α3, and β subunits encoded by the genes Glra1, Glra2, Glra3 and Glrb respectively (Lynch 2004). All cGlyRs are pentameric, but subtypes differ in their subunit composition to confer different functional properties (**Fig. 1.3**). Heteromeric cGlyRs are composed of both α and β subunits; although the exact stoichiometry has been extensively debated and historically considered 3α:2β (Durisic, Godin et al. 2012), recent findings support 4α:1β composition (Yu, Bai et al. 2021, Zhu and Gouaux 2021, Gibbs, Klemm et al. 2023). The α subunits are pore-forming, while the β subunit can bind to gephyrin to localise receptors to the postsynaptic membrane (Meyer, Kirsch et al. 1995). Homomeric cGlyRs can consist of pentamers of any of the α subunits and are extrasynaptic since they do not contain a β subunit. α1 and α2 homomeric cGlyRs have been most extensively studied (Gentet and Clements 2002, Mangin, Baloul et al. 2003) although α3 homomeric cGlyRs have been functionally identified (McCracken, Lowes et al. 2017).

Glycine receptors undergo a shift in subunit expression across the CNS over the course of development. The α2 subunit is initially expressed in neonates, before a transition of expression of the α1 subunit in juvenile animals (Mangin, Guyon et al. 2002). There is also a shift from predominantly homomeric cGlyR expression to heteromeric cGlyR expression across the CNS, with the introduction of the β subunit (Meyer, Kirsch et al. 1995). Classically, this is thought to coincide with the shift of

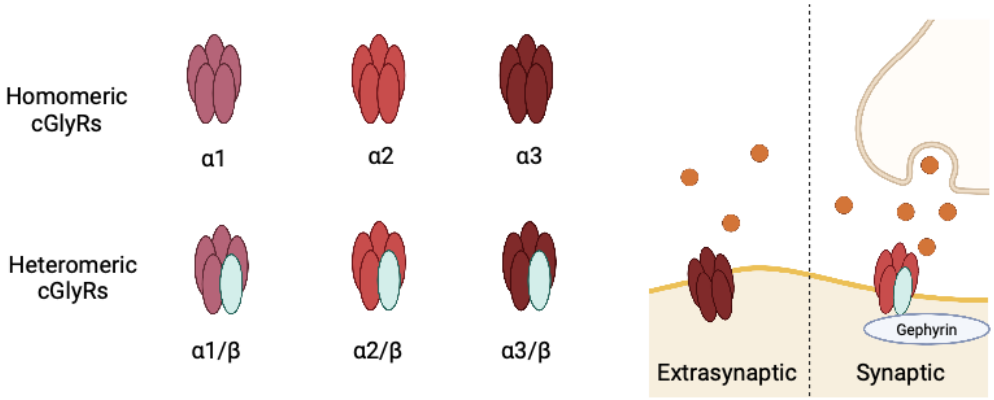

Figure 1.3. Schematic of cGlyR stoichiometry and localisation. Simplified diagram depicting the composition of receptors composed of α1, α2, α3, and β subunits. Recent findings show a 4α:1β stoichiometry for heteromeric cGlyRs. Heteromeric cGlyRs contain a β subunit that interacts with gephyrin, clustering them at the postsynaptic membrane. Homomeric cGlyRs do not contain a β subunit and are extrasynaptic. Created with BioRender.com

cGlyRs mediating tonic signalling during development to synaptic signalling (Lynch 2004). However, there is a growing understanding that α2 subunits are still expressed in cGlyRs in adult CNS, and homomeric cGlyRs have been functionally identified in adult CNS (Jiang, Krnjevic et al. 2004, Deleuze, Runquist et al. 2005, Salling and Harrison 2014, McCracken, Lowes et al. 2017). Most studies have investigated somatodendritic expression of cGlyRs, but homomeric cGlyRs have previously been identified on axons on rat supraoptic nucleus neurons (Deleuze, Runquist et al. 2005).

1.5.1.2. Kinetics

Single-channel kinetics experiments show that cGlyRs, similar to some other LGICs including nAChRs, exhibit rapid activation and desensitisation producing a steady-state current, and subsequent inactivation (Legendre 1998, Martin and Siggins 2002). The subunit composition strongly determines functional properties of the expressed channels. Homomeric cGlyRs have a higher channel conductance than heteromeric cGlyRs (100 pS versus 50 pS) but slower 2-fold slower activation kinetics with a longer mean open time and lower opening probability upon puff application of glycine (Mangin, Guyon et al. 2002). The rising phase of homomeric cGlyRs is slower than for heteromeric cGlyRs and may reflect a lower glycine affinity for these receptors (Gentet and Clements 2002). These characteristics show that homomeric cGlyRs are better suited to slower, tonic changes in extracellular glycine than

heteromeric cGlyRs. The activation state transitions of cGlyRs is still unclear, but there is strong evidence for homomeric cGlyRs that there are two phases of activation, including a partially liganded closed state linked to a desensitised state (Gentet and Clements 2002, Mangin, Baloul et al. 2003). The presence of a low, ambient concentration of glycine (10 μM) accumulates receptors in this partially liganded closed state, and upon application of a high concentration (10 mM puff) the receptor transitions directly into the closed desensitised state without opening (Mangin, Baloul et al. 2003). This reduces the peak amplitude of the glycine current. Since ambient extracellular glycine (or taurine) is present in most sites in the brain, it is likely that there is a mixed population of cGlyRs that are either not-activated or held in the partially liganded closed state (Palkovits, Elekes et al. 1986, Nagy, Marko et al. 2010, Salling and Harrison 2014).

1.5.1.3. Pharmacology

cGlyRs are gated by glycine as a full agonist, and d-serine, β-alanine, and taurine as partial agonists (Grenningloh, Pribilla et al. 1990, Hussy, Deleuze et al. 1997, Mori, Gähwiler et al. 2002, Jiang, Krnjevic et al. 2004, Grudzinska, Schemm et al. 2005). The EC50 of glycine at cGlyRs is in the range of 100-800 μM in most ex vivo striatal slice preparations (Sergeeva 1998, Martin and Siggins 2002, McCracken, Lowes et al. 2017, Molchanova, Comhair et al. 2017). This is higher than observed in heterologous expression systems and has been attributed to the function of glycine transporters in tissue and the diffusion of glycine through tissue to the recording site (McCracken, Lowes et al. 2017). Relatively few studies have investigated the pharmacology of taurine at cGlyRs, but these report EC50s in the 1-20 mM range (Grenningloh, Pribilla et al. 1990, Taleb and Heinrich 1994, Chattipakorn and McMahon 2001, Jiang, Krnjevic et al. 2004). Single-channel recordings show that taurine binding mediates a lower open probability than glycine, by increasing the probability of transition to an intermediate closed state (Lape, Colquhoun et al. 2008). α3 subunits have been observed to undergo RNA-editing, to confer high glycine sensitivity on the receptor (EC50 ~ 5 μM versus ~70 μM for WT α3 subunit) (Meier, Henneberger et al. 2005). The β subunit is also important for facilitating ligand-binding of glycine, strychnine, and picrotoxin (PTX) by increasing the binding affinity for these ligands,

and also confers greater efficacy and potency of taurine (Sergeeva and Haas 2001, Grudzinska, Schemm et al. 2005).

The pharmacology of cGlyR agonists and antagonists is poor, with no cGlyR specific ligands available without optimising the concentration to avoid desensitisation. Recent evidence identifying novel glycine-gated receptors including excitatory glycine receptors (eGlyRs) and metabotropic glycine receptors (mGlyRs) highlights the need for receptor specific compounds. Taurine is also a partial agonist at $GABA_A$Rs and needs to be considered during experiments (del Olmo, Bustamante et al. 2000, Nguyen, Bhattarai et al. 2013, Miles, Hawrysh et al. 2018).

Strychnine is a competitive antagonist at cGlyRs (Martin and Siggins 2002). It has a similar binding affinity to homomeric and heteromeric cGlyRs, and an IC50 of c. 10-100 nM for currents excited by either glycine or taurine (Siebler, Pekel et al. 1993, Sergeeva and Haas 2001, Martin and Siggins 2002, Farroni and McCool 2004). However, one study investigating glycine-currents in mouse ChIs found no significant inhibition of 10 mM glycine application in the presence of 50 μM strychnine (Sergeeva and Haas 2001). This may show difficulties in trying to antagonise the effect of glycine at higher concentrations. Higher concentrations of strychnine are avoided due to off-target effects as a competitive antagonist at α7-homomeric and a non-competitive antagonist at β2-containing nAChRs (Matsubayashi, Alkodon et al. 1998, Garcia-Colunga and Miledi 1999). This is likely due to the similarity in structure between nAChRs and cGlyRs. Strychnine has a greater inhibitory effect on α7-homomeric nAChRs (IC50 = 1 μM) than β2-containing nAChRs (IC50 = 38 μM) (Garcia-Colunga and Miledi 1999). This needs to be considered in any system containing functional nAChRs.

Picrotoxin (PTX) is a channel blocker at Cl^- permeable ion channels (Olsen 2006, Yang, Cromer et al. 2007). Although most often used as an antagonist at $GABA_A$Rs, PTX is also an antagonist at cGlyRs with greater efficacy at homomeric cGlyRs and is used to identify extrasynaptic cGlyR currents (Salling and Harrison 2014, Zhu and Gouaux 2021). At concentrations below 100 μM, PTX is effectively selective for homomeric cGlyRs, but is typically used at 30 μM to avoid flickering channel closing in heteromeric cGlyRs (Legendre and Korn 1994).

1.5.1.4. Nigrostriatal distribution

DA neurons in midbrain

cGlyR currents have been identified on DA neurons in the SNc, as defined by application of glycine and sensitivity to strychnine (Mercuri, Calabresi et al. 1990, Häusser, Yung et al. 1992). Glycine (3 mM) and taurine (10 mM) both mediate a reversible hyperpolarisation that is strychnine-sensitive, silencing these tonically active neurons. Cross-desensitisation of responses suggests that they act through a common mechanism - indicative of action via cGlyRs (Häusser, Yung et al. 1992). Intriguingly, another study identified differential responses, where 1 mM glycine either hyperpolarised, depolarised, or depolarised and subsequently hyperpolarised DA neurons (Mercuri, Calabresi et al. 1990). These currents were not PTX-sensitive, arguing against expression of extrasynaptic cGlyRs. Although during development DA neurons express α2-homomeric cGlyRs, these transition to the α1/β heteromeric receptors shortly after birth, with no evidence for α2 subunit expression or function in these neurons in adults (Mangin, Guyon et al. 2002). There is also no effect of strychnine application alone, suggesting no tonic activation of these receptors in SNc (Mangin, Guyon et al. 2002, Devoght, Comhair et al. 2022). These results show the presence of functional cGlyRs on DA neurons themselves, but the interaction between direct and indirect effects warrants further investigation. Immunohistochemistry has also identified cGlyR expression on DA neurons in human dorsal tier SNc, which may correspond to lower cGlyR expression in discrete "patches" of the striatum (where dorsal tier SNc DA neurons project preferentially to surrounding matrix in the patch-matrix organisation of striatum) (Baer 2009, Brimblecombe and Cragg 2017). cGlyRs have not yet been identified on DA axons within the striatum, but extrasynaptic cGlyRs have previously been identified on the axons of SON neurons, with a hypothesis that extrasynaptic cGlyRs may be preferentially located in the axonal compartment (Deleuze, Runquist et al. 2005).

Cholinergic Interneurons (ChIs)

Expression of cGlyRs on striatal ChIs has been extensively demonstrated in mouse, rat, and even human. Immunohistochemistry has shown expression of cGlyRs in 90% of rat ChIs, defined by

co-expression of ChAT (Darstein, Landwehrmeyer et al. 2000). RT-PCR has also identified the expression of the α2 and α3 subunits in the ChIs of mice, where 28% of ChIs only expressed the α2 subunit and the remainder expressing both α2 and α3 subunits (Sergeeva and Haas 2001). The β subunit was expressed in 80% of ChIs. These data indicate subpopulations of ChIs with differential expression of cGlyRs, including synaptic and extrasynaptic cGlyRs (Sergeeva and Haas 2001). There also appear to be species differences, where all rat ChIs express α2 and β subunits, with no α1 subunit expression in either species (Sergeeva and Haas 2001). In humans, immunohistochemistry has identified cGlyRs in ~75% of striatal ChIs (Waldvogel, Baer et al. 2007).

Electrophysiology has also shown functional cGlyRs expressed on ChIs, with two studies in particular characterising their subunit composition and function (Sergeeva 1998, Sergeeva and Haas 2001). Glycine and taurine both mediate strychnine-sensitive inhibitory currents, with 10 mM taurine not having any off-target effects at $GABA_A$Rs. The EC50 was reported as 125 μM and 2 mM for glycine and taurine respectively. ChIs not containing the β subunit have altered kinetics upon taurine application, with a larger EC50 of 2.5 mM and slower desensitisation kinetics. All ChIs recorded had a PTX-sensitive component of the glycine current (including majority of ChIs expressing β subunit). Together, these findings show that ChIs express both synaptic and extrasynaptic cGlyRs, with a subpopulation only expressing extrasynaptic cGlyRs.

Despite the investigation of these inhibitory currents, application of glycine has been shown to evoke the release of radio-labelled ACh from superfused striatal brain slices (Taylor, Tsai et al. 1988, Darstein, Löschmann et al. 1997, Hernandes, de Magalhaes et al. 2007). These studies find that 100 μM - 1 mM glycine was able to evoke ACh release, with an EC50 of ~100 μM and was inhibited in the presence of strychnine. This effect was also shown to be TTX-sensitive, and also shown to be present in 6-OHDA lesioned striatal tissue, arguing against an indirect mechanism via DA neurotransmission (Darstein, Löschmann et al. 1997). These findings show that cGlyRs are expressed on striatal ChIs and indeed mediate ACh release, although the underlying mechanism is unclear.

Medium Spiny Neurons (MSNs)

cGlyRs have also been identified on striatal MSNs in both the dorsal and ventral striatum (McCracken, Lowes et al. 2017). Investigation is primarily on MSNs in the NAc, in the context of ethanol potentiation of cGlyR currents in addiction (Forstera, Munoz et al. 2017). The majority of MSNs express cGlyRs, which could be activated by glycine or taurine (Martin and Siggins 2002). There is some variability in the reported efficacy between studies, with the EC50 of glycine lower in studies recording from dissociated cells (~110 μM) versus recording from cells in intact slice (~600 μM) (McCracken, Lowes et al. 2017). In young (12-20 days post-natal) rats with high intracellular Cl^-, glycine and taurine depolarise NAc MSNs. Application of the cGlyR antagonist strychnine mediates in shift in the holding current, suggesting that these receptors are tonically active (McCracken, Lowes et al. 2017, Molchanova, Comhair et al. 2017). There are discrepancies reported about sensitivity to PTX and the presence of extrasynaptic cGlyRs, even in adult animals where the developmental transition from homomeric to heteromeric cGlyRs has taken place (Martin and Siggins 2002, Forstera, Munoz et al. 2017, McCracken, Lowes et al. 2017, Molchanova, Comhair et al. 2017). *Glra2*-/Y and *Glra3*-/- mice have demonstrated that *Glra3* is required to mediate tonic cGlyR currents in NAc MSNs (suggesting expression of homomeric α3 cGlyRs) and *Glra2* is required to mediate exogenous activated currents (suggesting expression of heteromeric α2/β cGlyRs (McCracken, Lowes et al. 2017). There is also discrepancy about the expression of different cGlyR subunits within MSNs, particularly the presence or absence of the α1 subunit which is thought to be particularly sensitive to ethanol and potentiate glycine currents in its presence (Forstera, Munoz et al. 2017). Although these findings have discrepancies, it is likely that all subunits are expressed within the striatum, in a combination of homomeric and heteromeric cGlyRs. Furthermore, it is additional evidence for functional cGlyR expression within the striatum.

1.5.2. Excitatory glycine receptors (eGlyRs)

1.5.2.1. Structure and subunit composition

Although defined as excitatory glycine receptors (eGlyRs), these receptors are composed of NMDA receptor subunits and can also be described as atypical NMDA-Rs (Otsu, Darcq et al. 2019). Like other NMDA-Rs, eGlyRs are tetrameric cation-permeable receptors, composed of 4 subunits. NMDA-R subunits are divided into three groups based on their sequence homology: GluN1, GluN2, and GluN3 (Paoletti, Bellone et al. 2013). Within the GluN1 subunit family, 8 different isoforms have been identified (GluN1-1a-d and GluN1-2a-d) that are splice variants of the *Grin1* gene. There are four variants of the GluN2 subunit (GluN2a-d) each encoded by a separate gene, and two variants of the GluN3 subunit (GluN3a-b) also each encoded by a separate gene. All subunits contain an agonist binding domain, that consists of two segments with a clamshell assembly. GluN1 and GluN3 subunits contain a glycine binding site, while GluN2 subunits contain a glutamate binding site (Paoletti, Bellone et al. 2013).

Over the course of development, the stoichiometry of expressed NMDA-Rs varies with function (Paoletti, Bellone et al. 2013). All NMDA-Rs express GluN1 subunits, which are expressed ubiquitously across throughout development and adulthood. The GluN1 subunit is also required for ER export, hence why there are no GluN2-GluN3 di-heteromers (Pérez-Otaño, Schulteis et al. 2001). GluN2 and GluN3 subunits are differentially expressed over development, with GluN2 subunit expression increasing with age and GluN3 subunit expression at its greatest during development. NMDA-Rs usually exist as di-heteromers of 2 GluN1 and 2 GluN2 subunits, such that the receptor has both glutamate and glycine binding sites. During development, expression of tri-heteromeric NMDA-Rs consisting of 1 GluN1, 2 GluN2, and 1 GluN3 subunit are formed (Perez-Otano, Larsen et al. 2016). GluN1 and GluN3A di-heteromeric NMDA-Rs do not have a glutamate binding site, and are exclusively gated by glycine i.e. eGlyRs (**Fig. 1.4**) (Chatterton, Awobuluyi et al. 2002). Although demonstrated as being functional receptors in heterologous expression systems, eGlyRs were not identified *in vivo* until recently in 2018 in juvenile hippocampus, and subsequently in adult medial habenula and within the

basolateral amygdala and cortical interneurons (Chatterton, Awobuluyi et al. 2002, Otsu, Darcq et al. 2019, Bossi, Dhanasobhon et al. 2022).

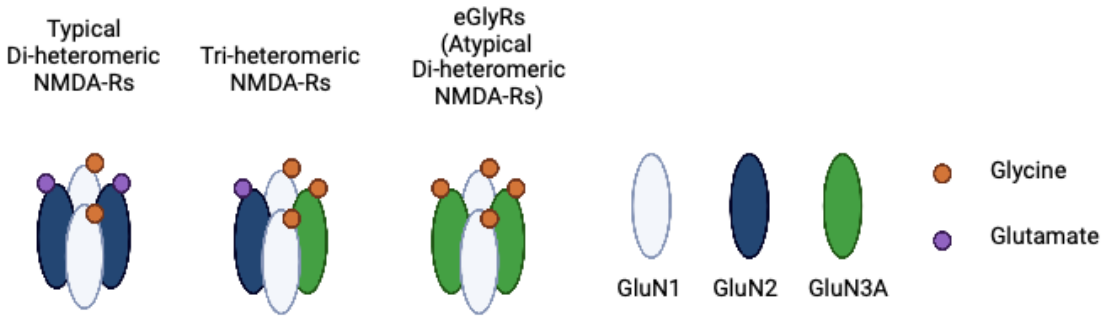

Figure 1.4. Schematic of NMDA-R and eGlyR stoichiometry. Simplified diagram depicting the composition of receptors composed of GluN1 (white), GluN2 (blue), and GluN3A (green) subunits. Agonist binding is depicted by glycine (orange) and glutamate (purple). eGlyRs are composed of GluN1 and GluN3A subunits, so contain only subunits with glycine binding sites. They are not gated by glutamate. Created with BioRender.com

1.5.2.2. Kinetics

Part of the reason why eGlyRs have not been more widely identified until recently is due to their rapid desensitisation, making their currents small, unstable and difficult to visualise. In HEK293 cells, 100 µM application of glycine results in a small current (~20 pA) that rapidly desensitises to a steady state current ~40% of peak amplitude (Grand, Abi Gerges et al. 2018). Glycine binding to the GluN3A subunit triggers channel opening, while glycine binding to the GluN1 subunit triggers a shift into a non-conducting desensitised state (Grand, Abi Gerges et al. 2018). This results in a bell-shaped concentration-response curve where glycine acts as both an agonist and functional antagonist (Bossi, Dhanasobhon et al. 2022). A single point mutation in the GluN1 agonist binding domain, preventing glycine binding, results in eGlyRs with large, non-desensitising glycine-gated currents (Madry, Mesic et al. 2007). The GluN3A subunit has a greater affinity for glycine than the GluN1 subunit (40 nM versus 26 µM) (Yao and Mayer 2006), hence why there is a concentration window where glycine is able to activate the receptor. eGlyRs have an EC50 of ~7 µM, and it is likely in tissue that a sub-population of these receptors are tonically activated by an ambient exogenous glycine concentration of 2-5 µM (Zhang, Herde et al. 2018), which may then cause them to transition more rapidly to a desensitised state.

1.5.2.3. Pharmacology

There are few ligands able to selectively target eGlyRs, due to off-target effects at NMDA-Rs that also express the same subunits. However, targeting the separate GluN1 and GluN3A subunits allows functional manipulation of eGlyRs. Grand et al. identified CGP-78608 as a GluN1 competitive antagonist with a 100-fold greater affinity for the GluN1 subunit than the GluN3A subunit. This blocks glycine binding to the GluN1 subunit that mediates desensitisation, allowing eGlyRs to remain in an active conformation (**Fig. 1.5**). CGP-78608 increased the peak current 100-fold and the steady-state current 300-fold, with an EC50 of 26 nM (Grand, Abi Gerges et al. 2018). The presence of CGP-78608 allows eGlyR currents to be revealed that otherwise would not be observed or measured. This enhancement of eGlyR current is state-dependent, with CGP-78608 having no effect where exogenous glycine (100 µM) was already applied and occupying the GuN1 subunit, keeping the eGlyR in a desensitised state (Grand, Abi Gerges et al. 2018). 5,7-dichlorokynurenic acid (DCKA) is an antagonist at both GluN1 and GluN3A agonist binding sites, and blocks eGlyR currents (Bossi, Dhanasobhon et al. 2022). Because these receptors do not contain a glutamate binding site, they are insensitive to AP-5

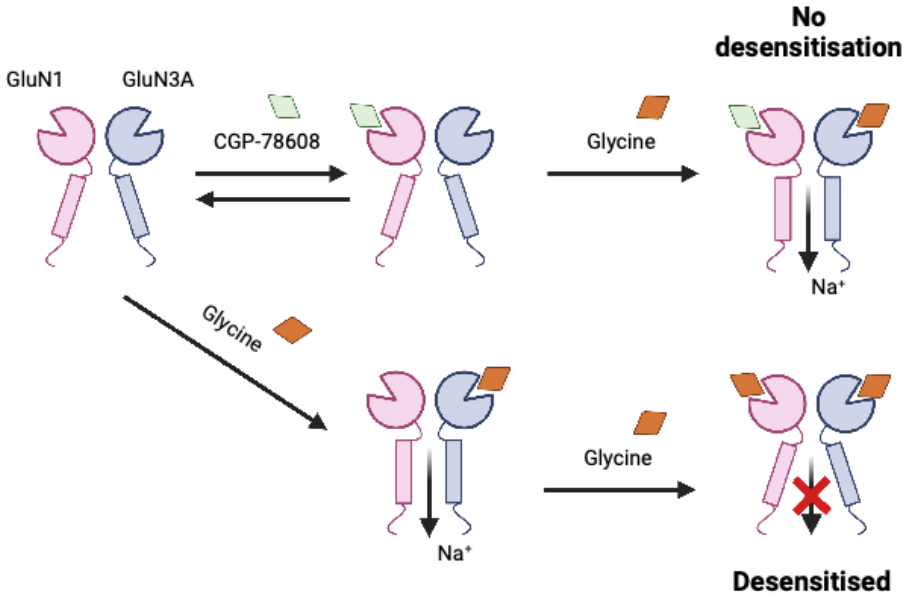

Figure 1.5. Simplified schematic of eGlyR gating and pharmacology. Simplified diagram depicting eGlyR composition of GluN1 (pink) and GluN3A (blue) subunits. Glycine binding to the GluN3A subunit opens the channel, but glycine binding to the GluN1 subunit shifts the channel into a desensitised state. CGP-78608 binding to the GluN1 subunit prevents glycine binding, stopping desensitisation if the channel is active. Adapted from Grand et al., 2018, doi: 10.1038/s41467-018-07236-4. Created with BioRender.com

as a typical NMDA-R antagonist. However, CNQX has been identified as an antagonist at eGlyRs, in addition to GluN1-GluN2 NMDA-Rs and AMPA-Rs, which should be considered for off-target effects (Madry, Mesic et al. 2007). eGlyRs are also redox state sensitive, whereby their sensitivity is increased in the presence of reducing agents by increasing the GluN3A binding affinity, where they mediate outward current shifts in the presence of ambient glycine concentrations (Bossi, Dhanasobhon et al. 2022). This may allow modulation of their function under different intracellular environmental conditions (Grand, Abi Gerges et al. 2018).

1.5.2.3. Distribution and function

There is still relatively little research identifying the distribution of eGlyRs, but they have been functionally characterised in the juvenile hippocampus, adult medial habenula, cortical SST+ interneurons and pyramidal neurons in the basolateral amygdala (BLA) (Grand, Abi Gerges et al. 2018, Otsu, Darcq et al. 2019, Bossi, Dhanasobhon et al. 2022). Commercially available antibodies have poor specificity for the GluN3A subunit, and RNA ISH methods are preferred for localisation of this subunit (Bossi, Dhanasobhon et al. 2022). Using ISH, the gene encoding GluN3A (*Grin3a*) expression is observed within the striatum, with punctate expression indicative of interneuron expression (**Fig.1.6, *left***) (Allen Institute for Brain Science, 2011, Experiment: 73907499). Although co-localisation of *Grin3A* expression has not yet been undertaken, a previous study used immunohistochemistry to identify GluN3A expression in striatal cells morphologically identified as putative ChIs (Marco, Giralt et al. 2013). There appears to be some *Grin3a* expression in the midbrain, but the staining pattern is not consistent with DA neurons (**Fig. 1.6*, right***).

In cortical SST+ interneurons, DCKA application mediates a tonic outward current, but exogenous application of low concentrations of glycine (10 μM) also mediates inward currents that are GluN3A- and DCKA-sensitive, suggesting that eGlyRs are tonically active and act by depolarising the neuron, increasing excitability (Bossi, Dhanasobhon et al. 2022). The hypothesis is that eGlyRs hold tonically active interneurons at a more depolarised resting membrane potential to facilitate action potential firing. This hypothesis is supported by findings on SST+ interneurons, but the lack of CGP-78608 potentiation of tonic eGlyR currents on BLA pyramidal neurons shows that different receptor

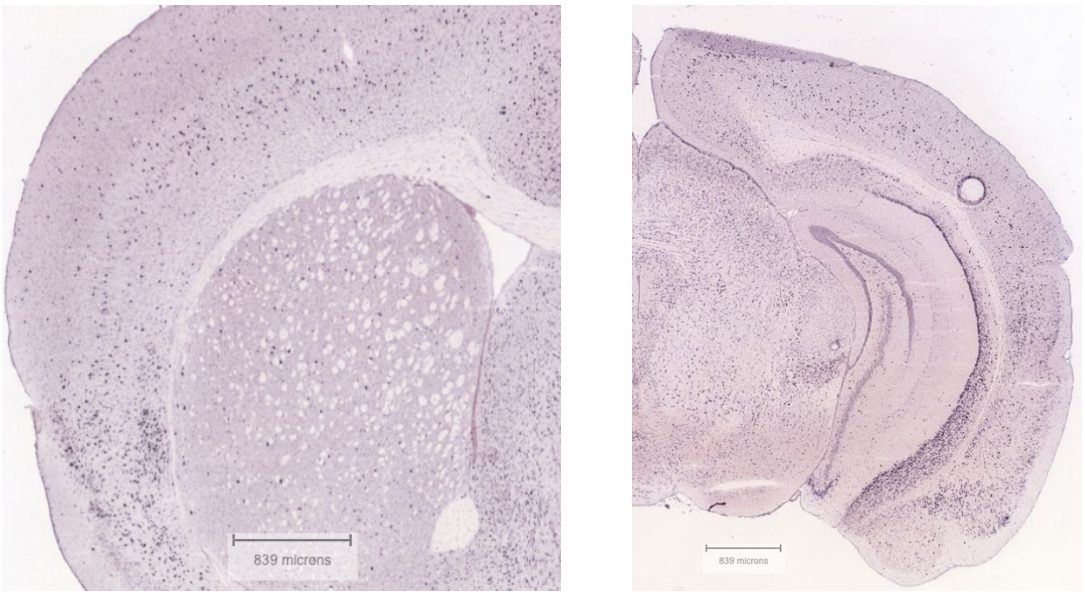

Figure 1.6. *Grin3a* expression in adult mouse brain

Images showing *Grin3a* expression in adult mouse brain, which encodes the GluN3A subunit. *Left*: There is punctate, distributed expression across dorsal and ventral striatum, suggesting expression of *Grin3a* in striatal interneurons. Right: There is some expression of *Grin3a* across the midbrain but does not appear to be enriched in DA neurons in SNc. From Allen Mouse Brain Atlas, https://mouse.brain-map.org/experiment/show/73907499

occupancy between eGlyR populations can result in different effects between brain regions (Bossi, Dhanasobhon et al. 2022). The complexity of the relationship between eGlyR gating is highlighted in an experiment using glycine oxidase to reduce extracellular glycine levels in slice, which would be expected to hyperpolarise SST+ interneurons but actually depolarised them further, possibly due to their atypical mechanism where glycine is both an agonist (binding to GluN3A subunits) and antagonist (binding to GluN1 subunits) (Bossi, Dhanasobhon et al. 2022).

In summary, eGlyRs are an under investigated receptor type with complex kinetics and pharmacology that can mediate an excitatory effect of glycine. Given initial ISH evidence and a hypothesis of a functional role in facilitating the excitability of tonically active interneurons, there is justification to investigate their expression and function in the striatum, especially on cholinergic interneurons that are known to powerfully regulate DA release.

1.5.3. Metabotropic glycine receptors (mGlyRs)

Until very recently, glycine was the only major neurotransmitter not to have an identified metabotropic receptor. However, a new study identified that an orphan GPCR (GPR158) functions as a metabotropic glycine receptor, which is now renamed as the mGlyR (Laboute, Zucca et al. 2023). Activation of this receptor alters the conformation of RGS7-Gβ5, reducing activation of Gα GTPase and ultimately causing an increase in intracellular cAMP. This mediates an excitatory effect, observed in layer II and layer III neurons in prelimbic cortex, where glycine mediated an excitatory effect by increasing the number of action potentials elicited by a depolarising current ramp, but interestingly did not alter resting membrane potential. The affinity of this receptor for glycine is high, with an EC50 of ~3 μM and with taurine also acting as a partial agonist (EC50 ~6 μM). This is lower than the affinity for ionotropic glycine receptors and may suggest differential regulation under different conditions of glycine or taurine release (Laboute, Zucca et al. 2023). Although GPR158 has only been recently identified as the mGlyR, it has been previously investigated as a widely expressed orphan receptor. GPR158 is expressed in the prefrontal cortex and is associated with control of affective states. Stress

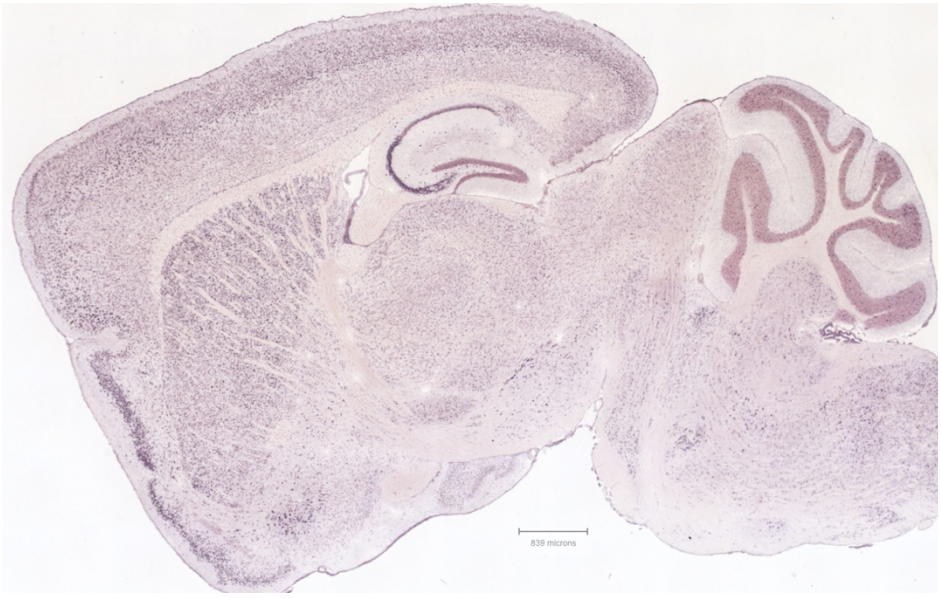

Figure 1.7. *GPR158* expression in adult mouse brain

Image showing *GPR158* expression in adult mouse brain, which encodes the re-assigned mGlyR. There is widespread distribution across the forebrain, including dorsal and ventral striatum. From Allen Mouse Brain Atlas, https://mouse.brain-map.org/experiment/show/73497162

causes up-regulation of GPR158 in prefrontal cortex, and knock-out of GPR158 results in mice with an anti-depressant and stress-resilient phenotype (Sutton, Orlandi et al. 2018). Although not (yet) investigated in striatum, ISH data shows expression within the striatum, which warrants further investigation (**Fig. 1.7**) (Allen Institute for Brain Science, 2011, Experiment: 73497162).

1.5.3. Glycine and taurine as the endogenous ligand at striatal glycine receptors

Although there is a large body of evidence for glycine receptors in striatum, there has been extensive debate over the past three decades around the identity of the endogenous ligand for these receptors. Although classically gated by glycine released from glycinergic fibres, there is little evidence for expression of glycinergic neurotransmission in the striatum, and alternative mechanisms of glycine release (Zeilhofer, Studler et al. 2005). This is why many studies investigating cGlyRs test the effect of taurine in addition to glycine (Sergeeva and Haas 2001). There is also a growing understanding of astrocyte-mediated gliotransmission as another source of either glycine or taurine, which may help to resolve some of these conflicts. There is extensive evidence for the tonic activation of striatal glycine receptors, but the identity of the endogenous ligand remains unclear.

1.5.3.1. Neuronal glycinergic transmission in striatum

Glycine is widely known as a fast inhibitory neurotransmitter, complementary to GABA. From neurons, it is release either alone or co-released from fibres expressing glycine and glycine transporter 2 (GlyT2) as presynaptic markers (Zeilhofer, Studler et al. 2005). GlyT2 is located on glycinergic neurons and is responsible for the re-uptake of glycine. However, there is very little evidence for the expression of glycinergic fibres or GlyT2 in striatum, with the vast majority of studies reporting negligible GlyT2 expression (Zafra, Aragon et al. 1995, Zeilhofer, Studler et al. 2005). There is some evidence for the co-release of glycine from GABAergic neurons that express the vesicular inhibitory amino acid transporter (VIAAT also known as VGAT in GABAergic neurons) (Wojcik, Katsurabayashi et al. 2006). In the striatum, only one study has identified strychnine-sensitive mIPSCs and used targeted optical stimulation of VGAT-expressing neurons to identify a strychnine-sensitive component of the

IPSC recorded in MSNs (Munoz, Yevenes et al. 2018). Other studies in striatum have not identified strychnine-sensitive mIPSCs (McCracken, Lowes et al. 2017). Although it is possible that there may be a neuronal component to striatal glycine release, it is only likely to have a very small role and is not considered be the most likely source of glycine.

1.5.3.2. Astrocytic glycinergic signalling via glycine transporter 1 (GlyT1)

The other possible source of striatal glycine are astrocytes. Glycine transporter 1 (GlyT1) is a member of the solute carrier family (SLC6A9) that is expressed on astrocytes (Shibasaki, Hosoi et al. 2017). It is responsible for the astrocytic release and re-uptake of glycine to maintain extracellular glycine concentrations. It has a stoichiometry of 2 Na^+: 1 Cl^-: 1 GLY, which are co-transported (Cherubino, Bossi et al. 2010, Zhang, Uchendu et al. 2021). Therefore, GlyT1 is also electrogenic, with a net movement of positive charge into the astrocyte as glycine is taken up from the extracellular environment. GlyT1 inhibitors have identified and developed to target extracellular glycine tone, as targets for schizophrenia, epilepsy, and pain via NMDA-Rs (Harvey and Yee 2013). Microdialysis studies have identified an ambient glycine tone in the striatum of 1-2 μM in rats, which is increased ~2.5-fold upon GlyT1 inhibition (Nagy, Marko et al. 2010). By contrast, the estimated peak glycine concentration upon synaptic release is c.1 mM, suggesting that astrocytes may use glycinergic signalling to target different glycine receptor populations (Legendre 1998, Vandenberg and Aubrey 2001). GlyT1 inhibition has been shown to enhance the magnitude of strychnine-sensitive currents in striatum, suggesting that elevation of extracellular glycine increases tonic activation of cGlyRs, and therefore that glycine is the endogenous ligand for these receptors (McCracken, Lowes et al. 2017). Furthermore, GlyT1 inhibition alone causes strychnine-sensitive shifts in the holding currents of recorded MSNs (Forstera, Munoz et al. 2017, McCracken, Lowes et al. 2017), again suggesting tonic activation of cGlyRs is mediated by glycine.

Although GlyT1 function as a sink of extracellular glycine is well-established, glycine release from astrocytes as a gliotransmitter is becoming more widely known, as a potential source of striatal glycine. Astrocytes are able to release glycine via reversal of GlyT1 (Huang, Barakat et al. 2004, Shibasaki, Hosoi et al. 2017), and in combination with previous studies showing effects of GlyT1

inhibition in striatum, it is possible that GlyT1 could mediate the release of glycine in striatum. This relationship of astrocytes acting as both a sink and source for extracellular striatal glycine warrants further investigation, but appears similar to astrocytic ENT1 acting as a sink and source for striatal adenosine (Roberts, Lambert et al. 2022). A recent study found that ablation of striatal astrocytes via application of fluorocitrate did not alter extracellular glycine levels recorded using *in vivo* microdialysis (Adermark, Lagstrom et al. 2022). Given the previous evidence, I would hypothesise this demonstrates a complex relationship for astrocytic release and re-uptake of glycine, rather than a lack of astrocytic regulation of striatal glycine levels. Local tissue trauma caused by the large diameter of microdialysis probes may also alter the levels of amino acids present in the extracellular space.

1.5.3.3. Astrocytic gliotransmission via volume regulating anion channels (VRACs)

A candidate mechanism for the striatal release of taurine, and possibly glycine, are volume regulating anion channels (VRACs) (Pasantes-Morales and Schousboe 1989). These are heteromeric channels that are almost ubiquitously expressed, and originally found to be activated by cell-swelling, upon which they mediate the release of organic osmolytes to reduce their volume (Jentsch 2016, Strange, Yamada et al. 2019). This includes taurine, which is released upon hypotonic challenge via VRACs, and is blocked in the presence of VRAC antagonists (Hussy, Bres et al. 2001). Furthermore, astrocytic release of taurine via VRACs has been shown to mediate tonic inhibition of neurons in the supraoptic nucleus, whereby depletion of taurine results in the loss of tonic inhibition, and the effect is strychnine-sensitive indicating cGlyRs as the effector (Choe, Olson et al. 2012). This shows that astrocytic VRACs can mediate cGlyR tonic inhibition via the release of taurine (Hussy, Deleuze et al. 1997). Although classically associated with molecules involved with osmoregulation, recent evidence shows that VRACs mediate the release of GABA from astrocytes in VTA to mediate tonic GABAergic inhibition in this region (Yang, Chen et al. 2023). Although not tested, I would hypothesise that this could also be a mechanism of astrocytic glycine release.

Although speculation of taurine as the endogenous ligand for cGlyRs arose from a lack of evidence for neuronal glycinergic transmission in striatum, there is also a large volume of positive evidence for taurine signalling within striatum. Although taurine is an abundant amino acid across the

CNS, but is particularly enriched in the striatum relative to other brain regions and is linked to high expression of the taurine transporter (TauT) that mediates taurine uptake (Clarke, Smith et al. 1983, Palkovits, Elekes et al. 1986, Sergeeva, Chepkova et al. 2003). Knockout of TauT also results in striatal disinhibition of extrasynaptic $GABA_AR$ currents, due to the lower taurine content in striatum (Sergeeva, Fleischer et al. 2007). The concentration of taurine is c. 25 μM in the extracellular space, but is found in the low mM range in neurons (Puka, Sundell et al. 1991, Molchanova, Oja et al. 2004). Within the striatum, inhibition of VRACs using 2 mM SITS decreases extracellular taurine by c. 40%, and inhibition of TauT using 1 mM GES increases extracellular taurine levels by c. 50%, showing the presence of a taurine tone that can be modulated (Molchanova, Oja et al. 2004). A caveat is the poor pharmacology for regulating taurine signalling - the TauT inhibitor GES is also a cGlyR antagonist, $GABA_AR$ antagonist, and GAT inhibitor at high concentrations, and the VRAC channel blocker is likely to have off-target indirect effects given the broad expression of VRACs to regulate the core function of osmoregulation (Sergeeva, Chepkova et al. 2003, Sergeeva, Fleischer et al. 2007). However, there is overall good evidence for functional taurine signalling in the striatum, that could act at glycine receptors.

Overall, there is evidence for both an ambient glycine and taurine tone within the striatum, but evidence of fast synaptic glycinergic transmission is less clear (Molchanova, Oja et al. 2004, Nagy, Marko et al. 2010). The mechanisms above are not mutually exclusive, and I would hypothesise that there is some component of both glycine and taurine signalling within the striatum. Testing this hypothesis is limited by the poor pharmacology of the transporters and channels involved in glycine and taurine signalling. An alternative approach is to deplete slices of glycine and taurine, either using channel blockers to stop taurine release or enzymatic approaches to degrade glycine but these can be difficult to execute based on residual glycine/taurine remaining in the slice, off-target effects of the drugs used, or the cost of enzymes such as glycine oxidase (Molchanova, Oja et al. 2004, Choe, Olson et al. 2012, Bossi, Dhanasobhon et al. 2022).

1.5.4. Glycine receptor modulation of striatal dopaminergic neurotransmission

There is evidence for functional glycine receptors in striatum and previous studies have explored how glycine receptors may regulate DA release. No research has accounted for functional roles of eGlyRs and mGlyRs, so research is focused on cGlyRs. This research has been undertaken using *ex vivo* tissue and *in vivo* recordings, with some discrepancies across methologies that may suggest different direct and indirect mechanisms across models.

1.5.4.1. *ex vivo* recordings

Several studies over the past 40 years have investigated how glycine regulates dopamine. These have mostly used ex vivo striatal tissue preparations loaded with radio labelled 3H-DA, and recording the subsequent quantity of 3H-DA in the slice superfusate after pharmacological manipulation. This technique allows measurement of DA release, but is limited by poor temporal resolution required to collect a sufficient volume of superfusate for subsequent analysis (typically at least 2 minutes per sample). Other aspects of this preparation are also non-physiological: this often measures the spontaneous release of DA in the absence of any intrinsic activity of DA axons, and where DA release is evoked it is often performed using chemical stimulation such as application of KCl or NMDA, resulting in intense prolonged stimulation rather than discrete brief pulses of stimulation. Most have explored the ability of glycine itself to regulate DA release, whilst others have explored the ability of glycine to modulate NMDA-evoked DA release. The earliest studies found that glycine evoked DA release in striatum and substantia nigra (Giorguieff-Chesselet, Kemel et al. 1979, Kerwin and Pycock 1979). These studies found that the release of DA after glycine application was strychnine-sensitive, suggesting that it is mediated by cGlyRs. However, a more recent study found no effect of glycine application on DA release (Hernandes, de Magalhaes et al. 2007). Studies also found that glycine and GlyT1 inhibitors that increase extracellular glycine inhibit NMDA-evoked DA release (Javitt, Sershen et al. 2000, Javitt, Hashim et al. 2005). These inconsistent results may arise from the different paradigms of recording evoked versus non-evoked DA release, but also recording extracellular DA levels over 2-4 minute fractions precludes more detailed investigation of the mechanisms involved, particularly given

the short sub-second timescales of both DA release events and cGlyR kinetics. Overall, however, these support a hypothesis that cGlyRs can control striatal DA release even though the mechanism is unclear.

Over the course of my project, a study used fast-scan cyclic voltammetry to investigate cGlyR regulation of DA release, as a potential mechanism of ethanol alteration of DA release (Yorgason, Wadsworth et al. 2022). Recording electrically evoked DA release in NAc of ex vivo striatal slices, they found that glycine reduced DA release at high concentrations (> 5 mM) and also observed that strychnine decreased DA release by ~25%. Interestingly, strychnine was not found to reduce DA release in vivo, which may again reflect different indirect mechanisms in an intact system. The glycine mediated reduction was found to be partially PTX-sensitive, although PTX (50-100 μM) was not used at a sufficiently high concentration to block synaptic heteromeric cGlyR currents that would be activated by 5-10 mM glycine. In combination with the data above, it supports a role for cGlyRs in regulating DA release, and that tonic activation of cGlyRs may contribute to this. However, there was no further investigation into the underlying mechanism of action.

1.5.4.2. *in vivo* recordings

In vivo microdialysis has been used in various studies to investigate how glycine and taurine may alter striatal DA levels. These have mostly recorded changes in DA levels in microdialysate following intra-striatal perfusion of either glycine or taurine, and as with the ex vivo literature have discrepancies: some studies show that glycine is able to increase extracellular DA levels, whilst others show mixed effects of either an increase or no effect (Yadid, Pacak et al. 1993, Molander and Soderpalm 2005). Similarly, although inhibition of GlyT1 increases striatal glycine levels, studies then report that causing a subsequent decrease in striatal DA levels (Nagy, Marko et al. 2010) or mixed effects with either a subtle increase in baseline DA levels or no response (Lidö, Stomberg et al. 2009, Lidö, Ericson et al. 2011). Taurine appears to increase striatal DA levels (Ruotsalainen and Ahtee 1996, Ericson, Molander et al. 2006). Where an effect is observed, it is consistently observed to be at least partly strychnine-sensitive, although this may be due to differences in concentration where > 10 mM glycine or taurine is usually needed to see an effect on DA release and concentrations of strychnine and PTX used go up to 100-200 μM where there may be off-target effects on nAChRs and $GABA_A$Rs (Jonsson,

Adermark et al. 2014, Clarke, Soderpalm et al. 2015). However, the experiments using GlyT1 inhibitors are able to block their effects using lower concentrations of strychnine (10 μM) more likely to act exclusively at cGlyRs. Strychnine alone was only appears to decrease DA levels at higher concentrations (< 20 μM) *in vivo*, which supports the findings of Yorgasson et al. who observed no effect at 10 μM (Molander and Soderpalm 2005, Jonsson, Adermark et al. 2014, Clarke, Soderpalm et al. 2015). Overall, these findings again support a role of glycine receptor regulation of DA neurotransmission in striatum, but again contains discrepancies that may reflect different experimental paradigms and a complex interplay between the direct and indirect mechanisms by which glycine receptors may regulate DA release.

1.5.5. Summary

In summary, there is a large body of evidence showing that functional glycine receptors are expressed in the striatum, but their role in the regulation of DA neurotransmission is poorly understood. For my DPhil project, I have revisited this question with techniques that can resolve DA release at sub-second timescales, and also detect other neurotransmitters that may indirectly regulate DA release. This is particularly important in the context of advances in our identification of striatal regulators of DA release, such as ChIs and astrocytes, which are strongly linked to glycine receptor function in striatum. The ultimate aim is for this project to contribute to our understanding of regulators of DA release which may then identify targets to be exploited for therapeutic purposes in disease.

1.6. Parkinson's disease

Parkinson's disease (PD) was originally identified by James Parkinson in 1817, primarily as a motor disorder but with non-motor features. It is the second most common neurodegenerative disease after Alzheimer's disease and is estimated to affect 1% of adults over the age of 60 (McGregor and Nelson 2019). With advances in healthcare resulting in an aging population, the number of people projected to develop PD is anticipated to nearly double from 7 million patients in 2015 to 12 million in

2040 (Darweesh, Raphael et al. 2018). Currently, there is no disease-modifying treatment available, and new treatments are needed to improve the quality of life for these patients, their families, and reduce the burden on already overstretched healthcare systems.

Parkinson's disease is caused by death of DA neurons in the SNc, resulting in degeneration of the nigrostriatal pathway (Poewe, Seppi et al. 2017). This reduces DA neurotransmission to the striatum, lowering the concentration of DA in the striatum and resulting in motor and non-motor symptoms. Parkinson's disease is typically diagnosed at a median age of 60, upon identification of key motor symptoms including dyskinesia, bradykinesia, and resting tremor (Obeso, Stamelou et al. 2017). However, there is also a long prodromal stage without motor symptoms that can include sleep disturbance and anosmia (Jankovic and Tan 2020). Progression of the disease is associated with further motor dysfunction and cognitive decline. This wide range of symptoms is associated with the core role of DA neurotransmission within the striatum.

Currently, the most common treatments available for Parkinson's disease are Levodopa (L-DOPA) which is the precursor for DA to increase DA synthesis, and deep brain stimulation which targets stimulation of the subthalamic nucleus or globus pallidus (Jankovic and Tan 2020). The difficulty in developing treatments for PD is caused by the many causes of DA neuron death, such that there are no single targets for PD (Surmeier, Obeso et al. 2017). Although aggregation of α-synuclein into Lewy bodies is a common hallmark of PD, most patients have idiopathic PD, which is unidentified but may be caused by factors including lysosomal transport disorders, Ca^{2+} mis-handling, and mitochondrial disorder (Braak, Tredici et al. 2003, Schapira 2015, Zampese and Surmeier 2020). Environmental factors can include certain pesticides that inhibit mitochondrial function (Ascherio and Schwarzschild 2016). DA neurons have a large energy requirement due to their extensive axonal arbour and so are particularly susceptible to mitochondrial dysfunction (Zampese and Surmeier 2020).

To help identify new treatments for PD, we aim to better understand the mechanisms that regulate DA release in health and disease. Mouse models of PD have been developed, aiming to mimic the pathology and progression of PD. Duplication and triplication of the α-synuclein gene (*SNCA*) are known to cause PD due to overexpression of α-synuclein that is prone to aggregate and form Lewy body inclusions (Book, Guella et al. 2018). At the Oxford Parkinson's Disease Centre, we have

developed and use a mouse model based on the overexpression of α-synuclein, *SNCA*-OVX (Janezic, Threlfell et al. 2013). This model does not express mouse α-synuclein but over-expresses human α-syn at a level similar to SNCA multiplication mutations. These mice exhibit a progressive decline of tyrosine hydroxylase positive cells in SNc, a progressive motor phenotype, and exhibit a deficit in electrically- and optically-evoked DA release in the dorsal but not ventral striatum before the loss of DA neurons in the midbrain. This model therefore shows a prodromal stage of DA release dysfunction, and may be particularly well-suited to study axonal dysfunction in PD, including alterations in DA release and re-uptake.

1.7. Diabetes

Diabetes is a metabolic disease caused by dysfunctional insulin signalling resulting in the inability of the body to regulate blood glucose levels (**Section 5.1.1**) (Petersen and Shulman 2018). It can be divided into type 1 diabetes caused by impaired endogenous insulin synthesis that results in low serum insulin levels, and type 2 diabetes caused by insufficient insulin release in response to elevations in blood sugar that is also described as insulin resistance (DeFronzo, Ferrannini et al. 2015). Some research indicates that patients with diabetes are at a greater risk of developing neurodegenerative diseases, including Parkinson's disease (De Pablo-Fernandez, Goldacre et al. 2018). Parkinson's disease is also hypothesised to be, at least in part, a metabolic disease caused by insufficient energy production in DA neurons that require large amounts of energy to maintain healthy function (Song and Kim 2016). Insulin resistance is associated with more rapid disease progression and motor impairment in Parkinson's disease (Athauda and Foltynie 2016).

Given this evidence, diabetes may also result in dysfunctional dopaminergic neurotransmission. As part of my DPhil project, I took part in a collaboration investigating whether dopaminergic neurotransmission was altered in mouse models of type 1 and type 2 diabetes. This hypothesis was based in part on the clinical association between type 2 diabetes and Parkinson's disease, but also findings from our collaborators that DAT expression was significantly reduced in both type 1 and type 2 mouse models of diabetes, which we would expect to alter DA neurotransmission (Perez-Taboada,

Alberquilla et al. 2020). Insulin receptors expressed on striatal ChIs have also been shown to indirectly regulate DA release, and we hypothesised that dysregulated insulin signalling in both type 1 and type 2 models of diabetes may also alter DA release via a presynaptic cholinergic mechanism (Stouffer, Woods et al. 2015). A better understanding of the mechanistic links between diabetes and Parkinson's disease may allow further understanding of the metabolic hypothesis of Parkinson's disease and identify new therapeutic approaches.

The aim of my DPhil project is to help identify novel mechanisms that regulate DA release, with the aim of identifying new treatments for Parkinson's disease. In **Chapter 3** and **Chapter 4** of this thesis, I investigate how glycine receptors may regulate dopamine release under normal conditions, which may then be used for future studies exploring relevance in PD models. In **Chapter 5** of this thesis, I investigate possible dysfunction in dopaminergic neurotransmission in mouse models of diabetes, as part of a collaboration investigating co-morbidity between diabetes and Parkinson's disease. I hope that this research will contribute to the field and help to bring forward new treatments for Parkinson's disease and other diseases associated with dysfunctional dopaminergic neurotransmission.

Chapter 2:
General Methods

2.1 Animal models used investigate dopaminergic striatal circuits

2.1.1. Ethical statement for the use of animals

The primary aim of this thesis is to understand the mechanisms by which mammalian striatal DA release is regulated, with the goal of using these findings to identify new targets for the treatment of diseases in humans with dysfunctional dopaminergic neurotransmission. Therefore, it is crucial to use a model system that is similar enough to humans that the research findings here have some translational potential, while mitigating against pain and distress caused to a more sentient being than necessary. Although there have been advances in computer modelling for individual components of the mesostriatal dopaminergic pathway, the total mapping of interacting regulatory circuits is currently unknown and therefore biological tissue must be used (Muddapu and Chakravarthy 2021).

Mice were used as the model organism throughout this project because they are the least sentient species with similar neural organisation to humans, particularly relating to mesolimbic DA transmission. Mice have been widely used in previous research in this field, allowing for more straightforward comparison between my findings and the findings of others, without having to consider species differences. Finally, genetic manipulation has been undertaken most routinely in mice, and there are many transgenic lines readily available for experimental use – including the Slc6A3$^{IRES\text{-}Cre}$ and *db/db* mouse lines used in this project.

Experimental procedures using animals were undertaken in accordance with University of Oxford guidelines and the UK Home Office Animals (Scientific Procedures) Act of 1986. All mice were housed at the Biomedical Services Building, University of Oxford. These were group-housed, with environmental conditions between 22-24°C and 40-60% humidity on a 12-hour light-dark cycle, and provided access to food and water *ad libitum*.

2.1.2. Animals & Transgenic mouse lines

Most experiments used adult wild-type C57BL6/J mice. This strain was selected because these mice carry the wild-type gene for α-synuclein, which is important both in the regulation of DA release and the pathology of Parkinson's disease (Janezic, Threlfell et al. 2013). Spontaneous deletion of α-synuclein has been observed in other C57BL/6 strains, such as C57BL/6S (Specht and Schoepfer 2001). Male and female mice were used across all experiments, to reduce under-representation of female subjects in animal research and also to investigate any sex-specific mechanisms, that ultimately better reflects the human population and will contribute to improved clinical trial design (Prendergast, Onishi et al. 2014, Clayton and Tannenbaum 2016). Results from male and female animals are plotted together unless a sex-specific effect is identified.

To activate DA axons selectively using an optogenetic approach, I used heterozygous DAT-Cre mice that express Cre-recombinase under the control of the DA transporter (Slc6A3). These animals were generated locally from homozygous $Slc6A3^{IRES\text{-}Cre}$ mice from a C57BL/6J background (B6.SJL-$Slc6A3^{tm1.1(cre)Bkmn}$/J, Jax ID 006660).

2.1.3. Stereotaxic intracranial injections for viral transfection

Stereotaxic intracranial injection was performed in the striatum or midbrain of wild-type (C57BL/6J) or DAT-Cre ($Slc6A3^{IRES\text{-}Cre}$) mice respectively to deliver adeno-associated viral (AAV) constructs for the targeted expression of either fluorescent GPCR-activation based (GRAB) sensors, or channelrhodopsin-2. Surgical procedures were performed as detailed below, in accordance with aseptic technique and the Project Licence approved by the UK Home Office.

Prior to surgery, mice were checked for overall health and condition. Isoflurane was used to induce and maintain anaesthesia over the course of the surgery. To induce anaesthesia, the mouse was placed into an induction chamber containing 4% isoflurane. Once the mouse was deeply anaesthetised, the fur over the scalp and cheeks was shaved using electrical clippers, and the mouse was then placed securely into the stereotaxic frame (Kopf Instruments). The isoflurane was then lowered to 1.5-2% for

the maintenance of anaesthesia, and dosage titrated throughout the surgery according to physiological responses such as the breathing rate and the presence of the pedal withdrawal reflex. Eye ointment was applied to protect the eyes, and internal body temperature was monitored and regulated using a rectally-inserted temperature probe linking to a heating mat with a set target temperature of 37°C. The scalp was thoroughly cleaned with chlorhexidine gluconate (Chloraprep) before local injection of bupivacaine hydrochloride (2 mg/kg) s.c. Meloxicam (5 mg/kg) was also injected s.c. for analgesia following surgery, and sterile saline (Vetivex) was also administered to prevent dehydration during the surgery or recovery in the heated Thermacage immediately post-op.

Incision along the scalp was made using a sterile scalpel, and stereotaxic co-ordinates set using the suture positions of bregma and lambda. Craniotomy was performed using a small drill, in either dorsolateral Caudate Putamen (ML ± 2.2 mm, AP + 0.70 mm, DV -2.7mm - -2.5mm), Nucleus Accumbens core (ML ± 0.9mm, AP + 1.35mm, DV -3.8mm - -3.55mm), or substantia nigra pars compacta (ML ± 1.2 mm, AP -3.1 mm, DV – 4.25 mm). Injection of viral construct was performed using a 32-gauge Hamilton syringe (Hamilton Company) with a volume of 1000 nL per site at a rate of 200 nL/min, with the needle removed 5 minutes after the end of the injection from each site.

After injections were complete, the incision was closed using monofilament suture (Monocryl), and animals were placed in a temperature-controlled cage for immediate recovery. After normal behaviour returned, the mice were returned to their long term post-operative recovery cage. Mice were closely monitored on days 0-7 post-operation and provided with Metacam jelly on days 0-2 post-operation to alleviate any pain. AAV-transfected mice were typically used 3-5 weeks after intracranial injection, to allow time for viral expression.

2.2. Investigating DA release in acute *ex vivo* slice preparation

2.2.1. Rationale

The activity of the mesolimbic dopaminergic system can be measured at various points, from the activity of the DA neuron cell bodies in the substantia nigra pars compacta (SNc) or the ventral

tegmental area (VTA), activity of the DA axons in their terminal-field in the striatum, or using *in vitro* preparation of DA neurons differentiated from iPSCs (Häusser, Yung et al. 1992, Beccano-Kelly, Cherubini et al. 2023). All approaches offer specific benefits to understanding DA release. Throughout this project, I have used an acute *ex vivo* brain slice preparation because this allows me to investigate the mechanisms that regulate DA release at the axonal level.

A coronal *ex vivo* slice preparation provides a well-characterised preparation for studying DA release from axons within the striatum. Axons are severed from the DA cell bodies allowing precise control of activity in DA axons. Alternative angle preparations such as sagittal, parasagittal or horizontal sections do not readily keep nigrostriatal or mesolimbic pathways intact, as the course of ascending axonal projections is not linear, and very thick sections would be required for intact pathways that are difficult to maintain as viable.

DA neurons differentiated from iPSCs are of particular interest for basic research to be applied for translational medicine. This is because they can be derived from humans, including Parkinson's disease patients (Lang, Campbell et al. 2019). With the ultimate goal of developing therapies for Parkinson's disease, using patient-derived iPSCs reduces the risk of species differences stopping the progress of candidate targets from pre-clinical to clinical validation. These can in some circumstances replace animals used in research, one of the objectives of the 3Rs. However, an advantage of *ex vivo* slice preparations is they include all other relevant cell types in the circuit (including neurons and glia) that have developed normally *in situ* and which may be critical to normal control of DA release (Rice and Cragg 2004, Roberts, Doig et al. 2020). Although iPSCs are increasingly co-cultured with astrocytes and other cell types, and are never purely differentiated to a single cell type, they do not reflect the complexity of the local striatal circuits acting on DA axons, and also omit cell types that we have identified as regulating DA release, such as cholinergic interneurons.

Using *in vivo* models is closer physiologically than using *ex vivo* acute brain slices. This is because the animal has neural circuitry intact and functioning, although at different levels based on anaesthetised or awake state. *In vivo* models can give a better representation of how specific mechanisms regulating DA release may act in the context of other local circuits, including tonically active local interneurons and afferent inputs such as glutamatergic inputs from cortex and thalamus, and

the somatodendritic component of axonal DA release. The ultimate goal is to regulate DA release in diseased states in humans that will also have multiple direct and indirect mechanisms interacting with each other, and *in vivo* models are a closer reflection of this. However, the purpose of my project is to identify the local striatal circuits and regulatory mechanisms that control DA release at the axon, which is most efficiently tested in *ex vivo* brain slices. Firstly, this preparation removes any component of somatodendritic regulation of DA release. Secondly, experimental manipulations and the measurement of DA is more straightforward using *ex vivo* slice preparation than recording *in vivo*. This is because DA release *in vivo* typically has a lower signal to noise ratio, and more easily allows manipulation of the extracellular environment and signalling networks by allowing local application of drugs, prior incubation of tissue, and closer control of variables including temperature and pH via constant perfusion of tissue with aCSF. Once the mechanism is understood in *ex vivo* slices, research can be taken *in vivo* to understand its physiological relevance.

2.2.2. Fast-scan cyclic voltammetry as a technique for the detection of DA release in real-time

I primarily used fast-scan cyclic voltammetry (FSCV) for the detection of DA during experiments performed in this thesis, with some pilot experiments measuring DA using the recently developed $GRAB_{DA}$ sensor (**Section 2.3 – Fluorescent Sensors**) (Sun, Zhou et al. 2020). FSCV is performed using carbon fibre microelectrodes (CFMs) inserted into a recording site of interest. This technique relies on the electroactive property of DA conferred by the presence of two hydroxyl groups that can be oxidised and reduced. A triangular scan wave between a potential of -0.7 V and + 1.3 V is applied at the recording electrode at a frequency of 8 Hz. If any DA is present, it is oxidised by the forward sweep from DA to dopamine-o-quinone at c. +600 mV. On the reverse sweep, this is reduced back to DA at c. -200 mV. The loss and gain of electrons via this change in oxidation state produces a faradaic current, which can then be plotted against the applied potential to produce a voltammogram (**Fig. 2.1**).

The shape of the voltammogram can help to identify the substrate present, and the amplitude of the peak indicates the quantity of substrate present. Each electrode is calibrated at the end of each day with a 2 µM concentration of DA to allow conversion of the faradaic currents into a concentration of DA. DA concentration is linearly related to current over the range of concentrations observed here.

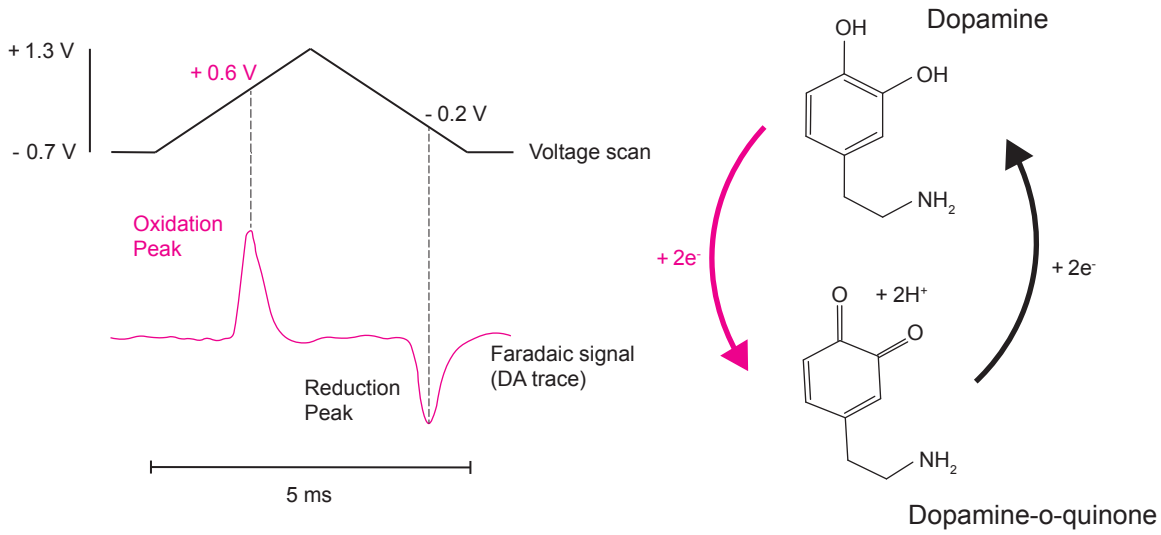

Figure 2.1. Fast-scan cyclic voltammetry uses the oxidation of dopamine to dopamine-o-quinone to generate a faradaic current

A triangular waveform of voltage is applied across the carbon-fibre recording microelectrode (CFM), between -0.7 V and + 1.3 V vs Ag/AgCl. The voltage scan is 5 ms in duration and performed at a scan rate of 800 V/s. Dopamine is oxidised to dopamine-o-quinone at +0.6 V and dopamine-o-quinone is reduced back to dopamine at -0.2 V. The resulting gain and loss of electrons produces a faradaic current, which can be mapped on the applied voltage scan to produce a voltammogram. This voltammogram is specific to dopamine, with the size of the current proportional to the amount of dopamine present.

To obtain the faradaic current, the relatively large background current produced by the charging of the electrode is subtracted digitally in real-time using the Millar voltammeter (Julian Millar, Barts and the London School of Medicine and Dentistry). Shifts in the background current may also be due to changes in the tissue environment, such as changes in tissue volume, Ca^{2+}, temperature and pH. To ensure that exogenously applied drugs do not cause shifts in the background current or alter the sensitivity of the electrode by interacting with the electrode surface directly, calibration of the electrode with a known concentration of DA is performed in the presence and absence of each exogenously applied drug. The amplitude of the faradaic current was then compared between conditions, to ensure the sensitivity of the electrode was not altered.

FSCV at a CFM is a powerful technique to measure DA release, particularly in an acute *ex vivo* striatal slice preparation. It detects DA within the concentration range (between high nanomolar and low micromolar) we expect to observe in our preparation, and with sufficient temporal resolution and signal to noise ratio at a subsecond sampling rate (8 Hz). Furthermore, the recording electrode diameter is sufficiently small (7 μm) to minimise tissue damage around the recording site, but their length of 50-100 μm allows recording across multiple release sites for extrasynaptic neurotransmitter release, such as DA, which functions as a volume transmitter (Rice, Patel et al. 2011). A longer length of exposed carbon fibre increases the sensitivity to DA but can detect higher levels of background noise and has greater capacitance limiting total amplification by the capped working range of the amplifier. Calibration of the recording electrode after use allows conversion of the faradaic currents recorded into a concentration of DA seen at the electrode.

We identify the neurotransmitter we record using FSCV as DA based on the combination of three factors. Firstly, DA has a characteristic voltammogram due to the electroactive properties of the DA molecule, which lead to a peak oxidation potential of ~600 mV and a peak reduction potential of ~-200 mV vs Ag/AgCl. The voltammograms we record during our experiments are compared to the calibration voltammograms performed at the end of each experimental day, applying a known concentration of DA to the recording electrode. However, this shape of the voltammogram alone is not sufficient to distinguish between other electroactive molecules with a similar structure (e.g. norepinephrine), which have a similar electrochemical profile. Secondly, we perform our recordings in the striatum, which has a significantly higher content of DA than norepinephrine due to the extensive DA axonal arbour present. Therefore, it is far more likely that any signal recorded will be due to DA. Finally, pharmacological manipulations are able to produce changes in the signal that are characteristic to DA release and are unlikely to significantly alter other neurotransmitters e.g. application of the DAT-blocker cocaine slows the decay of an evoked signal (Threlfell, Mohammadi et al. 2021).

There are a large number of alternative approaches to recording DA release including constant-potential amperometry, microdialysis with high-performance liquid chromatography (HPLC), radio-labelled DA, loaded DA synaptosome preparations, and the more recently developed genetically encoded fluorescence sensors (covered in more detail in **Section 2.3 – Fluorescent Sensors**). Recording

the activity of DA neurons using electrophysiology can also be used as an indicator of DA release. In this brief summary of alternative methods, I will focus on constant-potential amperometry and microdialysis with HPLC as the two most direct and widely used methods to detect DA itself (Zheng and Li 2023).

Constant-potential amperometry relies on the same principle that DA is oxidised at a given potential, producing a faradaic current that can be recorded. This technique allows sampling of extracellular DA at a higher or near continuous frequency because the potential at which DA is oxidised is maintained constantly rather than undergoing a cyclic sweep as for FSCV (Jiao, Liu et al. 2020). This gives greater temporal resolution and a more accurate recording of DA release and re-uptake. However, because a single potential is maintained rather than a voltage scan across a range of potential, this does not permit identification of the substrate of interest producing the faradaic current as readily as FSCV (Michael and Wightman 1999). Additionally, the enhanced temporal resolution provided by constant-potential amperometry is redundant for most use cases and is not advantageous over FSCV for detecting extracellular DA dynamics. Finally, stimulation of DA axons required for DA release in a coronal slice preparation causes a large stimulation artefact, that may disrupt the recording and can be avoided with FSCV by scanning out of phase with the stimulation.

Microdialysis with HPLC coupled to electrochemical detection is able to detect multiple neurotransmitters simultaneously from a given sample, and is also able to measure absolute concentrations of these neurotransmitters (Adermark, Lagstrom et al. 2022). Furthermore, microdialysis with HPLC has greater sensitivity than FSCV, allowing lower concentrations of DA to be detected, and also has greater chemical specificity, allowing it to distinguish between neurotransmitters with a similar chemical structure. However, the sampling resolution of microdialysis is much worse than FSCV, with maximal rates used of ~1 sample every 30 sec, which does not allow measurement of DA release and re-uptake that occurs on a sub-second timescale. Finally, microdialysis probes are relatively large (c. 250 μm diameter), which reduces the spatial resolution of recording but also causes more local tissue damage that can disrupt DA transmission.

Of the more established recording techniques, recording of DA release events using FSCV is the optimal method based on our acute *ex vivo* striatal slice preparation to address my question of

identifying regulators of striatal DA release acting at the axonal level. This is because we are confident that the signals we record can be attributed to DA in striatum. FSCV also has sufficient sensitivity for the detection of DA in the concentration range we observe, and temporal resolution to detect the sub second dynamics of DA release. Finally, the diameter of the recording electrode for FSCV are the optimal size to sample extrasynaptic DA release but not cause tissue damage as a microdialysis probe would.

2.2.3. Fabrication of Carbon Fibre Microelectrodes (CFMs)

All CFMs were manufactured in-house, with each electrode used for a single experiment due to changes in CFM sensitivity and kinetics caused by repeated exposure to DA and tissue damage. Borosilicate capillary tubes (2.0 mm outside diameter, 1.16 mm inside diameter, Harvard Apparatus) were immersed in acetone and threaded with an epoxy-free carbon fibre (7 µm diameter, Goodfellow Cambridge Ltd.). The capillary tube was then placed in a PE-2 vertical microelectrode puller (Narishige), and a high heat setting applied to form a tight seal between the glass and carbon fibre and enhance signal-to-noise ratio. Under 100x magnification, the seal was inspected for damage before the length of exposed carbon fibre from the seal was cut to a length of 50 – 100 µm using a scalpel. Finally, an insulated piece of copper wire (0.1 mm diameter) was coated with silver conducting paint and placed into the open end of the capillary tube, such that the wire was in contact with the carbon fibre at the tip. The wire was secured in place with cyanoacrylate glue.

2.2.4. Slice preparation

Acute *ex vivo* coronal slices of striatum were used during FSCV recordings. On the morning of experiments, the mouse was culled via cervical dislocation, with exsanguination performed as confirmation of death. The mouse was then decapitated, and the brain removed. 300 µm thick striatal coronal slices prepared using a vibratome (VT1200S, Leica) in ice-cold cutting solution saturated with 95% O_2 : 5% CO_2.

At the start of this project, I used an ice-cold HEPES-based buffer solution used commonly for FSCV across the lab. However, I switched to a high sucrose cutting solution during my project, as we standardised our cutting and recording solutions for FSCV and electrophysiology.

The HEPES-based buffer solution contains (mM): NaCl (120), $NaHCO_3$ (20), HEPES acid (6.7), KCl (5), HEPES salt (3.3), $CaCL_2$ (2), $MgSO_4$ (2), KH_2PO_4 (1.2), glucose (10). After cutting using this solution, slices were left to incubate for at least 1 hour in a storage chamber at room temperature using this solution, before being transferred to the recording chamber.

The high sucrose cutting solution contains (mM): Sucrose (194), NaCl (30), KCl (4.5), $MgCl_2$ (1), $NaHCO_3$ (26), NaH_2PO_4 (1.2), glucose (10). After cutting, the slices were left to incubate for 15 minutes in a storage chamber warmed by a water bath at 32°C containing electrophysiological aCSF containing (mM): NaCL (130), KCl (2.5), $NaHCO_3$ (26), $CaCL_2$ (2.5), $MgCl_2$ (2), NaH_2PO_4 (10). They were then removed from the water bath and left at room temperature for a further 45 minutes before being transferred to the recording chamber.

2.2.5. FSCV recording

Individual slices were hemisected, and then transferred to the recording chamber, perfused with artificial cerebrospinal fluid (aCSF) saturated with 95% O_2 : 5% CO_2. aCSF was either the electrophysiological recipe outlined above, or the previous bicarbonate-buffer based FSCV recipe containing (mM): NaCl (125), NaHCO3 (26), KCl (3.8), CaCl2 (2.4), MgSO4 (1.3), KH2PO4 (1.2), glucose (10). The slices were superfused with aCSF at a rate of c. 2 ml/min, between 31-33°C. Slices were placed in the bath and equilibrated for 30-45 minutes before recording. During this time, the recording electrode was left to charge and placed in striatal tissue with the voltammeter turned on, applying the voltage sweep at the carbon fibre electrode continuously. This is performed to equilibrate the electrode surface to recording conditions in advance of the experiment, to minimise baseline drift over the course of the experiment caused by the interaction of the electrode with electroactive substances present in the local extracellular environment.

To perform FSCV recording, the CFM was lowered 150 μm into striatal tissue at a chosen recording site – either the dorsolateral CPu (dlCPu) or the Nucleus Accumbens core (NAc). CFMs with a full signal gain between 3-10 mV/nA were used for recordings, and the full current was observed to evaluate the quality of the seal and subsequent signal to noise ratio. The full signal gain was set to a working range of 5 mV, and the sensitivity of the electrode was monitored over the course of experiments to prevent saturation of signal as electrodes become more sensitive during recording. Stimulation of a recording site was performed using electrical or optical stimulation (**section 2.2.6**), which was delivered every 2.5 minutes until stable release was observed (release variability of 10% across successive stimulations). If this could not be achieved, another recording site was chosen.

Extracellular DA concentration $[DA]_o$ was measured using FSCV (**Section 2.2.2**) with a CFM and a Millar voltammeter (Julian Millar, Barts and the London School of Medicine and Dentistry) producing a triangular waveform of voltage between +1.3V and -0.7V, vs Ag/AgCl reference electrode. This waveform was scanned across the CFM at a rate of 800 V/s, with a frequency of 8 Hz. Faradaic currents were identified as DA based on an oxidation potential at + 600 mV, a reduction potential at – 200 mV, and a recording location in striatum. At the end of each day, the CFM was calibrated in 2 μM DA in aCSF, prepared from a stock 2.5 mM or 5 mM DA solution in 0.1 M $HClO_4$ stored at 4°C in the dark, and used within 1 month of preparation. For experiments using different drugs, calibration was performed both in aCSF and at the working concentration of the drug used to ensure no interaction with the CFM that may alter electrode sensitivity.

Data were recorded and analysed using Axoscope 10.7 (Molecular Devices) and locally-written scripts in Visual Basic for Applications (Microsoft Excel). Transients depicting raw $[DA]_o$ are calculated from the conversion of the DA oxidation currents converted to the concentration of DA using the electrode calibration factor, plotted against time. The number of animals included for each dataset is $n \geq 3$, unless otherwise indicated for pilot data. Statistical analysis was performed using Prism (GraphPad), with the threshold for statistical significance set at $p < 0.05$. Statistical testing was performed as indicated for each experiment.

2.2.6. Electrical and light stimulation

In an acute *ex vivo* coronal striatal slice preparation, the cell body of the DA neuron is removed, leaving only the DA axon. Without the tonic activity of the DA neuron cell body, the axonal arbour needs external stimulation for DA release. Either electrical or optical stimulation of DA release was performed during this project (**Fig. 2.2)**.

Electrical stimulation was delivered using a bipolar concentric Pt/Ir electrode with 125 µm tip diameter (FHC, Inc.), with the tip positioned on the surface of the brain slice c. 100 µm away from the recording electrode. This delivered a 0.6 mA, 200 µs wide stimulation pulse, that was out-of-phase with the FCV scans to prevent signal interference. This current intensity was chosen to evoke near maximal (perimaximal) DA release while maintaining stable DA release from the site over time (Cragg 2003). One caveat of this stimulation method is that it is non-selective, causing co-incident depolarisation of

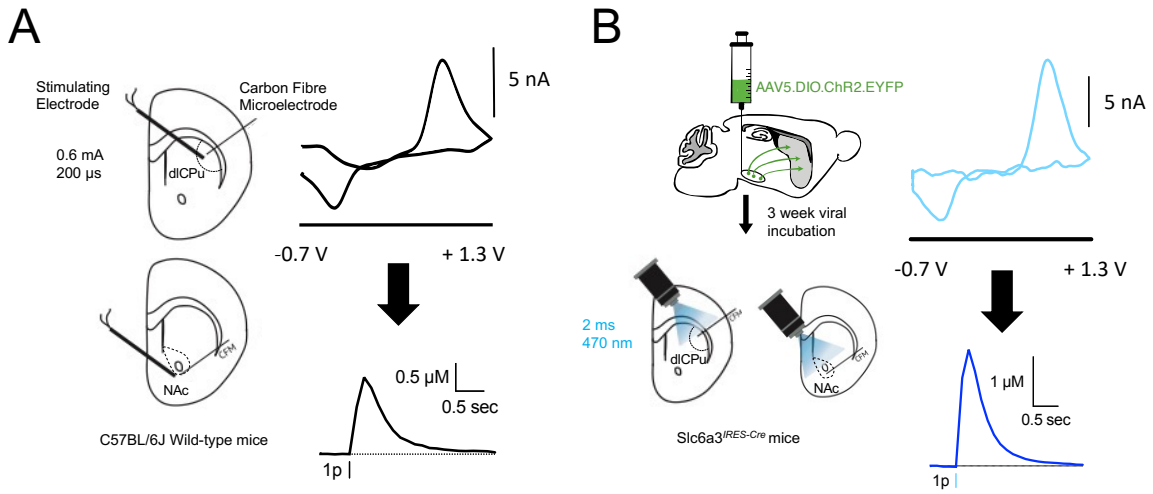

Figure 2.2. – Schematic representation of experimental configuration for FSCV experiments and cyclic voltammograms of $[DA]_o$ evoked by electrical and optical stimulation.

(A) *Left:* Schematic representation of acute *ex vivo* striatal coronal slice preparation, with dlCPu and NAc recording regions identified. *Right*: Representative cyclic voltammogram showing electrically evoked $[DA]_o$, and transient showing evoked $[DA]_o$ following a single electrical pulse.

(B) *Left*: Schematic showing injection and expression of viral-mediated ChR2-eYFP in midbrain and dlCPu of Slc6A3$^{IRES\text{-}Cre}$ mouse. *Right*: Representative cyclic voltammogram showing optically evoked $[DA]_o$, and transient showing evoked $[DA]_o$ following a single optical pulse.

all cell types within the local region. Since activation of these cell-types may mediate an indirect effect on DA release, I used an optogenetic approach to selectively activate DA axons only.

To investigate mechanisms regulating DA release without the coincident activation of neighbouring cell-types, I used optogenetic stimulation of DA axons in Slc6A3$^{IRES\text{-}Cre}$ mice (**Fig. 2.2**). These had undergone midbrain injection of AAV5-DIO-eYFP-ChR2 (rAAV5.hEF1α-DIO.hChR2(H134).EYFP.WPRE.PA, University of North Carolina Vector Core Facility, 8x10^{12} gc/ml), resulting in targeted expression of ChR2 and eYFP label in striatal DA axons. These were stimulated using a 470 nm wavelength LED (OptoLED, Cairn Research), delivering blue light pulses (2 ms wide) at c.5 mW intensity. Light intensity required to deliver perimaximal DA release was determined at the start of each experiment, due to variability of ChR2 expression across the slice. Expression was visualised using an upright microscope (Olympus BX50W1) with a x10 water-immersion lens to identify possible recording sites, but also minimising ChR2 activation before recording. DA release was evoked every 2.5 min by either electrical or optical stimulation. This period of recovery was sufficient for stable DA release to be achieved between stimulations.

2.3. Fluorescence Imaging

A new modality of sampling neurotransmitter release is the imaging of genetically encoded fluorescent sensors. These are based on a GPCR for the neurotransmitter of interest, linked to a cyclic permuted fluorescent protein (**Fig. 2.3**). Upon binding of a neurotransmitter to the binding site on the GCPR, this causes a conformational change in the protein structure, facilitating fluorescence. These sensors have been used both *ex vivo* and *in vivo*, and have high temporal and spatial resolution – similar to FSCV. They are particularly useful for measuring neurotransmitters that cannot be measured using FSCV because they are not electroactive, such as ACh (Jing, Zhang et al. 2018). In this project, I primarily used GRAB (GPCR-activation based) sensors for ACh to investigate how pharmacological manipulations may impact ACh release (**Chapter 4**). I also conducted pilot experiments using a GRAB

sensor to measure DA, both as a comparison versus FSCV but also attempting to measure changes to the tonic (non-evoked) levels of DA in the slice, which is not possible using FSCV (**Chapter 3**).

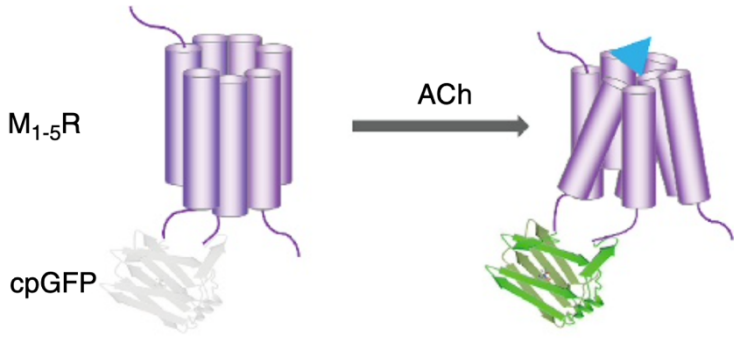

Figure 2.3. – Diagram depicting $GRAB_{ACh}$ sensor structure and conformational change upon ACh binding (From Jing et al., 2018; Figure 1a). The GRAB sensors are based on GPCRs for different neurotransmitters and neuropeptides attached to a circular permutated green fluorescent protein (cpGFP) via a linker region. Upon ligand binding, the sensor undergoes a conformational change, allowing cpGFP fluorescence. For example, $GRAB_{ACh}$ sensors are based on muscarinic ACh receptors (mAChRs). Upon ACh binding, there is an increase in $GRAB_{ACh}$ mediated fluorescence, indicating a change in the extracellular concentration of ACh.

2.3.1. GRAB sensor imaging

ACh was measured using $GRAB_{ACh3.0}$ (Jing, Li et al. 2020) and DA was measured using $GRAB_{DA2m}$ (Sun, Zhou et al. 2020). $GRAB_{ACh3.0}$ is based upon the human M3-mAChR with a circularly permutated green fluorescent protein (cpGFP) attached via a short linker region (Jing, Zhang et al. 2018). $GRAB_{DA2m}$ is based upon human D2 receptors linked to a cpGFP. Studies performed *in vitro* show these sensors have insignificant downstream coupling, preventing activation of the sensor mediating downstream effects (Sun, Zeng et al. 2018). However, these sensors do effectively act as a buffer, reducing available ACh or DA that has been released (Zheng and Li 2023). These sensors are a powerful and novel tool, but do require additional characterisation to understand any indirect effects on local circuits in which they are used, and interpretation of the fluorescence data generated to measure both evoked and tonic neurotransmitter release.

The GRAB sensors used in this project were packaged in AAV5 vectors, under control of the human Synapsin 1 (hSyn) gene for ubiquitous, long-term expression in neurons at the site of injection (**Fig. 2.4.**) (Kugler, Kilic et al. 2003). The viral constructs used were AAV5-hsyn-$GRAB_{ACh3.0}$ (BrainVTA) and AAV5-hSyn-$GRAB_{DA2m}$ (WZ Biosciences). These were injected into either the dlCPu

or NAc of mice during intracranial surgery (**Section 2.1.3**) and given 3-5 weeks for sufficient viral expression, before being culled for slice preparation as performed for FSCV (**Section 2.2.4**).

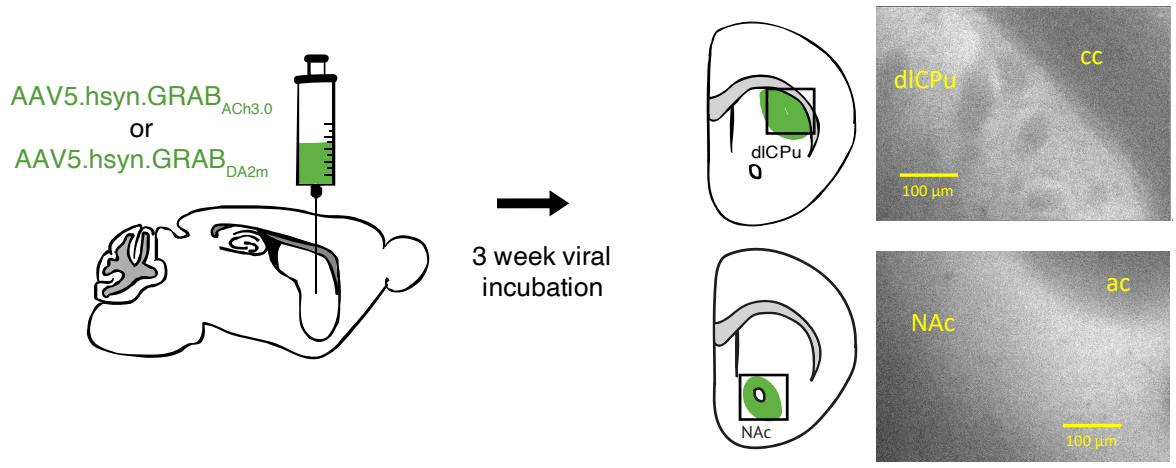

Figure 2.4. Schematic representation of GRAB sensor expression in mouse striatum
Either GRAB$_{ACh3.0}$ or GRAB$_{DA2m}$ were packaged within an AAV construct, and injected bilaterally into either the dlCPu or NAc within the mouse striatum. The virus is expressed across non-specific cell types, under control of the human synapsin 1 gene (hsyn) promoter. After at least 3 weeks of incubation, the mice are culled and slices prepared as described previously. Representative images show clear GRAB$_{ACh3.0}$ expression in dlCPu and NAc.

2.3.2. Image Acquisition

All solutions, temperature and recording chamber solution flow rate were the same as used for FSCV recordings. Upon being placed in the recording chamber, GRAB expression was visualised using a aCMOS camera (IRIS9, Teledyne Photometrics) with a 10x objective. The field of view and recording electrode were placed in the region with greatest expression.

Image acquisition protocol was performed using an ImageJ software package (MicroManager). Evoked release events were recorded at a sampling rate of 100 Hz (100 fps), with a light exposure time of 10 ms. A longer exposure time enhances the signal amplitude but would reduce the temporal resolution, and these parameters were selected as the optimal combination of both factors. Tonic neurotransmitter levels were recorded with an image taken every 5-30 seconds, again with an exposure time of 10 ms. Both sensors use a cpGFP as the fluorophore, and were visualised using a blue light LED (470 nm) at a power of 5 mW for fluorophore excitation. This light power was sufficient for

large signal amplitude, but reduced bleaching of the fluorophore over the course of the experiment, resulting in a stable signal over time.

2.3.3. Data Processing

Extraction of fluorescence data was undertaken using ImageJ (**Fig. 2.5A**). For evoked neurotransmitter release, a 100 µm x 100 µm region of interest (ROI) was positioned with its centre 100 µm away from the centre of the stimulating electrode to maintain consistency with FSCV experiments. Another ROI was also positioned on the stimulating electrode, to sample a region of the

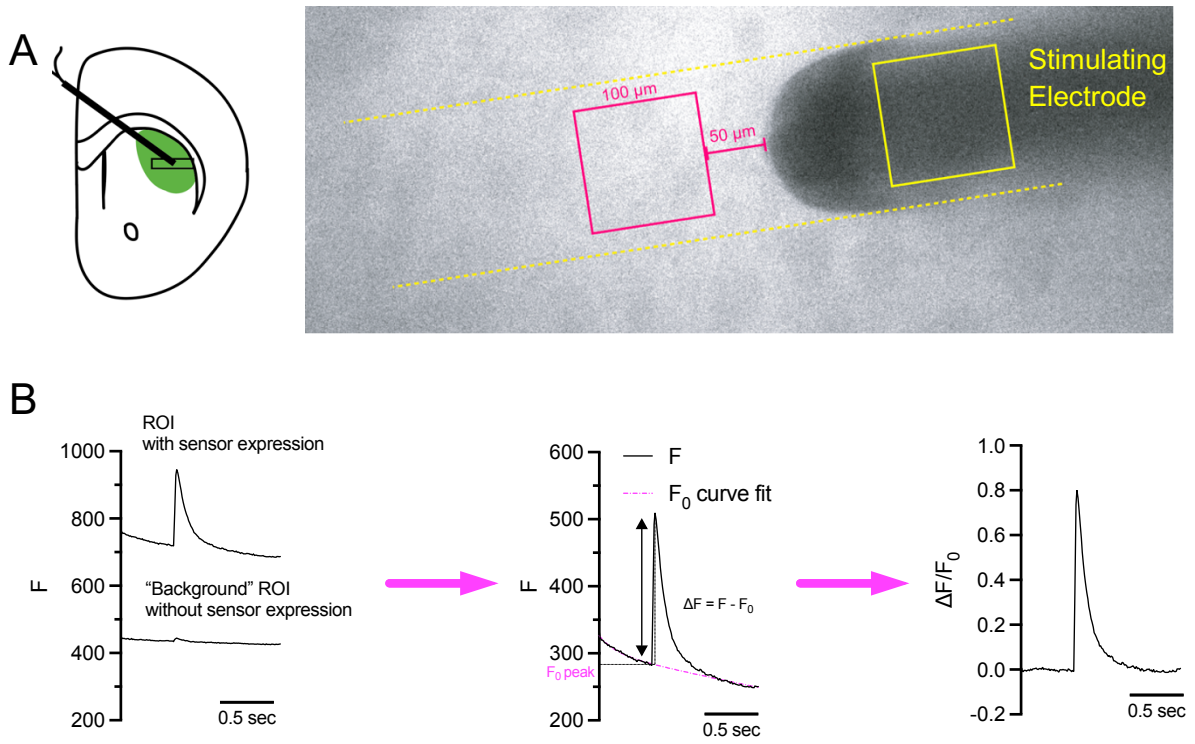

Figure 2.5. Data extraction and analysis of evoked GRAB fluorescence imaging

(A) *Left:* Diagram depicting recording configuration for evoked stimulus GRAB fluorescence imaging in dlCPu. *Right*: Representative image of evoked $GRAB_{ACh}$ imaging in dlCPu. Fluorescence data was extracted from a square 100 µm x 100 µm region of interest (ROI). The edge of the ROI is positioned 50 µm away from the stimulating electrode, so that the centre of the ROI is 100 µm away from the stimulating electrode, similar to the distance between the stimulating electrode and recording electrode for FSCV (~ 100 µm) to allow for comparison between techniques.

(B) Analysis workflow of evoked stimulus GRAB fluorescence imaging. *Left*: The raw fluorescence traces obtained from the magenta ROI positioned in a region of sensor expression (*upper*) and from the yellow ROI positioned on the stimulating electrode without sensor expression (*lower*). *Centre*: An exponential decay fit is performed on fluorescence values (F) of the background subtracted fluorescence trace before and after stimulation, to predict the value of baseline fluorescence at the time of stimulation (F_0). ΔF is the change in fluorescence from baseline ($\Delta F = F - F_0$). *Right*: ΔF is divided by F_0 at each timepoint, to provide $\Delta F/F_0$ trace.

image without sensor expression to allow subtraction of background fluorescence (**Fig. 2.5B, *left and centre***). The fluorescence value and corresponding frame number was extracted for each ROI using a custom developed ImageJ macro. Subsequent analysis was undertaken using a custom developed MATLAB script (MATLAB R2020_b, MathWorks). Background subtraction of the stimulated ROI from the background ROI was undertaken as described previously (Condon, Platt et al. 2019). In brief, a two-term exponential decay function ($f(x) = a^{bx} + c^{dx}$) was used to model the expected decay in fluorescence over time, to also provide an estimate of baseline fluorescence without stimulation (F_0) (**Fig. 2.5B**). Where raw signal peak amplitude is defined as F, normalised fluorescence responses were calculated as:

$$\frac{\Delta F}{F_0} = \frac{F - F_0}{F_0}$$

The value of F_0 itself was also of interest as a measure of non-evoked fluorescence intensity, that may indicate changes of tonic neurotransmitter levels occurring with time or pharmacological manipulation. Analysis of experiments investigating non-evoked (tonic) levels of neurotransmitter also used ImageJ to extract fluorescence values from a square (100 µm x 100 µm) ROI over an area of high GRAB expression, and corresponding frame numbers (**Fig. 2.6**). The percentage change in fluorescence over time was calculated as F/F_0, where F_0 is defined as the mean ROI fluorescence before drug application. We hypothesised that baseline fluorescence could be used as an indicator of tonic (non-evoked) neurotransmitter levels, which is investigated in **Chapter 4**.

The number of animals included for each dataset is $n \geq 3$, unless otherwise indicated for pilot data. Statistical analysis was performed using Prism (GraphPad), with the threshold for statistical significance set at $p < 0.05$. Statistical testing was performed as indicated for each experiment.

2.4. Approach for Statistical testing

Over the course of this project, the data points binned for analysis are indicated in the wash-on data for each experiment by highlight with a grey box. Unless otherwise indicated, these are three

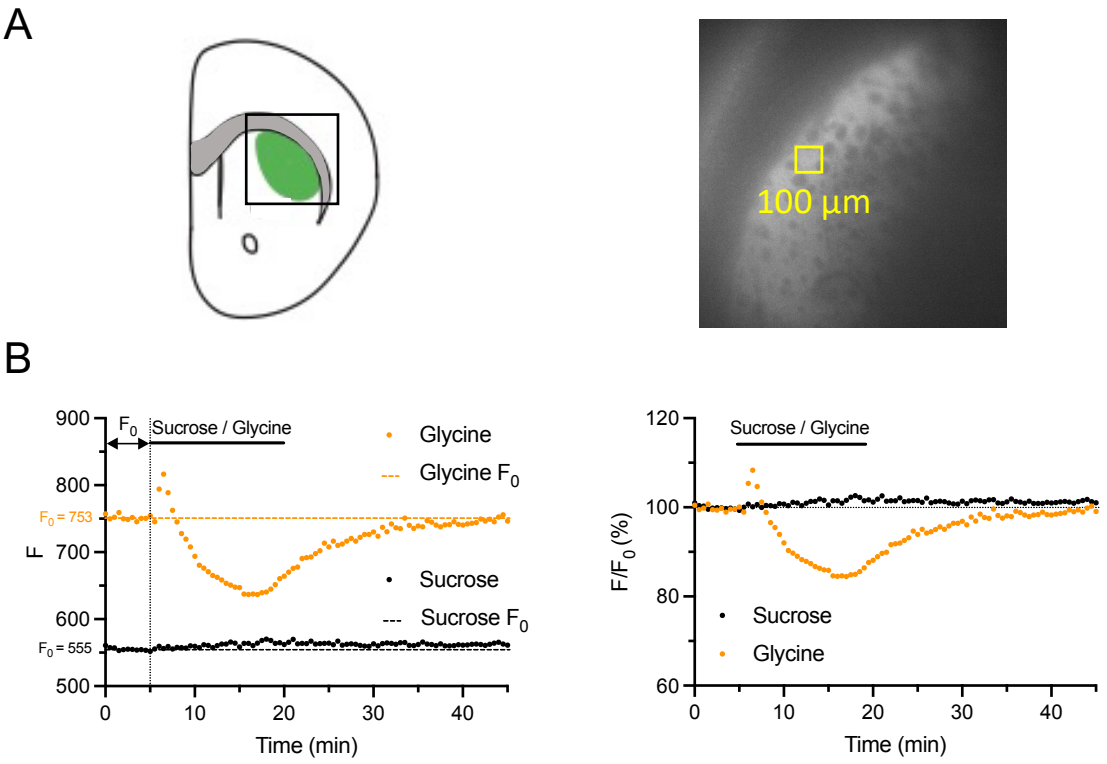

Figure 2.6. Data extraction and analysis of non-evoked (tonic) GRAB fluorescence imaging

(A) *Left:* Diagram depicting recording configuration for non-evoked stimulus GRAB fluorescence imaging in dlCPu. *Right*: Representative image of evoked $GRAB_{ACh}$ imaging in dlCPu. An image was acquired every 5 sec or 30 sec as indicated in each experiment. Fluorescence data was extracted from a square 100 µm x 100 µm ROI to maintain consistency with evoked recording ROIs. ROI location was selected based on high level of sensor expression within the target area.

(B) Analysis workflow of non-evoked stimulus GRAB fluorescence imaging. *Left*: Representative raw fluorescence levels during 10 mM sucrose or 10 mM glycine (in the presence of ambenonium) application. Each value of F is the mean fluorescence of the ROI at that timepoint. F_0 is defined as the mean fluorescence for the 5 minute period before drug application. *Right*: The values of F are divided by F_0 to give a percentage change in fluorescence from the pre-drug baseline over the course of the experiment. The variation in the starting values of F between the sucrose and glycine wash-on experiments is due to different brain slices with different levels of $GRAB_{ACh}$ expression.

values of evoked DA release in a given condition that are averaged per site due to regression of the mean, to give a single value for comparative analysis for each replicate in an experiment, giving us greater confidence in each condition. This is not valid in some experiments where there is a significant effect of time such that the effect of drug is not stable, and in these cases only a single "snapshot" value of evoked DA release at a given timepoint is used.

Unless otherwise indicated, the units of analysis used for the FSCV and GRAB-imaging data in this thesis are the number of brain slices recorded, the units of analysis for the electrophysiology is the number of cells recorded, and the units of analysis for the RNAscope data is the number of animals used. For the FSCV, GRAB-imaging, and electrophysiology data, the number of animals also recorded from for each experiment is also reported, where "n = 5 slices/animals" would indicate an experiment was completed in 5 brain slices from 5 different animals. Where possible, each experiment has been performed in one slice from each animal, but some experiments use multiple slices from an individual animal. The number of slices were treated as independent units of analysis. This is because we observe no difference in variation in results obtained between experiments conducted in different slices from the same animal, or between different animals. Therefore, performing the same experiment in multiple slices from the same animal was not considered to be pseudoreplication, and as part of the 3Rs (Replacement, Reduction, Refinement) would also reduce the number of animals needed for use in this project.

Appropriate statistical testing was performed for each experiment, as indicated. Throughout this project, parametric testing was used. The rationale used by our lab is that the population of DA release events are normally distributed, and therefore it is appropriate to use parametric tests when testing comparisons between samples drawn from this normally distributed population. Parametric tests are also more sensitive and therefore better suited to small sample sizes in alignment with the 3Rs. However, an alternative approach would be to perform normality testing on each dataset and ensure that other criteria of those normality tests (such as sample size) are met before using parametric tests, otherwise reverting to non-parametric statistical tests. Alternatively, if there was unequal variance between conditions, the data could be log-transformed and still use a parametric test for comparative analysis.

2.5. Summary

FSCV and GRAB imaging are the main sampling methods that I use in **Chapter 3** and **Chapter 4**, for the detection of DA and ACh respectively. The detection of DA by FSCV is well

characterised, but the detection of ACh and other neurotransmitters using the newly developed GRAB sensors will allow me to better investigate indirect mechanisms that regulate striatal DA release. The GRAB sensors also allow detection of non-evoked changes in neurotransmitter level occurring over longer timecourses than is readily detectable with FSCV, and will be complementary to investigating changes in evoked DA and ACh release. This is particularly useful given the increasing understanding we have for neurotransmitters regulating striatal DA release via tonic inhibition (Roberts, Doig et al. 2020, Roberts, Lambert et al. 2022). Other chapter-specific methods will be described within each chapter.

Chapter 3: Classical and Excitatory Glycine Receptors Inhibit Striatal Dopamine Release

3.1. Introduction

3.1.1. Local regulation of DA release at the axon

DA neurons in the midbrain project to the striatum, where DA is released from a widely branched axonal arbour. While neurotransmitter release is usually predominantly determined by somatodendritic activity, DA release within the striatum is powerfully regulated by local neurotransmitters and neuromodulators that act on the DA axon (Sulzer, Cragg et al. 2016). These can powerfully modulate the release of DA independent of changes of somatodendritic activity, either acting directly on receptors expressed on the DA axon, or indirectly via local circuits. ACh is a powerful regulator of DA release that acts on nAChRs that are expressed on DA axons, which modulate DA releases and can even drive DA release, independent of DA neuron somatodendritic activity (Rice and Cragg 2004, Threlfell and Cragg 2011, Threlfell, Lalic et al. 2012). GABA also mediates a tonic inhibition of DA release via $GABA_A$Rs expressed on DA axons, as a result of ambient striatal GABA that is regulated by GABA transporters (GATs) expressed on astrocytes (Lopes, Roberts et al. 2019, Kramer, Twedell et al. 2020, Roberts, Doig et al. 2020). Other neurotransmitters and neuropeptides mediate indirect regulation of DA release, for example glutamate, nitric oxide and insulin acting via ChIs (Hartung, Threlfell et al. 2011, Stouffer, Woods et al. 2015, Kosillo, Zhang et al. 2016). The striatum is rich in neurotransmitters and neuropeptides that have not yet been investigated for their contribution to regulation of DA release at the axonal level.

3.1.2. Evidence for glycinergic signalling in striatum and midbrain

There is a large body of evidence supporting a role for glycine and glycine receptors in the striatum. Functional cGlyRs have been identified in cell types across the striatum including MSNs, ChIs, and GABAergic interneurons (Sergeeva and Haas 2001, Martin and Siggins 2002, Forstera, Munoz et al. 2017, McCracken, Lowes et al. 2017, Molchanova, Comhair et al. 2017, Munoz, Yevenes et al. 2018). Many of these studies show the tonic activity of striatal cGlyRs, and an enhancement of

cGlyR currents in the presence of GlyT1 inhibition, indicating the presence and function of GlyT1 that regulates an ambient glycine tone in striatum (McCracken, Lowes et al. 2017, Molchanova, Comhair et al. 2017). There is debate within the field as to whether glycine is the endogenous ligand at striatal cGlyRs given a lack of evidence for glycinergic neurotransmission within the striatum (Zeilhofer, Studler et al. 2005). It is hypothesised that taurine may act as the endogenous ligand, given that it is enriched within the striatum and acts as a partial agonist at cGlyRs (Palkovits, Elekes et al. 1986, Sergeeva and Haas 2001, Sergeeva, Chepkova et al. 2003). There is also functional evidence for the expression of cGlyRs in the somatodendritic compartment of DA neurons in the midbrain, which raises the possibility of the expression of cGlyRs on DA axons and glycine acting directly on DA axons to regulate DA release (Mercuri, Calabresi et al. 1990, Häusser, Yung et al. 1992).

We also have a new understanding of functional excitatory glycine receptors (eGlyRs), composed of GluN1 and GluN3A NMDA-R subunits that only contain glycine binding sites and hence are gated by glycine and not glutamate (Grand, Abi Gerges et al. 2018). These have been recently identified in neurons within the basolateral amygdala and cortical interneurons, but have not previously been investigated within striatum (Bossi, Dhanasobhon et al. 2022). Experiments performing ISH of *Grin3A* (encoding the GluN3A subunit) show expression within the striatum, with a punctate and sparse distribution indicative of expression within interneurons, including ChIs (Allen Institute for Brain Science, 2011, Experiment: 73909499).

3.1.3. Previous investigations of glycinergic regulation of DA release

Previous studies have investigated the effects of glycine on striatal DA release using *ex vivo* and *in vivo* models. *in vivo* studies have observed mixed responses, with some studies observing an elevation of striatal dopamine levels upon intrastriatal glycine application or glycine transporter inhibition, with others observing a decrease, no effect, or variability within populations of responders and non-responders (Yadid, Pacak et al. 1993, Molander and Soderpalm 2005, Nagy, Marko et al. 2010). *ex vivo* studies also report variable results upon manipulation of striatal glycine levels, with some studies reporting an elevation of striatal dopamine concentration (Giorguieff-Chesselet, Kemel et al. 1979) and

others reporting a decrease or no change (Javitt, Sershen et al. 2000, Hernandes, de Magalhaes et al. 2007, Yorgason, Wadsworth et al. 2022). Until recently, the effect of glycine and glycinergic regulation of DA release had not been investigated using FSCV. However, this study did not account for possible indirect mechanisms that might regulate evoked DA release, or the contribution of eGlyRs. The role and mechanisms of glycinergic regulation of DA release remain unclear.

The aim of this chapter is to understand how cGlyRs and eGlyRs regulate DA release at the level of the axon, the effects of glycine and taurine, and any indirect mechanisms by which this takes place. I will revisit the question of glycinergic regulation of DA release with techniques using better temporal resolution, and a better understanding of the contribution of other neuromodulators and neurotransmitters to indirectly modulate DA release.

3.2. Methods

3.2.1. Animals and Slice Preparation

For experiments recording electrically-evoked DA release with FSCV, 7-25 week-old, mixed-sex, wild-type C57BL/6J mice (Charles River) were used. For experiments recording optically-evoked DA release with FSCV, 12-15 week-old heterozygous Slc6A3$^{IRES\text{-}Cre}$ mice selectively expressing ChR2-eYFP in DA axons were used after intracranial injection of AAV5-hsyn-DIO-ChR2-eYFP (University of North Carolina Vector Core Facility, 8x10^{12} gc/ml), in SNc (ML ± 1.2 mm, AP -3.1 mm, DV -4.25 mm) 3-4 weeks prior, as described in **Section 2.2.3**. For experiments recording optically-evoked DA release with GRAB$_{DA2m}$ (WZ Biosciences, 0.8 x10^{13} gc/ml, YL002009-AV5), 12 week-old male wild-type C57BL/6J mice (Charles River) were used after intracranial injection with AAV5.hSyn.GRAB$_{DA2m}$. Acute coronal *ex vivo* striatal slices were prepared as described in **Section 2.1.1**. All experimental procedures were carried out in accordance with University of Oxford guidelines and the UK Animals (Scientific Procedures) Act 1986.

3.2.2. Fast-scan Cyclic Voltammetry

DA release was recorded using FSCV, as described in **Section 2.2.4**, at a single recording site per slice in either dlCPu or NAc where indicated. Data are expressed as either the absolute extracellular concentration of dopamine ($[DA]_o$) or normalised to mean peak $[DA]_o$ during the three stimulations before drug application within the individual experiment. DA release was evoked every 2.5 min using either electrical or optical stimulation as described in **Section 2.2.5**. For experiments using electrical stimulation, single pulse stimulation was delivered every 2.5 min at a given site until stable DA release with maximum 10% variability across successive stimulations was achieved, before a drug wash-on was performed. For optical stimulation, the light power was titrated upwards until stable, peri-maximal DA release was obtained. During experiments using electrical stimulation, either single pulse or a burst stimulation protocol of 4 pulses at 100 Hz frequency was performed to test the pulse-number dependence of DA release. During experiments using optical stimulation, only single-pulse stimulation was used.

Data was acquired using Axoscope 10.7 (Molecular Devices) and analysed using locally-written macros on Microsoft Excel. As described in **Section 2.3.1**, faradaic currents recorded from the oxidation of DA were converted to $[DA]_o$ using the specific electrode calibration factor for that recording, and then plotted against time to obtain $[DA]_o$ transients. For each experiment, $n \geq 3$ animals unless where indicated. The data points binned for analysis are indicated in the wash-on data for each experiment by highlight with a grey box. Unless otherwise indicated, these are three values of evoked DA release in a given condition that are binned to give a single value for comparative analysis for each replicate in an experiment. Statistical analysis was performed using GraphPad Prism, using unpaired t-tests, paired t-tests, two-way RM ANOVA, one-way RM ANOVA, and *post hoc* Sidak's multiple comparisons tests where indicated.

3.2.2. $GRAB_{DA}$ Imaging

This chapter includes pilot experiments using $GRAB_{DA2m}$ to record evoked DA release and non-evoked extracellular DA levels (**Fig. 3.10**). These experiments were performed as described in **Section 2.3.3** after injection of AAV5-hSyn-$GRAB_{DA2m}$ into dlCPu (ML ± 2.2 mm, AP + 0.70 mm, DV -2.7mm - -2.5mm). Images were captured at a frequency of 100 Hz, with an image exposure time of 10 ms and pixels binned 2x2 to reduce image file size. Light for excitation of the cpGFP moiety (470 nm) was used at a power of ~5 mW and turned on continuously for 4 sec over the course of recording each stimulation every 2.5 min. For experiments recording non-evoked DA levels, excitation light (470 nm) was used at a power of ~5 mW and turned on for a duration of 1 sec every 30 sec or 10 sec where indicated, obtaining an image with exposure time of 10 ms. Pixels were binned 2x2 to minimise image size. Data were extracted and analysed as described in **Section 2.3.4**. Due to the small number of observations, no statistical analysis was performed on these data.

3.3.3. Drugs

Most drugs were dissolved in either diH_2O, dimethyl sulfoxide (DMSO) or sodium hydroxide (NaOH) to 1000x aliquots and stored frozen at -20°C. On the day of experiments, these were diluted in oxygenated aCSF to their working concentration immediately before use. 10 mM glycine was made up on the morning of each experiment due to a maximum solubility of 100 mM. The final concentrations used and source of each drug are shown in **Table 3.1**.

Table 3.1. Drugs used in Chapter 3

Drug	Supplier	Action	Concentration	Solvent	References
Glycine	Sigma-Aldrich & SLS Labs	GlyR agonist	1-10 mM	diH_2O	(McCracken, Lowes et al. 2017)
Strychnine	Abcam	cGlyR antagonist	10 µM	diH_2O	(Häusser, Yung et al. 1992)
Sarcosine	Sigma-Aldrich	GlyT1 inhibitor	500 µM	diH_2O	(McCracken, Lowes et al. 2017)
Taurine	Alfa Aesar	cGlyR partial agonist	10 mM	diH_2O	(Sergeeva and Haas 2001)
CGP-78608 hydrochloride	Tocris Bioscience	GluN1 antagonist	2 µM	2.2 eq. NaOH	(Bossi, Dhanasobhon et al. 2022)
5,7-Dichlorokynurenic acid sodium salt (DCKA)	Tocris Bioscience	GluN3A antagonist	500 µM	2 eq. NaOH	(Bossi, Dhanasobhon et al. 2022)
Caffeine	Sigma	Ado-R antagonist	20 µM	diH_2O	(Roberts, Lambert et al. 2022)
Oxotremorine-M	Tocris Bioscience	mAChR agonist	1 µM	diH_2O	(Threlfell, Clements et al. 2010)
Amphetamine	Sigma	DAT reversal	5 µM	diH_2O	(Hedges, Obray et al. 2018)
DHβE	Tocris Bioscience	β2-nAChR antagonist	1 µM	diH_2O	(Threlfell, Lalic et al. 2012)
AP-5	Abcam	NMDAR antagonist	10 µM	diH_2O	(Roberts, Doig et al. 2020)
Bicuculline	Abcam	$GABA_AR$ antagonist	10 µM	DMSO	(Roberts, Doig et al. 2020)
CGP-55845 hydrochloride	Abcam	$GABA_BR$ antagonist	4 µM	DMSO	(Roberts, Doig et al. 2020)
L-741,626	Abcam	D2-R Antagonist	1 µM	DMSO	(Condon, Platt et al. 2019)

3.3 Results

3.3.1. Strychnine inhibits dopamine release

The two glycine receptors I am investigating in the project are the classical glycine receptors (cGlyRs) composed of cGlyR-specific subunits, and excitatory glycine receptors (eGlyRs) composed of NMDA receptor subunits. To investigate whether cGlyRs regulate DA release in striatum, I applied the cGlyR-specific antagonist strychnine and measured $[DA]_o$ using fast-scan cyclic voltammetry. A concentration of 10 µM strychnine was chosen based on previous experiments in the literature, aiming to observe a maximal effect without off-target effects. I found that strychnine decreased $[DA]_o$ detected following electrical stimulation by 40% in dlCPu and NAc (**Fig. 3.1A-C**, paired t-test, dlCPu: $p = 0.0020$, $n = 9$ slices/animals; NAc: $p = 0.038$ $n = 5$ slices/animals). There was no difference in the effect of strychnine between these regions (**Fig. 3.1D**, unpaired t-test, $p = 0.9595$). These results suggest that cGlyRs in both dlCPu and NAc can modulate DA release. Furthermore, the ability of the antagonist alone to mediate a response without exogenous application of an agonist suggests that these cGlyRs are tonically active, either via an endogenous ligand being present or some constitutive activity.

To test whether the action of strychnine required concurrent stimulation of striatal circuits that might input to DA axons, I investigated the effect of strychnine on optically-evoked DA release, in DAT-Cre ($Slc6a3^{IRES\text{-}Cre}$) mice after viral expression of channelrhodopsin 2 (ChR2) targeted to DA neurons and axons (**Fig. 3.1E-F**). Light activation of striatum allows selective stimulation of DA axons, without non-specific activation of all other striatal cells and inputs. Strychnine also reduced optically-evoked DA release (**Fig.3.1G**, paired-t-test, $p = 0.0127$, $n = 5$ slices/animals). These data suggest that cGlyR tone is not produced by non-specific activation of a cellular population driven by electrical stimulation but is present under tonic conditions, indicating the presence of an ambient cGlyR tone in striatum. This result supports existing evidence for ambient levels of glycine present in the striatum (Harsing and Matyus 2013).

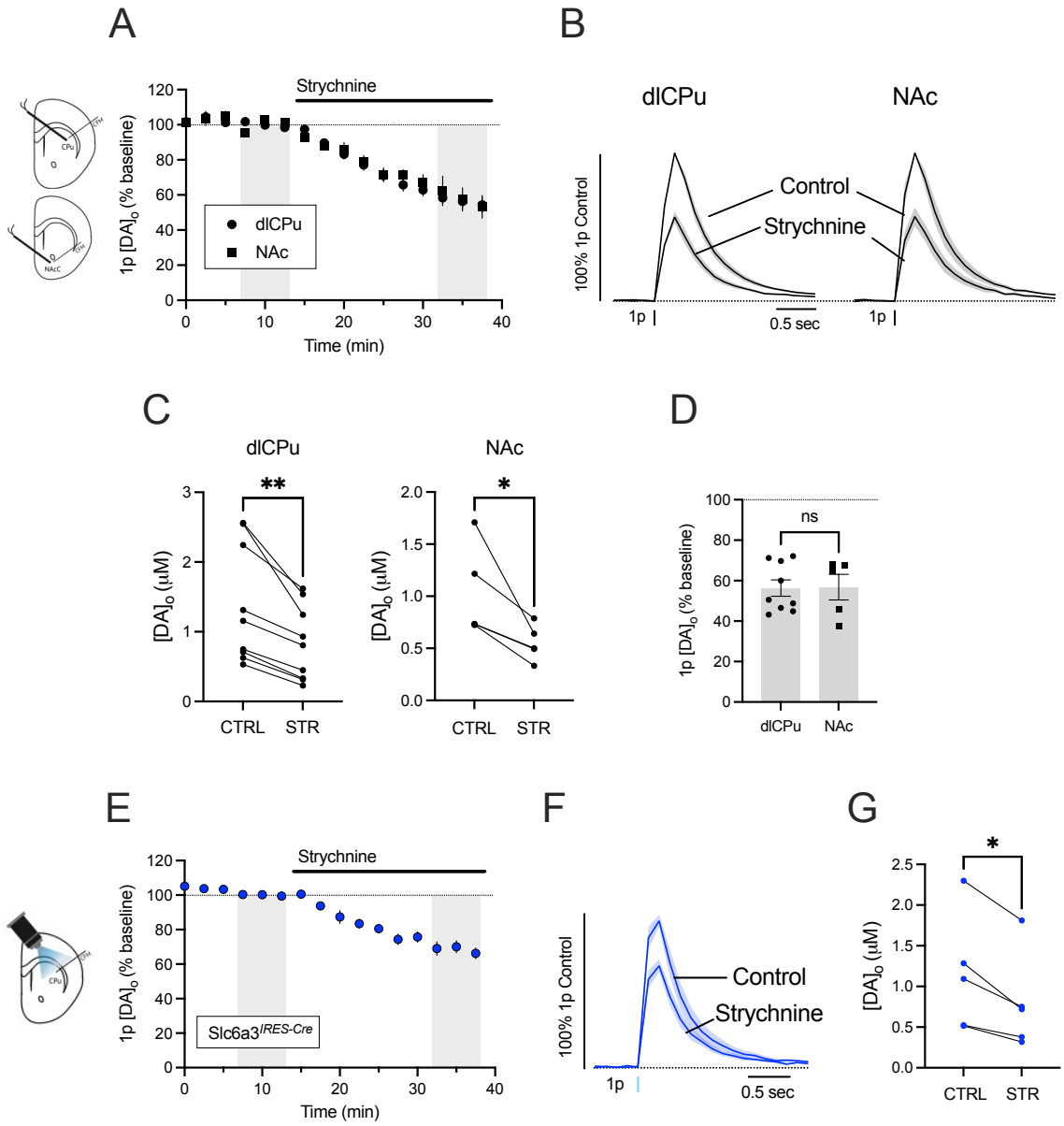

Figure 3.1: cGlyR antagonist strychnine reduces evoked DA release in dlCPu and NAc

(A) Mean peak $[DA]_o$ (±SEM) versus time, evoked by 1 electrical pulse in dlCPu or NAc, before and after application of strychnine. dlCPu: n = 9 slices/animals. NAc: n = 5 slices/animals.

(B) Mean $[DA]_o$ (±SEM) transients versus time in dlCPu or NAc, before and after application of strychnine. dlCPu: n = 9 slices/animals. NAc: n = 5 slices/animals.

(C) Mean peak $[DA]_o$ (±SEM) following application of strychnine in dlCPu and NAc. Paired t-test for each region. dlCPu: p = 0.0020 (**); n = 9 slices/animals. NAc: p = 0.0377 (*); n = 5 slices/animals.

(D) Mean peak $[DA]_o$ (±SEM) following application of strychnine in dlCPu and NAc, normalised to pre-drug control. Unpaired t-test. p = 0.9505

(E) Mean peak $[DA]_o$ (±SEM) versus time, evoked by 1 optical pulse in dlCPu, before and after application of strychnine. n = 5 slices/animals

(F) Mean $[DA]_o$ (±SEM) transients versus time in dlCPu, before and after application of strychnine. n = 5 slices/animals

(G) Mean peak $[DA]_o$ (±SEM) following application of strychnine in dlCPu. Paired t-test. p = 0.0127 (*), n = 5 slices/animals

3.3.2. Strychnine mediated inhibition is independent of nAChRs

Beyond acting as a high affinity, competitive antagonist at cGlyRs, strychnine has several off-target pharmacological effects including as an antagonist at some nAChRs, particularly α7 homomeric but also β2-containing nAChRs (Matsubayashi, Alkodon et al. 1998, Garcia-Colunga and Miledi 1999). We could not find a role for α7 nAChRs in the modulation of DA release in striatum (Exley, Clements et al. 2008), but by contrast, β2-containing nAChRs are known to powerfully regulate DA release, including initial probability of release and activity-dependence of release (Rice and Cragg 2004). I therefore investigated whether the effect of strychnine was altered in the presence of 1 μM DHβE, a β2-containing nAChR antagonist (**Fig. 3.2A-B**). I found nonetheless that strychnine reduced DA release in the presence of DHβE (**Fig. 3.2C**, paired t-test, $p = 0.0022$, n = 5 slices/animals), and that there was no difference between the effect of strychnine in the presence or absence of DHβE (**Fig. 3.2D**, unpaired t-test, $p = 0.4215$. Control: n = 9 slices/animals, DHβE: n = 5 slices/animals). These data show that the effects of strychnine are not mediated via β2-containing nAChRs.

Published immunohistochemical and electrophysiological data show that striatal cholinergic interneurons express cGlyRs (Darstein, Landwehrmeyer et al. 2000, Sergeeva and Haas 2001). Together, these findings suggest that although there is a tonic cGlyR tone that controls DA release, any cGlyR tone on ChIs is not required for the regulation of DA release by cGlyRs. The effect of strychnine on ACh release is investigated separately in **Chapter 4**.

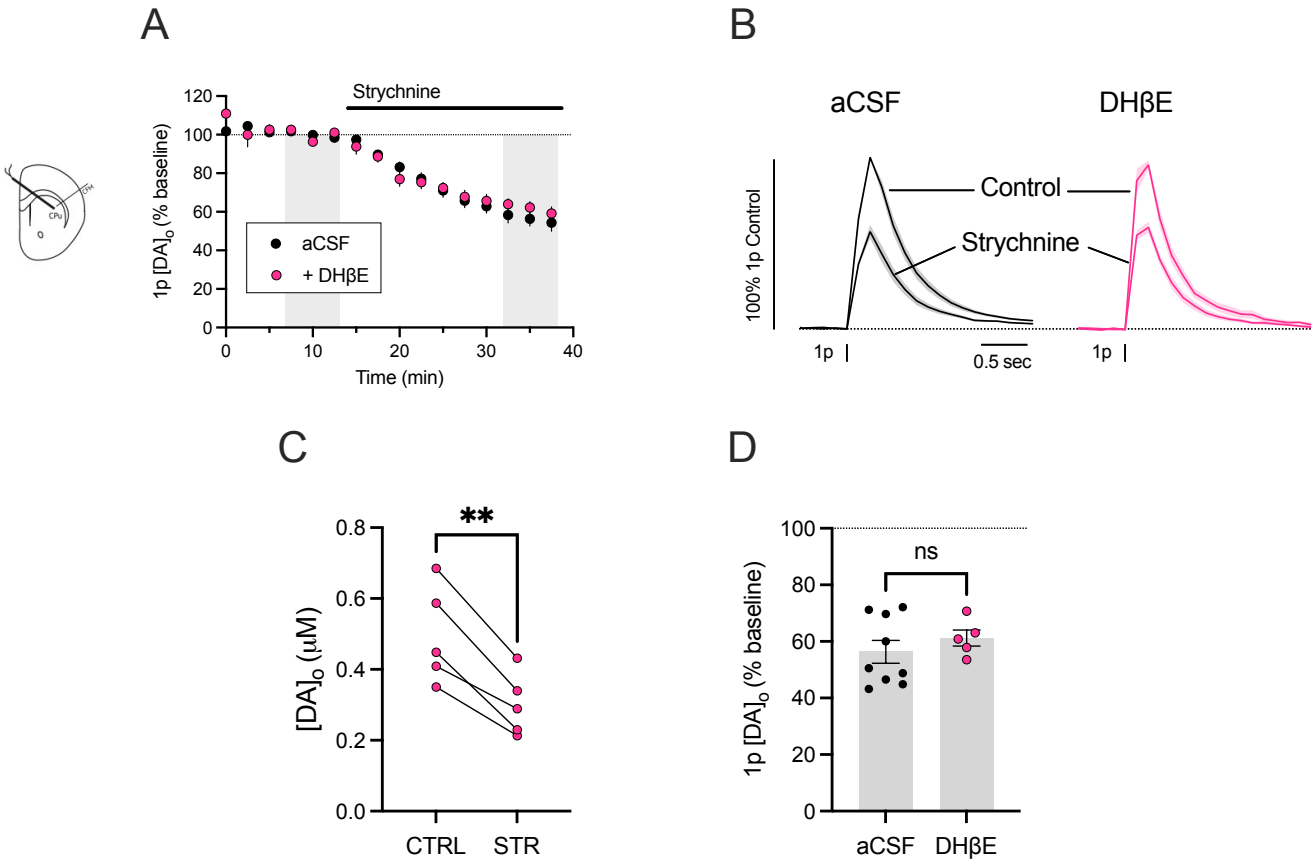

Figure 3.2. The effect of strychnine is independent of nAChRs

(A) Mean peak $[DA]_o$ (±SEM) versus time, evoked by 1 electrical pulse in the presence or absence of DHβE, before and after application of strychnine. Data for aCSF condition is same as Fig 3.1. aCSF: n = 9 slices/animals, DHβE: n = 5 slices/animals.

(B) Mean $[DA]_o$ (±SEM) transients versus time, normalised to pre-drug control, in the presence or absence of DHβE, before and after application of strychnine. Data for aCSF condition is same as Fig 3.1. aCSF: n = 9 slices/animals, DHβE: n = 5 slices/animals.

(C) Mean peak $[DA]_o$ (±SEM) following application of strychnine in the presence or absence of DHβE. Paired t-test: DHβE: p = 0.0022 (**). Data for aCSF condition is same as Fig 3.1. aCSF: n = 9 slices/animals, DHβE: n = 5 slices/animals.

(D) Mean peak $[DA]_o$ (±SEM) following application of strychnine in dlCPu and NAc, normalised to pre-drug control. Data for aCSF condition is same as Fig 3.1. aCSF: n = 9 slices/animals, DHβE: n = 5 slices/animals. Unpaired t-test. p = 0.4215 (n.s.)

3.3.3. Striatal glycine tone is enhanced by inhibition of Glycine Transporter 1

Given the apparent presence of an ambient cGlyR tone that controls DA release, I next aimed to alter the glycine tone to test for an impact on DA release. There is previous evidence for functional GlyT1 in striatum, and for inhibition of GlyT1 leading to an increase the extracellular glycine tone (McCracken, Lowes et al. 2017, Molchanova, Comhair et al. 2017). To achieve this, I used 500 µM sarcosine, used previously as a GlyT1 inhibitor (McCracken, Lowes et al. 2017). The hypothesis was that inhibition of GlyT1 by sarcosine would elevate extracellular glycine concentration, and in turn enhance activation of cGlyRs, which may in turn alter DA release. Since cGlyR antagonist strychnine reduces DA release, we might expect the sarcosine to increase DA release. However, application of sarcosine alone did not alter electrically evoked DA release, in dlCPu or NAc (**Fig. 3.3A-D**, paired t-test, dlCPu: $p = 0.1294$, $n = 5$ slices/animals; NAc: $p = 0.0707$, $n = 5$ slices/animals). Nonetheless, sarcosine did enhance the effect of cGlyR antagonist strychnine on evoked $[DA]_o$, leading to a greater inhibition of DA release (**Fig. 3.3E-G**, paired t-test, $p = 0.0046$, $n = 5$ slices/animals) (**Fig. 3.3H,** **u**npaired t-test, effect of strychnine in control versus sarcosine, $p = 0.0099$, control: $n = 9$ slices/animals, sarcosine: $n = 5$ slices/animals). These data suggest that the GlyT1 is acting modestly to limit an ambient glycine tone that alone does not have a detectable added or net effect on the levels of DA release evoked, but can nonetheless act to limit how cGlyRs are regulating DA release. Note that the inability for sarcosine to increase evoked $[DA]_o$ might be limited by the use of the perimaximal stimulus, or by the ability of cGlyRs to desensitize (Legendre 1998, Mangin, Baloul et al. 2003).

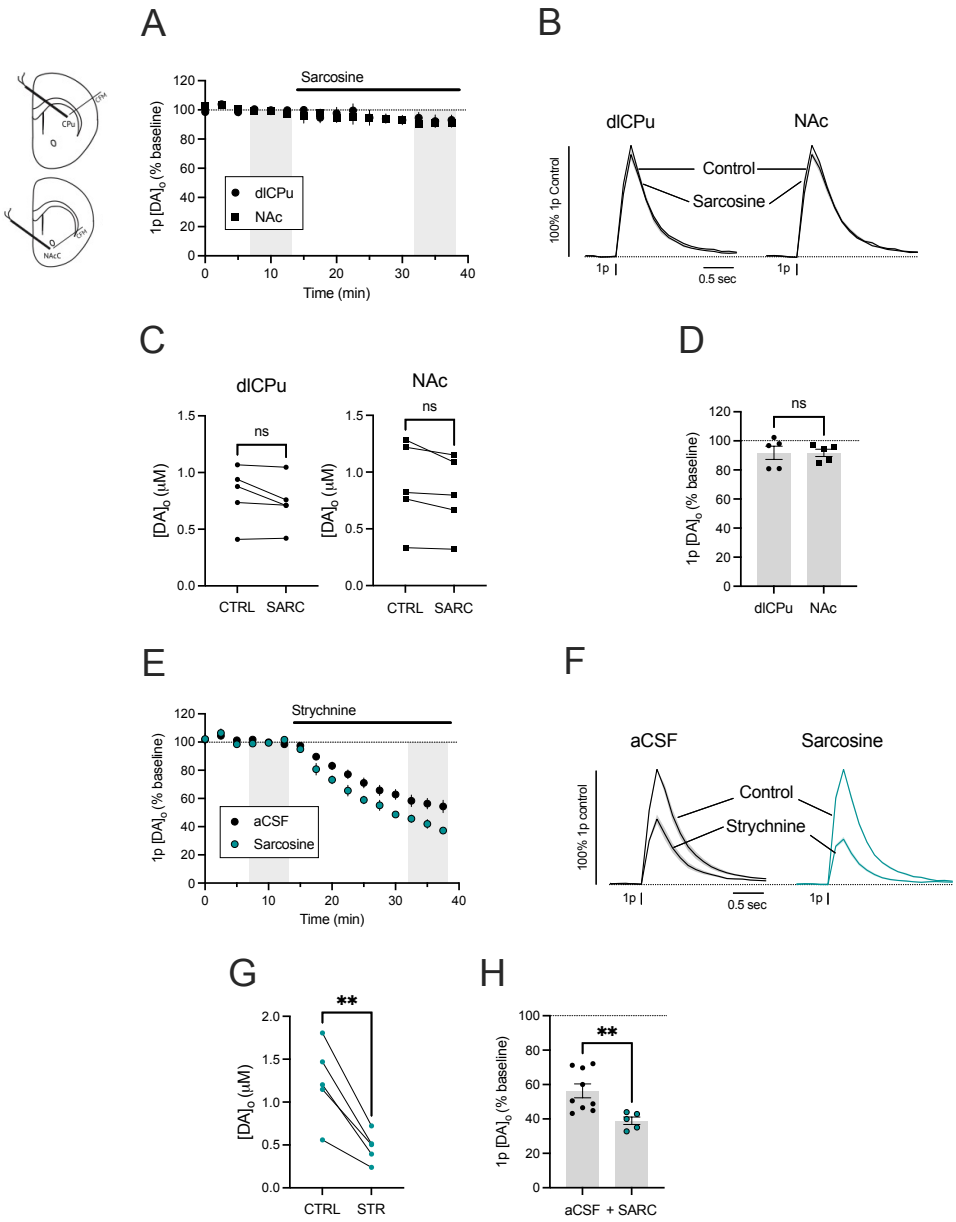

Figure 3.3. Striatal GlyR tone is enhanced by GlyT1 inhibition

(A) Mean peak $[DA]_o$ (±SEM) versus time, evoked by 1 electrical pulse in dlCPu or NAc, before and after application of sarcosine. dlCPu: n = 5 slices/animals. NAc: n = 5 slices/animals.

(B) Mean $[DA]_o$ (±SEM) transients versus time in dlCPu or NAc, normalised to pre-drug control, before and after application of strychnine. Mean peak $[DA]_o$ (±SEM) following application of strychnine in dlCPu and NAc. dlCPu: n = 5 slices/animals. NAc: n = 5 slices/animals.

(C) Mean $[DA]_o$ (±SEM), in dlCPu and NAc, before and after application of strychnine. Paired-t test for each region. dlCPu: p = 0.1294 (n.s.); n = 5 slices/animals. NAc: p = 0.0707 (n.s.); n = 5 slices/animals.

(D) Mean peak $[DA]_o$ (±SEM) following application of strychnine in dlCPu and NAc, normalised to pre-drug control. Unpaired t-test. p = 0.9991 (n.s.). dlCPu: n = 5 slices/animals. NAc: n = 5 slices/animals.

(E) Mean peak $[DA]_o$ (±SEM) versus time, evoked by 1 electrical pulse in dlCPu, in the presence or absence of sarcosine, before and after application of strychnine. Data for aCSF condition is from Fig.3.1. aCSF: n = 9 slices/animals. Sarcosine: n = 5 slices/animals.

(F) Mean $[DA]_o$ (±SEM) transients versus time in dlCPu or NAc, before and after application of strychnine. aCSF: n = 9 slices/animals. Sarcosine: n = 5 slices/animals.

(G) Mean peak $[DA]_o$ (±SEM) following application of strychnine, in the presence of sarcosine. Paired t-test: p = 0.0046 (**); n = 5 slices/animals.

(H) Mean peak $[DA]_o$ (±SEM) following application of strychnine in dlCPu and NAc, normalised to pre-drug control. Unpaired t-test. p = 0.0099 (**). aCSF: n = 9 slices/animals. Sarcosine: n = 5 slices/animals.

3.3.4. Glycine application results in prolonged decline of DA release

I next investigated the effect of glycine itself. I performed bath application of glycine, using concentrations used by others for previous studies in acute *ex vivo* slice preparation (Sergeeva and Haas 2001, Mangin, Baloul et al. 2003, McCracken, Lowes et al. 2017, Yorgason, Wadsworth et al. 2022). Application of 10 mM glycine reduced electrically-evoked DA release (**Fig. 3.4A-C**, paired-t-test, p = 0.0051, n = 5 slices/4 animals). There are two distinct phases of the glycine effect on DA release: an initial decrease in peak $[DA]_o$ which stabilises for roughly 10-15 minutes, followed by a prolonged decline that continues during glycine application. The initial reduction occurred rapidly after administration (**Fig. 3.4A**, one-sample t-test, e-stim 7.5 min after wash-on, p = 0.0011, n = 5 slices/4 animals), but then proceeded to continue until DA release was below detection threshold rather than stabilise. In experiments using optically-evoked DA release to eliminate potential artefacts of electrical stimulation, a similar pattern of rapid reduction in DA release followed by a prolonged decline was also observed (**Fig. 3.4A-C,** paired t-test, p = 0.0498, n = 3 slices/animals). This two-phase response was surprising. I primarily focused on the mechanisms behind the initial decline of DA release in my subsequent experiments, with assistance from a project student to investigate the prolonged decline (**Chapter 3, Section 3.3.15**).

The findings that strychnine, the cGlyR antagonist, and glycine, a GlyR agonist both decrease DA release might seem counterintuitive. However, cGlyRs are pentameric ligand-gated ionotropic channels that readily exhibit desensitisation on exposure to agonist (Mangin, Baloul et al. 2003). The similar outcome on DA release of cGlyR antagonism and agonism might readily be explained by desensitisation of cGlyRs by glycine.

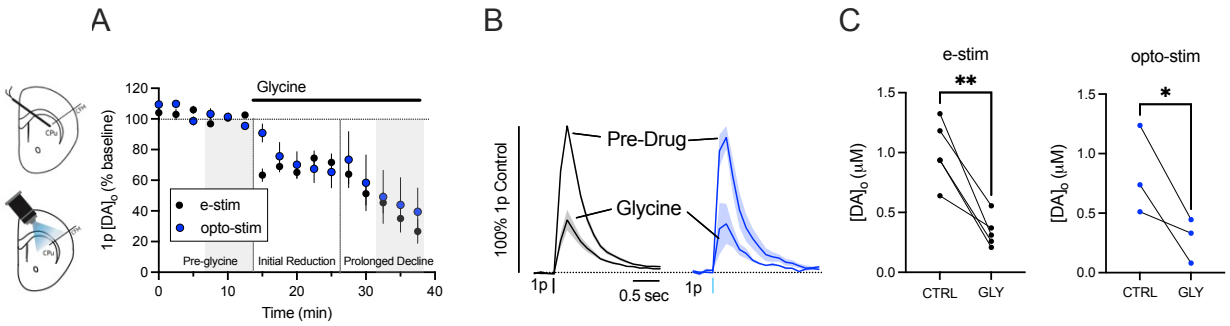

Figure 3.4. Glycine application results in a prolonged decline of DA release

(A) Mean peak $[DA]_o$ (±SEM) versus time, evoked by 1 electrical or optical pulse in dlCPu, before and after application of glycine. e-stim: n = 5 slices/4 animals. opto-stim: n = 3 slices/animals

(B) Mean $[DA]_o$ (±SEM) transients versus time, normalised to pre-drug control, before and after application of glycine. e-stim: n = 5 slices/4 animals. opto-stim: n = 3 slices/animals

(C) Mean peak $[DA]_o$ (±SEM) before and after application of glycine, evoked by electrical or optical stimulation. Paired t-test. e-stim: p = 0.0051 (**). opto-stim: p = 0.0498 (*). e-stim: n = 5 slices/4 animals. opto-stim: n = 3 slices/animals

3.3.5. Glycine reduces DA release in a concentration- and region-dependent manner

I investigated whether the effects of glycine on evoked $[DA]_o$ were concentration- or region-dependent. I washed on 1-10 mM glycine sequentially and then washed it off, in dlCPu and NAc (**Fig. 3.5A**). These experiments were long in duration (2 hours) and there was a large amount of decline in DA release over this period, as an effect of time. To correct for this, I completed experiments providing electrical stimulation over the same duration but without application of glycine, to show the effect of time on DA release. I then subtracted the normalised values of DA release, from the time control experiments, from the normalised values of DA release from the glycine application experiments to control for the effect of time. I observed a concentration-dependent effect in both regions (**Fig. 3.5B**), with increasing concentration of glycine causing a greater reduction of DA release (**Fig. 3.5C**, one-way ANOVA, dlCPu: $F_{(4,10)} = 74.10$, $p < 0.0001$; NAc: $F_{(4,10)} = 27.82$, $p < 0.0001$). Although these were the concentrations of glycine applied exogenously, the concentration of glycine in tissue during recording might not equate these levels. This is likely due to the limited speed of perfusion of glycine through the tissue, and putative activity of GlyT1 in striatal slices (McCracken, Lowes et al. 2017). The concentration of glycine required to see an effect is high (5 mM) but in agreement with a previous study

also investigating the concentration-response of DA release to glycine in an *ex vivo* striatal coronal slice preparation (Yorgason, Wadsworth et al. 2022).

In comparing effects between regions, glycine had a larger effect on DA release in dlCPu than NAc (**Fig. 3.5B**, non-linear fit and test if one curve fits both data sets, dlCPu: $R^2 = 0.96$, NAc: $R^2 = 0.92$, $F_{(2,20)} = 4.323$, $p = 0.0275$), indicating a region-dependent effect. By contrast, the effects of cGlyR antagonist strychnine on DA release did not vary with region (**Fig. 3.1D**). Although strychnine does not have a region-dependent effect, this might be due to glycine altering DA release via other mechanisms not mediated via cGlyRs, such as eGlyRs or the recently identified mGlyRs (Laboute, Zucca et al. 2023).

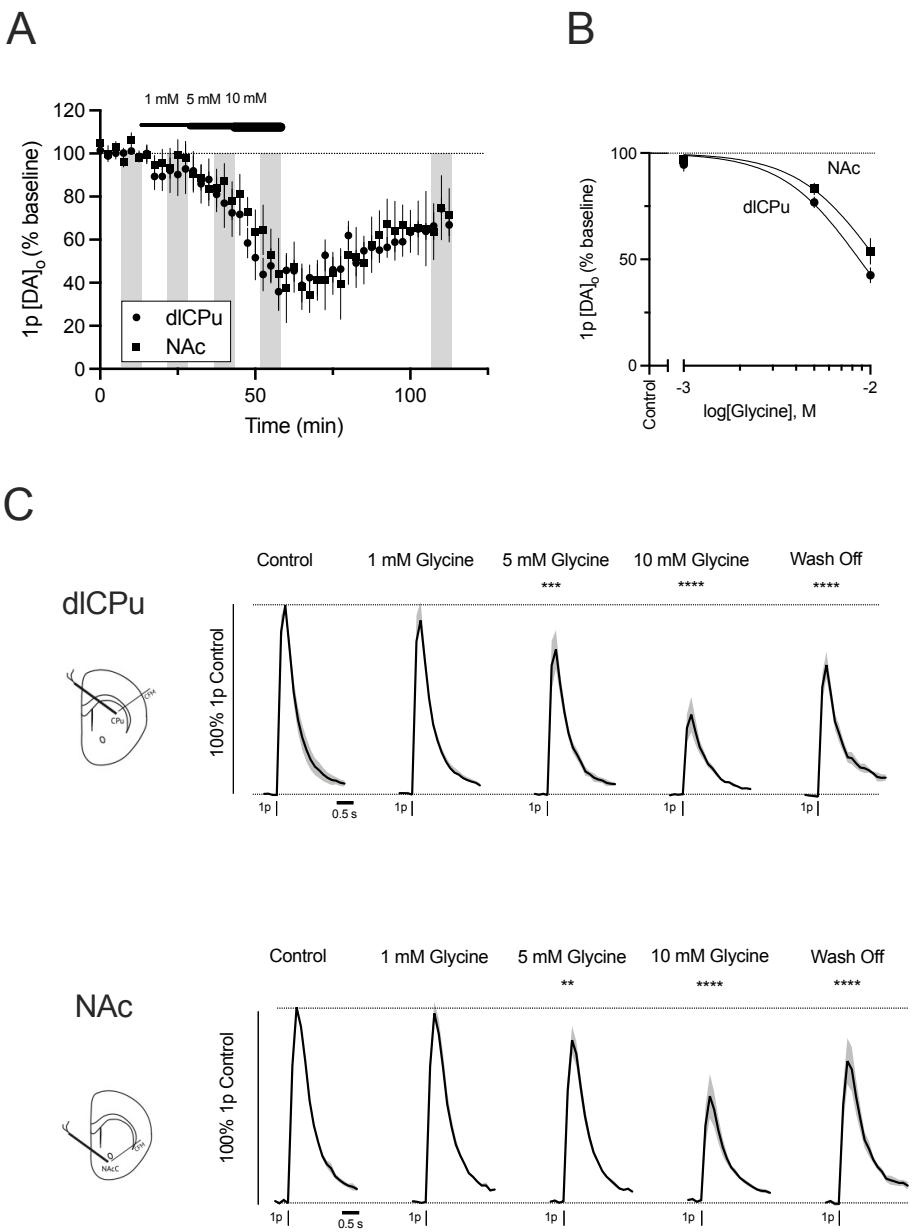

Figure 3.5. Glycine reduces DA release in a concentration- and region-dependent manner

(A) Mean peak $[DA]_o$ (±SEM) versus time evoked by 1 electrical pulse in dlCPu or NAc, before and following application of ascending concentrations of glycine. dlCPu: n = 3 animals/slices, NAc: n= 3 animals/slices.

(B) Concentration-response curve depicting mean peak $[DA]_o$ (±SEM) in dlCPu and NAc from. Data used are the final 3 data points from each condition. Non-linear fit and test if one curve fits both data sets: dlCPu: $R^2 = 0.96$, NAc: $R^2 = 0.92$, $F_{(2,20)} = 4.323$, $p = 0.0275$. dlCPu: n = 3 animals/slices, NAc: n= 3 animals/slices.

(C) Mean $[DA]_o$ (±SEM) transients versus time, normalised to pre-drug control, before and after application of glycine, in dlCPu and NAc. One-way ANOVA: dlCPu: $F_{(4,10)} = 74.01$, $p < 0.0001$. NAc: $F_{(4,10)} = 27.82$, $p < 0.0001$. *Post-hoc* Tukey's multiple comparisons test: ** $p < 0.01$, *** $p < 0.001$, **** $p < 0.0001$. Data used are the final 3 data points from each condition. dlCPu: n = 3 animals/slices, NAc: n= 3 animals/slices.

To correct for an effect of time, the mean ± SEM of time-control experiments (performed in the absence of glycine) was subtracted from the mean ± SEM of the wash off experiments in each region. All data are normalised to pre-drug condition within each region.

3.3.6. Brief glycine application reduces DA release in dlCPu but not NAc

Continuous glycine application caused a prolonged decline of DA release that did not stabilise (**Fig. 3.4**). This experimental protocol would be difficult to use in further experiments aiming to investigate the mechanism of action. I therefore used a brief application protocol for 7.5 minutes, to focus on the initial decline caused by glycine in both dlCPu and NAc. In dlCPu, I found that a brief application of glycine reduced electrically evoked $[DA]_o$ (**Fig. 3.6A-C,** paired t-test, $p = 0.0066$, $n = 5$ slices/animals). Pilot experiments with optically evoked DA release also showed a decrease upon glycine application (**Fig. 3.6C**, paired t-test, $p = 0.031$, $n = 3$ slices/animals). However, in NAc, brief application of glycine did not reduce DA release in NAc using either electrical or optical stimulation (**Fig. 3.6D-F**, paired t-test, e-stim: $p = 0.9439$, $n = 3$ slices/animals; opto-stim: $p = 0.4637$, $n = 5$ slices/animals). This reflects the region-dependence shown using the longer application of glycine (**Fig. 3.5**), but also showed that it would be possible to record the effects of glycine using a shorter protocol to dissect the mechanism mediating the reduction of DA release over this initial period.

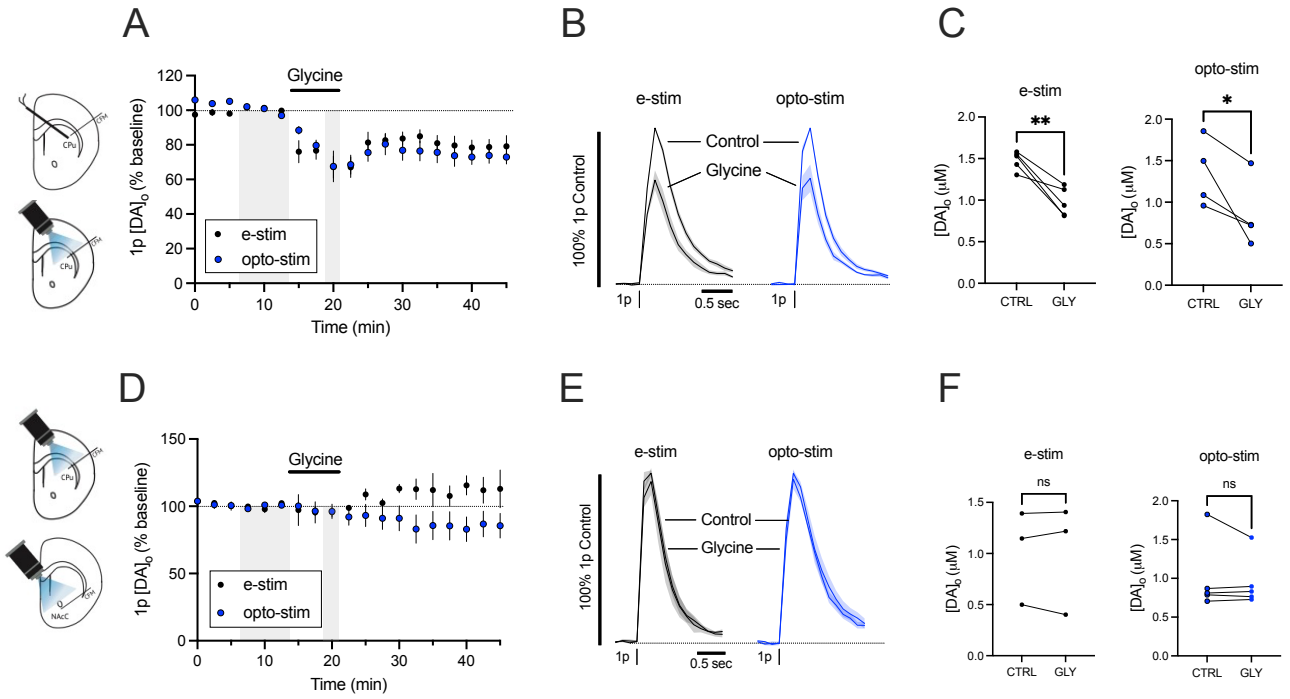

Figure 3.6. Brief application of glycine reduces DA release in dlCPu but not NAc

(A) Mean peak $[DA]_o$ (±SEM) versus time, evoked by 1 electrical or optical pulse in dlCPu, before and after application of glycine. e-stim: n = 5 slices/5 animals. opto-stim: n = 4 slices/animals.

(B) Mean $[DA]_o$ (±SEM) transients versus time, normalised to pre-drug control, before and during application of glycine, evoked by 1p electrical (e-stim) or optical (opto-stim) pulse. e-stim: n = 5 slices/5 animals. opto-stim: n = 4 slices/animals.

(C) Mean peak $[DA]_o$ (±SEM) before and after application of glycine, evoked by electrical or optical stimulation. Paired t-test. e-stim: p = 0.0066 (**). opto-stim: p = 0.0310 (*). e-stim: n = 5 slices/5 animals. opto-stim: n = 4 slices/animals.

(D) Mean peak $[DA]_o$ (±SEM) versus time, evoked by 1 electrical or optical pulse in NAc, before and after application of glycine. e-stim: n = 3 slices/animals. opto-stim: n = 5 slices/animals.

(E) Mean $[DA]_o$ (±SEM) transients versus time, normalised to pre-drug control, before and during application of glycine, evoked by 1p electrical or optical pulse. e-stim: n = 3 slices/animals. opto-stim: n = 5 slices/animals

(F) Mean peak $[DA]_o$ (±SEM) before and after application of glycine, evoked by electrical or optical stimulation. Paired t-test. e-stim: p = 0.9439 (n.s.). opto-stim: p = 0.4637(n.s.). e-stim: n = 3 slices/animals. opto-stim: n = 5 slices/animals

3.3.7. GlyT1 activity contributes to the high concentration of glycine required to observe an effect

5-10 mM glycine was required to see an effect on DA release (**Fig. 3.5**). I hypothesised that this high concentration could be partly due to activity of GlyT1, that might act to limit the concentration of glycine in the extracellular space. I tested this hypothesis by using the GlyT1 inhibitor sarcosine, to see if this would increase the effect of glycine. I found that the effect of 1 mM glycine on evoked $[DA]_o$ was significantly greater in the presence of sarcosine (**Fig. 3.7A-C**, two-way ANOVA, glycine x sarcosine interaction, $F_{(1,12)} = 9.274$, $p = 0.0102$). The ~30% decrease of DA release by 1 mM glycine in the presence of sarcosine is greater than the ~10 % decrease seen without sarcosine, and is similar to the ~35% decrease of DA release by 10 mM glycine alone over the same time course (**Fig. 3.4A**). These data indicate that GlyT1 are operating within the striatum to limit extracellular glycine and are a factor in explaining the high concentration of exogenous glycine required to modulate DA release.

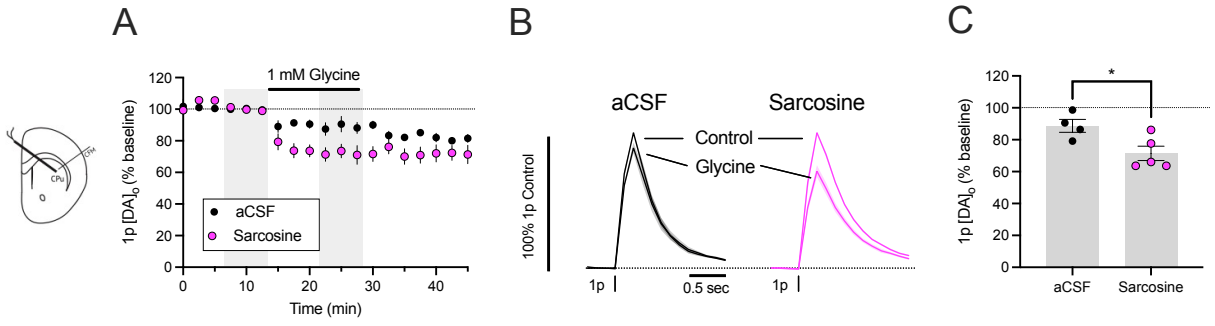

Figure 3.7. Effect of exogenously applied glycine is enhanced in sarcosine

(A) Mean peak $[DA]_o$ (± SEM) versus time evoked by 1 electrical pulse in dlCPu showing application of 1mM glycine, in the presence and absence of 500 µM sarcosine. aCSF: n = 4 slices/animals; Sarcosine: n = 5 slices/animals.

(B) Mean $[DA]_o$ (± SEM) versus time evoked by 1p electrical pulse in dlCPu, before and after application of 1mM glycine in the presence or absence of 500 µM sarcosine. aCSF: n = 4 slices/animals; Sarcosine: n = 5 slices/animals.

(C) Mean peak $[DA]_o$ (± SEM) following application of 1mM glycine in the presence and absence of 500 µM sarcosine. Unpaired t-test, $p = 0.0278$ (*). aCSF: n = 4 slices/animals; Sarcosine: n = 5 slices/animals.

3.3.8. The effects of glycine on DA release are subtly altered in DHβE

There is evidence that cGlyRs are also expressed on striatal ChIs, raising the possibility that glycine might modulate the activity of ChIs and in turn alter striatal ACh levels. ACh is a powerful regulator of DA release via nAChRs expressed on DA axons. I investigated whether the effects of glycine on DA release are indirectly mediated via a change in ACh levels that acts on nAChRs.

I performed a brief (7.5 min) wash-on of 10 mM glycine followed by a wash-off, in the presence of nAChR antagonism (DHβE 1 μM). Under control conditions (the absence of DHβE), brief application of glycine mediates a rapid decrease in peak evoked $[DA]_o$ that plateaus, similar to the initial effect seen during prolonged application of glycine (Fig. 3.5A), and then partially reverses. In the presence of DHβE, the initial decrease in evoked $[DA]_o$ mediated by glycine also occurred (**Fig. 3.8A-C**). However, during the wash-off period in the presence of DHβE, evoked $[DA]_o$ did not recover but remained at a low plateau. These data suggest that glycine is acting to regulate DA release through multiple component mechanisms, that can involve in part the regulation of ACh acting at nAChRs. They also suggest that an action of glycine on ACh acting at nAChRs helps to support the rebound in DA release as glycine concentration decays.

I investigated whether glycine altered the pulse-number dependence of DA release, as an indicator of the activation state of nAChRs on DA axons. I found that glycine subtly but significantly increased the ratio of DA released by 4p 100 Hz versus 1p stimulation (**Fig. 3.8D-E**), suggesting a change in nAChR activation consistent with either a reduction in ACh, or conversely an increase that might promote nAChR desensitisation (Rice and Cragg 2004). To explore the effects of glycine on striatal ACh levels, I used the $GRAB_{ACh}$ sensor to measure ACh directly (**Chapter 4**).

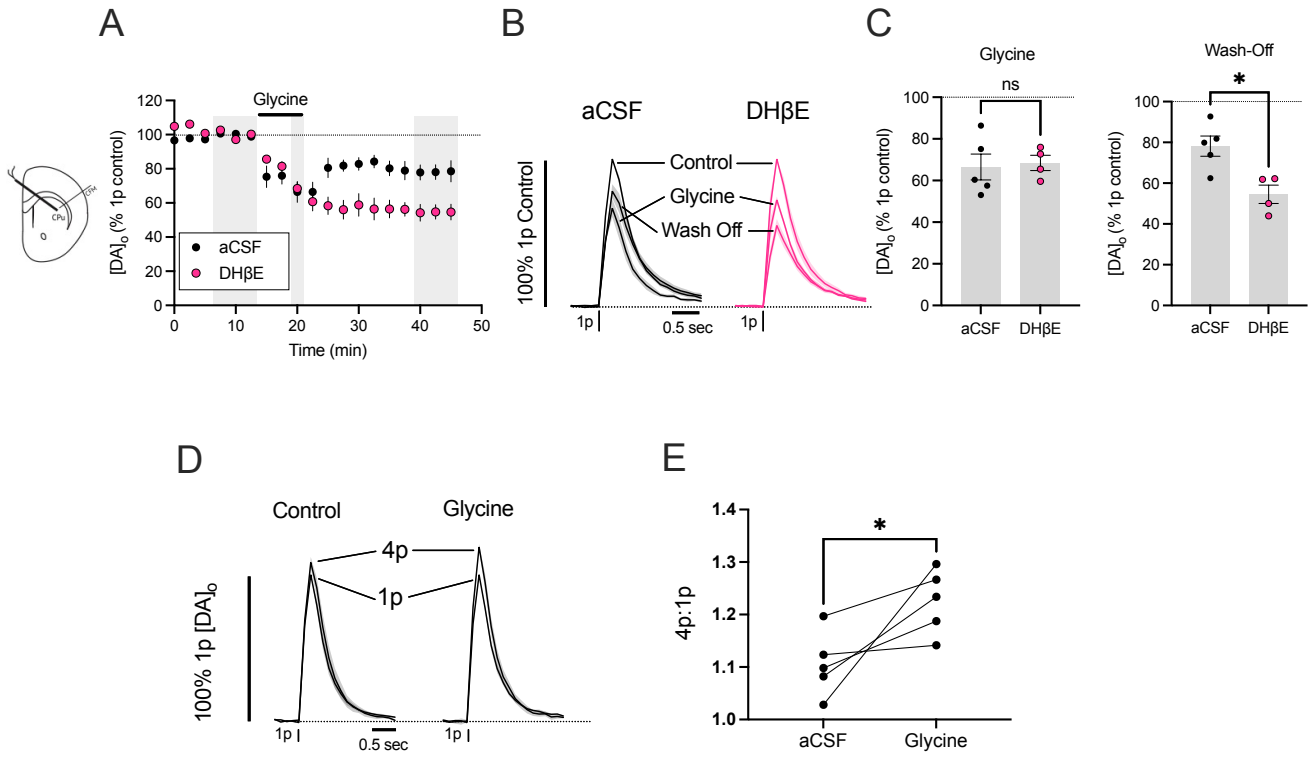

Figure 3.8. The effect of glycine is subtly altered in DHβE and glycine enhances 4p:1p

(A) Mean peak $[DA]_o$ (±SEM) versus time evoked by 1 electrical pulse in dlCPu showing application of 10 mM glycine, in the presence and absence of 1 µM DHβE. aCSF: n = 5 animals/slices. DHβE: n = 4 animals/slices.

(B) Mean $[DA]_o$ (±SEM) transients versus time, normalised to pre-drug control, before and during application of glycine, in the presence and absence of DHβE. aCSF: n = 5 animals/slices. DHβE: n = 4 animals/slices.

(C) *Left*: Mean peak $[DA]_o$ (±SEM) during application of glycine, in the presence and absence of DHBE. Unpaired t-test, glycine application, p = 0.8079 (n.s.); *Right:* Mean peak $[DA]_o$ (±SEM) during wash off of glycine, in the presence and absence of DHβE. Unpaired t-test, p = 0.0110 (*) . aCSF: n = 5 animals/slices. DHβE: n = 4 animals/slices.

(D) Mean peak $[DA]_o$ (±SEM) evoked by 1p or 4p 100 Hz electrical stimulation. Transients normalised to 1p evoked release in each condition. n = 5 slices/animals.

(E) Ratio of evoked $[DA]_o$ evoked by 4p 100 Hz and 1p electrical stimulation. Paired t-test: p = 0.0498 (*). n = 5 slices/animals.

3.3.9. The effects of glycine on DA release are not mediated via NMDA-Rs or GABA-Rs

I next investigated other indirect mechanisms by which glycine could modulate DA release. Glycine is a co-agonist at NMDA-Rs, which is required for channel opening. Although thalamic glutamatergic inputs have been shown to regulate DA release via NMDA-Rs expressed on ChIs following optogenetic activation, NMDA-Rs are not thought to be a significant regulator of evoked DA release (Kosillo, Zhang et al. 2016). A recent study confirmed that the NMDA-R antagonist AP-5 did not alter single pulse evoked DA release, recorded using FSCV in NAc core (Yorgason, Wadsworth et al. 2022). However, it is possible that exogenously applied glycine may drive an NMDA-R dependent effect. There is also evidence for GlyRs present on GABAergic striatal cell types including MSNs and interneurons. Although the source of ambient striatal GABA tone is not defined (Roberts, Doig et al. 2020), it is possible that altering the activity of GABAergic cells either directly or indirectly may contribute to the reduction in DA release observed upon application of glycine. I tested whether the effect of glycine on evoked DA release were modified by the presence of NMDA-R and GABA-R antagonists (also in the presence of DHβE, to remove any confounding effects of nAChR regulation of DA release).

The NMDA-R antagonist AP-5 (50 µM) did not alter single-pulse evoked DA release in dlCPu (**Fig. 3.9A-C**, paired t-test, $p = 0.3212$, $n = 5$ animals/slices) as observed in NAc (Yorgason, Wadsworth et al. 2022). The effect of glycine on evoked $[DA]_o$ was not significantly altered by the presence of AP-5 (**Fig. 3.9D-F**, unpaired t-test, $p = 0.5901$). Similarly, the effect of glycine on evoked $[DA]_o$ was not significantly altered by the presence of $GABA_AR$ and $GABA_BR$ antagonists (4 µM Bicuculline + 10 µM CGP-55845) (**Fig. 3.9G-I**, unpaired t-test, $p = 0.2953$). These experiments suggest that the effects of glycine are not indirectly mediated via NMDA-Rs, or $GABA_ARs$ or $GABA_BRs$.

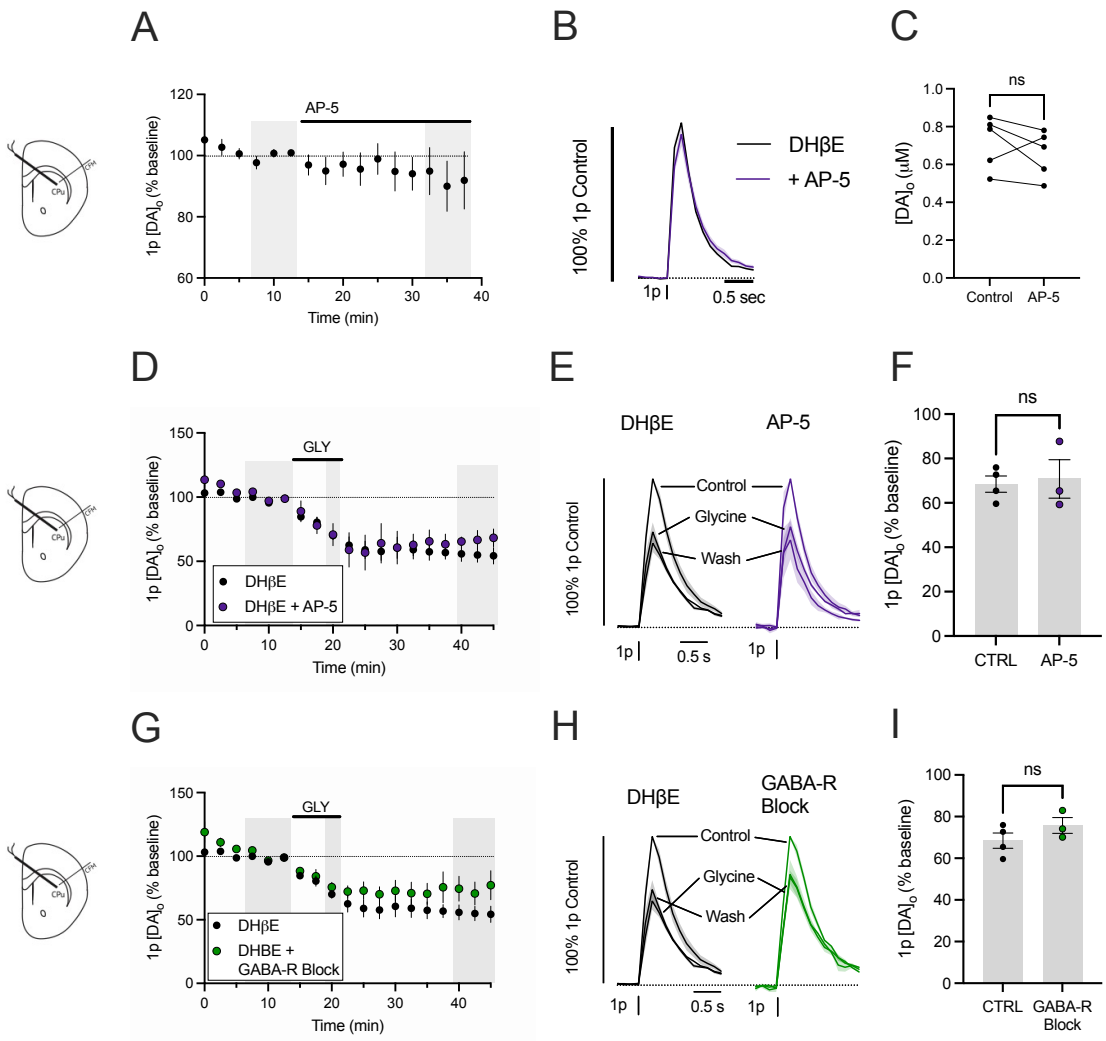

Figure 3.9. The effect of glycine on DA release is not mediated via NMDA-Rs or GABA-Rs

(A) Mean peak $[DA]_o$ (±SEM) versus time, evoked by 1 electrical pulse in dlCPu, before and after application of AP-V, in presence of DHβE. n = 5 animals/slices.

(B) Mean $[DA]_o$ (±SEM) transients versus time, normalised to pre-drug control, before and during application of AP-V, in presence of DHβE. n = 5 animals/slices.

(C) Mean peak $[DA]_o$ (±SEM) after application of AP-V, in presence of DHβE. Paired t-test. p =0.3212 (n.s.). n = 5 animals/slices.

(D) Mean peak $[DA]_o$ (±SEM) versus time, normalised to pre-drug control, following brief application of glycine in presence of DHβE and AP-V, or DHβE only. DHβE: n = 4 animals/slices. DHβE + AP-V: n = 3 animals/slices.

(E) Mean $[DA]_o$ (±SEM) transients versus time, normalised to pre-drug control, following brief application of glycine in presence of DHβE and AP-V, or DHβE only. DHβE: n = 4 animals/slices. DHβE + AP-V: n = 3 animals/slices.

(F) Mean peak $[DA]_o$ (±SEM) following brief application of glycine, in presence of DHβE and AP-V, or DHβE only, normalised to pre-drug control. Un-paired t-test p =0.5901 (n.s.). DHβE: n = 4 animals/slices. DHβE + AP-V: n = 3 animals/slices.

(G) Mean peak $[DA]_o$ (±SEM) versus time, normalised to pre-drug control, following brief application of glycine in presence of DHβE and GABA-R antagonists, or DHβE only. DHβE: n = 4 animals/slices. DHβE + GABA-R antagonists: n = 3 animals/slices.

(H) Mean $[DA]_o$ (±SEM) transients versus time, normalised to pre-drug control, following brief application of glycine in presence of DHβE and GABA-R antagonists, or DHβE only. DHβE: n = 4 animals/slices. DHβE + GABA-R antagonists: n = 3 animals/slices.

(I) Mean peak $[DA]_o$ (±SEM) after application, following brief application of glycine in presence of DHβE and GABA-R antagonists, or DHβE only, normalised to pre-drug control. Un-paired t-test p =0.2953 (n.s.). DHβE: n = 4 animals/slices. DHβE + GABA-R antagonists: n = 3 animals/slices.

3.3.10. Glycinergic regulation of spontaneous DA release and autoinhibition (Pilot)

Having recorded DA release using FSCV, I also tried using the $GRAB_{DA2m}$ sensor to see whether I could observe the same effect of glycine using this technique. This was partly due to concern that bath application of 10 mM glycine may indirectly affect FSCV recording via alteration of the chemical microenvironment that currents detected by FSCV are sensitive to. Using the $GRAB_{DA}$ sensor might also permit detection of changes in non-evoked DA levels occurring over slower or longer timecourses than is readily detectable with FSCV.

I completed a pilot experiment, using the same brief application protocol of 10 mM glycine as for the FSCV experiments (**Fig. 3.6**), but recording using $GRAB_{DA}$. Glycine appeared to reduce evoked DA release by a similar proportion to that detected with FCV (**Fig. 3.10A-C**). I also found that this glycine effect was reversible on wash-off. Another pilot experiment also showed that prolonged application of glycine mediated a continuous decline of evoked DA release similar to that observed using FSCV (data not shown). Although these are pilot data, it suggests that my effect of glycine on evoked DA is not purely due to a chemical interaction with the carbon fibre recording microelectrode.

I next undertook pilot experiments to investigate the effect of glycine application on tonic DA levels in striatum. My data seemed to show a very slight (~1%) increase in fluorescence upon application of glycine before a decline in DA levels that did not wash-off but remained stable (**Fig. 3.10D**). This sensor had not been used for recording non-evoked DA levels in our lab, and I was initially using a sampling rate of 30 sec interval per frame. To obtain better temporal resolution of this peak, I increased the sampling rate to a 10 sec interval per frame, and appeared to see a more clear increase in fluorescence, albeit of very small amplitude (**Fig. 3.10E**). This suggested that glycine may mediate a small increase in non-evoked DA release. To test if this might be occurring, I tried to enhance this effect by repeating a glycine application experiment in the DAT-blocker cocaine, to slow DA re-uptake, and in D2-R antagonist, to reduce any inhibitory effect mediated by a leak of DA on subsequent DA release. Although pilot data, this did not appear to enhance the DA signal (**Fig. 3.10D**). As a positive control, I used amphetamine (5 μM) to evoke spontaneous DA release and observed a ~ 1.5-fold increase in

fluorescence. These data suggest that the c. 1% increase in fluorescence observed with 30 sec sampling rate (**Fig. 3.10D**), even if it is DA release and not an artefact, may not be meaningful.

If glycine mediates a small leak of DA from DA axons, it would then be expected to result in subsequent inhibition of any evoked DA release via activation of D2-Rs, expressed on DA axons and which function as autoreceptors. To test this hypothesis, I performed a pilot experiment applying glycine in the presence of the D2-R antagonist L-741,626. Under these conditions, glycine still appeared to reduce evoked DA release by a similar amount, and also partially wash-off as under control conditions (**Fig. 3.10G-I**).

Although pilot data, these experiments suggest that the effect of glycine on evoked DA release is not an artefact of using FSCV as a recording technique. Glycine may mediate a small non-evoked increase in extracellular DA levels, but this does not then appear to be potentiated by DAT inhibition or D2-R block. Further, this does not appear to mediate any subsequent inhibition of evoked DA release via D2-Rs. However, further optimisation of recording protocols for $GRAB_{DA}$, particularly for non-evoked DA levels, may allow a better understanding of meaningful non-evoked DA release events.

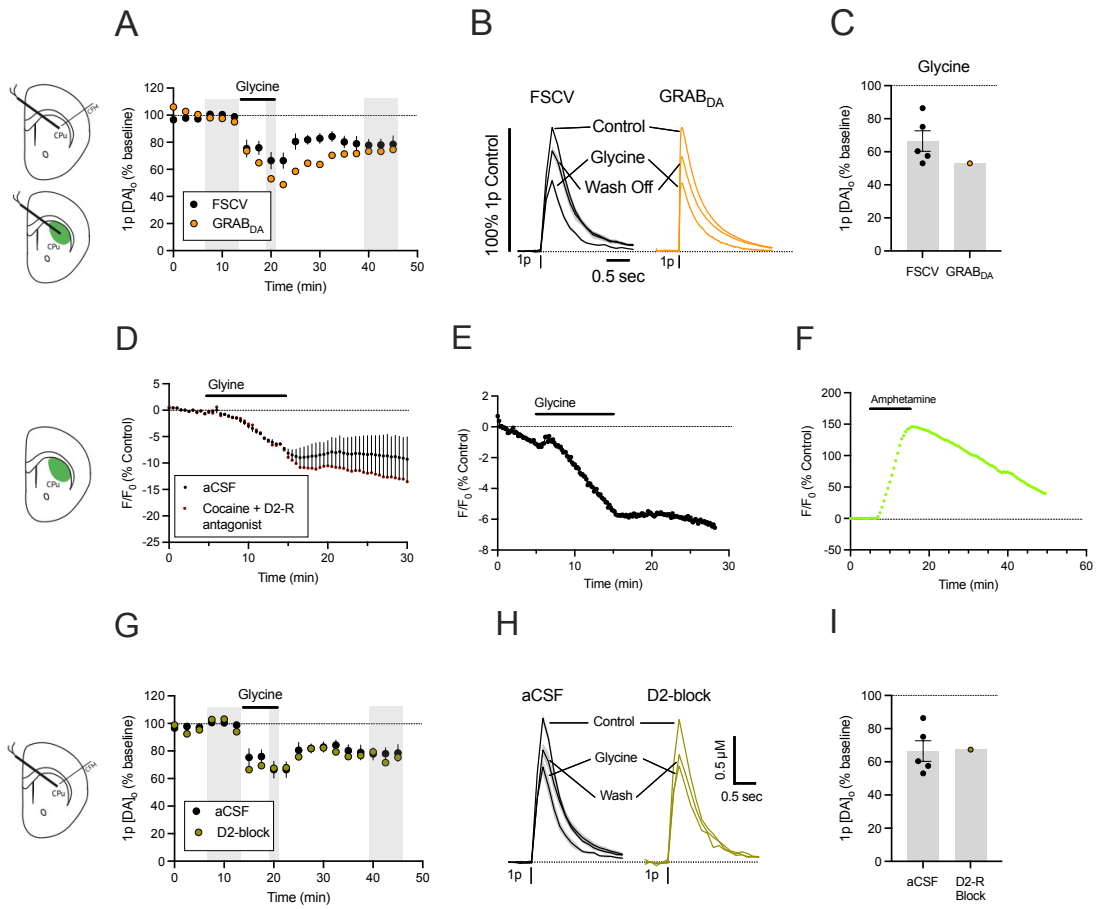

Figure 3.10. Glycinergic regulation of spontaneous DA release and autoinhibition (Pilot)

(A) Mean peak $[DA]_o$ (±SEM) versus time, evoked by 1 electrical pulse in dlCPu, before and after application of glycine, recorded using FSCV or GRAB$_{DA2m}$. DA release measured using GRAB$_{DA}$ is normalised to pre-glycine application $\Delta F/F_0$ fluorescence. FSCV: n = 5 animals/slices (same data as Fig. 3.6A). GRAB$_{DA}$: n = 1 animal/slice.

(B) Mean $[DA]_o$ (±SEM) transients versus time, normalised to pre-drug control, before and after application of glycine, recorded using FSCV or GRAB$_{DA}$. FSCV: n = 5 animals/slices (same data as Fig. 3.6A). GRAB$_{DA}$: n = 1 animal/slice.

(C) Mean peak $[DA]_o$ (±SEM) after application of glycine, in the presence or absence of D2-R antagonist, normalised to pre-drug control. FSCV: n = 5 animals/slices (same data as Fig. 3.6A). GRAB$_{DA}$: n = 1 animal/slice.

(D) Non-evoked GRAB$_{DA}$ fluorescence normalised to pre-glycine application (F/F_0) before and after application of glycine, in the presence or absence of cocaine and D2-R antagonist. aCSF: n = 2 slices/1 animal; Cocaine + D2-R block: n = 1 slice/1 animal.

(E) Non-evoked GRAB$_{DA}$ fluorescence normalised to pre-glycine application (F/F_0) before and after application of glycine, sampling at 10 sec interval per frame. n = 1 slice/1 animal.

(F) Non-evoked GRAB$_{DA}$ fluorescence normalised to pre-glycine application (F/F_0) before and after application of amphetamine. n = 1 slice/1 animal.

(G) Mean peak $[DA]_o$ (±SEM) versus time, evoked by 1 electrical pulse in dlCPu, before and after application of glycine in the presence or absence of D2-R antagonist. aCSF: n = 5 animals/slices (same data as Fig. 3.6A). D2-R block: n = 1 animal/slice.

(H) Mean $[DA]_o$ (±SEM) transients versus time, normalised to pre-drug control, before and after application of glycine, in the presence or absence of D2-R antagonist. aCSF: n = 5 animals/slices (same data as Fig. 3.6A). D2-R block: n = 1 animal/slice.

(I) Mean peak $[DA]_o$ (±SEM) after application of glycine, in the presence or absence of D2-R antagonist, normalised to pre-drug control. aCSF: n = 5 animals/slices (same data as Fig. 3.6A). D2-R block: n = 1 animal/slice.

3.3.11. Effect size of glycine is maintained following repeat application

cGlyRs are known to rapidly desensitise upon activation, similar to nAChRs and other pentameric ligand-gated ion channels. This is a hypothesis for why glycine and the cGlyR antagonist strychnine both reduce DA release. Although difficult to investigate using bath application of glycine and conscious that continuous application would cause a prolonged decline in DA release, I attempted to investigate whether repeat application of glycine would reduce DA release by a similar amount. Any reduced effect may indicate continued desensitisation of glycine receptors. I found that the effect of a second application of glycine was not significantly different to the initial glycine application, in either the presence or absence of DHβE (**Fig. 3.11A-B**, paired t-test, aCSF: p = 0.88714, n = 5 slices/animals; DHβE: p = 0.9265, n = 3 slices/animals). However, given the rapid kinetics of cGlyR desensitisation, this experiment would be better performed using puff-application of glycine and using electrophysiology to record cGlyR desensitisation kinetics more directly, or FSCV to record the effects of glycine application on DA release at shorter time-points.

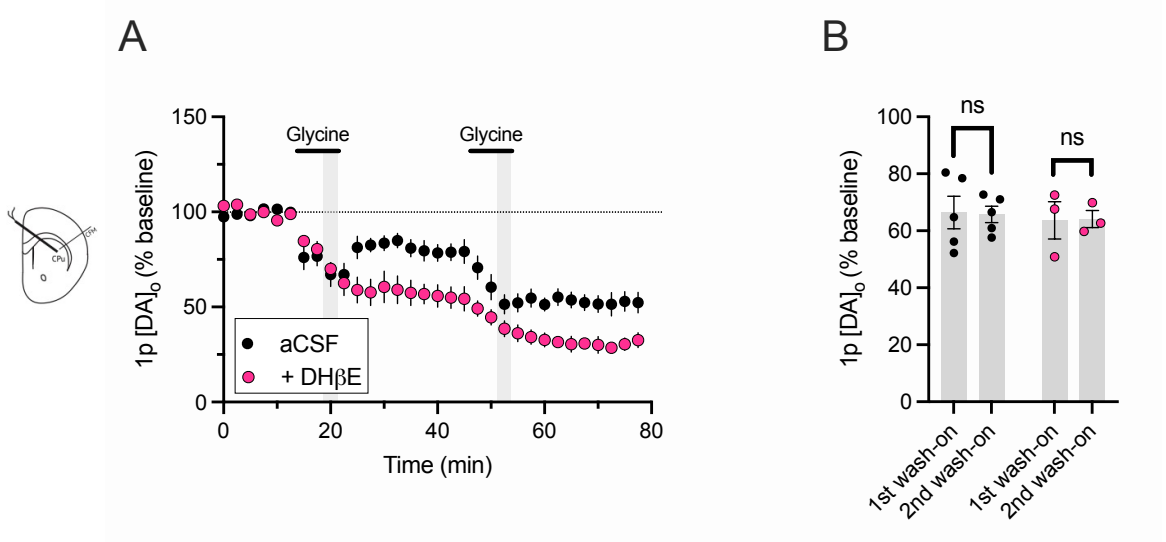

Figure 3.11. Effect size of glycine is maintained following repeat application

(A) Mean peak $[DA]_o$ (±SEM) versus time, normalised to pre-drug control, during repeat application of glycine. aCSF: n = 5 slices/animals. DHβE: n = 3 slices/animals.

(B) Mean peak $[DA]_o$ (±SEM) and after application of glycine, normalised to the 3 stimulations before the 1st and 2nd glycine wash-ons respectively. Paired t-test. aCSF: p = 0.8714 (n.s.), n = 5 animals/slices. DHβE: p = 0.9265 (n.s.), n = 3 animals/slices

3.3.12. The initial effect of glycine is reduced in the presence of strychnine

I tested whether the effects of glycine (10 mM) on DA release detected using FSCV were prevented by the presence of the cGlyR antagonist strychnine (10 μM). In the previous experiments using the long application of glycine, there appeared to be two distinct components of the reduction in DA release – a rapid initial decrease that plateaued, and a subsequent prolonged decline (**Fig. 3.4**). I performed an exploratory experiment to investigate whether strychnine could occlude the any of these effects of glycine.

There was a significant interaction between the effects of glycine and strychnine overall (**Fig. 3.12A**, two-way RM ANOVA, strychnine x glycine, $F_{(15,90)} = 3.562$, $p < 0.0001$), showing that the presence of strychnine alters the effect of glycine. Within the initial decrease, strychnine limits the inhibition of evoked DA release by glycine after 2.5 min application, but by 7.5 min of application the effects of glycine are the same, with or without strychnine (**Fig. 3.12A-B**, *post-hoc* Sidak's multiple comparisons test: 2.5 min after application, $p = 0.0004$; 7.5 min after application, $p = 0.9999$). This suggests that glycine is not simply desensitising cGlyRs, as glycine would not have a further effect in strychnine. This might be due to a combination of glycine acting via cGlyRs, eGlyRs, and the recently identified mGlyRs, each of which may also have a mixed population of receptors in different activation states. Glycine itself may also be out-competing strychnine given the 1000x difference in concentration (10 mM glycine versus 10 μM strychnine), exacerbated by a bath application protocol. The prolonged decline is still present, with no difference on the effect of DA release in the presence or absence of strychnine, and was investigated further in subsequent experiments.

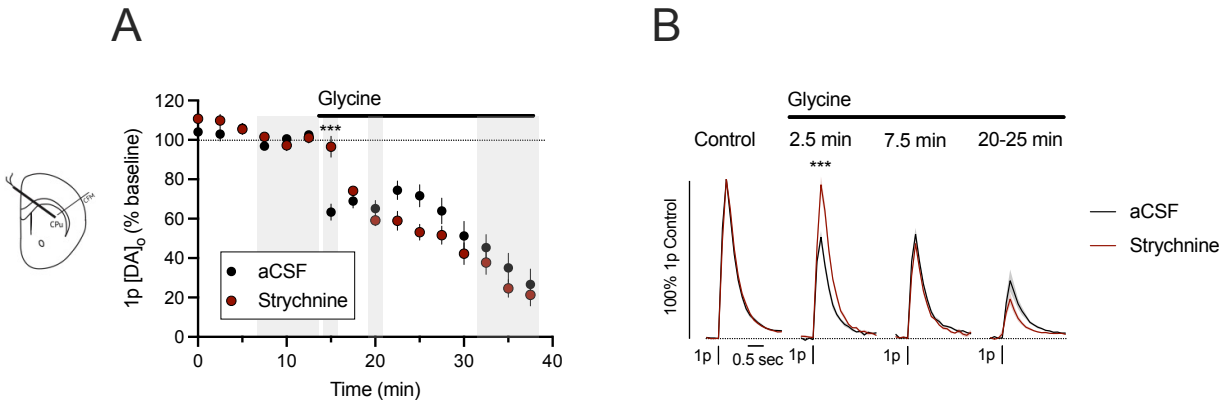

Figure 3.12. The initial effect of glycine is reduced in the presence of strychnine

(A) Mean peak $[DA]_o$ (±SEM) versus time, evoked by 1 electrical pulse in dlCPu, before and during application of glycine, in the presence or absence of strychnine. Two-way RM ANOVA: strychnine x glycine, $F_{(15,90)} = 3.562$, $p < 0.0001$. *post-hoc* Sidak's multiple comparisons test, $p = 0.0004$ (***). aCSF: n = 5 slices / 4 animals. Strychnine: n = 3 slices/animals. Shaded areas depict time-points used for transients in Fig. 3.13B and statistical analysis.

(B) Mean $[DA]_o$ (±SEM) transients versus time, normalised to pre-drug control, before and during application of glycine, in the presence or absence of strychnine.

3.3.13 CGP-78608 reduces DA release, via nAChRs

In addition to acting at cGlyRs with Cl^--permeable channels, it has recently been defined that glycine can act at excitatory glycine receptors (eGlyRs) (Bossi, Dhanasobhon et al. 2022). These eGlyRs have been identified in neurons of cortex and baslolateral amygdala, and I investigated whether eGlyRs contribute to the control of DA release. Previous ISH results for the expression of the critical eGlyR subunit Grin3A appears to show sparse, punctate expression in striatum (Allen Institute for Brain Science, 2011, Experiment: 73907499). Our collaborators in the Meletis lab (Karolinska Institutet, Stockholm) performed RNAscope and clearly identified the expression of Grin3A enriched in striatal ChIs (**Section 4.3.13**).

I pharmacologically manipulated the activity of eGlyRs to understand their role in DA release. As for cGlyRs, eGlyRs have a very limited pharmacological toolbox since these drugs typically also target the GluN3A subunit. One ligand available is CGP-78608, which binds to the GluN3A subunit that mediates the conformational switch from the active to inactive state. When CGP-78608 is bound, this stops the receptor pore closing, and therefore stops desensitisation, leading to pronounced increase in eGlyR function. Effects of CGP-78608 should therefore reflect on an extended timescale the effects of eGlyR activation. I found that application of CGP-78608 reduces electrically-evoked DA release by ~30% (**Fig. 3.13A-B**, one-sample t-test, $p = 0.0002$). I also found that this effect was nAChR-dependent as it was lost in the presence of DHβE (**Fig. 3.13C**, unpaired t-test, $p = 0.0003$). Given that these receptors are found on ChIs (Chapter 4), I also tested if there was a change in the ratio of DA released evoked by 4p 100 Hz electrical stimulation versus 1p. I found that there was a non-significant trend towards a greater 4p:1p ratio in the presence of CGP-78608 (**Fig. 3.13D-E**, paired t-test, $p = 0.0640$), but is likely underpowered. This effect is consistent with a change in the activation state of nAChRs expressed on DA axons. This would suggest a change in striatal ACh levels, and in turn a change in the activity of ChIs.

Overall, my data show that eGlyRs appear to regulate DA release in the striatum. The ability of the CGP-78608 to have an effect in the absence of an exogenously applied agonist, suggests a mixed-

receptor population where some of these receptors are tonically active and some desensitised. Regulation of eGlyRs on ChIs is investigated further in **Chapter 4**.

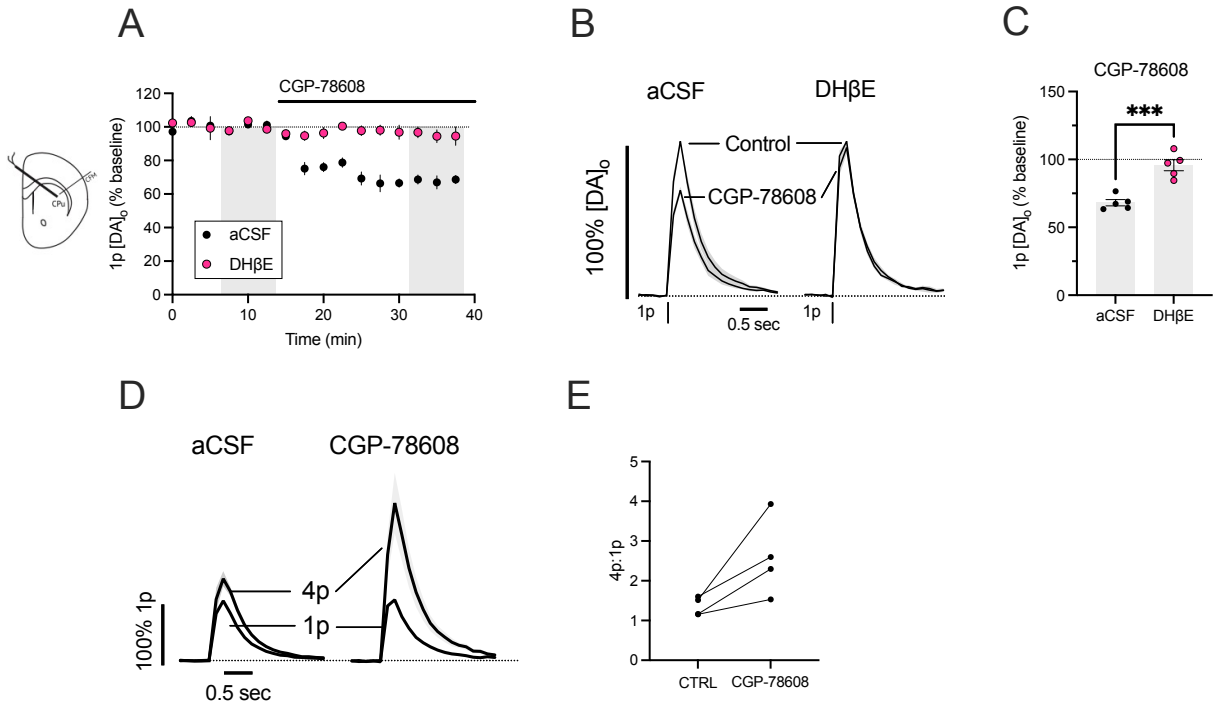

Figure 3.13. Stopping desensitisation of eGlyRs reduces DA release, via nAChRs

- **(A)** Mean peak $[DA]_o$ (±SEM) versus time, evoked by 1 electrical pulse in dlCPu, before and during application of CGP-78608, in the presence or absence of DHβE. n = 5 animals/slices per group.
- **(B)** Mean $[DA]_o$ (±SEM) transients versus time, normalised to pre-drug control, before and during application of CGP-78608, in the presence or absence of DHβE. n = 5 animals/slices per group.
- **(C)** Mean peak $[DA]_o$ (±SEM) after application of CGP-78608, normalised to pre-drug control. Un-paired t-test. p =0.0003 (***), n = 5 animals/slices per group.
- **(D)** Mean peak $[DA]_o$ ± SEM normalised to 1p evoked release in each condition. Evoked by 1p or 4p 100 Hz electrical stimulation in the presence or absence of CGP-78608. n = 4 animals/slices.
- **(E)** Ratio of 4p 100 Hz versus 1p evoked release, in either the presence or absence of CGP-78608. Paired t-test, p = 0.0640 (n.s.). n = 4 animals/slices.

3.3.14. Stopping inactivation of eGlyRs significantly alters effect of glycine

Given that eGlyRs can modulate DA release, I investigated the role of these receptors in mediating the effects of exogenously applied glycine on DA release. My hypothesis was that the effects of glycine that are mediated by eGlyRs would be enhanced in the presence of CGP-78608, because the eGlyRs would be stopped from desensitising. I also hypothesised that these effects would be nAChR-dependent because the effects of CGP-78608 are nAChR dependent.

Although there is no difference in the effect of glycine on DA release at the snapshot timepoint used previously for comparison of the effect of brief application of glycine (**Fig.3.14A-C**, one-way ANOVA, $F_{2,11} = 1.626$, $p = 0.2407$), there is a difference in the timecourses of action of glycine on evoked DA release in the presence of CGP-78608 or CGP-78608 and DHβE (Two-way RM ANOVA, Drug x Time, $F_{(36,198)} = 2.454$, $p < 0.0001$). This supports a role of eGlyRs in regulating the effect of exogenous glycine application modulating DA release. This effect of CGP-78608 on DA release following glycine application may be reduced in the presence of DHβE, indicating involvement via ChIs. These data suggest that the onset and offset of glycine's inhibitory effects on DA release are dependent on eGlyR activation on ChIs, consistent with the differences in both of these aspects seen with and without DHβE (Fig. 3.8) and suggesting that ChIs and ACh release might be rapidly and dynamically gated by eGlyRs. This will be further interrogated in **Chapter 4**.

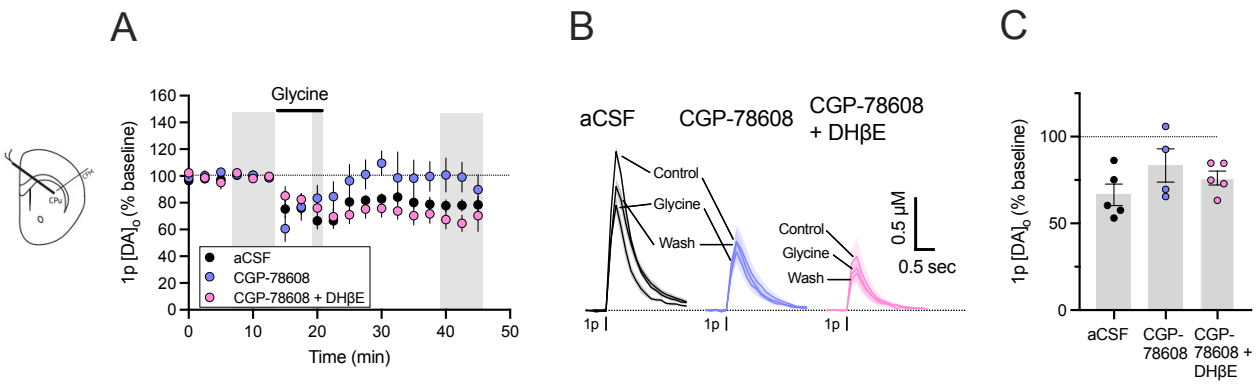

Figure 3.14. Stopping inactivation of eGlyRs significantly alters effect of glycine on DA release

(A) Mean peak $[DA]_o$ (±SEM) versus time, evoked by 1 electrical pulse in dlCPu, before and after application of glycine, in the presence or absence of CGP-78608 and CGP-78608 + DHβE. Two-way RM ANOVA, Drug x Time, $F_{(36,198)}$= 2.454, $p < 0.0001$). aCSF: n = 5 slices/animals, CGP-78608: n = 4 slices/animals, CGP-78608+DHβE: n = 5 slices animals.

(B) Mean $[DA]_o$ (±SEM) transients versus time, before and after application of glycine, in the presence or absence of CGP-78608 and CGP-78608 + DHβE. aCSF: n = 5 slices/animals, CGP-78608: n = 4 slices/animals, CGP-78608+DHβE: n = 5 slices animals.

(C) Mean peak $[DA]_o$ (±SEM) during application of glycine, in the presence or absence of CGP-78608 and CGP-78608 + DHβE, normalised to pre-drug control. One-way ANOVA, $F_{(2,11)}$ = 1.626, p = 0.2407 aCSF: n = 5 slices/animals, CGP-78608: n = 4 slices/animals, CGP-78608+DHβE: n = 5 slices animals.

3.3.15. The prolonged decline in DA release involves adenosine receptors (Elliot Yates)

We explored an alternative contributing mechanism for the prolonged decrease in DA release upon continuous, prolonged application of glycine. These experiments were completed by Elliot Yates, a Part II Biochemistry undergraduate student in our lab. Given previous findings from our lab that adenosine is able to reduce DA release via A1 receptors (Roberts, Lambert et al. 2022), we investigated whether adenosine release could be a mechanism by which glycine mediates a prolonged decline in DA release.

We investigated whether the prolonged decline of DA release by glycine could be mediated via adenosine receptors. We tested this by performing application of glycine in the presence of caffeine, a non-specific adenosine receptor antagonist. We found that the prolonged decline of DA release during glycine application was significantly reduced in the presence of caffeine (**Fig. 3.15A-C**, unpaired t-test, p = 0.0190). This finding suggests that the prolonged decline of DA release mediated by glycine is via adenosine receptors.

We performed long application of glycine in the presence of CGP-78608, preventing desensitisation of eGlyRs, to investigate if enhancement of eGlyRs would potentiate the prolonged decline, via release of adenosine. We found that, similar to the brief application of glycine in CGP-78608, there was a sharp initial decrease in release followed by a rebound (**Fig. 3.15D**. As with the glycine application, DA release started to drop, but still remained significantly higher than DA release at the same time-points in the absence of CGP-78608 (**Fig. 3.15E-F**, unpaired t-test, $p < 0.0001$). However, DA release at this point is still declining rather than stable, and I hypothesise that the presence of CGP-78608 does not occlude the prolonged decline of DA release but rather delays it by elevating DA release during it. Continuing the experiment for a longer duration would allow this to be tested.

Finally, we explored the source of this adenosine. A candidate mechanism is the co-release of ATP from cholinergic interneurons, which is then degraded to adenosine (Saunders, Granger et al. 2015). This would be consistent with other findings from this project, that glycine can have an excitatory effect on ChIs, although the literature surrounding ATP co-release from cholinergic interneurons is controversial. To test the hypothesis that the source of adenosine are ChIs, we performed application of glycine in the presence of oxotremorine (Oxo-M), an mAChR agonist that activates autoreceptors expressed on ChIs, stopping their firing activity (albeit that they will still be activated during electrical stimulation) and neurotransmitter release. However, the presence of Oxo-M did not significantly alter the prolonged decline of evoked DA release caused by glycine application (**Fig. 3.15G-H**, unpaired t-test, $p = 0.7680$). This suggests that ATP co-transmission from ChIs is not the source of striatal adenosine mediating these effects, or that oxo-M does not diminish its release during this protocol. These results show that the prolonged component of the reduction in DA release by glycine is mediated via adenosine receptors, but that the source of adenosine is not resolved

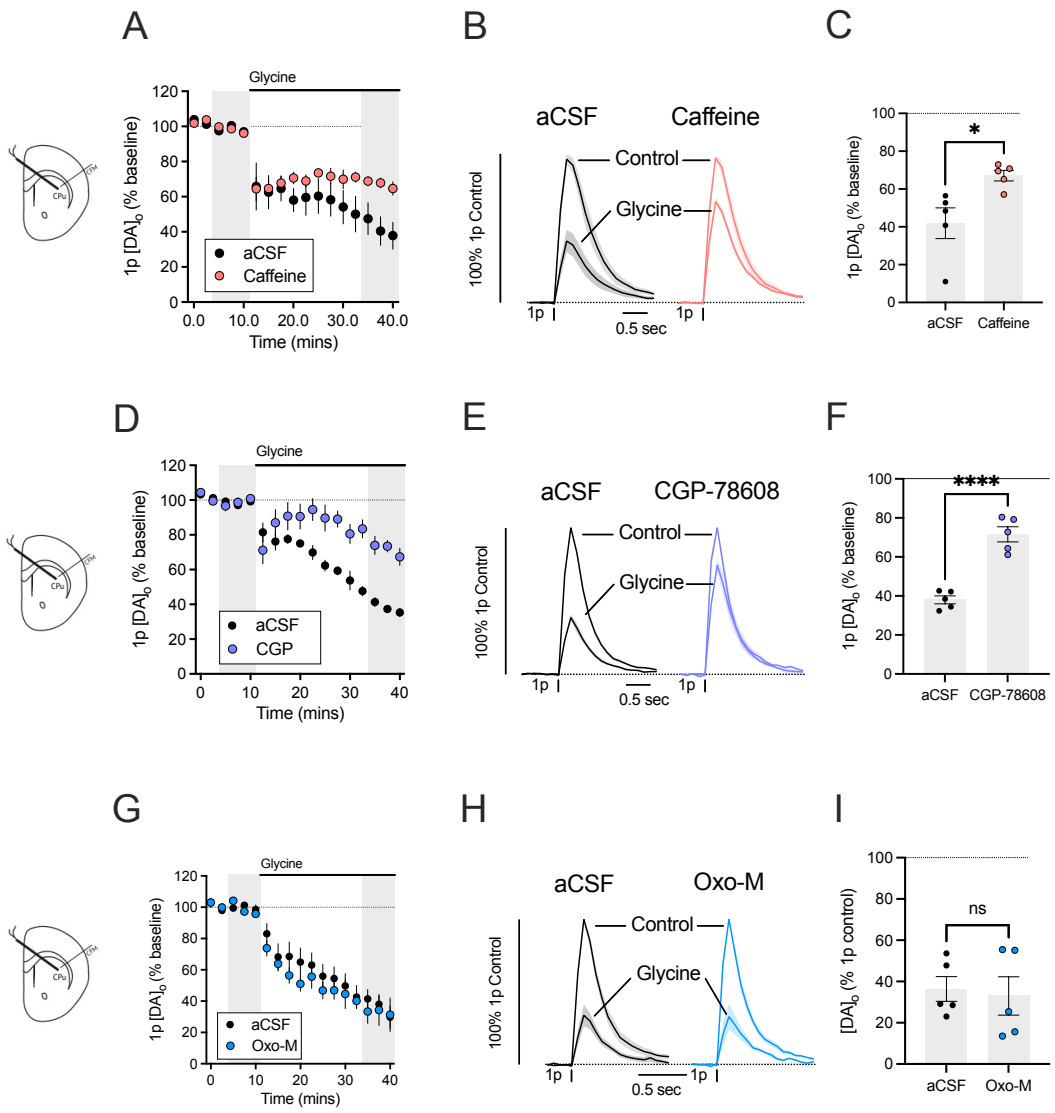

Figure 3.15. The prolonged decline in DA release by glycine is mediated via adenosine receptors.

(A) Mean peak $[DA]_o$ (±SEM) versus time, normalised to pre-drug control, before and during application of glycine, in the presence and absence of caffeine. n = 5 slices/animals per condition.

(B) Mean $[DA]_o$ (±SEM) transients versus time, normalised to pre-drug control, before and during application of before and during application of glycine, in the presence and absence of caffeine. n = 5 slices/animals per condition.

(C) Mean peak $[DA]_o$ (±SEM) after application of glycine, in presence or absence of caffeine. Unpaired t-test, $p < 0.0001$. n = 5 slices/animals per condition.

(D) Mean peak $[DA]_o$ (±SEM) versus time, normalised to pre-drug control, before and during application of glycine, in the presence and absence of CGP-78608. n = 5 slices/animals per condition.

(E) Mean $[DA]_o$ (±SEM) transients versus time, normalised to pre-drug control, before and during application of before and during application of glycine, in the presence and absence of CGP-78608. n = 5 slices/animals per condition.

(F) Mean peak $[DA]_o$ (±SEM) after application of glycine, in presence or absence of CGP-78608. Unpaired t-test, $p = 0.0190$. n = 5 slices/animals per condition.

(G) Mean peak $[DA]_o$ (±SEM) versus time, normalised to pre-drug control, before and during application of glycine, in the presence and absence of Oxo-M. n = 5 slices/animals per condition.

(H) Mean $[DA]_o$ (±SEM) transients versus time, normalised to pre-drug control, before and during application of before and during application of glycine, in the presence and absence of Oxo-M. n = 5 slices/animals per condition.

(I) Mean peak $[DA]_o$ (±SEM) after application of glycine, in presence or absence of Oxo-M. Unpaired t-test, $p = 0.7680$. n = 5 slices/animals per condition.

3.3.16. Taurine also reduces striatal DA release

Taurine is an amino acid that is a partial agonist at cGlyRs (Mangin, Guyon et al. 2002, Lewis, Schofield et al. 2003). I investigated whether taurine was also able to reduce DA release. Prolonged application of taurine also reduced evoked DA release initially (**Fig. 3.16G**, one-sample t-test, Taurine 2.5 min after application, $p = 0.0266$), but in contrast to glycine did not exhibit the same prolonged decline in DA release (**Fig.3.16A-C**, unpaired t-test, $p = 0.0003$). This is further evidence to consider dividing the effects of glycine into its initial reduction of DA release, which is similar to taurine, and the secondary prolonged decline effects, which is different to taurine.

I then investigated whether, as with glycine, there is a greater effect in dlCPu than NAc. However, I did not find a significant difference of the effect of taurine between these two regions (**Fig.3.16D-F**, unpaired t-test, $p = 0.3529$). This may be due to a very small difference at lower concentrations that becomes larger as concentration increases, as for glycine (**Fig.3.5B**).

There are few specific tools for the investigation of GlyRs, and taurine is known to have off-target effects at different receptors and transporters, including as a weak, partial agonist at $GABA_A$Rs, which could also contribute to the reduction of DA release directly. To test this, I performed taurine application in the presence of NMDA-R or GABA-R block (**Fig.3.16G-I**). I did not find any significant interaction between the effect of glycine or taurine and the receptor antagonists present (**Fig. 3.16I**, two-way ANOVA, glycine/taurine x receptor antagonists, $F_{(2,20)} = 0.2222$, $p = 0.8027$), suggesting the effect of taurine is not mediated via NMDA-Rs or GABA-Rs.

These data show that taurine, like glycine, reduces DA release. Moreover, taurine in its own right is an important modulator of DA release. Although likely acting via cGlyRs, it may also act via other mechanisms specific to taurine signalling. It also supports a hypothesis the multiphase hypothesis of the effects of glycine, where taurine mediates a similar initial decline but not the subsequent prolonged decline.

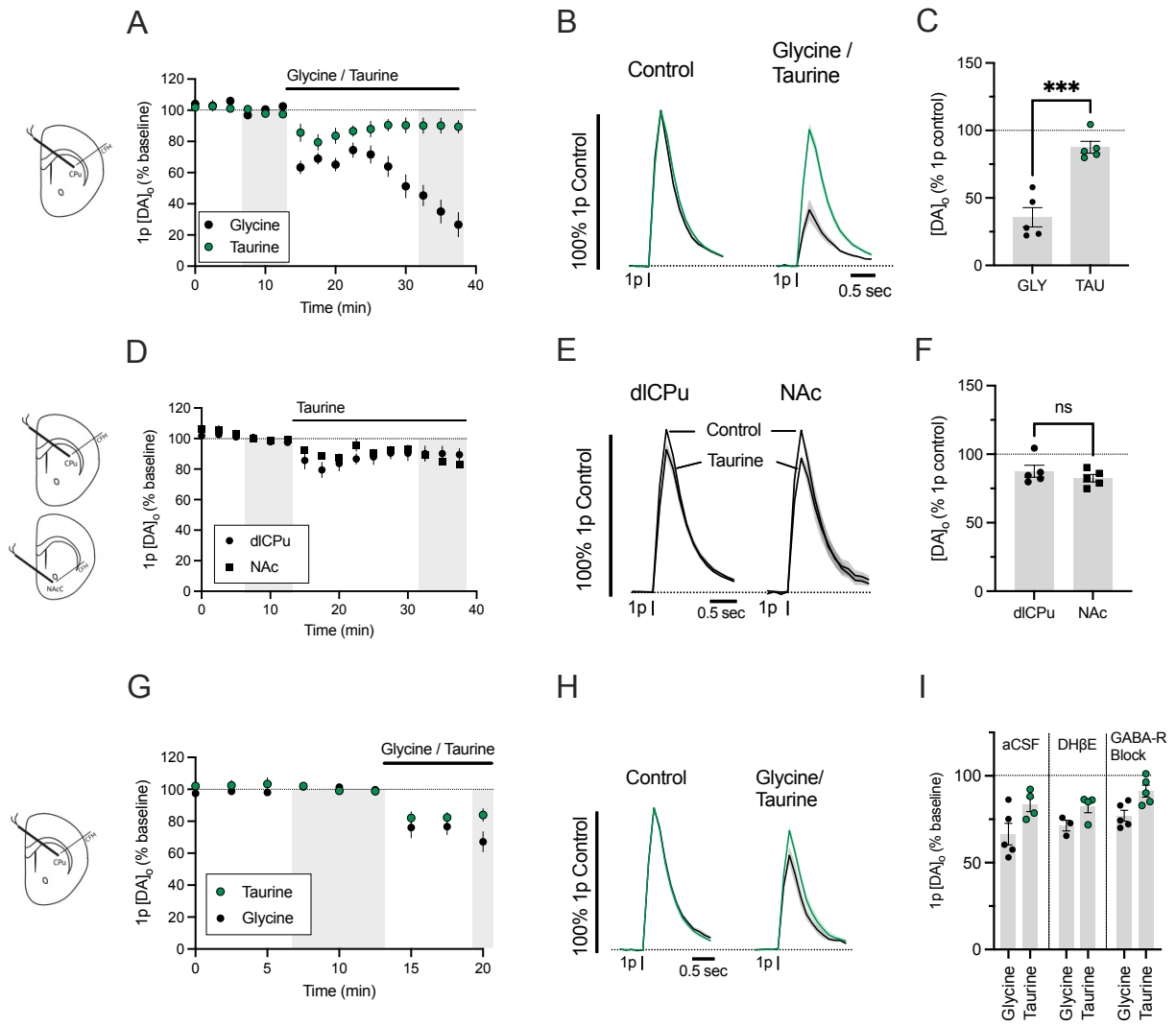

Figure 3.16. Taurine also reduces striatal DA release

(A) Mean peak $[DA]_o$ (±SEM) versus time, evoked by 1 electrical pulse in dlCPu, before and after application of taurine or glycine. n = 5 animals/slices per group.

(B) Mean $[DA]_o$ (±SEM) transients versus time, normalised to pre-drug control, before and during application of glycine or taurine, evoked by 1p electrical pulse. n = 5 animals/slices per group.

(C) Mean peak $[DA]_o$ (±SEM) after application of glycine or taurine, normalised to pre-drug control. Un-paired t-test. p =0.0003 (***), n = 5 animals/slices per group.

(D) Mean peak $[DA]_o$ (±SEM) versus time, following brief application of taurine in dlCPu or NAc. n = 5 animals/slices per region.

(E) Mean $[DA]_o$ (±SEM) transients versus time, normalised to pre-drug control, before and after brief application of taurine, in dlCPu or NAc. n = 5 animals/slices per region.

(F) Mean peak $[DA]_o$ (±SEM) after application of taurine, in dlCPu or NAc, normalised to pre-drug control. Un-paired t-test. p =0.3529 (n.s.), n = 5 animals/slices per region.

(G) Mean peak $[DA]_o$ (±SEM) versus time, evoked by 1 electrical pulse in dlCPu, before and during brief application of taurine or glycine. Taurine: n = 4 slices/animals. Glycine: n = 5 slices/animals.

(H) Mean $[DA]_o$ (±SEM) transients versus time, normalised to pre-drug control, before and during brief application of glycine or taurine. Taurine: n = 4 slices/animals. Glycine: n = 5 slices/animals.

(I) Mean peak $[DA]_o$ (±SEM) after application of taurine or glycine, either in aCSF only, DHβE, or GABA-R block, normalised to pre-drug control. Two-way ANOVA: Drug x antagonist: $F_{(2,20)} = 0.2222$, p = 0.8027 (n.s.). aCSF: Glycine: n = 5 slices/animals. Taurine: n = 4 slices/animals. DHβE: Glycine: n = 3 slices/animals. Taurine: n = 4 slices/animals. GABA-R Block: Glycine: n = 5 slices/animals. Taurine: n = 5 slices/animals.

3.4. Discussion

In these series of experiments, we have shown that functional cGlyRs and eGlyRs are present in striatum and modulate evoked DA release. The effect of excitatory (eGlyRs) but not classical GlyRs are mediated via nAChRs, most likely via alteration of the activity of ChIs. Both types of receptors are tonically active, with GlyT1 regulating an ambient glycine tone that acts on at least classical GlyRs. The putative endogenous agonist for these receptors, glycine, also reduces DA release in a region-dependent manner with two distinct phases of reduction. This initial phase appears to be at least partially mediated via cGlyRs and eGlyRs, and the secondary phase is mediated via adenosine receptors. Taurine, another candidate endogenous ligand at cGlyRs, also reduces DA release.

3.4.1. Classical glycine receptors are tonically active and inhibit DA release

cGlyRs regulating DA release are tonically active in both dorsal and ventral striatum, and under the control of an ambient glycine tone. This is demonstrated by the experiments showing that cGlyR antagonist strychnine application alone reduces DA release, even in the absence of a GlyR agonist being added (Fig. 3.1A). This finding is consistent with a recent study that found strychnine reduced electrically-evoked DA release in NAc core (Yorgason, Wadsworth et al. 2022). To minimise the confound that non-specific electrical stimulation is stimulating glycine release, I used targeted optical stimulation of DA axons, for which there is no evidence of glycinergic co-transmission (Fig. 3.1E-G**)**. Under these conditions, strychnine still reduced DA release and by a similar magnitude. This shows that the endogenous agonist is present even without stimulation, as opposed to the antagonist blocking the effect of an endogenous agonist that is co-incidentally release following the electrical stimulation to evoke DA release. Overall, this supports a hypothesis of an ambient glycine tone acting on cGlyRs to regulate DA release, and is consistent with tonic cGlyR activity in striatum observed on MSNs (McCracken, Lowes et al. 2017) .

cGlyRs are also expressed in the somatodendritic compartment of DA neurons in midbrain (Häusser, Yung et al. 1992, Mangin, Guyon et al. 2002), and I hypothesise that they may also be located

directly on DA axons in striatum, similar to $GABA_A$Rs (Lopes, Roberts et al. 2019, Kramer, Twedell et al. 2020). This would be consistent with the effect of strychnine on optically-evoked DA release we observe. However, it is important to understand that this approach does not control for any non-evoked changes in neurotransmitter levels, that can still modulate DA release. As our understanding of the striatal neurotransmitter and neuromodulator network grows, we are beginning to appreciate the role of ambient neurotransmitters and neuromodulators, such as adenosine and GABA that may regulate DA release, without their release needing to be evoked (Roberts, Doig et al. 2020, Roberts, Lambert et al. 2022).

To test the hypothesis of direct expression of cGlyRs on DA axons in the future, electrophysiological recordings from DA axons directly could investigate whether strychnine-sensitive glycine currents are present, as has been performed for $GABA_A$R currents (Kramer, Twedell et al. 2020). Alternatively, recently developed approaches for targeted ligand localisation via drugs acutely restricted by tethering (DART) could be developed and deployed: Targeted expression of the HaloTag protein in Slc6a3$^{IRES\text{-}Cre}$ mice and bath application of a HaloTag ligand based on strychnine would allow targeted application of strychnine to DA axons (Shields, Kahuno et al. 2017). If this strychnine-based construct reduced DA release, this would suggest the expression of GlyRs directly on DA axons. However, the purpose of this project is to understand the role of neurotransmitters to regulate DA release; although cell-type localisation of receptors is of interest, striatal DA release is intrinsically a complicated process mediated by many interacting circuits, and the overall net effect of GlyR regulation on DA release is arguably more important.

cGlyRs have also been identified on several striatal cell types, including ChIs, MSNs, and other striatal interneurons (Sergeeva and Haas 2001, Martin and Siggins 2002, Forstera, Munoz et al. 2017, McCracken, Lowes et al. 2017, Molchanova, Comhair et al. 2017, Munoz, Yevenes et al. 2018), making them a strong candidate for indirect modulation of DA release. ChIs are known to powerfully regulate DA release and were a candidate indirect mechanism for the effects of strychnine (Rice and Cragg 2004). We found that the effects of strychnine were nAChR-independent (Fig. 3.2). Previous findings have shown that strychnine can have off-target effects as an antagonist at nAChRs, mostly at α6-homomeric nAChRs and to a lesser extent at β2-containing nAChRs (Matsubayashi, Alkodon et al.

1998, Garcia-Colunga and Miledi 1999). Although our lab does not find that α7-nAChRs regulate DA release, any action on β2-containing nAChRs would be a significant confound. Our results have two implications: firstly, that strychnine does not have an off-target effect at nAChRs in this experimental protocol, but secondly that this effect is also not mediated indirectly via nAChRs. There is a subtle increase in the pulse-number dependence of DA release in the presence of glycine (Fig. 3.8D-E) but this is small in comparison to the overall effect on 1p release of strychnine, and may be mediated by eGlyRs rather than cGlyRs. The mechanisms of glycinergic receptor regulation of ChI activity will be investigated in greater detail in **Chapter 4**. However, future experiments should investigate alternative indirect mechanisms of DA release via GlyRs, such as GABAergic transmission given cGlyR expression on GABAergic cell-types.

3.4.2. Excitatory glycine receptors are present in striatum, are tonically active, and inhibit DA release via nAChRs

My results show that eGlyRs are present in striatum, are tonically active and indirectly regulate DA release via nAChRs. The recent identification of eGlyRs in cortex and BLA raised the possibility of their presence in striatum, and as a receptor responding to glycine, may modulate DA release (Bossi, Dhanasobhon et al. 2022). Localisation in striatum was supported by initial *in situ* hybridisation data from the Allen Brain Atlas, but also findings from our collaborators at the Karolinska Institutet (Dr Ioannis Mantas and Prof. Konstantions Meletis) using RNAscope to identify expression of the Grin3A subunit in striatum, and specifically co-localisation within ChIs (**Chapter 4**).

The pharmacology available for the manipulation of eGlyRs is limited, with CGP-78608 used to block the desensitisation of eGlyRs by binding to the GluN3A subunit, and DCKA used as an antagonist by binding to the GluN1 subunit. We show that application of CGP-78608 reduce DA release, in an nAChR-dependent manner (Fig. 3.13A-C). This shows that functional eGlyRs are present in striatum, and secondly that they are tonically active – necessary for the blocking of eGlyR desensitisation to mediate an effect. This also suggests a mixed population of eGlyRs, that are not all active together simultaneously. The finding that this effect is nAChR-dependent supports the

localisation data that these receptors are located on ChIs, and supports the data suggesting that there is a trend towards increased pulse-number dependence of DA release in the presence of CGP-78608 (Fig. 3.13D-E). Furthermore, the rapid reduction in DA release upon glycine application and the subsequent rebound, enhanced by CGP-78608, supports a mechanism where eGlyR activation reduces DA release, mediating a rebound as nAChR activity returns. The mechanism of action of eGlyRs on ChIs will be investigated in greater depth in **Chapter 4**, but this suggests a mechanism whereby eGlyRs indirectly regulate DA release, by modulating the activity of ChIs, affecting the release of ACh and the activation of nAChRs expressed on DA axons.

3.4.3. Glycine reduces DA release in a multiphasic manner

We found that exogenous glycine reduces DA release across the striatum, with a greater effect in dlCPu than NAc (Fig. 3.5). Initially, I had hypothesised that glycine and strychnine should have opposing effects, due to their agonist and antagonist activity respectively at cGlyRs. However, cGlyRs are part of the family of pentameric ligand-gated ion channels, including nAChRs, which exhibit rapid desensitisation. Thus, agonist-mediated desensitisation and antagonism would be expected to have the same functional outcome, as seen in nAChRs. This is supported by a recent study showing that both strychnine and glycine reduce electrically evoked DA release, recorded using FSCV, in NAc core (Yorgason, Wadsworth et al. 2022). Using bath application of glycine and recording DA release every 2.5 min lacks the temporal resolution to record these events, and puff application with direct recording of cGlyR currents may be more appropriate to investigate this aspect.

Since antagonism of cGlyRs reduces DA release, it would suggest that activation of cGlyRs is excitatory. This would be counterintuitive, since cGlyRs and Cl^- conductance is typically inhibitory. However, within the previous studies reporting on glycinergic modulation of DA release, some studies find that glycine promotes DA release. I hypothesised that this might be due to an indirect, disinhibitory mechanism, whereby glycinergic inhibition of GABAergic neurons may reduce tonic GABAergic inhibition of DA release, but I did not find that the effect of glycine is significantly altered in GABA-R block (Fig. 3.9). I alternatively hypothesised that glycine application might facilitate NMDA-R

mediated signalling, that may enhance DA release. However, I did not find that DA release is modulated by NMDA-Rs using single-pulse stimulation where glycine modulates DA release, nor that the effect of glycine is altered under the antagonism of NMDA-Rs (Fig. 3.9). DA axons are hyperpolarised under normal conditions, and under these circumstances increased Cl^- conductance could be depolarising. However, electrophysiological investigation at the level of the axon whether this would manifest in increased DA axon firing or shunting inhibition would be required, and based on previous findings looking at $GABA_AR$ currents in DA axons, a Cl^- conductance mediated via cGlyRs should be inhibitory (Kramer, Twedell et al. 2020).

In our experiments, a concentration of at least 5 mM glycine was required to reduce striatal DA release (Fig. 3.5). This is a relatively large concentration of ligand to apply and raises the question of non-specific effects mediated by exogenous application of a high concentration of any ligand. However, my results complement those of previous studies, supporting that this is an effect mediated by glycine. Firstly, my findings that a concentration of at least 5 mM glycine is needed to reduce DA release in striatum is supported by the results of Yorgason et al., who also completed a concentration-response curve of glycine application while measuring DA in NAc core in *ex vivo* brain slices and found that only concentrations greater than 5 mM glycine altered DA release (Yorgason, Wadsworth et al. 2022). Secondly, endogenous striatal GlyT1 activity takes up exogenously applied glycine, as shown in results where the effect of exogenously applied glycine is enhanced in the presence of GlyT1 inhibition (Fig. 3.7). Finally, the reduction of DA release by glycine is at least partially mediated by strychnine-sensitive cGlyRs at an early timepoint (Fig. 3.12). This inhibition of the effect of glycine by strychnine is lost at later timepoints, likely due to the difference in applied concentration (10 mM glycine vs 10 µM strychnine) resulting in glycine out-competing strychnine. Puff application, rather than bath application, of glycine in the presence of strychnine may be a better experimental approach to show antagonism of glycine more clearly. However, there are clear parallels to investigations of GABAergic regulation of DA release; high concentrations of 5 mM GABA is required to elicit a large reduction of DA release, likely due to activity of GABA transporters expressed in striatum that reduce the effective concentration of GABA reaching GABA-Rs (Lopes, Roberts et al. 2019, Roberts, Doig et al. 2020).

The prolonged application of glycine shows an initial reduction in DA release, followed by a prolonged decline (Fig. 3.4). An initial hypothesis was that this may be a pathological effect, due to a combination of high concentration of exogenous ligand application, and non-specific electrical stimulation. However, the prolonged decline was also observed in optically-evoked, targeted DA release, arguing against this hypothesis (Fig. 3.4). An important finding is that this component is receptor mediated, via adenosine receptors (Fig. 3.15). This emerged as a hypothesis when application of DCKA appeared to cause the spontaneous release of adenosine, visualised on a voltammogram and subsequently observed upon application of glycine in the presence of CGP-78608 in a GRAB-adenosine pilot experiment. The mechanism by which adenosine is released is unclear, and there is no consensus around the source of striatal adenosine(Roberts, Lambert et al. 2022). Our initial hypothesis was that glycine causes excitation of ChIs, causing the release of ACh and the co-release of ATP, which could then be degraded into adenosine. However, the prolonged decline was still present in Oxo-M under which ACh release should be stopped (Fig. 3.15). This suggests that the source of adenosine is not ChIs, but a secondary candidate are astrocytes. Previous evidence has shown that astrocytes release adenosine as a gliotransmitter, and this possibility should be explored further.

3.4.4. Glycine as the endogenous agonist at striatal GlyRs

The finding that GlyT1 inhibition modulates the size of the striatal glycine tone supports previous findings of an ambient glycine tone in striatum acting on medium spiny neurons (Forstera, Munoz et al. 2017, McCracken, Lowes et al. 2017). However, GlyT1 inhibition alone did not alter DA release (Fig. 3.3A-C). This was surprising finding given the clear enhancement of the reduction in DA release mediated by strychnine when in the presence of sarcosine (Fig. 3.3D-F). It may be that GlyT1 inhibition alone has a relatively small effect on DA release that could not be determined by these experiments, or alternatively that a small increase in DA release may not be visualised in comparison to an effect of time, where DA release at a given site progressively declines independently of pharmacological manipulation. With the hypothesis that there is a mixed population of cGlyRs in different activation states, sarcosine elevating extracellular glycine could promote one population of

cGlyRs to desensitise and another to become more active, therefore mediating no net effect. Alternatively, a longer incubation time-period may be required for sufficient striatal glycine accumulation to mediate an effect on DA release, which is more apparent upon exogenous glycine application.

A broader debate within the field is whether glycine is the endogenous ligand at cGlyRs in striatum. This is historically due to the lack of evidence for glycinergic innervation within the striatum, identified via GlyT2 expression on presynaptic glycinergic neuron terminals, and the potential for other ligands such as taurine to act as a partial agonist at cGlyRs; we show in our data that exogenously applied taurine reduces striatal DA release (Fig. 3.16). Taurine is present across the brain as an osmoregulator, and in particularly high mM concentrations in striatum (Sergeeva, Chepkova et al. 2003). Furthermore, previous studies have shown that taurine is able to regulate neuronal activity via the tonic activation of cGlyRs following release from astrocytes via volume-regulating anion channels (VRACs) (Choe, Olson et al. 2012), and that taurine can activate cGlyRs in NAc (Jiang, Krnjevic et al. 2004). Thus, the molecular components for taurine signalling are present in striatum, supporting a role for taurine as the endogenous ligand.

However, there is a growing understanding that astrocytes can also contribute to neuronal signalling directly via gliotransmission. Previous studies have shown that GlyT1 is expressed on astrocytes, and moreover that GlyT1 can be reversed to provide a source for glycine (Huang, Barakat et al. 2004, Shibasaki, Hosoi et al. 2017). Pilot data from our lab using striatal astrocytes selectively expressing GCaMP6f suggests that exogenous glycine application mediates a large increase in intracellular [Ca^{2+}]. The most parsimonious explanation is that striatal astrocytes express GlyT1, and that application of glycine increases inward transport of glycine into astrocytes. Due to the co-transport of Na^{+}, this depolarises the astrocyte, mediating an increase in intracellular [Ca^{2+}] via the opening of voltage-gated Ca^{2+} channels and/or the release of intracellular stores of Ca^{2+}. This provides functional evidence that striatal astrocytes express GlyT1, supporting previous studies that indirectly show downstream effects of GlyT1 modulation (Forstera, Munoz et al. 2017, McCracken, Lowes et al. 2017). If glycine is the endogenous ligand for cGlyRs, this raises the question of how astrocytes via GlyT1 can act as both a sink and source of glycine. This is a similar question for the role of adenosine-mediated

regulation of striatal DA release via ENT1 on astrocytes (Roberts, Lambert et al. 2022), and warrants further investigation.

Given the above evidence, it is possible that both glycine and taurine are present in striatum and could act as the endogenous ligand at cGlyRs. Experimental approaches to isolate the contribution of each transmitter would not be straightforward. Previous studies have used incubation of tissue in glycine oxidase to remove extracellular glycine and then investigate the presence of glycine-mediated currents recorded using electrophysiology (Bossi, Dhanasobhon et al. 2022). However, this approach is incredibly expensive, and negative result (i.e. a strychnine-sensitive cGlyR tone is still present) would be difficult to interpret as either the tone being mediated by taurine, or the enzymatic degradation approach being insufficient. Removing taurine from the slice is also difficult; GES is a taurine transport inhibitor that is also a reversible antagonist of cGlyRs (Sergeeva, Chepkova et al. 2003), and requires incubation of the slice in GES followed by incubation of the slice in GES-free aCSF for one hour to ensure cGlyRs are still active (Choe, Olson et al. 2012). Both glycine and taurine are likely released from astrocytes, and so an upstream approach of targeting astrocytes (e.g. using flurocitate to selectively ablate astrocytes) will also not provide any additional information, as well as residual glycine/taurine likely being present in the slice – or extracellular concentrations even increasing as supported by the GlyT1 inhibition data (Fig. 3.3). However, this is an interesting question that would help to expand our understanding of striatal gliotransmission and warrants further investigation.

3.4.5. Summary

In summary, we have shown that both classical and excitatory glycine receptors are able to modulate striatal DA release. This is likely to be regulated by an ambient glycine tone regulated by astrocytic GlyT1 but taurine is another candidate ligand that may also act at these receptors. The effects of eGlyRs are dependent on nAChRs, showing another indirect regulatory mechanism of DA release via ChIs. Overall, these findings will aid our understanding of the local regulatory mechanisms that control DA release at the axonal level, including through the involvement of astrocytes. It has been difficult to dissect the contribution of cGlyRs and eGlyRs (and now account for the contribution of

mGlyRs) due to the lack of receptor-specific ligands. My data show that both cGlyRs and eGlyRs have powerful regulatory effects in striatum.

More broadly, this has highlighted the diversity of neurotransmitters and regulatory mechanisms that are able to regulate DA release. This chapter has identified a novel mechanism via the recently identified eGlyR that again shows the importance of indirect regulation of DA release. Future work should investigate whether this mechanism is altered in models of Parkinson's disease, and whether this may represent a new therapeutic target. The identification of an endogenous cGlyR tone modulated by the activity of astrocytic GlyT1 is similar to previous findings of a striatal GABA tone regulated by astrocytic GATs (Roberts, Doig et al. 2020). Furthermore, GAT function was reduced in a mouse model of Parkinson's disease, and the activity of GlyT1 should also be investigated in this model as well. However, it is also important to progress this research *in vivo* to further understand the contribution of these mechanisms in an intact system to regulate DA release. Finally, these findings should be of interest to pharmaceutical companies exploring new targets to develop receptor-specific tool compounds, to help elucidate these mechanisms and may form the basis of new therapeutics for patients.

In **Chapter 4**, I test how glycinergic signalling affects ChIs.

Chapter 4: Classical and Excitatory Glycine Receptors Regulate Cholinergic Interneuron activity

4.1. Introduction

4.1.1. Cholinergic interneuron regulation of DA release

ACh is a powerful, local regulator of DA release within the striatum, mediated via nAChRs expressed directly on DA axons. ACh is able to modulate DA release, and also drive DA release (Rice and Cragg 2004, Threlfell, Lalic et al. 2012). Synchronised stimulation of a small population of ChIs is able to directly generate action potentials in DA axons (Liu, Cai et al. 2022) and evoke DA release via nAChR activation, independently of DA neuron somatodendritic activity (Threlfell, Lalic et al. 2012). After nAChRs have been activated, subsequent DA release is transiently limited and so evoked DA release become independent of neuronal firing rate (Rice and Cragg 2004). When nAChRs are inactive, DA release more faithfully corresponds to stimulus intensity or neuronal firing rate (Exley and Cragg 2008). Thus, not only can ChIs regulate DA neurotransmission via ACh release, but altering the activity of ChIs would be expected to alter DA neurotransmission. Indeed, ChIs can be a gate or mediator through which many striatal neurotransmitters, modulators and receptors can gate DA release (Hartung, Threlfell et al. 2011, Stouffer, Woods et al. 2015, Kosillo, Zhang et al. 2016).

Data presented in Chapter 3 indicates that glycine regulates striatal DA release through multiple striatal GlyR types, in part mediated through effects that depend on ACh action at nAChRs. In this chapter, I explore how cGlyRs and eGlyRs govern activity in ChIs and control ACh release and test the hypothesis that cGlyRs expressed on ChIs inhibit ACh release, whilst eGlyRs facilitate ACh release.

4.1.2. Glycinergic Regulation of Cholinergic Interneurons

Previous studies have investigated cGlyR expression and function on ChIs. Immunohistochemical evidence has identified cGlyRs on ChIs in rat (Darstein, Landwehrmeyer et al. 2000), and single-cell RT-PCR has shown expression of the α2, α3, and β cGlyR subunits in both rat and mouse (Sergeeva and Haas 2001). Functional strychnine-sensitive glycine currents have also been observed in striatal ChIs, which are also gated by taurine (Sergeeva and Haas 2001). These studies

demonstrate the presence and function of cGlyRs on ChIs, making cGlyR activity a candidate for indirect regulation of striatal DA neurotransmission.

There have also been a small number of studies that have investigated the effects of glycine on ACh release. These have measured the release of radiolabelled ACh loaded into rat striatal tissue upon application of glycine. Two studies found that glycine was able to evoke ACh release (Taylor, Tsai et al. 1988, Hernandes, de Magalhaes et al. 2007). These provide evidence that glycine can evoke ACh release, supporting a hypothesis that glycine may indirectly regulate DA release via modulation of ACh release. However, these studies were restricted to sampling at 3- and 6-minute intervals, and the underlying mechanism mediating ACh release was unclear.

4.1.3. Recording ACh levels using $GRAB_{ACh}$

Until recently, it has been difficult to measure ACh release with sub-second temporal resolution. Unlike DA, ACh is not electroactive and so cannot be directly detected using FSCV or amperometry. However, $GRAB_{ACh}$ is a recently developed fluorescent sensor that can be used to detect extracellular ACh (Jing, Zhang et al. 2018). In this chapter, I use this sensor to investigate how glycinergic signalling alters ACh release, with a significantly greater temporal resolution than previous approaches. I explore use of this sensor to record evoked ACh release but also ambient, non-evoked ACh levels, similar to those observed in previous studies using radiolabelled ACh efflux from striatal tissue (Taylor, Tsai et al. 1988, Hernandes, de Magalhaes et al. 2007). It should be noted that we are still exploring and optimising our use of the GRAB family of sensors, and have not yet taken a precautionary approach to probe whether GRAB-ACh signals are exclusive to this sensor and are not also evident in the mutant control sensor, the non-ligand binding mutant control. Since the cpGFP reporter of the GRAB sensor is located intracellularly, the sensor is also potentially sensitive to changes in redox state and pH (Wu, Cui et al. 2023), and also temperature, which might disproportionately impact on low level or slowly fluctuating signals.

4.1.3. Excitatory glycine receptor regulation of ChIs

The recently described excitatory GlyRs (eGlyRs) are cation permeable ion channels consisting of NMDA-R subunits that only contain glycine binding sites, and therefore are gated by glycine. They have only recently been described, and have to date have been identified in interneurons in cortex, BLA, and medial habenula, where their function appears to hold interneurons at a more depolarised potential to facilitate AP firing (Otsu, Darcq et al. 2019, Bossi, Dhanasobhon et al. 2022). eGlyR expression and function in the striatum has not yet been investigated but we might speculate about their potential role here given that earlier studies have shown that glycine evokes ACh release (Taylor, Tsai et al. 1988, Hernandes, de Magalhaes et al. 2007). Indeed, the Allen Brain Atlas ISH data shows that eGlyR subunit gene *Grin3a* is expressed in striatum (Allen Institute for Brain Science, 2011, Experiment: 73907499) with a distributed and punctate pattern that is consistent with expression in a sparse population of striatal interneurons. In cortex, eGlyRs were found in SST+ interneurons (Bossi, Dhanasobhon et al. 2022). The striatum contains a sparse population of SST+ interneurons, but also a sparse population of ChIs, and our hypothesis was that eGlyRs might be expressed on ChIs through which they might mediate the excitatory effects of glycine. To visualise the distribution of GluN3A subunit expression, RNAscope was performed in collaboration with Prof. Dinos Meletis at the Karolinska Institutet.

4.1.4. Synthesis from Chapter 3

My FSCV results show that the effect of glycine is altered in DHβE, mediating a loss of rebound of DA release upon wash-off. The effect of CGP-78608 on DA release was entirely dependent on DHβE, showing that it is mediated via nAChRs. However, the effect of strychnine was unaltered in DHβE. This suggests that eGlyRs regulate the activity of ChIs, and the release of ACh, altering the activation state of nAChRs, which may then contribute to the rapid initial decline in DA release. The aim of this chapter is to investigate how glycine controls the activity of ChIs, and the contributions that cGlyRs and eGlyRs each play, that may then indirectly alter DA release.

4.2. Methods

4.2.1. Animals and slice preparation

For experiments using GRAB sensor imaging, 9-17 week old, mixed-sex, wild-type C57BL6/J mice (Charles River) were used. These underwent intracranial injection 3-5 weeks previously with an AAV-vector viral construct into either dlCPu (ML ± 2.2 mm, AP + 0.7 mm, DV -2.7- -2.5 mm) or NAc (ML ± 0.9 mm, AP + 1.35 mm, DV -3.8- -3.5 mm), as described in **Section 2.2.3**. The sensors used in this chapter (including pilot experiments) are listed in **Table 4.1**. For experiments using electrophysiology where ChIs were labelled for visualisation, heterozygous *ChAT*-Cre mice between 10-16 weeks of age were used. These underwent intracranial injection 3 weeks before use with an AAV-vector viral construct into dorsal striatum (ML ±1.75 mm, AP + 0.8 mm, DV -2.40). Acute coronal *ex vivo* slices were prepared as described in **Section 2.2.1**. All experimental procedures were carried out in accordance with University of Oxford guidelines and the UK Animals (Scientific Procedures) Act 1986.

4.2.2. GRAB Imaging

GRAB sensor imaging was used to record evoked and baseline fluorescence. These experiments were performed as described in **Section 2.3.3**. Each experiment was performed in an individual site in either dlCPu or NAc of each slice. Neurotransmitter release was evoked using electrical stimulation as described in **Section 2.2.5**, with single pulse stimulation delivered every 2.5 minutes. A baseline of at least 3 stimulations was collected before performing drug application, with up to 6 stimulations performed as the experimental protocol was refined over the course of this project. Evoked neurotransmitter release was recorded at a frequency of 100 Hz, with an image exposure time of 10 ms and pixels binned 2x2 to reduce image size. Excitation light (470 nm) was used at a power of ~5 mW and turned on continuously over the course of recording each stimulation every 2.5 min.

For experiments recording non-evoked DA levels, excitation light (470 nm) was used at a power of ~5 mW and turned on for a duration of 1 sec every 30 sec or 5 sec where indicated, obtaining an image with exposure time of 10 ms. Pixels were binned 2x2 to minimise image file size. A baseline of 5 minutes fluorescence was collected before drug application for most experiments, with some pilot experiments using a shorter duration baseline as the experimental protocol was refined.

Data were extracted and analysed as described in **Section 2.3.4**, from a 100 µm square ROI . For evoked recordings, the data points binned for analysis are indicated in the wash-on data for each experiment by highlight with a grey box. Unless otherwise indicated, these are three values of evoked ACh release in a given condition that are binned to give a single value for comparative analysis for each replicate in an experiment. For non-evoked recordings, the peak F/F_0 values used in statistical analysis was the maximal value observed during drug application. For each experiment, $n \geq 3$ animals unless where indicated. Statistical analysis was performed using GraphPad Prism, using unpaired t-tests, paired t-tests, one-way RM ANOVA, and *post hoc* Tukey's multiple comparisons tests where indicated.

4.2.3. RNAscope (Dr Ioannis Mantas & Ms Vasiliki Skara)

FISH (RNAscope™) was performed using the RNAscope™ Multiplex Fluorescent Detection Kit v2 (Advanced Cell Diagnostics, Cat. No 323110). Cryostat (Leica CM 3050 S) fresh-frozen thaw mounted sections (12 µm thick) were post-fixated with 4% paraformaldehyde (dissolved in 1× PBS). The slides were dehydrated with graded ethanol solutions (80%, 90%, 95% and 100%). Protease IV Reagent (Advanced Cell Diagnostics) was then applied for 30 min at room temperature. Afterwards, the sections were hybridized for 2 h at 40 °C with the following probes: Mm-Grin3a (Cat No. 551371), Mm-Glra2 (Cat No. 510301), Glra3 (Cat No. 490591), Mm-Chat (Cat No. 408731-C2), Mm-Npy (Cat No. 313321-C3). The hybridization step was followed by standardized steps of amplification (Amp 1-FL 30 min at 40 °C, Amp 2-FL 15 min at 40 °C, Amp 3-FL 30 min at 40 °C, HRP for each channel 15 min at 40 °C, TSA-Fluo for each channel 5 min at 40 °C, HRP-blocker for each channel 20 min at 40 °C) . The last amplification step was followed by DAPI (Advanced Cell Diagnostics) counterstaining and mounting with Dako fluorescent mounting medium. For quantifying the number of cells, the brain

sections were imaged on a Carl Zeiss LSM 880 confocal microscope using a 20 × 0.8 NA objective. For close-up images, a 63 × 1.4 NA oil immersion objective was used. We used Imaris 7.4.2 to count the cells. First, we applied background substruction for each channel separately. For Chat and Npy channels, the cells were automatically segmented in spherical ROIs (15 µm diameter) according to fluorescent filter applied by the software. The quality of the segmentation was evaluated, and false positive or negative cells were removed or added manually. After that, we applied defined Grin3a, Glra2 or Glra3 positive cells by applying fluorescent threshold only in the Chat or Npy positive ROIs defined by the previous process. The fluorescent threshold was selected according to the number of the fluorescent dots per cell. Cells with less than 3 fluorescent dots were considered negative. False positive or negative cells that occurred form fluorescent thresholding process were removed or added manually.

4.2.4. Electrophysiology (Drs Jeffrey Stedehouder & Simon Bossi)

4.2.4.1. Whole-cell recording of ChI firing rate – Dr Jeffrey Stedehouder

Acute brain slices for patch clamp electrophysiology were obtained from 8-16-week-old mice using standard techniques. Anesthesia was induced within ~2 hrs after start of light ON period of light cycle using sodium pentobarbital and mice were decapitated in ice-cold, NMDG-based cutting solution containing (in mM): 93 N-methyl-d-glucamine (NMDG), 93 HCl, 30 $NaHCO_3$, 25 D-glucose, 20 HEPES, 5 Na-ascorbate, 2 thiourea, 7 $MgCl_2$, 3 Na-pyruvate, 2.5 KCl, 1.25 NaH_2PO_4 and 0.5 $CaCl_2$ (310 mOsm, pH 7.4) oxygenated with 95% O_2/5% CO_2 before decapitation. After decapitation, the brain was quickly dissected on ice. Coronal 300 µm slices containing the striatum (bregma: +1.50 till +0.50 mm) were cut with a vibrating slicer (Leica VT1200S) and incubated in cutting solution at 34°C for 15 min., followed by oxygenated (95% O2/5% CO2) aCSF at 34°C for 15 min. aCSF contained (in mM) 127 NaCl, 25 $NaHCO_3$, 25 D-glucose, 2.5 KCl, 1.25 NaH_2PO_4, 1.5 $MgSO_4$ and 1.6 $CaCl_2$. Slices were allowed to recover at room temperature for at least 1 hr before recordings.

mCherry-positive cholinergic interneurons (ChIs) in NAc (within <200 µm from anterior commissure) were identified using a TXRed filter. Whole-cell recordings were made from using borosilicate glass pipettes (3–6 MΩ resistance) with intracellular solution containing (in mM) 120 K-

gluconate, 10 KCl, 10 HEPES, 10 K-phosphocreatine, 4 ATP-Mg, and 0.4 GTP (pH was adjusted to 7.4 using KOH, and osmolarity measured ~290 mOsm). Recordings were performed in aCSF at near-physiological temperatures (32–33°C) using a Multiclamp 700B amplifiers and Digidata 1440A acquisition board digitized at 20 kHz sampling rate. Data were acquired using Clampex 10.0.

Series resistance was typically <20 MΩ and fully compensated for bridge balance and capacitance; recordings in which the series resistance exceeded 20 MΩ were not included in the averages. No correction was made for liquid junction potential. Data analysis was performed offline using custom written Python software.

To examine firing rate changes in response to glycine/drug application, ChIs were held in current clamp with a holding potential of 0-100 pA for a stable spontaneous firing rate between 0.5-5 Hz. For glycine-only experiments, following a 30-second baseline recording, glycine (10 mM) dissolved in ACSF was bath perfused, followed by a washout after 3 mins. For combined drug experiments, following a 30-second baseline recording, CGP78608 (2 μM) and strychnine (10 μM) dissolved in ACSF were bath perfused, followed by additional bath perfusion of glycine (10 mM), similarly dissolved in ACSF. All drugs were washed out after 5.5 mins.

4.2.4.2. Cell-attached recording of cGlyR currents – Dr Simon Bossi

Adult (>2 months old) mice were culled by cervical dislocation before decapitation. The brain was quickly removed and immerged in an ice-cold cutting solution containing (in mM): 86 NaCl; 2.5 KCl; 25 Na_2HCO_3; 1.2 Na_2HPO_4; 25 Glucose; 75 Sucrose, 7 $MgCl_2$ and 0.5 $CaCl_2$. The cutting solution was continuously bubbled with a 95% O_2/ 5% CO_2 mix, equilibrating the pH at 7.3-7.4. Coronal brain slices (300 μm) containing the striatum were cut using a vibratome (VT1200S, Leica Microsystems) in ice-cold cutting solution. Slices were then transferred for 30 minutes in warm artificial cerebrospinal fluid (ACSF) containing (in mM): 127 NaCl; 2.5 KCl; 25 Na_2HCO_3; 1.25 Na_2HPO_4; 25 Glucose; 1.5 $MgSO_4$ and 1.6 $CaCl_2$ (34°C) before placing them for the rest of the experimental day in ACSF at room temperature.

For electrophysiological recordings in striatum, brain slices were moved to a recording chamber on an Olympus BX51WI microscope and continuously perfused with oxygenated ACSF (2mL/min; 30-34°C). Recorded neurons were located in the dorsolateral part of the striatum and were visually identified using an Iris 9 Scientific CMOS camera (Teledyne Photometrics, USA) run by Micro-Manager 1.4 (NIH, USA). For whole-cell experiments, patch pipettes (4-7 MΩ tip resistance) were filled with an intracellular solution containing (in mM): 120 K-Gluconate; 10 KCl; 10 HEPES; 10 K-phosphocreatine, 4 Mg-ATP; 0.4 Na_3-GTP, pH 7.4 with KOH (290 mOsm). Whole-cell recordings were carried out using a Multiclamp 700B amplifier (Molecular Devices, United Kingdom) run by the Multiclamp 700B interface and Digidata 1440A (Molecular Devices, United Kingdom) acquisition board digitized at 20 kHz sampling rate. Data were acquired using Clampex 10.0. In the whole-cell configuration, series resistances were compensated up to 65% maximum.

For puff experiments, glycine (10 mM) was puffed locally at the surface of the slice near the recorded cell through a pipette (3-5 MΩ tip resistance; 1000 msec puff duration) with a pneumatic drug ejection system [PicoPump PV 830 (WPI, Germany)]. During glycine puff experiments, the extracellular batch solution and the puff pipettes contained antagonists of $GABA_A$ (10 µM Bicuculine), glycine (10 µM strychnine), AMPA (10 µM NBQX) and NMDA (50 µM D-AP5) receptors as well as TTX (200 nM). With the exception of glycine, all the drugs were bath applied: D-AP5 (HelloBio or Abcam), NBQX (Abcam), Bicuculline (Cayman Chemical), Strychnine (Abcam), TTX (Abcam), CGP-78608 (Tocris), 5,7-Dichlorokynurenic acid (DCKA; Tocris).

4.2.5 Drugs

Drugs were dissolved in either diH_2O or sodium hydroxide (NaOH) to 1000x aliquots and stored frozen at -20°C. On the day of experiments, these were diluted in oxygenated aCSF to their working concentration immediately before use. 10 mM glycine was made up on the morning of each experiment due to a maximum solubility of 100 mM. The final concentrations used and source of each drug are shown in **Table 4.2.**

Table 4.1. Viruses used in Chapter 4

Viral Construct	Volume	Titre	Supplier	Product Code	Function
AAV5-hsyn-$GRAB_{ACh.3.0}$	1000 µl per hemisphere	0.8 $x10^{13}$ gc/ml	BrainVTA	PT-1335	Detection of ACh
AAV5-hsyn-$GRAB_{ACh.3.0.Mut}$	1000 µl per hemisphere	~ 0.2 x 10^{13} gc/ml	BrainVTA	PT-1336	Control sensor, insensitive to ACh binding
AAV5-hysn-$GRAB_{DA.2m}$	1000 µl per hemisphere	0.8 $x10^{13}$ gc/ml	WZ Biosciences	YL002009-AV5	Detection of DA
AAV5-hsyn-DIO-mCherry	1000 µl per hemisphere	1.3 $x10^{13}$ gc/ml	ETH Viral Vector Facility	v214	Labelling of ChIs for electrophysiology recordings

Table 4.2. Drugs used in Chapter 4

Drug	Supplier	Action	Concentration	References
Glycine	Sigma-Aldrich & SLS Labs	GlyR agonist	1-10 mM	(McCracken, Lowes et al. 2017)
Strychnine	Abcam	cGlyR antagonist	10 µM	(Häusser, Yung et al. 1992)
Sarcosine	Sigma-Aldrich	GlyT1 inhibitor	500 µM	(McCracken, Lowes et al. 2017)
Taurine	Alfa Aesar	cGlyR partial agonist	10 mM	(Sergeeva and Haas 2001)
CGP-78608	Tocris Bioscience	GluN1 antagonist	2 µM	(Bossi, Dhanasobhon et al. 2022)
DCKA	Tocris Bioscience	GluN3A antagonist	500 µM	(Bossi, Dhanasobhon et al. 2022)
TTX	Tocris Bioscience	Voltage-gated Na^+ channel blocker	200 nM - 1 µM	(Roberts et al., 2020)
D-AP5	HelloBio & Abcam	NMDA-R antagonist	50 µM	(Bossi, Dhanasobhon et al. 2022)
NBQX	Abcam	AMPA-R antagonist	10 µM	(Bossi, Dhanasobhon et al. 2022)
Bicuculline	Cayman Chemical	$GABA_AR$ antagonist	10 µM	(Bossi, Dhanasobhon et al. 2022)

4.3. Results

4.3.1. Strychnine increases evoked ACh release

Given the previous evidence for strychnine-sensitive classical glycine receptors (cGlyRs) expressed on ChIs, I investigated whether strychnine alters evoked ACh release. I found that strychnine did not significantly alter peak of ACh transients evoked by a single pulse (1p) (**Fig. 4.1A**) but did increase the area under the curve (AUC) of ACh transients (**Fig. 4.1B-D**, AUC, paired t-test, $p = 0.017$, $n = 4$ slices/animals). This is consistent with our previous findings using the GRAB sensors that manipulations expected to increase the amplitude of neurotransmitter release (e.g. GABA-receptor antagonist) can manifest as increases in AUC rather than $\Delta F/F_0$ peak release (Dr Stefania Vietti-Michelina, personal communication). Strychnine did not significantly alter baseline fluorescence (**Fig. 4.1E**, F_0, paired t-test, $p = 0.60$, $n = 4$ slices/animals).

4.3.2 Classical glycine receptor RNAscope data (Dr Ioannis Mantas & Ms Vasiliki Skara)

We explored the expression of cGlyRs on ChIs. Prior immunohistochemical studies against cGlyR α subunits, and RT-PCR for specific subunits of cGlyRs have previously shown expression of α2 and α3 subunits in ChIs (Darstein, Landwehrmeyer et al. 2000, Sergeeva and Haas 2001). We collaborated with Prof. Dinos Meletis and his lab at the Karolinska Intitutet, who performed RNAscope (Dr Ioannis Mantas and Ms Vasiliki Skara) to investigate the expression of the *Glra2* and *Glra3* genes that encode the α2 and α3 subunit of cGlyRs in ChIs (using expression of gene for choline acetyltransferase *Chat* as a marker). For comparison, expression of these cGlyR subunits was also tested in cells expressing NPY (using expression of neuropeptide-Y gene *Npy* as a marker). Approximately 75% NPY+ striatal neurons are SST-positive GABAergic low-threshold spiking interneurons (LTSIs), and the remaining ~ 25% are neurogliaform cells (NGFs) (Ibanez-Sandoval, Tecuapetla et al. 2011). These results show striatal expression of *Glra2* and co-expression with *Chat* or *Npy*: *Glra2* was expressed in ~ 95% of ChIs (Total *Chat*+: n = 3 animals. #1 = 329 cells, #2 = 303 cells, #3 = 352 cells)

but only ~25% of NPY+ cells (Total *Npy*+: n = 3 animals. #1 = 358 cells, #2 = 353 cells, #3 = 339 cells), without a clearifference along the rostral-caudal axis. Similarly for *Glra3*, there is striatal co-expression of *Glra3* with *Chat* or *Npy: Glra3* was expressed in ~85% of ChIs (Total *Chat*+: n = 3 animals. #1 = 302 cells, #2 = 319 cells, #3 = 349 cells) and ~5% of NPY+ cells (Total *Npy*+: n = 3 animals. #1 = 309 cells, #2 = 420 cells, #3 = 383 cells). These data support previous findings that cGlyRs are found in ChIs, and show for the first time the expression of cGlyRs in a subset of NPY+ cells. The presence of cGlyRs in ChIs provides a site through which cGlyR antagonist strychnine can inhibit ACh release (**Fig. 4.1**). but perhaps ultimately has an insignificant effect on DA release (**Fig. 3.2**).

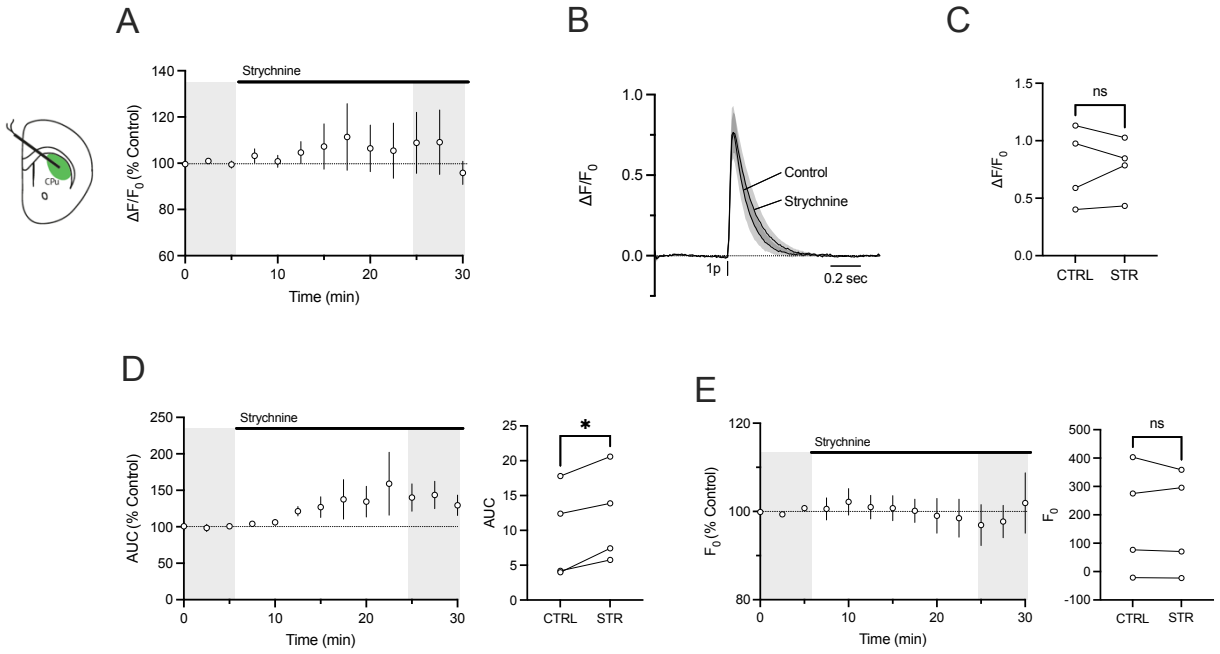

Figure 4.1. Strychnine increases evoked ACh release

- **(A)** Mean (±SEM) peak $\Delta F/F_0$ of evoked ACh release in dlCPu before and after application of strychnine. n = 4 slices/animals.
- **(B)** Mean (±SEM) transient $\Delta F/F_0$ of evoked ACh release in dlCPu before and after application of strychnine. n = 4 slices/animals.
- **(C)** Mean peak $\Delta F/F_0$ of evoked ACh release before and after application of strychnine. Paired t-test; p = 0.98 (n.s.), n = 4 slices/animals.
- **(D)** *Left:* Mean (±SEM) AUC of evoked ACh release in dlCPu before and after application of strychnine. *Right:* Mean AUC of evoked ACh release in dlCPu before and after application of strychnine. Paired t-test; p = 0.017 (*), n = 4 slices/animals.
- **(E)** *Left:* Mean (±SEM) F_0 of evoked ACh release in dlCPu before and after application of strychnine. *Right:* Mean F_0 of evoked ACh release in dlCPu before and after application of strychnine. Paired t-test; p = 0.60 (n.s.), n = 4 slices/animals.

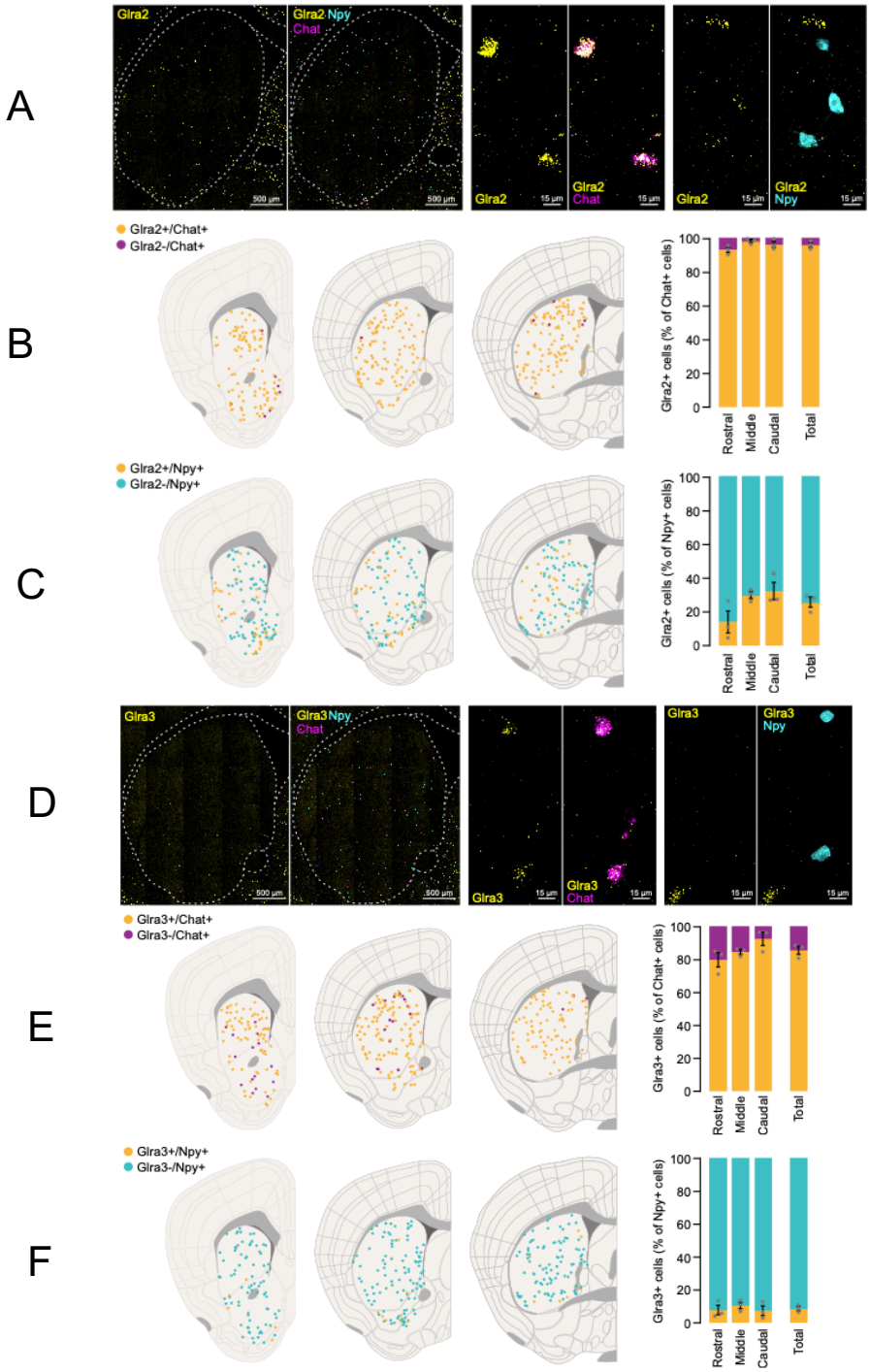

Figure 4.2. Glra2 and Glra3 are expressed in ChIs and *Npy*+ cells

(A+D) Representative images showing Glra2 (A) and Glra3 (D) expression within a coronal striatal slice, and co-expression for Chat and npy as markers for ChIs and *Npy*+ cells respectively.

(**B+E)** *Left:* Diagrams depicting distribution of ChIs and co-expression of Glra2 (B) or Glra3 (E) in striatum across a rostral to causal axis. *Right*: Quantification of ChIs either positive or negative for Glra2 (B) or Glra3 (E) co-expression, across a rostral to caudal axis. n = 3 animals

(**C+F**) *Left:* Diagrams depicting distribution of *Npy*+ cells and co-expression of Glra2 (C) or Glra3 (F) in striatum across a rostral to causal axis. *Right*: Quantification of *Npy*+ cells either positive or negative for Glra2 (C) or Glra3 (F) co-expression, across a rostral to caudal axis. n = 3 animals

Data collected and analysed by Dr Ioannis Mantas and Ms Vasiliki Skara

4.3.3. Sarcosine does not alter evoked ACh release

I previously found that sarcosine (GlyT1 inhibitor) application alone was not sufficient to alter DA release, but enhanced the effect of cGlyR antagonist strychnine, suggesting an effect on the ambient striatal glycine tone. Here, I investigated whether sarcosine could alter evoked ACh release. However, sarcosine did not significantly alter evoked ACh release (**Fig. 4.3A-C**, $\Delta F/F_0$, paired t-test, p = 0.76, n = 4 slices/animals), or baseline fluorescence F_0 (**Fig. 4.3D-E**, F_0, paired t-test, p = 0.21, n = 4 slices/animals). These data are consistent with the results showing that sarcosine alone cannot alter DA release, and it would be interesting for future experiments to explore whether sarcosine can enhance the effect of strychnine on ACh release.

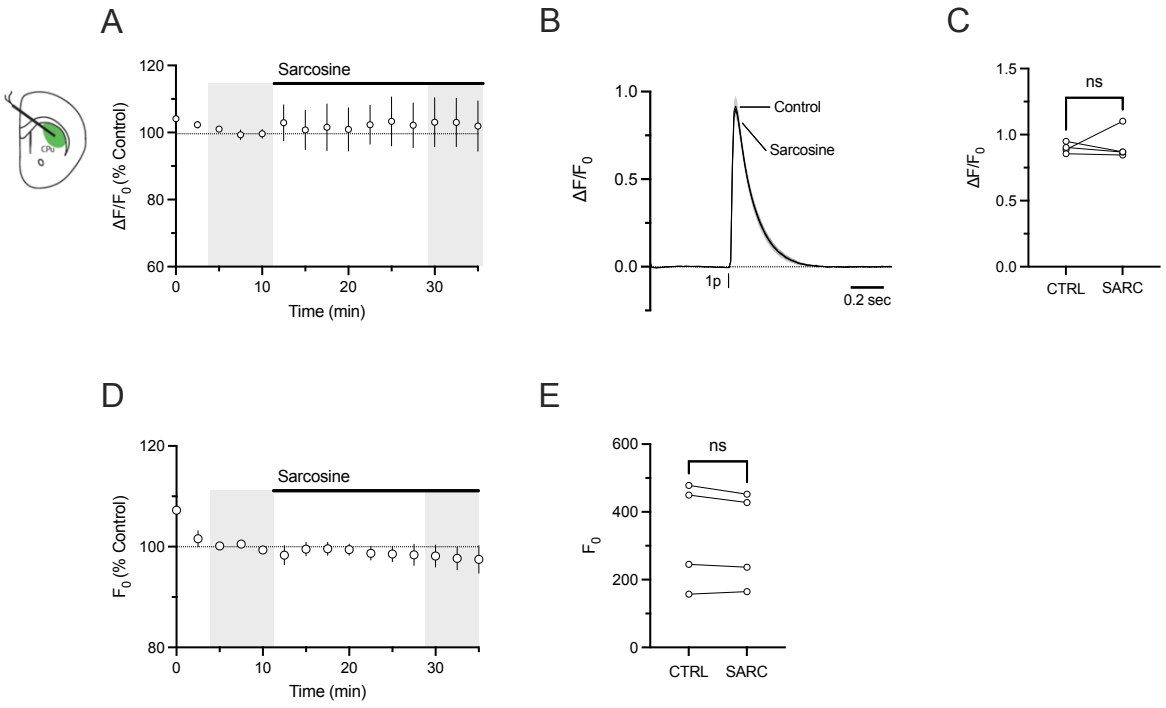

Figure 4.3. Sarcosine does not alter evoked ACh release

(A) Mean (±SEM) peak $\Delta F/F_0$ of evoked ACh release in dlCPu before and after application of sarcosine. n = 4 slices/animals.
(B) Mean (±SEM) transient $\Delta F/F_0$ of evoked ACh release in dlCPu before and after application of sarcosine. n = 4 slices/animals.
(C) Mean peak $\Delta F/F_0$ of evoked ACh release before and after application of sarcosine. Paired t-test; p = 0.76 (n.s.), n = 4 slices/animals.
(D) Mean (±SEM) ΔF and F_0 of evoked ACh release in dlCPu before and after application of sarcosine. n = 4 slices/animals.
(E) Mean F_0 of evoked ACh release before and after application of sarcosine. Paired t-test; p = 0.21 (n.s.), n = 4 slices/animals.

4.3.4. Brief glycine application reduces evoked ACh levels

In **Chapter 3**, I found that glycine exhibited multiphasic effects on DA release. Glycine caused an initial decrease of DA release, with varying onset kinetics, and this inhibition was partially reversible when nAChRs were operating, but was persistent in the absence of nAChRs effects or upon continued application of glycine (**Fig. 3.8**). The long-acting component appeared to be mediated via adenosine receptors (**Fig. 3.15**). To understand the role of ACh in effects of glycine on DA release during brief exposure, I investigated whether ACh release might be altered following brief application of glycine. I focused my experiments on the dlCPu because that was the region where I observed the greatest effects of glycine. I collected only preliminary data in the NAc that is not sufficiently powered to perform statistical analysis. In dlCPu, glycine reversibly reduced evoked ACh release, with a reduction in peak $\Delta F/ F_0$ (**Fig. 4.4A-D**, one-way ANOVA, dlCPu: $F_{(1.601,6.405)} = 58.08$, $p = 0.0001$, $n = 5$ slices/animals, *post-hoc* Tukey's multiple comparisons test, (ns) $p > 0.05$, (**) $p < 0.01$, (***) $p < 0.001$), on a similar time course seen to the regulation of DA release. There is a trend towards reduction in the NAc by a similar amount.

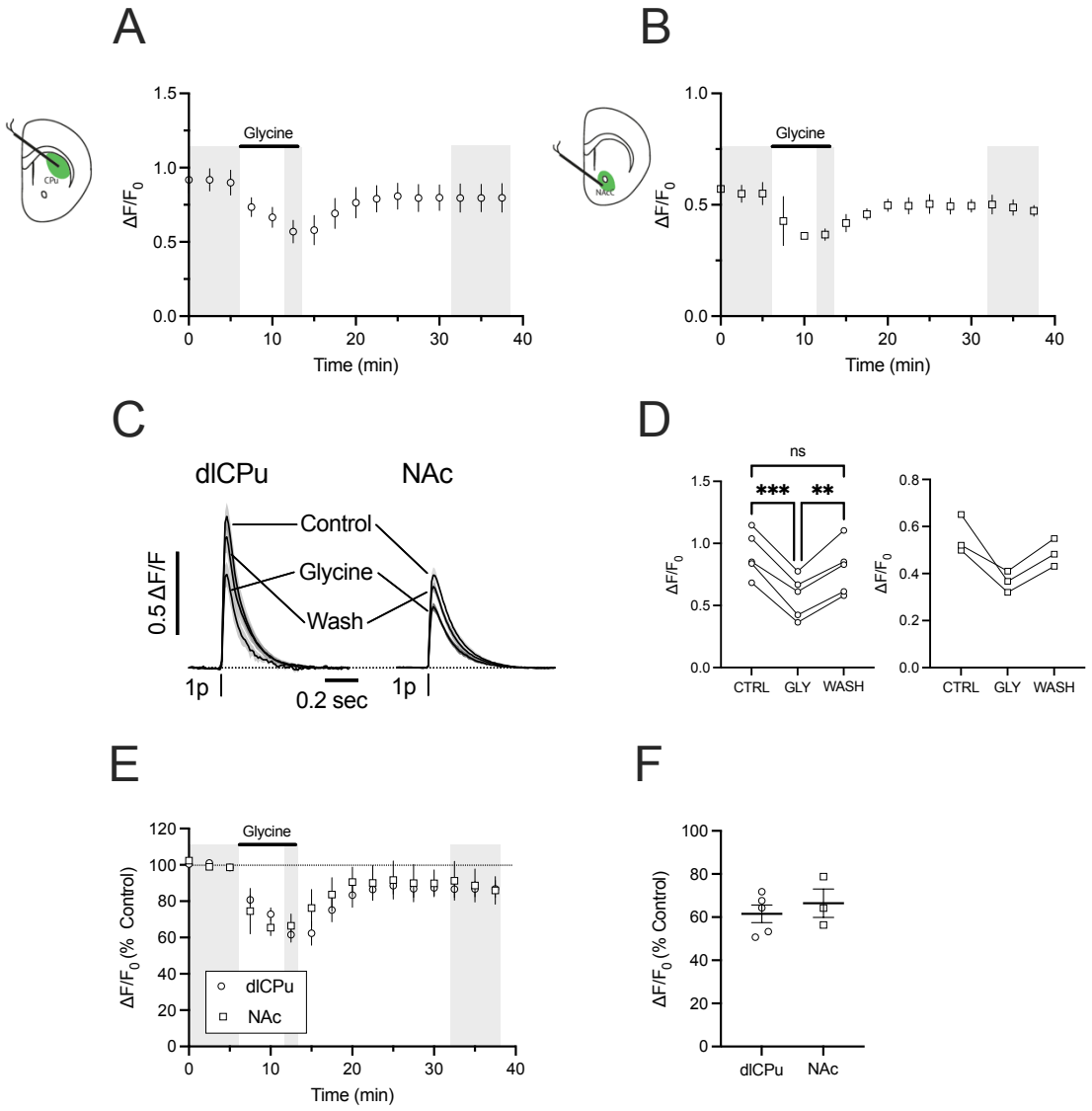

Figure 4.4. Brief glycine application reduces evoked ACh release

(A) Mean (±SEM) peak $\Delta F/F_0$ of evoked ACh release in dlCPu, before and after application of glycine. n = 5 slices/animals.

(B) Mean (±SEM) peak $\Delta F/F_0$ of evoked ACh release in NAc, before and after application of glycine. n = 3 slices/animals.

(C) Mean (±SEM) transient $\Delta F/F_0$ of evoked ACh release in dlCPu before, during, and after application of glycine in dlCPu and NAc. dlCPu: n = 5 slices/animals. NAc: n = 3 slices/animals.

(D) Mean (±SEM) peak $\Delta F/F_0$ of evoked ACh release before, during and after application of glycine. *Left*: dlCPu, One-way RM ANOVA, $F_{(1.601,6.405)} = 58.08$, p = 0.0001, n = 5 slices/animals. *Right:* NAc, n = 3 animals/slices

(E) Mean (±SEM) peak $\Delta F/F_0$ of evoked ACh release, normalised to pre-glycine control, in dlCPu and NAc, before, during after application of glycine. dlCPu: n = 5 slices/animals. NAc: n = 3 slices/animals.

(F) Mean (±SEM) peak $\Delta F/F_0$ of evoked ACh release during application of glycine in dlCPu and NAc, normalised to pre-glycine control. dlCPu: n = 5 slices/animals. NAc: n = 3 slices/animals.

4.3.5. Extended glycine reduces both ACh baseline signal and evoked amplitude

I next investigated whether prolonged glycine application produced a prolonged decline of evoked ACh release, similar to evoked $[DA]_o$. Analysis does not show a significant reduction in peak $\Delta F/F_0$ ACh release, but did show an overall reduction in AUC (**Fig. 4.5A-D,** $\Delta F/F_0$ paired t-test, p = 0.096; AUC paired t-test, p = 0.037, 5 slices/animals).However, I found that glycine significantly reduced the amplitude of the signal (**Fig. 4.5F-G, *right*)**, ΔF paired t-test, p = 0.017) but also significantly reduced the baseline of the signal (**Fig. 4.5F-G, *left*)**, F_0 paired t-test = 0.013). This is also apparent on the raw traces showing change in fluorescence in each condition upon electrical stimulation (**Fig. 4.4.E**). Since both the numerator and denominator are reducing in size, any change in the normalised value will be reduced. We hypothesised that this reduction in baseline signal would be consistent with glycine inhibiting ChI activity, reducing ambient ACh tone and therefore non-evoked $GRAB_{ACh}$-mediated fluorescence. However, this change in baseline fluorescence is a confound in analysis of the $GRAB_{ACh}$ evoked signal and would be investigated further to establish whether it reflects a change in tonic ACh levels activating the sensor, or is an artefact via interaction with the sensor.

4.3.6. The effect of glycine is concentration-dependent

I investigated whether the effect of glycine was concentration-dependent. Based on the previous analysis of the prolonged glycine application data, I divided my analysis into the effects on signal amplitude (ΔF) and baseline (F_0) for application of 1 mM glycine (**Fig. 4.6A**) and 10 mM glycine (**Fig. 4.6B** – data from **Fig. 4.5F**). I found that the reduction of both ΔF and F_0 by glycine was significantly greater by 10 mM than 1 mM glycine (**Fig. 4.6D**, ΔF, unpaired t-test, p = 0.0004; **Fig. 4.6C**, F_0, unpaired t-test, p = 0.0006; 1 mM: n = 5 slices/animals, 10 mM: n = 5 slices/animals, data from **Fig. 4.5F**). I then performed a pilot experiment to test whether the presence of strychnine would reduce the effect of glycine, but strychnine does not appear to alter the effect of glycine on either ΔF or F_0 parameters of the ACh signal (**Fig.4.6E-F**).

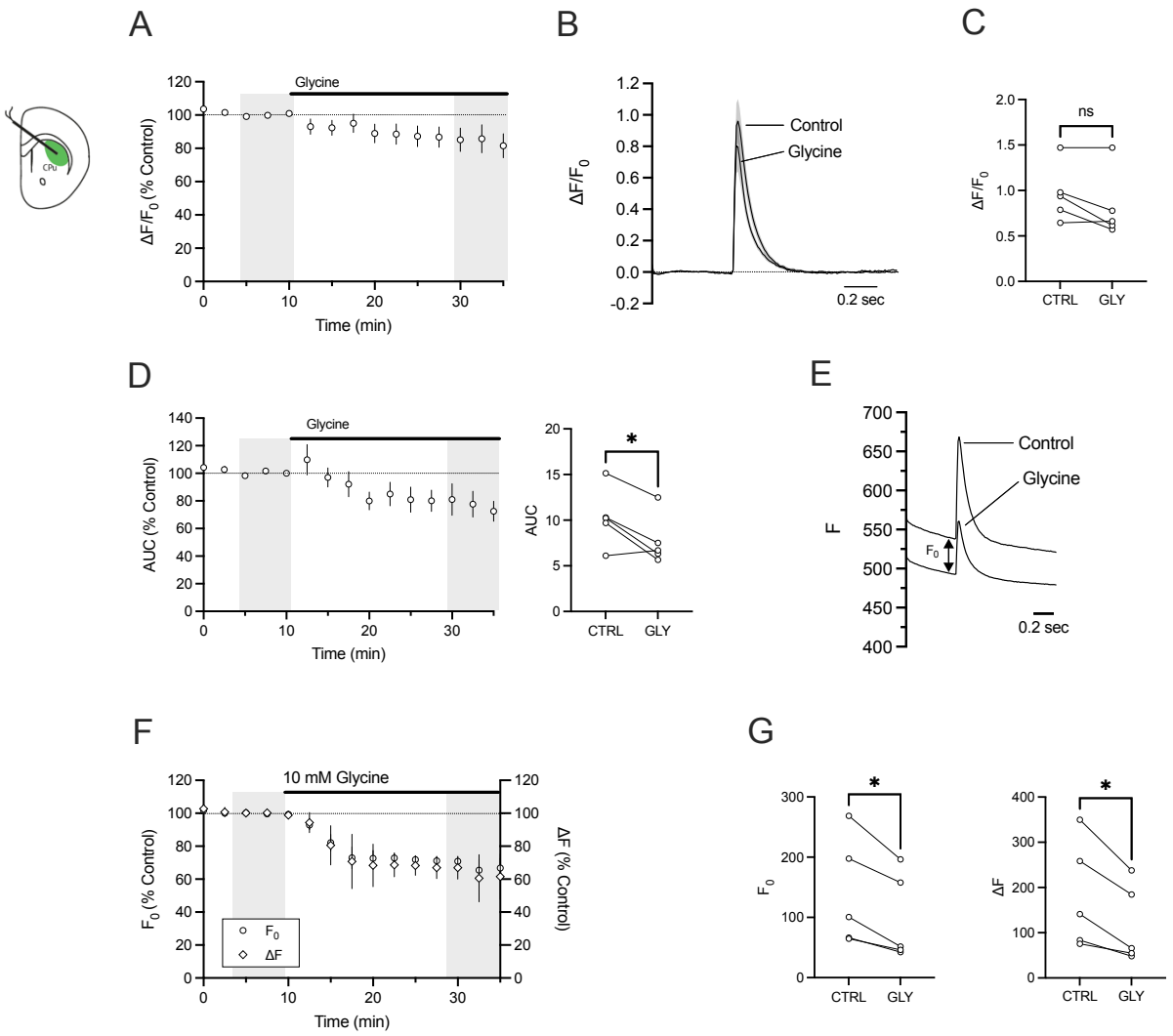

Figure 4.5. Extended glycine application reduces evoked ACh release

(A) Mean (±SEM) peak $\Delta F/F_0$ of evoked ACh release in dlCPu before and after application of glycine. n = 5 slices/animals.

(B) Mean (±SEM) transients $\Delta F/F_0$ of evoked ACh release in dlCPu before and after application of glycine. n = 5 slices/animals.

(C) Mean $\Delta F/F_0$ of evoked ACh release before and after application of glycine. Paired t-test; p = 0.096 (n.s.), n = 5 slices/animals.

(D) *Left:* Mean (±SEM) AUC of evoked ACh release in dlCPu before and after application of glycine. *Right:* Mean AUC of evoked ACh release in dlCPu before and after application of glycine. Paired t-test; p = 0.037 (*), n = 5 slices/animals.

(E) Representative transients of raw F of evoked ACh release in dlCPu before and after application of glycine.

(F) Mean (±SEM) F_0 and ΔF of evoked ACh release in dlCPu before and after application of glycine. n = 5 slices/animals

(G) *Left:* Mean F_0 of evoked ACh release in dlCPu before and after application of glycine. Paired t-test; p = 0.013 (*), n = 5 slices/animals. *Right*: Mean ΔF of evoked ACh release in dlCPu before and after application of glycine. Paired t-test; p = 0.017 (*), n = 5 slices/animals.

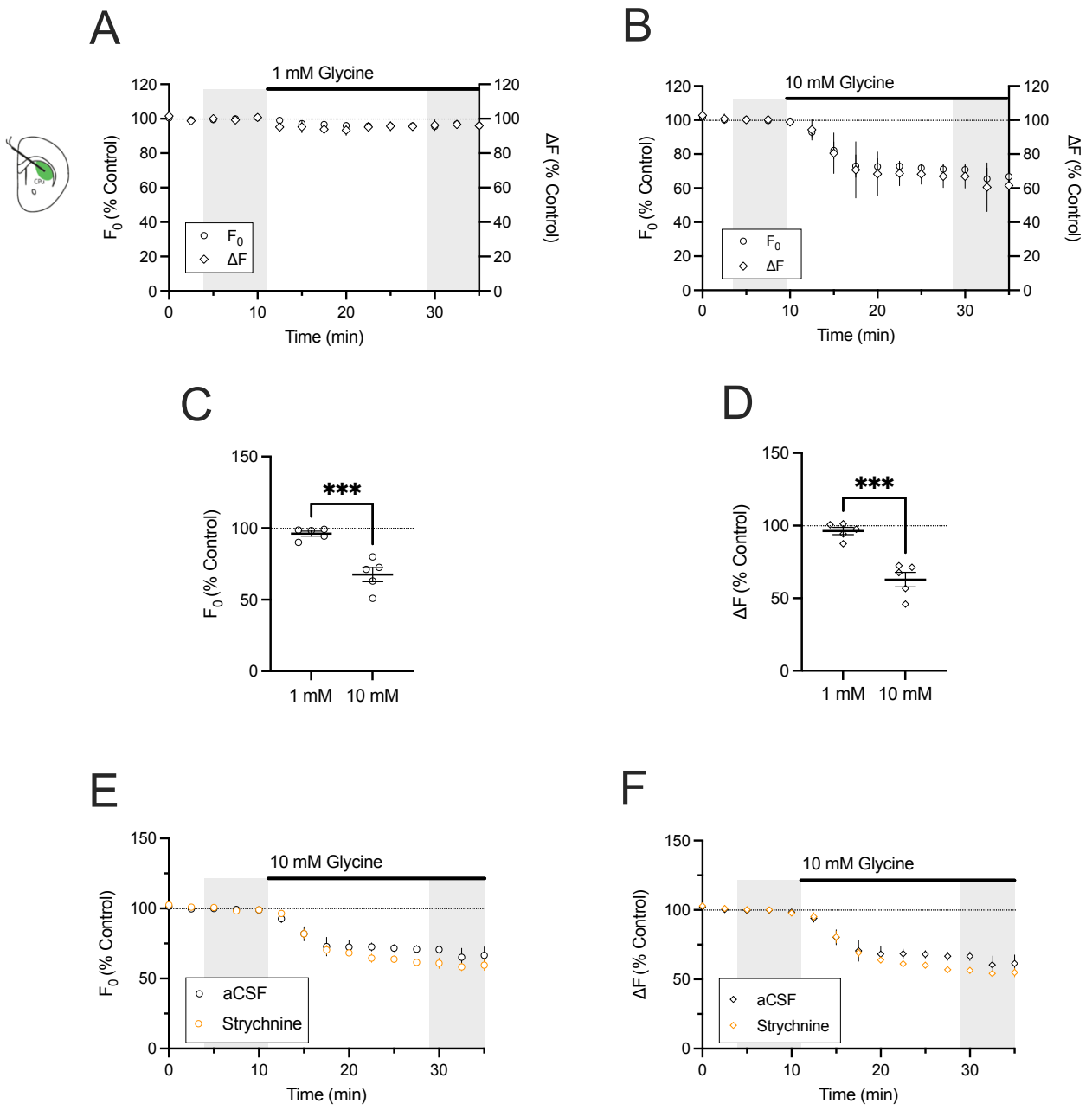

Figure 4.6. The effect of glycine is concentration-dependent

(A) Mean (±SEM) ΔF and F_0 of evoked ACh release before and after application of 1 mM glycine. n = 5 slices/animals.

(B) Mean (±SEM) ΔF and F_0 of evoked ACh release before and after application of 10 mM glycine. 10 mM: n = 5 slices/animals (from **Fig. 4.5**).

(C) Mean F_0 of evoked ACh after application of either 1 mM or 10 mM glycine. Paired t-test; p = 0.0006. 10 mM: n = 5 slices/animals (from **Fig. 4.5**), 1 mM: n = 5 slices/animals.

(D) Mean ΔF of evoked ACh release after application of 1 mM or 10 mM glycine. Paired t-test; p = 0.0004. 10 mM: n = 5 slices/animals (from **Fig. 4.5**), 1 mM: n = 5 slices/animals.

(E) Mean (±SEM) F_0 of evoked ACh release before and after application 10 mM glycine, in the presence or absence of 10 µM strychnine. aCSF: n = 5 animals/slices (from **Fig. 4.5**). Strychnine: n = 2 slices/animals.

(F) Mean (±SEM) ΔF of evoked ACh release before and after application of 10 mM glycine, in the presence or absence of 10 µM strychnine. aCSF: n = 5 animals/slices (from **Fig. 4.5**). Strychnine: n = 2 slices/animals.

4.3.7. Taurine evoked ACh release (Pilot)

Given the role of taurine as a partial agonist at cGlyRs, I conducted pilot experiments to explore whether taurine like glycine can reduce ACh release, to corroborate that the effects of glycine represent effects of cGlyR action. Taurine (10 mM) appears to reduce evoked ACh release (**Fig. 4.7A-B**), with a decrease in both ΔF and F_0 (**Fig. 4.7C**). Interestingly, the change in F_0 appears to be smaller upon application of taurine than glycine (**Fig. 4.7D-E**). This greater reduction in ΔF than F_0 may support the apparently greater reduction in $\Delta F/F_0$ for taurine than glycine. The reduction of ACh release by taurine suggests regulation via cGlyRs, which could be tested further by repeating experiments in the presence of strychnine.

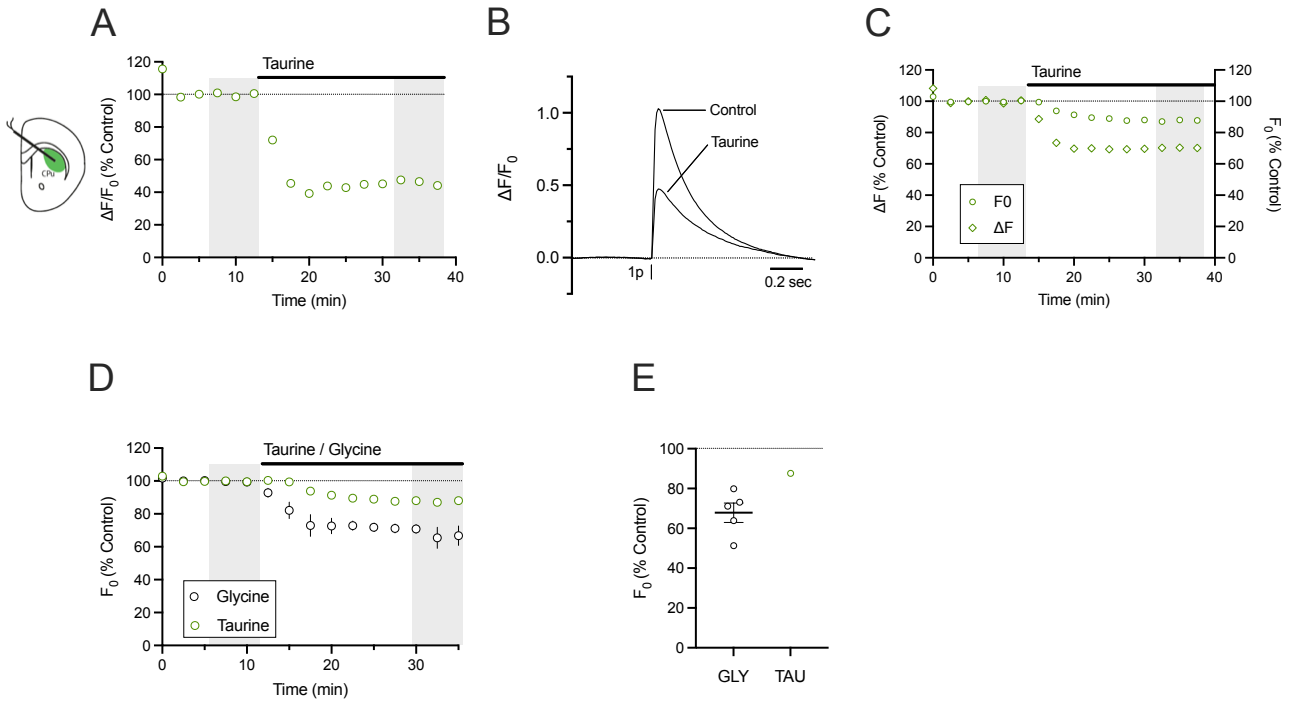

Figure 4.7. Effect of taurine on evoked ACh release

(A) Peak $\Delta F/F_0$ of evoked ACh release in dlCPu before and after application of taurine. n = 1 slice/animal.
(B) Transient $\Delta F/F_0$ of evoked ACh release before and after application of taurine. n = 1 slice/animal.
(C) Mean ± SEM ΔF and F_0 of evoked ACh release before and after application of taurine. n = 1 slice/animal.
(D) Mean (± SEM) F_0 of evoked ACh release before and after application of either taurine or glycine. Taurine: n = 1 slice/animal; Glycine: n = 5 slices/animals (data from **Fig. 4.5G**).
(E) Mean F_0 (± SEM) of evoked ACh release after application of either taurine or glycine. Taurine: n = 1 slice/animal; Glycine: n = 5 slices/animals (data from **Fig. 4.5G**).

4.3.8. Reduction of baseline fluorescence is TTX-insensitive

Having observed that glycine reduces baseline fluorescence F_0, we hypothesised this was due to glycine inhibiting tonic ChI activity, reducing the ambient striatal ACh tone. To test this hypothesis, we investigated whether this reduction was TTX-sensitive. Electrically-evoked ACh release is TTX-sensitive (Dr Stefania Vietti-Michelina, personal communication), and we hypothesised that ACh release arising from tonic activity of ChIs would also be TTX-sensitive. We found that the reduction of F_0 was present in 1 µM TTX, with no significant difference versus aCSF control (**Fig. 4.8A-C**, unpaired t-test, p = 0.78, aCSF: n = 5 slices/animals (data from **Fig. 4.5**); TTX: n = 3 slices/animals). The higher levels of absolute (not normalised) fluorescence in the representative TTX trace is due to a different recording site in a different slice being used. Our lab has previously observed that TTX itself does not alter F_0 (Dr Stefania Vietti-Michelina, personal communication). This suggests that the reduction in baseline fluorescence mediated by glycine is not via TTX-sensitive ACh release. It is possible that alternative mechanisms independent of action potentials mediate tonic ACh release may be responsible, or that other factors are changing baseline fluorescence e.g. pH, or that glycine is interacting with the $GRAB_{ACh}$ sensor.

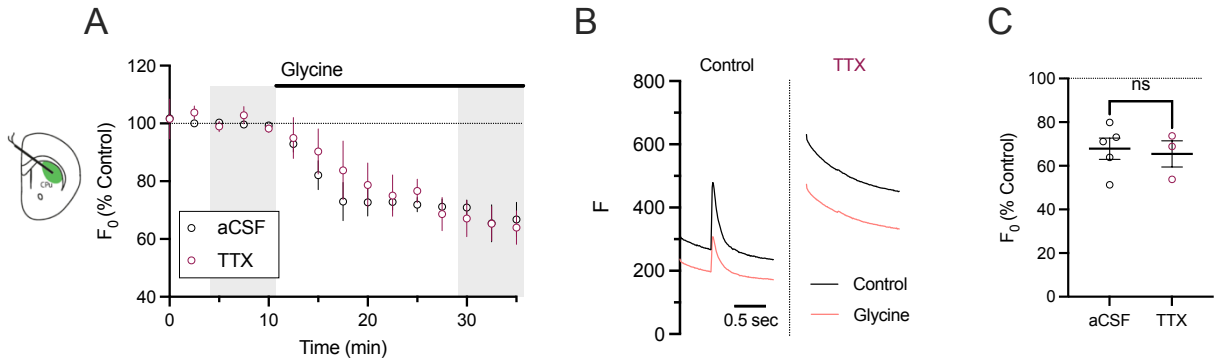

Figure 4.8. Reduction of baseline fluorescence is TTX-insensitive

(A) Mean (± SEM) F_0 of evoked ACh release in dlCPu before and after application of glycine, in the presence or absence of TTX, normalised to pre-glycine control. aCSF: n = 5 slices/animals (Data from **Fig. 4.5F**); TTX: n = 3 slices/animals.

(B) Representative transients of evoked ACh release in dlCPu before and after application of strychnine, in the presence and absence of TTX. aCSF: n = 5 slices/animals (Data from **Fig. 4.5F**); TTX: n = 3 slices/animals.

(C) Mean F_0 of evoked ACh release, in the presence and absence of TTX. Un-paired t-test; p = 0.77. aCSF: n = 5 slices/animals (Data from **Fig. 4.5F**); TTX: n = 3 slices/animals.

4.3.9. Glycine does not alter the sensitivity of $GRAB_{ACh3.0}$ (Pilot)

Having seen that glycine reduces $GRAB_{ACh3.0}$ baseline fluorescence (F_0), I investigated whether glycine altered the sensitivity of the sensor to ACh. I performed brief application of 50 µM ACh in the presence of AChE inhibitor ambenonium (5 µM), to reduce the catabolism of ACh and allow visualisation of ACh signals. Ambenonium increases baseline fluorescence, due to elevation of ambient striatal ACh, so the slices were incubated in ambenonium for at least 20 minutes before starting the experiment to allow the full effect of ambenonium to take place.

ACh was applied twice in each experiment, before and after application of 10 mM glycine, recording non-evoked $GRAB_{ACh}$ fluorescence levels in dlCPu. Exogenous application of ACh mediated a transient increase raw fluorescence, before reducing fluorescence upon glycine application, and a second increase in raw fluorescence upon application of ACh again (**Fig. 4.9A**). I normalised the amplitude of each transient increase evoked by ACh by the mean fluorescence for the 5 minutes preceding ACh application to give a normalised $\Delta F/F_0$ signal (**Fig. 4.9B, *left***), and this showed that the signal evoked by the second application of ACh, in the presence of 10 mM glycine, was significantly smaller than the first application of ACh (**Fig. 4.9B, *right*)**, $\Delta F/F_0$, paired t-test, $p = 0.017$, 3 slices/animals).

To control for an effect of time, I repeated this experiment but with application of vehicle (aCSF) instead of 10 mM glycine (**Fig. 4.9C**), and pilot data appear to show a similar decline for the second application of ACh (**Fig. 4.9D**). Direct comparison of the signals evoked by the first (**Fig. 4.9E**) and second (**Fig. 4.9F**) applications of ACh show no difference with the presence or absence of glycine. Although pilot data, these results suggest that glycine does not affect the sensitivity of $GRAB_{ACh}$ to detect ACh, but the sensitivity may decrease over time.

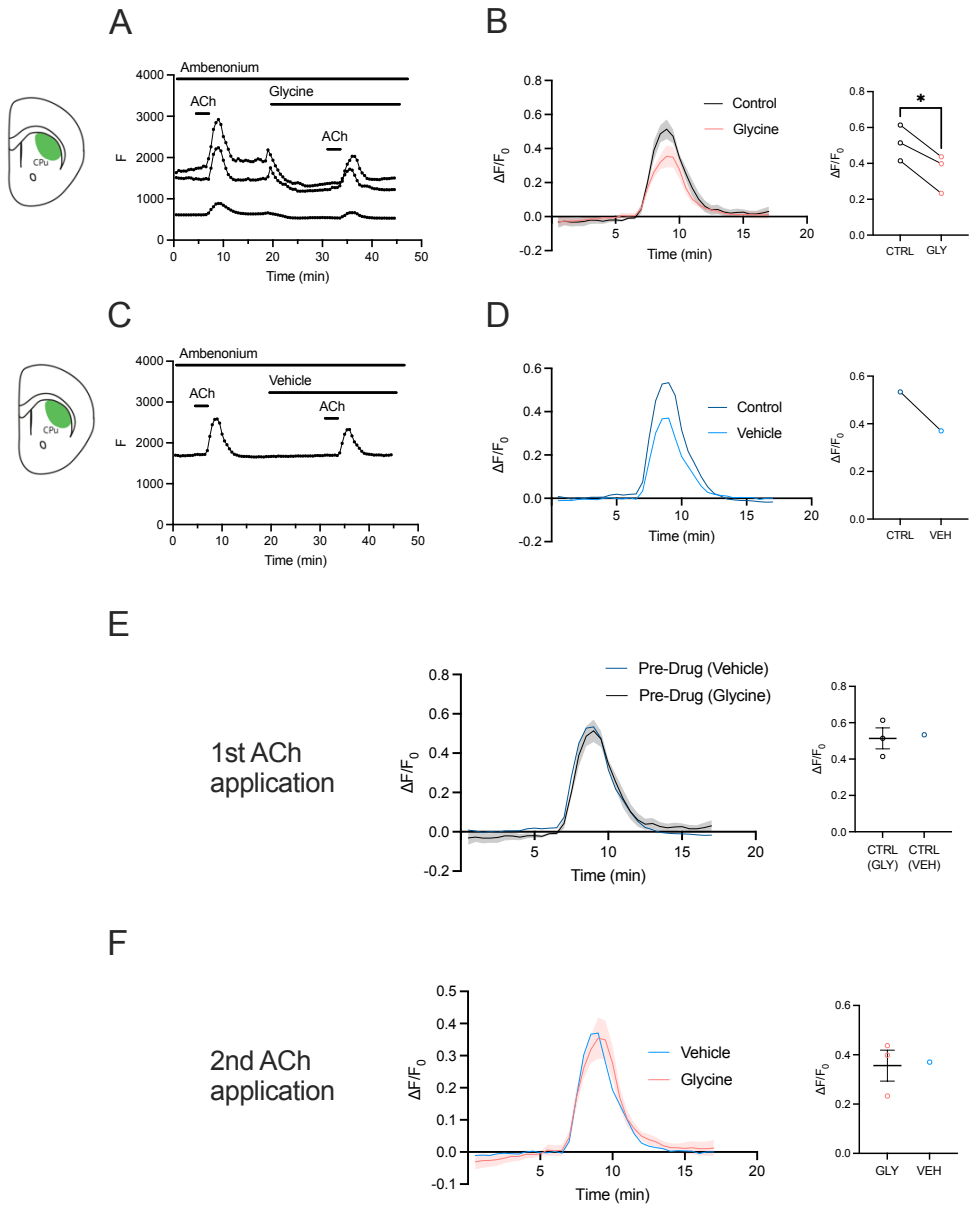

Figure 4.9. Glycine does not alter sensitivity of $GRAB_{ACh}$ sensor (Pilot)

(A) Individual traces showing raw fluorescence (F) values during the application of 50 µM ACh, in the presence of 5 µM Ambenonium throughout and in the presence of 10 mM glycine during the second application. n = 3 slices/animals.

(B) *Left:* Mean (±SEM) $\Delta F/F_0$ fluorescence evoked by the first application of 50 µM ACh (black) and the second application of 50 µM ACh in the presence of 10 mM glycine (red). *Right:* Peak $\Delta F/F_0$ fluorescence upon application of ACh, in the absence (black) or presence of 10 mM glycine (red). Paired t-test: p = 0.017, n = 3 slices/animals.

(C) Individual trace showing raw fluorescence (F) values during the application of 50 µM ACh, in the presence of 5 µM Ambenonium throughout and after application of vehicle (aCSF) during the second application. n = 1 slice/animal.

(D) *Left:* $\Delta F/F_0$ fluorescence evoked by the first application of 50 µM ACh (dark blue) and the second application of 50 µM ACh in the presence of vehicle (light blue). *Right:* Peak $\Delta F/F_0$ fluorescence upon application of ACh, in the absence (dark blue) or presence of vehicle (light blue). n = 1 slice/animal.

(E) *Left*: Mean (±SEM) $\Delta F/F_0$ fluorescence evoked by the first application of 50 µM ACh, in either the vehicle control experiment or where glycine was applied later. *Right*: Peak $\Delta F/F_0$ fluorescence upon application of ACh for both experimental protocols. Pre-Drug (Glycine): n = 3 slices/animals. Pre-Drug (Vehicle): n = 1 slice/animal.

(F) *Left*: Mean (±SEM) $\Delta F/F_0$ fluorescence evoked by the second application of 50 µM ACh, in either the vehicle control experiment or where glycine was applied later. *Right*: Peak $\Delta F/F_0$ fluorescence upon application of ACh for both experimental protocols. Pre-Drug (Glycine): n = 3 slices/animals. Pre-Drug (Vehicle): n = 1 slice/animal.

4.3.10. Characterising determinants of changes in $GRAB_{ACh3.0}$ baseline fluorescence (Pilot)

My experiments in Figure 4.8 showed that the glycine-mediated reduction in baseline fluorescence was TTX-insensitive. I conducted pilot experiments to explore further what might be causing the underlying change in baseline (non-evoked) fluorescence. Changes in non-evoked fluorescence were measured as a percentage from the mean fluorescence before drug application (F/F_0).

I tested whether this was due to the presence of a 10 mM increase in osmolarity. However, application of a similar 10 mM concentration of sucrose did not alter baseline fluorescence (**Fig. 4.10A**, n = 3 slices/animals). This suggests that the reduction of baseline fluorescence is not due to osmolarity of solution, and is an effect of glycine. In a pilot experiment, I also tested whether the reduction in non-evoked fluorescence mediated by glycine was dependent on ambenonium perhaps altering ChI activity, but still observed this effect in the presence and absence of TTX (**Fig. 4.10B**, n = 1 slice/animal per condition).

We next investigated whether the reduction in baseline fluorescence was dependent on ACh binding to the $GRAB_{ACh}$ sensor. We tested this by performing a pilot experiment of ACh application in a slice expressing $GRAB_{ACh3.0.Mut}$, a variant of the $GRAB_{ACh3.0}$ sensor that has a mutation to the ligand binding site, preventing ligand binding and therefore changes in fluorescence due to changes in extracellular ACh concentration (Jing, Li et al. 2020). We found that ACh was unable to evoke a response in the $GRAB_{ACh3.0.Mut}$ sensor, showing that it is insensitive to ACh (**Fig. 4.10C**). However, application of glycine mediated a partially reversible reduction in baseline fluorescence of the $GRAB_{ACh3.0.Mut}$ sensor (**Fig. 4.10D**), similar to the $GRAB_{ACh3.0}$ sensor (**Fig. 4.10E**). These data suggest that the reduction in baseline fluorescence detected by $GRAB_{ACh3.0}$ is not due to changes in extracellular ACh, and may be an interaction with, or other impact on, the sensor itself. A previous study reported changes of the fluorescence of the cpGFP of the GRAB construct, sensitive to changes in intracellular conditions such as pH (Wu, Cui et al. 2023). Although the pH of 10 mM glycine in aCSF is not different from aCSF alone, glycine may have downstream impact on intracellular pH, e.g. via networks of coupled co-transporters or local metabolic changes.

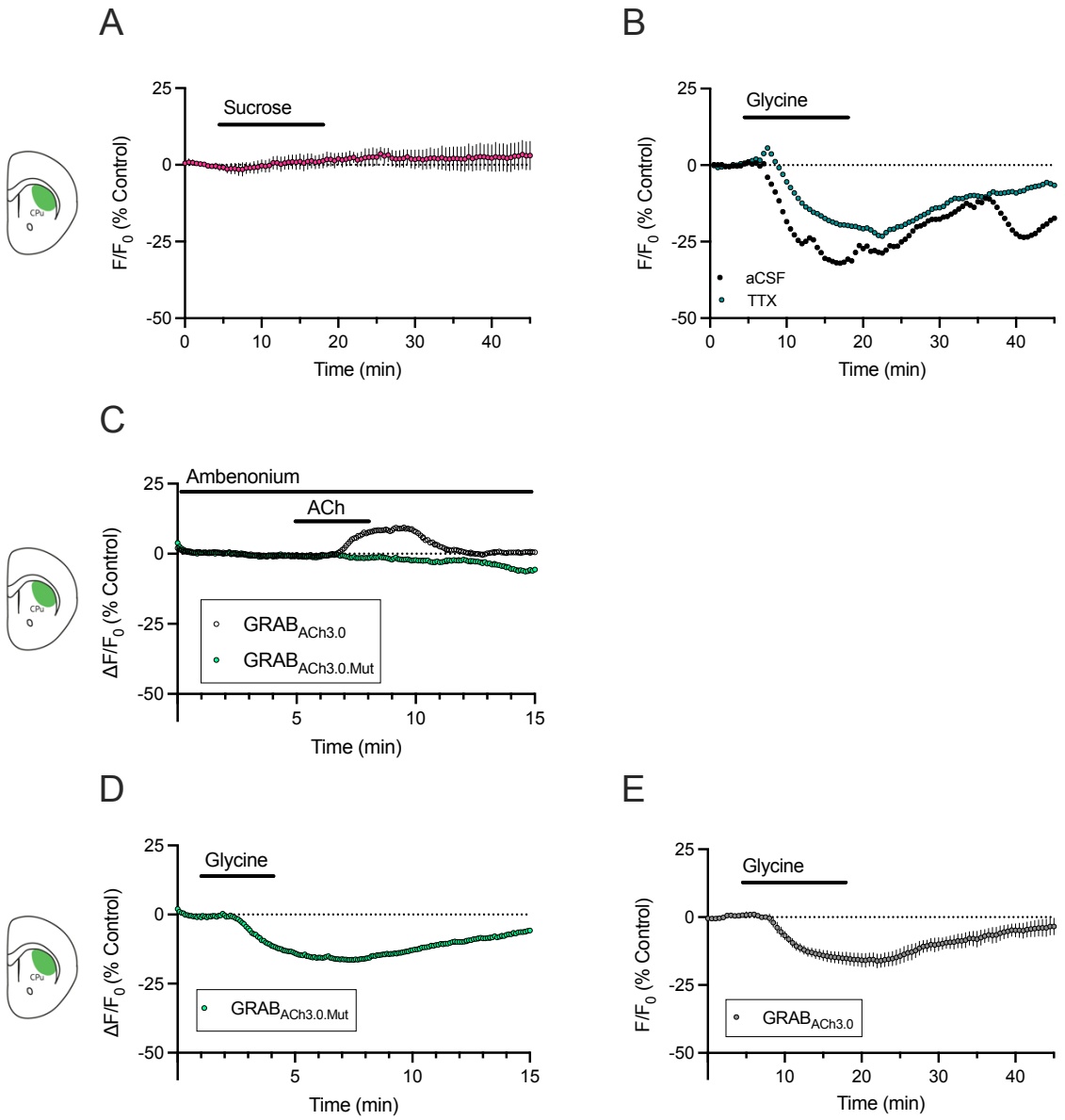

Figure 4.10. Characterising determinants of changes in $GRAB_{ACh3.0}$ baseline fluorescence (Pilot)

(A) Mean (±SEM) F/F_0 upon application of 10 mM sucrose, normalised to pre-sucrose control. n = 3 slices/animals.

(B) F/F_0 upon application of 10 mM glycine, in the presence (teal) or absence (black) of TTX, normalised to pre-glycine control. n = 1 slice/animal per condition

(C) Mean (±SEM) F/F_0 upon application of 50 µM ACh, recorded using either $GRAB_{ACh3.0}$ or $GRAB_{ACh3.0.Mut.}$ n = 1 slice/animal per sensor.

(D) Mean (±SEM) F/F_0 upon application of glycine, recorded using a mouse expressing $GRAB_{ACh3.0.Mut}$ sensor. n = 1 slice/animal

(E) Mean (±SEM) F/F_0 upon application of glycine, recorded using a mouse expressing $GRAB_{ACh3.0}$ sensor. n = 1 slice/animal

4.3.11. Glycine evokes ACh release

I observed during the calibration experiments in **Fig. 4.9** that application of glycine in the presence of ambenonium caused a transient increase in fluorescence. I hypothesised that glycine might cause the release of ACh but this might only be observed in ambenonium because active AChE would otherwise degrade the released ACh too rapidly to be observed. I performed experiments with a higher sampling interval of 5 seconds between images to have better temporal resolution of any release event. I found that in the presence of ambenonium, glycine mediated a TTX-sensitive increase in fluorescence (**Fig. 4.11A-B**, unpaired t-test, p = 0.0004; aCSF: n = 6 slices/animals, TTX: n = 4 slices/animals). This suggests that the increase of fluorescence is caused by the release of ACh from ChIs upon glycine application.

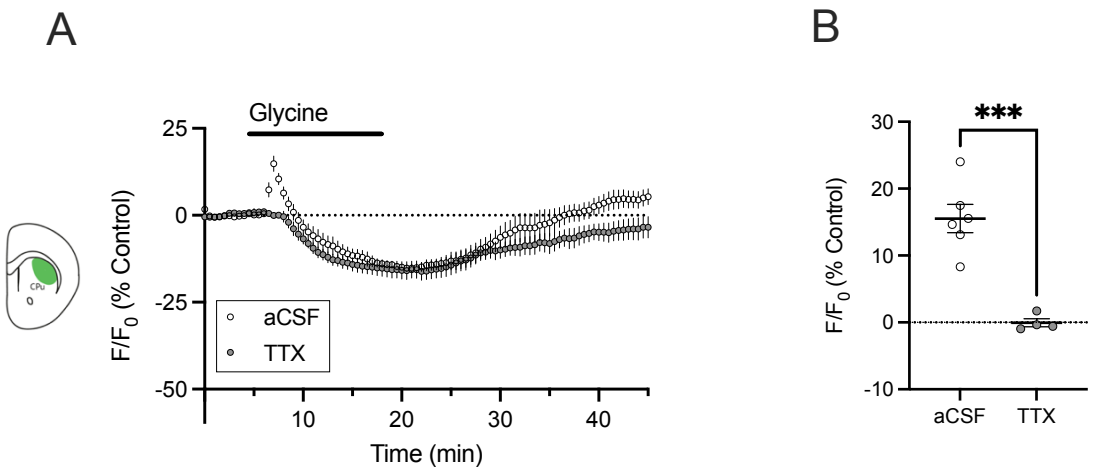

Figure 4.11. Glycine evokes ACh release

(A) Mean (±SEM) F/F_0 upon application of glycine, in the presence of ambenonium and the presence or absence of TTX, normalised to pre-glycine control.

(B) Peak F/F_0 during glycine application, in the presence or absence of TTX. Unpaired t-test: p = 0.0004. aCSF: n = 6 slices/animals; TTX: n = 4 animals/slices.

4.3.12. Glycine regulates the excitability of ChIs (Dr Jeffrey Stedehouder)

We tested whether glycine can directly excite ChIs, using the cell-attached patch-clamp configuration to record the firing rate of ChIs upon the application of glycine under a range of different GlyR conditions. ChIs were labelled using viral expression of mCherry in ChAT-Cre mice (**Fig. 4.12A**). Recorded ChIs responded appropriately to current injection (**Fig. 4.12B**) and we observed spontaneous activity in the absence of current injection (**Fig. 4.12C**). However, in the 11 cells recorded, bath application of 10 mM glycine stopped ChI firing and produced an initial hyperpolarisation followed by a slow repolarisation in the membrane potential, but firing did not readily return upon wash-off (**Fig. 4.12D-E**, paired t-test, $p < 0.0001$, n = 11 cells/3 animals). To isolate and identify potential effects of eGlyRs, without effects of cGlyRs, we antagonised cGlyRs using strychnine, and prolonged eGlyR activation by limiting eGlyR desensitisation using CGP-78608, as described in Chapter 3, and as performed in Bossi et al (Bossi, Dhanasobhon et al. 2022). In the presence of strychnine and CGP-78608, glycine caused a rapid increase in ChI firing rate and a reduction in action potential amplitude, that partially reverse on wash-off (**Fig. 4.12F-G,** one-way RM ANOVA, $F_{(1.619,22.66)} = 21.20$, $p < 0.0001$, *post hoc* Sidak's comparison, n = 15 cells/3 animals). These data show that glycine is able to mediate an excitatory effect on ChIs via eGlyRs, by preventing desensitisation of the eGlyR and by occluding the effects of cGlyRs. However, the net effect of glycine was one of inhibition, suggesting that cGlyR effects dominate over eGlyRs during application of high concentrations of glycine alone. This net outcome does not parallel the finding that glycine evoked ACh release (Fig 4.11), seen in the presence of AChE inhibition. It is possible that elevation of ambient ACh tone during AChE inhibition might have led to a different net effect, leading to a brief dominance of excitation via eGlyRs excitation, perhaps via elevated activation of autoreceptors on ChIs that might shunt the ability of cGlyRs to further inhibit, and allowing impact of eGlyRs to manifest. Future experiments should test whether in the presence of ambenonium, or elevated mAChR activation, the effects of eGlyRs on excitation might be revealed.

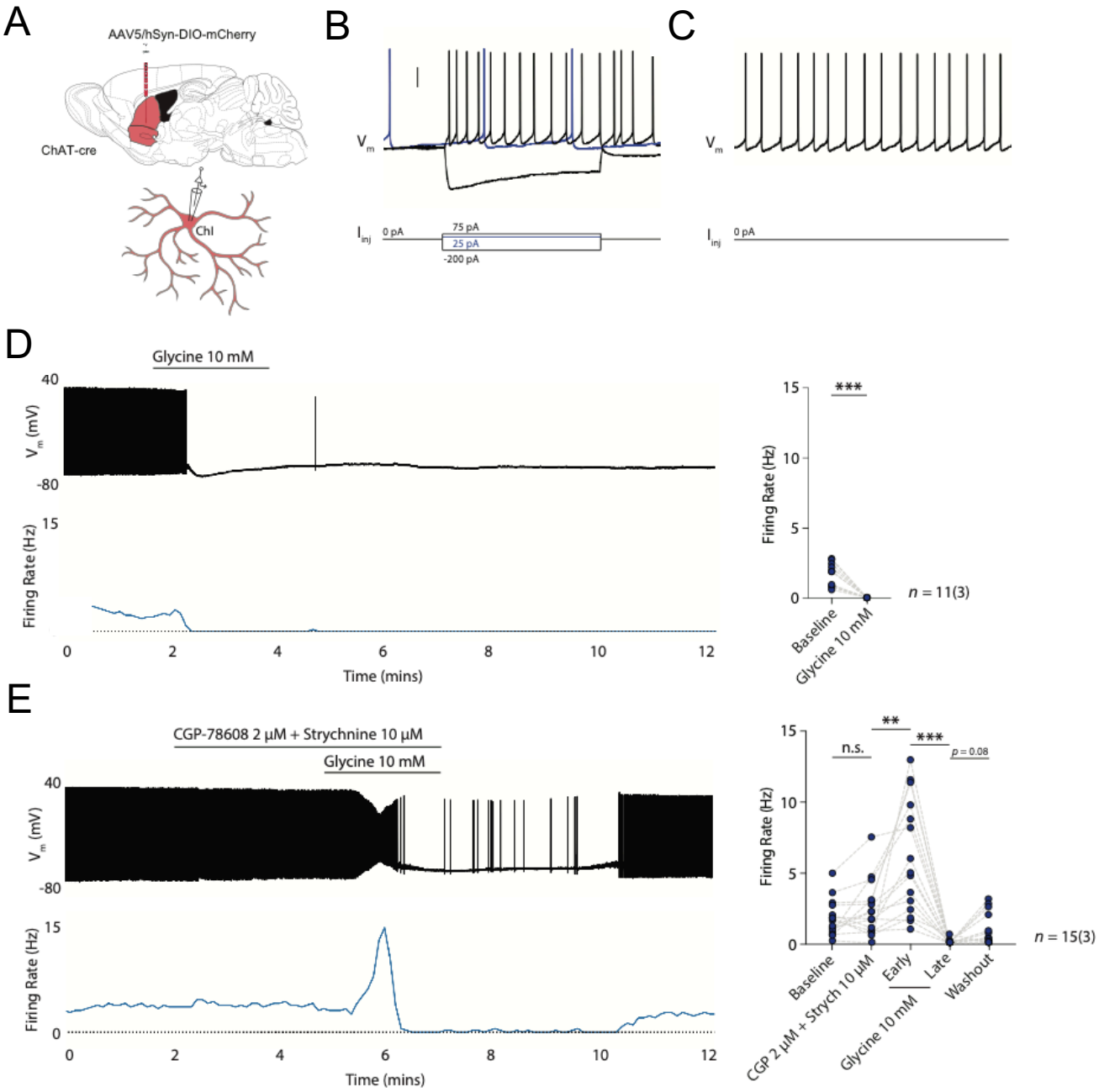

Figure 4.12. Glycine regulates the excitability of ChIs

(A) Schematic representation of mCherry expression in ChIs in ChAT-Cre mice for identification, and cell-attached recording.
(B) Representative trace of ChI firing upon current injection, recorded in cell-attached configuration.
(C) Representative trace of ChI firing without current injection
(D) Recording of ChI firing rate before, during, and after bath application of 10 mM glycine. Unpaired t-test, $p < 0.001$. n = 11 slices/3 animals
(E) Recording of ChI firing rate under drug-free conditions, in the presence of strychnine and CGP-78608, the addition of 10 mM glycine, and wash off. One-way RM ANOVA, $F_{(1.619,22.66)} = 21.20$, $p < 0.0001$, and *post hoc* Sidak's multiple comparisons test. n = 15 slices/3 animals

Data collected and analysed by Dr Jeffrey Stedehouder

4.3.13. CGP-78608 application reduces evoked ACh levels

My earlier results showed that CGP-78608, a GluN1-subunit antagonist that functionally stops the desensitisation of eGlyRs, was able to decrease DA release via an nAChR-dependent mechanism. My hypothesis was that CGP-78608 mediates this effect by altering striatal ACh levels, in turn altering the activation of nAChRs on DA axons that powerfully control DA release. I found that CGP-78608 did not significantly reduce peak evoked ACh release (**Fig. 4.13A-C**, $\Delta F/F_0$, paired t-test, $p = 0.12$, $n = 3$ slices/animals), but did reduce AUC (**Fig. 4.13D**, AUC, paired t-test, $p = 0.020$, $n = 3$ slices/animals). There was no significant effect on baseline F_0 (**Fig. 4.13E**), showing that CGP-78608 does not alter ambient striatal ACh tone or interact with the $GRAB_{ACh}$ sensor. These data show that CGP-78608 reduces evoked ACh release, consistent with a change to eGlyR regulation of ACh release.

I also performed pilot experiments investigating whether the release of ACh evoked directly by glycine is mediated via eGlyRs (**Fig. 4.13F**). My initial hypothesis was that stopping eGlyR desensitisation with CGP-78608 would enhance ACh release, based on a greater excitatory current mediated by glycine causing a greater release of ACh, and application of the antagonist DCKA would reduce ACh release. My pilot data suggest the opposite, with DCKA appearing to increase the AUC of glycine release but CGP-78608 reducing this. Although these data do suggest that eGlyRs regulate the release of ACh upon glycine application, further investigation is needed to understand how eGlyR activation state contributes to the excitability of ChIs and subsequent ACh release.

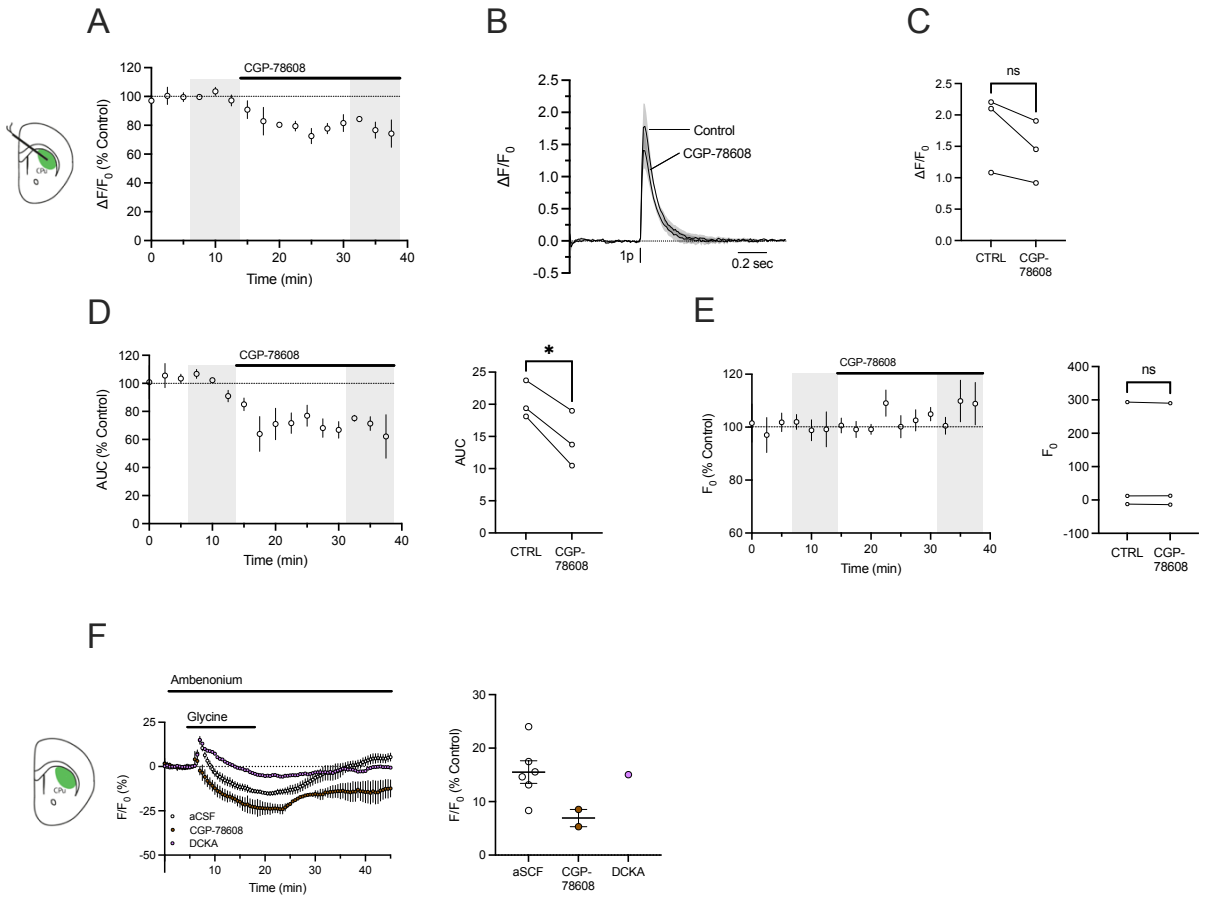

Figure 4.13. CGP-78608 reduces ACh release

(A) Mean (±SEM) peak $\Delta F/F_0$ of evoked ACh release in dlCPu before and after application of CGP-78608

(B) Mean (±SEM) transient $\Delta F/F_0$ of evoked ACh release in dlCPu before and after application of CGP-78608.

(C) Mean peak $\Delta F/F_0$ of evoked ACh release before and after application of CGP-78608. Paired t-test; p = 0.12, n = 3 slices/animals.

(D) *Left:* Mean (±SEM) AUC of evoked ACh release in dlCPu before and after application of CGP-78608. *Right:* Mean AUC of evoked ACh release in dlCPu before and after application of CGP-78608. Paired t-test; p = 0.020, n = 3 slices/animals.

(E) *Left:* Mean (±SEM) F_0 of evoked ACh release in dlCPu before and after application of CGP-78608. *Right:* Mean F_0 of evoked ACh release in dlCPu before and after application of CGP-78608. Paired t-test; p = 0.32, n = 3 slices/animals.

(F) *Left:* Mean (±SEM) F/F_0 upon application of glycine, in the presence of ambenonium and the presence or absence of CGP-78608 or DCKA, normalised to pre-glycine control. *Right:* Peak F/F_0 during glycine application, in the presence or absence of CGP-78608 or DCKA. Unpaired t-test: aCSF: n = 6 slices/animals (from **Fig. 4.11A**); CGP-78608: n = 2 animals/slices; DCKA: n = 1 slice/animal

4.3.14. Effect of CGP-78608 and glycine on ACh release

Having observed the effects of glycine on ACh release and both the ΔF and F_0 components of the ACh signal, I next investigated how CGP-78608 modulated the effects of glycine on ACh release, hypothesising a similar response to evoked DA with a more rapid, immediate reduction in release in comparison to the effect of glycine alone. I found a very variable effect on $\Delta F/F_0$ peak evoked release (**Fig. 4.3.14A-C**, $\Delta F/F_0$, paired t-test, p = 0.45, n = 3 animals/slices) due to variability in the effects on ΔF (**Fig. 4.3.14D**, paired t-test, p = 0.06) and F_0 **(Fig. 4.3.14E**, paired t-test, p = 0.019), whereby a greater reduction in F_0 than ΔF results in an increase of $\Delta F/F_0$. There is no significant difference between either the ΔF or F_0 values in the presence or absence of CGP-78608 upon application of glycine, but this is difficult to interpret given the confounding effects on F_0.

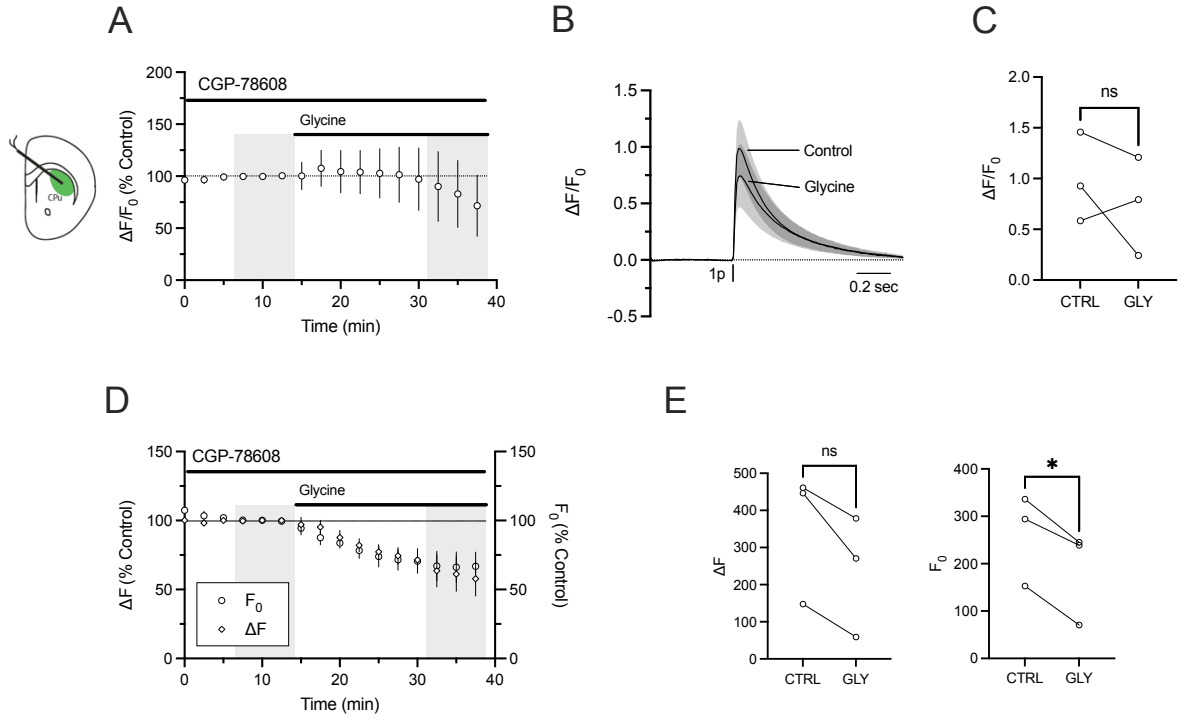

Figure 4.14. Effect of CGP-78608 and glycine on ACh release

(A) Mean (± SEM) peak $\Delta F/F_0$ of evoked ACh release in dlCPu before and after application of glycine, in the presence or absence of CGP-78608

(B) Mean (±SEM) transient $\Delta F/F_0$ of evoked ACh release in dlCPu before and after application of glycine, in the presence or absence of CGP-78608.

(C) Mean peak $\Delta F/F_0$ of evoked ACh release before and after application of glycine, in the presence or absence of CGP-78608. Paired t-test; p = 0.45, n = 3 slices/animals

(D) Mean (± SEM) F_0 of evoked ACh release in dlCPu before and after application of glycine, in the presence of CGP-78608.

(E) Mean ΔF (*left*) and F_0 (*right*) of evoked ACh release in dlCPu before and after application of glycine, in the presence of CGP-78608. ΔF: Paired t-test, p = 0.0609 (n.s.), n = 3 slices/animals. F_0: Paired t-test; p = 0.0192 (*), n = 3 slices/animals.

4.3.15. Functional eGlyRs are expressed on striatal ChIs (Dr Ioannis Mantas, Ms Vasiliki Skara, and Dr Simon Bossi)

To support the pharmacological data supporting the presence of functional striatal eGlyRs that can regulate DA release, our collaborators also performed RNAscope experiments investigating striatal expression of *Grin3A*, encoding the GluN3A subunit present in eGlyRs. Our FSCV and $GRAB_{ACh}$ data strongly supports *Grin3A* expression in ChIs, and Grin3A expression has previously been observed in SST+ interneurons in cortex. There is previous ISH evidence for the expression of *Grin3A* in striatum (Allen Brain Atlas, 2011, Experiment: 73907499) but this has not been co-localised to specific neuronal subtypes. Our collaborators investigated the co-expression of Grin3A with markers for ChIs and cells expressing *Npy*. They found expression of *Grin3A* in striatum, including co-expression with *ChAT* and *Npy*, with expression of *Grin3A* in ~90% of ChIs (Total *Chat*+: n = 3 animals. #1 = 282 cells, #2 = 311 cells, #3 = 348 cells) and ~80% of *Npy*+ cells (Total *Npy*+: n = 3 animals. #1 = 302 cells, #2 = 260 cells, #3 = 347 cells) (**Fig. 4.15A-C**). These data show the expression of *Grin3A* in ChIs and *Npy*+ cells for the first time and support my findings that eGlyRs are expressed on ChIs.

To confirm the functional expression of eGlyRs on ChIs, Dr Simon Bossi in our lab conducted a pilot experiment testing the pharmacology of glycine-mediated currents in ChIs, as he had done previously for cortical interneurons (Bossi, Dhanasobhon et al. 2022). Puff application of 10 mM glycine in a cocktail of antagonists to isolate a putative eGlyR current showed a very small (~20 pA), rapidly desensitising inward current (**Fig. 4.15D**). In the presence of CGP-78608, a GluN1 subunit antagonist that stops receptor desensitisation, the amplitude of the evoked current increases significantly (~1.4 nA) and does not appear to desensitise. Upon addition of DCKA, the GluN3A subunit antagonist that blocks channel gating, puff application of glycine does not mediate a current (**Fig. 4.15D**). Additionally, application of CGP-78608 and DCKA shifted the holding current of ChIs during recording (**Fig. 4.15E**). This suggests that the eGlyRs on ChIs are tonically active and mediate a depolarising effect on the neuronal resting membrane potential. This is consistent with previous findings of cortical interneurons (Bossi, Dhanasobhon et al. 2022). These are pilot data that requires further investigation, but very strongly suggest the expression of functional eGlyRs on striatal ChIs.

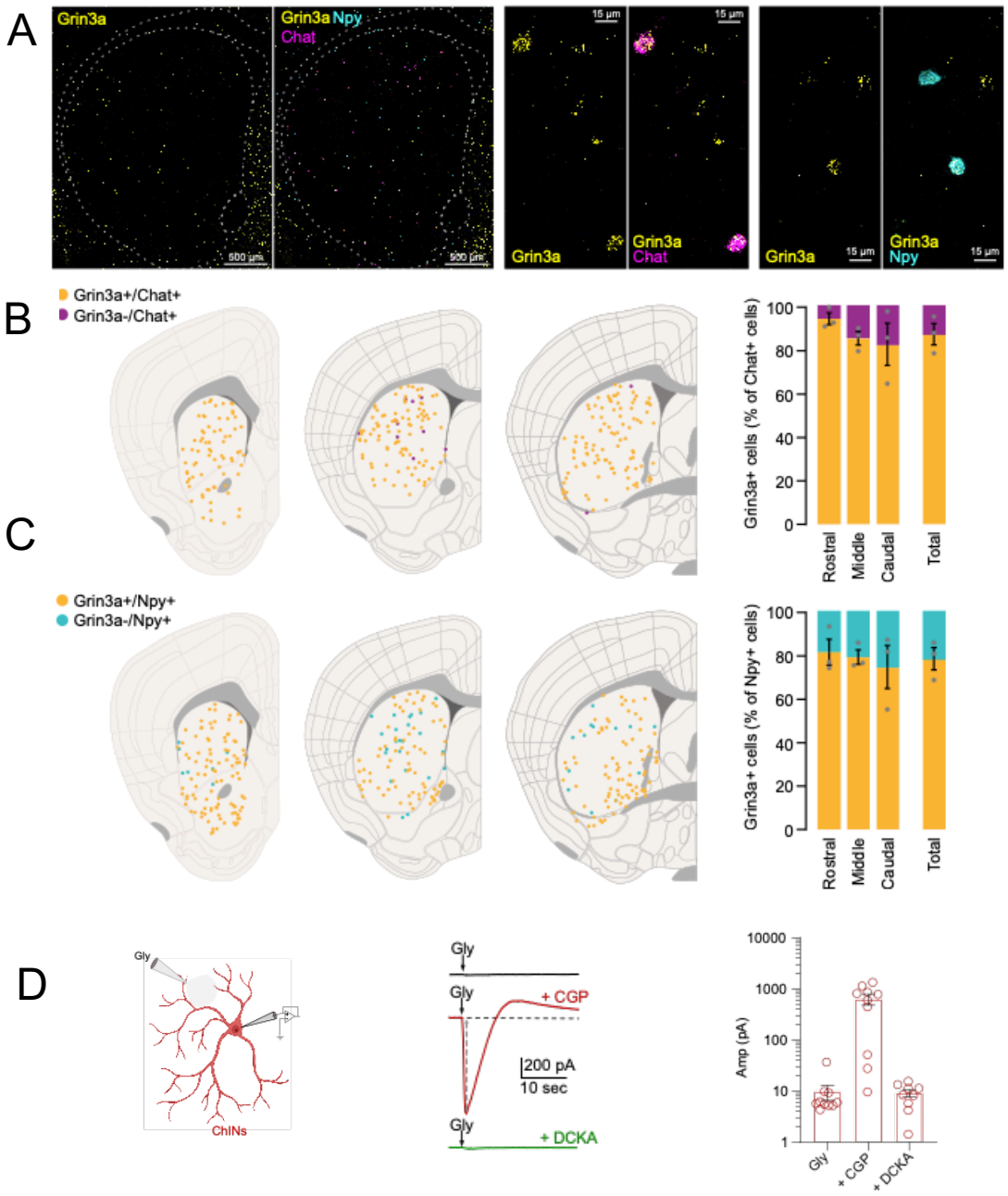

Figure 4.15. eGlyRs are expressed and functional on striatal ChIs

(A) Representative images showing *Grin3A* expression within a coronal striatal slice, and co-expression for *Chat* and *Npy* as markers for ChIs and NPY+ cells respectively.

(B) *Left:* Diagrams depicting distribution of ChIs and co-expression of *Grin3A* in striatum across a rostral to causal axis. *Right*: Quantification of ChIs either positive or negative for *Grin3A* co-expression, across a rostral to caudal axis. n = 3 animals

(C) *Left:* Diagrams depicting distribution of NPY+ cells and co-expression of *Grin3A* in striatum across a rostral to causal axis. *Right*: Quantification of NPY+ cells either positive or negative for *Grin3A* co-expression, across a rostral to caudal axis. n = 3 animals

(D) *Left*: Schematic of 10 mM glycine puff application onto ChI. *Right*: Example traces and amplitude of inward current mediated by puff application of 10 mM glycine in presence of cocktail of antagonists (black), CGP-78608 (red), and CGPO-78608 + DCKA (green). n = 10 neurons / 3 animals

(E) Example traces showing shifts in holding current in the presence of cocktail of antagonists (black), CGP-78608 (red), and CGPO-78608 + DCKA (green). n = 10 neurons / 3 animals

Data collected and analysed by Dr Ioannis Mantas, Ms Vasiliki Skara and Dr Simon Bossi

4.4. Discussion

These results provide evidence for the expression and function of cGlyRs and eGlyRs on ChIs, that can regulate ACh release. The genes encoding the α2 and α3 subunits of cGlyRs were shown to be expressed in ChIs (Fig. 4.2), and application of the cGlyR antagonist strychnine enhanced evoked ACh release (Fig. 4.1), suggesting that cGlyRs are tonically active on ChIs. Application of CGP-78608 to stop eGlyR desensitisation reduced evoked ACh release (Fig. 4.13), and the gene encoding the GluN3A subunit of eGlyRs was also shown to be expressed in ChIs (Fig. 4.15). Glycine itself evoked spontaneous ACh release (Fig. 4.11) and in the presence of CGP-78608 increased the firing rate of ChIs (Fig. 4.12), suggesting an excitatory effect via eGlyRs. Glycine appeared to reduce evoked ACh release (Fig. 4.4) but there was an effect on the baseline fluorescence (Fig. 4.5) that might be independent of any change in extracellular ACh (Figs. 4.8-4.10) and should be investigated further. Despite this confound, these data support the hypothesis that cGlyRs and eGlyRs regulate ChI activity and ACh release. These effects will mediate some of the multicomponent processes through which glycine regulates DA release.

4.4.1. Functional cGlyRs are located on ChIs

Previous research had shown the presence of cGlyRs on striatal cholinergic interneurons in rats and mice, using electrophysiology, immunohistochemistry, and single-cell RT-PCR (Sergeeva 1998, Darstein, Landwehrmeyer et al. 2000, Sergeeva and Haas 2001, Martin and Siggins 2002). Our RNAscope data supports the single-cell RT-PCR findings; we observe expression of both α2 and α3 subunits in ChIs, with almost ~95% ChIs expressing the α2 subunit and ~85% expressing the α3 subunit (Fig. 4.2), where Sergeeva and Haas observe that all ChIs express the α2 subunit and 72% expressing the α3 subunit (Sergeeva and Haas 2001). The subunit composition is a determining factor of cGlyR function. There is some discrepancy in the literature, but homomeric α3 cGlyRs predominantly mediate tonic extrasynaptic currents, and can be exposed pharmacologically using picrotoxin that selectively blocks this receptor population (in addition to $GABA_A$Rs) (McCracken, Lowes et al. 2017). There is

some evidence that α2-containing cGlyRs can also mediate tonic currents, and it would be interesting to further explore the subunit composition of cGlyRs on ChIs to understand the contributions between synaptic and extrasynaptic cGlyR activity better. The RNAscope data also showed expression of cGlyR subunits in a sub-population of NPY+ interneurons. cGlyRs have not previously been described in other striatal interneurons, and their distribution in LTSIs versus neurogliaform interneurons, in addition to any functional role, should also be further investigated.

Given the strength of evidence for the expression of cGlyRs on ChIs, I wanted to investigate how they might control ACh release, which can now be measured using the recently developed $GRAB_{ACh}$ sensors. My data show that strychnine enhances evoked ACh, as measured by AUC (Fig. 4.1), suggesting that tonic cGlyR activity inhibits ACh release. Previous data collected by our lab shows that modest increases in ACh release manifest as an increase in AUC rather than an increase in peak amplitude ($\Delta F/F_0$). This data is complementary to previous data showing the expression and function of cGlyRs on ChIs, now demonstrating an effect on ACh release itself.

I investigated the regulatory effects of cGlyRs on ACh release in the context of indirect regulation of DA release. I found that the effects of strychnine on DA release could be seen independently from nAChR function (Fig. 3.2). This suggests that although cGlyRs can regulate ACh release from ChIs, this mechanism is insufficient to alter ACh release enough to alter the activity of nAChRs on DA axons and ultimately affect DA release. This is very consistent with the finding that increases in extracellular ACh do not further increase evoked DA release (Zhou, Liang et al.). It does not discount a role for cGlyRs on ChIs in the regulation of DA, but shows rather that cGlyRs elsewhere, perhaps on DA axons, can regulate DA release.

4.4.2. Functional eGlyRs located on ChIs

There is no previous evidence for the expression of eGlyRs on striatal ChIs. ISH data for *Grin3A* from the Allen Brain Atlas suggests expression of the GluN3A subunit in striatal interneurons, supporting recent findings of eGlyRs expressed in cortical interneurons (Bossi, Dhanasobhon et al. 2022). A previous study also observed glycine-evoked ACh release in rat striatal tissue, but the

underlying mechanism was unclear (Hernandes, de Magalhaes et al. 2007). My data show that CGP-78608 reduces evoked ACh release (Fig. 4.13) and that glycine is able to mediate non-evoked ACh release (Fig. 4.11), indicating eGlyR expression and function in ChIs. Our findings using RNAscope clearly show expression of the GluN3A subunit in ~90% of ChIs, and pilot data using electrophysiology shows glycine-gated excitatory currents that are potentiated by CGP-78608 and blocked by DCKA, characteristic of eGlyRs (Fig. 4.15).

These data also support my findings that the effects of CGP-78608 on DA release are dependent on nAChRs. This suggests a mechanism where CGP-78608 stops the desensitisation of eGlyRs on ChIs, ultimately reducing the activity and subsequent release of ACh, altering the activation of nAChRs expressed on DA axons, reducing DA release. My initial hypothesis was that CGP-78608 should increase evoked ACh release, given that this would stop the desensitisation of eGlyRs, that should have an overall excitatory effect on ChIs. However, a reduction of ACh release is observed, including in pilot data investigating glycine-evoked ACh release (Fig. 4.13). This suggests a mixed population of receptors, some active and some inactive, where CGP-78608 may have different effects on ChI excitability. Previous findings hypothesise that eGlyRs mediate a tonic depolarising current that maintain tonically active neurons closer to their membrane firing potential (Bossi, Dhanasobhon et al. 2022). It is possible that sustained depolarisation may shift ChIs into depolarisation block, but this should be investigated in greater depth using electrophysiology to understand exactly how eGlyRs regulate ChI activity.

4.4.3. Glycine and taurine data interpretation with F_0

The family of GRAB sensors have allowed the visualisation and monitoring of a wide variety of neuropeptides and neuromodulators, including those that cannot be measured using electrochemical techniques because they are not electroactive (Sabatini and Tian 2020). This includes ACh, which is known to have a powerful regulatory effect on striatal DA release, but has been difficult to monitor directly at a sub-second temporal resolution until now. Although the focus of my project is not characterisation of the properties of these sensors, monitoring how individual components of the GRAB

sensor signals respond to pharmacological manipulation is important as we are still optimising their use for our experiments.

Initially, my glycine wash on data appear to show that glycine reduces evoked ACh release (Fig. 4.4). However, glycine appears to reduce both the absolute fluorescence (F_0) and the amplitude of the signal (ΔF) (Fig. 4.5). Changes in ΔF will be due to the change in the number of $GRAB_{ACh}$ ligand-binding sites occupied by ACh, upon electrical stimulation of ACh release. $\Delta F/F_0$ normalisation works on the assumption that F_0 does not change over the course of an experiment. Therefore, where F_0 is changing over the course of an experiment, it is difficult to ascribe any change in $\Delta F/F_0$ to a change in evoked neurotransmitter release, or a change in the function of the sensor.

F_0 itself is defined here as the baseline fluorescence which should be a function of:

1. The number/availability of ligand-binding sites
2. How many of those ligand-binding sites are occupied by ambient (non-evoked) ACh
3. The fluorescence of each activated sensor.

A change in ambient ACh would be a mechanism by which a pharmacological manipulation is altering tonic ACh release or breakdown by AChE via a biological mechanism, whereas a change in the number/availability of ligand-binding sites or the fluorescence of an activated sensor would be an interaction with the sensor itself, and a technical artefact. The key question is whether the effects of glycine are truly modifying tonic ACh release or interacting with the $GRAB_{ACh}$ sensor.

$GRAB_{ACh3.0}$ is not a ratiometric sensor, and therefore it is difficult to ascertain any change in the number of ligand-binding sites. Theoretically, the sensor should only fluoresce upon ligand-binding – unless the sensor can also stochastically transition into the active state or exhibit constitutive activity, as a biological receptor might, but this would not be expected to be a significant component. Our hypothesis is that F_0 reflects tonic activation of the sensor by non-evoked extracellular ACh. This is supported by data showing that ambenonium (AChE inhibitor) application increases F_0, likely via inhibition of AChE reducing the rate of extracellular ACh breakdown, enhancing extracellular ACh. This is supported by the rationale that exogenous application of ACh increases non-evoked fluorescence (Fig. 4.9A).

Some of my data suggest that the effect of glycine is specific to glycine, arguing for a pharmacological mechanism. Firstly, application of an equimolar solution of sucrose does not cause a reduction in baseline fluorescence, showing that this is not an effect due to the osmolarity of solution (Fig. 4.10A). Secondly, the TTX-sensitive increase in non-evoked fluorescence upon application of glycine (Fig. 4.11) could be explained by the corresponding increase in ChI firing rate (Fig. 4.12). After the increase in non-evoked fluorescence, there is the reduction in fluorescence, which could correspond to the silencing in ChI firing rate at this timepoint.

Glycine causes a reduction in baseline fluorescence of the $GRAB_{ACh.3.0.Mut}$ sensor, designed as a control where ACh-binding should not alter fluorescence (Fig. 4.10D). This suggests that the effect of glycine is not due to a change in extracellular ACh, but rather an interaction with the sensor. The change in F_0 does not appear to alter the sensitivity of the sensor to ACh (Fig. 4.9), with a known concentration of ACh eliciting a similar $\Delta F/F_0$ response in the presence or absence of ACh. The relationship between ligand-binding and F_0 is also unclear; data from our lab shows that application of the mAChR antagonist atropine (that should also block the sensor) does not alter F_0. This is despite a hypothesis that atropine would displace ambient ACh bound to the sensor, reducing the number of sensors activated, and therefore reducing baseline fluorescence.

Nevertheless, a change in the fluorescence of the sensor independent of ACh-binding is a large confound in the interpretation of both the non-evoked ACh data, and the evoked ACh data where it is normalised to F_0. Data exploring effects of strychnine, CGP-78608 and sarcosine did not show a change in F_0, but still showed glycine receptor regulation of ACh release. The non-evoked increase in fluorescence upon glycine application is TTX-sensitive, strongly indicative of a pharmacological mechanism whereby glycine is stimulating ACh release. However, the subsequent decrease that is also present in the $GRAB_{ACh.3.0.Mut}$ should not be considered without further investigation into the determinants of background fluorescence.

This raises the question of what could alter baseline fluorescence of $GRAB_{ACh.3.0}$, independent of changes in changes in extracellular ACh. Initially we considered whether high concentrations of glycine might cause membrane turnover and subsequent internalisation of the GRAB sensor. However, this the relatively rapid response of baseline fluorescence to application of glycine, the reversibility of

this mechanism, and the different magnitudes of response across different GRAB sensors argues against this. Another possibility is that the fluorophore itself is sensitive to changes in intracellular state. This was recently shown where neuronal activation resulted in intracellular acidification, resulting in a reduction of fluorescence of $GRAB_{Ado1.0}$ and $GRAB_{Ado1.0.Mut}$ (Wu, Cui et al. 2023). Therefore, it is possible that glycine may interact with the fluorophore to reduce its fluorescence. Although speculative, I have two hypotheses for how glycine may mediate a similar neuronal excitation:

Striatal astrocytes express GlyT1, which is electrogenic and should depolarise astrocytes upon transport of glycine into the astrocyte (McCracken, Lowes et al. 2017 , Erdem, Ilic et al. 2019). This could in turn lead to the excitation of astrocytes and release of gliotransmitters, such as ATP. These data need to be fully investigated, but I hypothesise that this release of ATP could be sufficient to mediate downstream excitation of striatal cells expressing the $GRAB_{ACh}$ sensor, altering intracellular metabolism leading to a local change in pH and a reduction in the fluorescence of the cpGFP fluorophore. This could be tested by performing this experiment in the presence of fluorocitrate, a toxin that selectively kills astrocytes and would stop any increase in extracellular ATP if the source is astrocytic.

An alternative hypothesis for glycine mediating neuronal excitation across a large number of striatal cells is via the newly assigned mGlyRs (Laboute, Zucca et al. 2023). Activation of these receptors increases intracellular cAMP and has been shown to be excitatory in electrophysiological recordings of neurons in prefrontal cortex. Although it is unclear on which cell types they are expressed, ISH data in the Allen Brain Atlas for the original orphan receptor GPR185 shows striatal expression. It is possible that bath application of 10 mM glycine causes mass excitation of these receptors on striatal neurons, resulting in neuronal excitation and again altering the intracellular environment and reducing fluorescence of the cpGFP fluorophore. Until we have a better understanding of these mechanisms, data that show a reduction of baseline fluorescence, either during evoked or non-evoked recordings, should be interpreted with caution.

4.4.4. Composite effect on ChIs

My data show glycine receptors mediating excitatory and inhibitory effects on ChIs. This is likely due to the contribution of cGlyRs and eGlyRs. Both populations of receptors appear to be tonically active, with the cGlyR antagonist strychnine and the eGlyR desensitisation blocker CGP-78608 both modulating ChI activity without needing exogenous application of an agonist to reveal their effects. Further investigation is needed to understand the circumstances under which they both act.

Inhibition of cGlyRs via strychnine application increased evoked ACh release (Fig. 4.1). ChIs express both α2 and α3 cGlyR subunits (Fig. 4.2). It is likely that they express both synaptic and extrasynaptic cGlyRs, which generally mediate synaptic and tonic glycine-mediated currents respectively. The α3 homomeric cGlyRs that preferentially mediate tonic glycine currents are picrotoxin-sensitive, and a change in the ChI membrane potential upon application of picrotoxin (in the presence of a $GABA_AR$ antagonist) would indicate the presence of these receptors on ChIs.

Glycine itself mediates a spontaneous release of ACh (Fig. 4.11). This response is TTX sensitive, and therefore likely due to ACh release and not an artefact of glycine interaction with the $GRAB_{ACh}$ sensor. Although the time course of this response appears relatively long (~2.5 min), this is likely due to the presence of ambenonium, slowing the clearance of any ACh release by glycine. This result also supports a previous finding that glycine was able to evoke ACh release, in rat striatal tissue superfused with radiolabelled ACh (Hernandes, de Magalhaes et al. 2007). Although likely to be mediated via eGlyRs, this response is surprising in the absence of CGP-78608 given the rapid desensitisation of these receptors (Fig. 4.15). There may be off-target effects via ATP gliotransmission or mGlyR signalling that could contribute. Puff-application of glycine would be a more refined approach that would limit some of these possible off-target effects.

4.4.4. Conclusion

These data demonstrate the expression of both cGlyRs and eGlyRs on ChIs, and that they both regulate the activity of ChIs and ACh release. This supports a theme that glycinergic signalling is an important regulator of neuronal activity, and within my project also shows how eGlyR activity contributes to the nAChR-dependent regulation of DA release.

More broadly, these results further support a hypothesis that eGlyRs are important regulators of neuronal activity, that is only starting to be fully appreciated (Bossi, Dhanasobhon et al. 2022). Our findings are the first to show eGlyR function within the striatum, and further research will elucidate how eGlyR function on ChIs may regulate other striatal circuits, and indeed if they may represent a therapeutic target for other diseases associated with striatal dysfunction. Additionally, I hope these findings encourage future studies investigating the presence and function of these receptors in other brain regions.

My results have also identified specific limitations of using the GRAB sensors and identify a possible interaction between intracellular activity and fluorescence of the fluorophore itself. This may represent a particularly large confound for *in vivo* studies that take place over a longer timescale and it is more difficult to identify the cause of subtle changes in baseline fluorescence after data are normalised. My findings should undergo additional investigation, particularly *in vivo*, to ensure accurate data interpretation where an experimental manipulation results in a change of the baseline, non-evoked, fluorescence level. This is especially important as more research groups are using the GRAB sensors for the first time and should be aware of any limitations or considerations before starting to use them in their experiments.

Chapter 5: Diabetes alters dopaminergic neurotransmission in mouse models of diabetes

5.1. Introduction

5.1.1. Diabetes is caused by metabolic dysfunction

Diabetes is a metabolic disease caused by an inability of the body to regulate blood glucose levels, via dysfunctional insulin signalling (Petersen and Shulman 2018). Insulin is a hormone synthesised by β-cells in the pancreatic Islets of Langerhans, which is released upon elevated blood glucose levels and stimulates glucose uptake from the blood primarily by skeletal muscle and promotes the conversion of glucose to glycogen via glycogenesis. This allows the maintenance of blood glucose within a healthy range, and the conversion of glucose into a form for longer-term storage.

Diabetes is caused by dysfunction in insulin signalling. Type 1 diabetes is caused by the death of the pancreatic β-cells, typically as the result of auto-immune disease, and results in low serum insulin levels (Katsarou, Gudbjornsdottir et al. 2017). Onset of type 1 diabetes is typically in childhood and requires daily injection of insulin for treatment. Type 2 diabetes is caused by the β-cells not releasing enough insulin in response to an increase in blood sugar, and is also described as insulin resistance (DeFronzo, Ferrannini et al. 2015). In these patients, serum insulin levels can still be high. This is caused by a range of risk factors, including age, genetic pre-disposition, nutrition and obesity. Onset arises usually after 50 years of age, and longer-term complications include cardiac and vascular disease, blindness, stroke, and neuropathy. Treatment consists of supplemental insulin, changes in diet, or drugs - either aiming to further increase insulin secretion (sulphonylureas) or promote glucose uptake (biguanides) (Artasensi, Pedretti et al. 2020).

The number of patients with type 2 diabetes has been increasing rapidly as advances in healthcare have contributed to people living longer lives, and eating diets with a greater proportion of fat than before. Accompanying this has been research indicating that patients with diabetes are at a greater risk of developing neurodegenerative diseases, including Parkinson's disease (Martins, Hone et al. 2006, De Pablo-Fernandez, Goldacre et al. 2018). However, there are conflicting reports in the literature, especially since age is a major risk factor for both Parkinson's disease and type 2 diabetes (Cereda, Barichella et al. 2011). It is important to understand if there is a mechanistic link between the two diseases, which may provide further information on how to treat PD and reduce this co-morbidity.

5.1.2. Metabolic dysfunction may contribute to Parkinson's disease

A major hypothesis suggests that PD is partly a metabolic disease, specifically caused by insufficient energy production in DA neurons (Song and Kim 2016). These neurons have the most branched axonal arbours in the CNS and require a vast amount of energy to maintain their function (Pissadaki and Bolam 2013). Several PD models including toxin MPTP administration induce mitochondrial dysfunction, reducing the ability of the DA neurons to meet their energy requirements, resulting in cell death (Meredith and Rademacher 2011). Previous findings show that insulin resistance in PD patients is associated with increased disease progression and motor impairment (Bosco, Plastino et al. 2012, Athauda and Foltynie 2016). Thus, metabolic dysfunction may contribute as a cause of PD or exacerbate symptoms of PD.

Insulin receptors (InsRs) in the brain are also known to regulate DA release mediated by via striatal cholinergic interneurons (ChIs) (Stouffer, Woods et al. 2015). Circulating insulin acts on InsRs expressed on ChIs, increasing ChI excitability, and increasing the activation of nAChRs on DA axons to enhance DA release. Given that insulin signalling is dysregulated in both type 1 and type 2 diabetes, this may be a mechanism contributing to altered DA neurotransmission.

5.1.3. Mouse models of type 1 and type 2 diabetes

Mouse models of diabetes aim to replicate the pathophysiology of type 1 and type 2 diabetes observed in humans. The death of pancreatic β-islet cells present in type 1 diabetes is modelled by treatment of mice with streptozotocin (STZ), a broad-spectrum antibiotic administered via i.p. injection over a 5-day period (Like and Rossini 1976, Furman 2015). STZ is transported into pancreatic β-islet cells via a glucose transporter (GluT2) and results in the alkylation of DNA within these cells, resulting in poly ADP-ribosylation that disrupts cellular metabolism and promotes the generation of super oxide radicals (Szkudelski 2001). Ultimately, this leads to necrotic cell death, and the loss of insulin synthesis. These mice develop stable hyperglycaemia within a week of STZ-treatment. The protocol of STZ-treatment can be adapted for the severity of diabetes induced, with STZ-treatment also used as a model of diabetic neuropathy (Furman 2015).

Development of type 2 diabetes in humans is typically slow and multifactorial, including age, obesity, and genetic pre-disposition that arises over a prolonged period. As an approximate model, leptin and leptin receptor KO mice (*ob/ob* and *db/db* respectively) are used (Friedman, Leibel et al. 1991, Lee, Proenca et al. 1996). Leptin is a neuropeptide and hormone that is released after eating and from adipose tissue to mediate satiety, and cessation of eating. These mice lose satiety signalling, causing early onset and severe obesity from 4 weeks of age, and resultant hyperglycaemia, which develops between 4-8 weeks of age (Wang, Chandrasekera et al. 2014).

The hypothesis that diabetic mice may have altered dopaminergic neurotransmission predominantly arises from human clinical studies identifying co-morbidity between diabetes and Parkinson's disease. A previous study in 10 week-old *db/db* mice did not report loss of TH-positive cells in midbrain, suggesting no death of DA neurons at that timepoint (Wang, Zhai et al. 2014). However, they did report activated microglia and increased aggregation of α-synuclein in midbrain, and increased vulnerability of *db/db* mice to 6-OHDA lesion. In the present study, our collaborators did not find a decrease in the number of TH-positive cells expressed in either midbrain or striatum for either *db/db* or STZ-treated models of diabetes. However, they also reported increased vulnerability to 6-OHDA lesion. These results could be indicative of a prodromal parkinsonian phenotype, where a reduction of evoked $[DA]_o$ can be observed before DA neuron death in midbrain (Janezic, Threlfell et al. 2013).

5.1.4. DAT dysregulation is implicated in both Parkinson's Disease and diabetes

Our collaborators collected data showing lower protein levels of DAT and GIRK2 channels in the CPu using Western blot in two different mouse models of diabetes: STZ-treated and *db/db* mice (see Sections 5.2.1.1 and 5.2.1.2) (Perez-Taboada, Alberquilla et al. 2020). The core function of DAT is to remove released DA from the extracellular space (Cragg and Rice 2004), but DAT inhibition also independently enhances DA release (John and Jones 2007), and regulates short-term plasticity of DA release (Condon, Platt et al. 2019). Therefore, it is difficult to predict what effect any alteration of DAT expression or function may have on DA release and re-uptake.

Furthermore, there is also evidence that DAT expression and function is altered in Parkinson's disease. DAT takes up metabolic toxins such as MPTP and rotenone that disrupt the mitochondrial

electron transport chain, reducing ATP production and resulting in DA neuron death (Hirata, Suzuno et al. 2008). DAT function itself may contribute to Parkinson's disease etiology via its depolarising action as an electrogenic transporter, requiring energy to maintain ionic gradients across the axonal membrane (Pissadaki and Bolam 2013). *SLC6A3* variants that have enhanced striatal cell surface expression are associated with enhanced risk of developing Parkinson's disease (Richter, Gabby et al. 2017). Threlfell et al. previously found that DAT function is enhanced in the *SNCA-OVX* model of Parkinson's disease (Threlfell, Mohammadi et al. 2021); the rate of DA transient decay is greater in *SNCA-OVX* mice, and Michaelis-Menten-like plots found V_{max} and K_m is greater in *SNCA-OVX* than *Snca*-null mice. However, it is unclear how changes in DAT function may manifest in diabetes models showing reduced DAT expression.

5.1.5. Fast-Scan Cyclic Voltammetry in acute *ex vivo* slices as a model

Our collaborators wanted to investigate whether dopaminergic neurotransmission was altered in diabetes models, given their results showing that diabetic mice have increased vulnerability to 6-OHDA lesion, and may indicate a prodromal Parkinson's disease phenotype(Perez-Taboada, Alberquilla et al. 2020). This was partly because synaptic dysfunction has been shown to precede neurodegeneration in some animal models, including the *SNCA-OVX* mouse model of PD (Janezic, Threlfell et al. 2013). Originally, they attempted to measure DA release in a striatal synaptosome preparation from mouse models of diabetes, evoking DA release using KCl and recording this using fast-scan cyclic voltammetry. However, they encountered technical difficulties performing FCV and asked if we could complete these experiments using an acute *ex vivo* brain slice preparation from the diabetic mouse models, evoking dopamine release using electrical stimulation.

This approach has some advantages. Firstly, brain slices contain intact neurons, and have endogenous sources of dopamine, making it more physiologically relevant. Secondly, electrical stimulation is closer physiologically than KCl mediated depolarisation, and the shorter time-course allows better resolution of changes in DA re-uptake. This will allow for a better understanding of any alterations in dopaminergic transmission that arise from changes in DAT expression or function.

5.1.2. Aim and hypothesis

We used FCV to record electrically-evoked DA release in mouse models of type 1 and type 2 diabetes, in comparison to control animals for each condition. We investigated whether DA release or the shape of the DA transients were altered, indicating a change in DA re-uptake. Given the previous findings that insulin receptors also regulate DA release via ChIs, we also wanted to investigate whether nAChR control of DA release is altered in diabetes.

5.2. Methods

Methods are as described in Chapter 2 unless detailed here.

5.2.1. Animals

We used mouse models of type 1 (STZ-induced) and type 2 diabetes (db/db) (Damasceno, Netto et al. 2014, Wang, Chandrasekera et al. 2014, Furman 2015). The background strain of the STZ-treated mice was C57BL/6J. All animals were male and aged between 15-20 weeks old at the time of experiments. Only male animals were used for these experiments to align with the results of our collaborators, who also only did their experiments in male mice and provided us with these animals, Particularly given that this is translational focused research, inclusion of female mice would better reflect the human population and highlight any sex-specific effects (**Section 2.1.2**). They were housed under a 12:12 hour light-dark cycle, with food and water access *ad libitum*. Blood glucose levels were monitored weekly before experiments were performed. Experimental protocols were approved by the Consejo Superior de Investigaciones Científicas (CSIC) under European Union (63/2010/EU) and Spanish (RD53/2013) regulation, and the University of Oxford Ethical Review Board under the United Kingdom Animals (Scientific Procedures) Act (1986).

5.2.1.1. Streptozotocin-dependent diabetes mouse model

Streptozotocin (STZ) (50 mg/kg, i.p.; Sigma-Aldrich, St. Louis, MO) was given for 5 consecutive days to induce death of the pancreatic β-cells. Mice were defined as diabetic when blood

glucose levels after a 4-hour fast were >250 mg/dL. Normal blood glucose levels (observed in the control mice) were below 250 mg/dL. Mice underwent vehicle administration (10 mM sodium citrate, i.p., 0.9% NaCl, pH 4.5) to provide a control.

5.2.1.2. *db/db* diabetes mouse model

The background strain of the *db/db* mice was BKS. The BKS-D-Lepr *db/db* mice are homozygous for a point mutation in the gene encoding the leptin receptor, resulting in a loss of function and inability to signal satiety (Chen, Charlat et al. 1996). These mice develop obesity and hyperglycaemia between 4-8 weeks, defined as when blood glucose levels after a 4-hour fast were >250 mg/dL. Littermate heterozygous *db/+* mice were used as a control. This is because a single functioning copy of the leptin receptor is sufficient to mediate satiety, and these mice remain lean and do not develop hyperglycaemia, but are still littermates with the same environmental background of the hyperglycaemic *db/db* mice.

5.2.2. Fast-scan cyclic voltammetry

5.2.2.1. Slice preparation

Diabetic animals were randomly assigned a paired control animal. On the day of experiments, the blood glucose levels of a diabetic animal and its paired control would be determined by blood drawn via lateral tail vein nick and measured on a glucose meter. The animals would then be culled and slice preparation would be undertaken as described in **Chapter 2, Section 2.2.4**. The order diabetic mouse and control mouse to undergo slice preparation alternated with each experimental day.

5.2.2.2. Experimental design

To evaluate any differences in dopaminergic neurotransmission between the diabetic animal and its control, a multi-site experimental protocol was used, as done previously (Janezic et al., 2013). In brief, 6 defined recording sites were chosen, with 3 in the dlCPu, 2 in the NAc core and 1 in the NAc shell. At the time of recording, a hemisphere of the diabetic mouse brain slice would be placed in the

recording chamber alongside a brain slice from the control animal. Electrically-evoked extracellular concentrations of DA ($[DA]_o$) would then be recorded from each defined site first in one brain slice, and then the other brain slice, in a randomised order. Each site would undergo electrical stimulation 3 times, with a 2.5min inter-stim interval. The order of stimulations would be 1p:1p, 1p:4p 100 Hz, 1p:4p 100 Hz. There is a 4 second interval between each successive pulse within a stimulation. The mean first 1p evoked DA release from each site (i.e. 3 technical replicates) was considered an independent unit of analysis, and the possibility of pseudoreplication across sites was considered.

5.2.3. Drugs

Experiments were either conducted drug-free conditions (aCSF only) or in the presence of 1 μM DHβE, to remove the contribution of nAChRs expressed on DA axons that regulate DA release (Threlfell and Cragg 2011).

5.3. Results

5.3.1. Dopamine release is altered in diabetes

We first used a multi-site recording protocol to characterise differences in DA release characteristics in diabetes models versus paired controls, also comparing dorsolateral caudate putamen (dlCPu) and nucleus accumbens core (NAc) within each model (**Fig. 5.1A**).

We found that the shape of $[DA]_o$ transients were altered in the dlCPu of both STZ-treated type 1 diabetes model mice (**Fig. 5.1B**, two-way RM ANOVA, treatment x time interaction, $F_{(8,960)} = 2.862$, $p = 0.0064$) and *db/db* type 2 diabetes model mice (**Fig. 5.1C**, two-way RM ANOVA, genotype x time interaction, $F_{(8,752)} = 4.452$, $p < 0.0001$). We also observed a subtle increase in evoked $[DA]_o$ in *db/db* mice versus *db/+* mice (**Fig. 5.1C**, paired t-test, $p = 0.0015$) but this was not observed in STZ-treated versus vehicle-treated mice (**Fig. 5.1B,** paired t-test, $p = 0.0674$). In contrast, we did not find any difference in the transient shape in the NAc in either STZ-treated mice (**Fig. 5.1D**, two-way RM

ANOVA, treatment x time interaction, $F_{(8,624)} = 0.07524$, p = 0.9997) or *db/db* mice (**Fig. 5.1E**, two-way RM ANOVA, genotype x time interaction, $F_{(8,512)} = 1.896$, p = 0.0585).

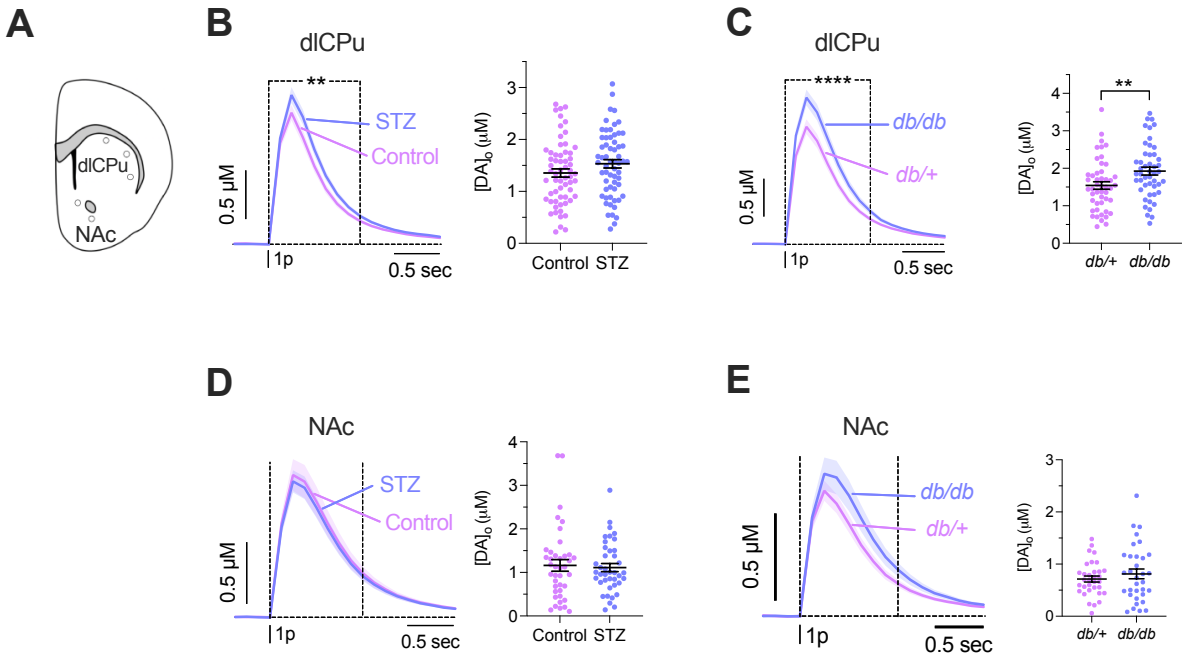

Figure 5.1. Dopamine release is altered in the dlCPu of STZ- and *db/db* models of diabetes

(A) Diagram showing recording sites used to record DA release in dlCPu and NAc using FSCV.

(B) *Left*: Transients showing mean $[DA]_o$ (±SEM) versus time evoked by 1p stimulus in dlCPu of STZ-treated diabetic and vehicle-treated non-diabetic control mice. Two-way RM ANOVA between dotted lines, treatment x time interaction, $F_{8,960} = 2.682$, p = 0.0064 (**). *Right:* Peak $[DA]_o$ (± SEM) in STZ-treated or vehicle treated mice. Paired t-test, p = 0.0674 (n.s.). n = 61 sites, 21 slices, 10 animals per treatment

(C) *Left*: Transients showing mean $[DA]_o$ (±SEM) versus time evoked by 1p stimulus in dlCPu of *db/db* diabetic and *db/+* non-diabetic mice. Two-way RM ANOVA between dotted lines, treatment x time interaction, $F_{8,752} = 4.452$, p < 0.0001 (****). *Right:* Peak $[DA]_o$ (±SEM) in *db/db* or *db/+* mice. Paired t-test, p = 0.0015 (**). n = 48 sites, 17 slices, 8 animals per genotype

(D) *Left*: Transients showing mean $[DA]_o$ (± SEM) versus time evoked by 1p stimulus in NAc of STZ-treated diabetic and vehicle-treated non-diabetic control mice. Two-way RM ANOVA between dotted lines, treatment x time interaction, $F_{8,624} = 0.07524$, p = 0.9997 (n.s.). *Right:* Peak $[DA]_o$ (±SEM) in STZ-treated or vehicle treated mice. Paired t-test, p = 0.6823 (n.s.). n = 40 sites, 20 slices, 10 animals per treatment

(E) *Left*: Transients showing mean $[DA]_o$ (±SEM) versus time evoked by 1p stimulus in NAc of *db/db* diabetic and *db/+* non-diabetic mice. Two-way RM ANOVA between dotted lines, treatment x time interaction, $F_{8,512} = 1.896$, p = 0.0585 (n.s.). *Right:* Peak $[DA]_o$ (±SEM) in *db/db* or *db/+* mice. Paired t-test, p = 0.3491 (n.s.). n = 33 sites, 17 slices, 8 animals per genotype

5.3.2. Dopamine re-uptake is altered in diabetes

These data show a change in the profile of $[DA]_o$ in both models in dlCPu but not NAc, trending towards increased $[DA]_o$ which was significant in the *db/db* model. Given our collaborators previously found reduced DAT protein levels in both STZ-treated and *db/db* mice, we hypothesised that the changes in the transient shape were due to reduced DAT expression, and that dopamine re-uptake would be slower in both models. This could also contribute to elevated peak $[DA]_o$.

We tested changes in the falling-phases of the DA transients in the recordings from dlCPu sites (**Fig. 5.2.A**) using two alternative methods: approximation of the decay rate to a first-order exponential and approximation to a Michaelis-Menten relationship.

The falling phase of $[DA]_o$ can be approximated by a one-phase exponential decay curve (**Fig. 5.2.B**. $R^2 = 0.99$). The decay constant of $[DA]_o$ falling phase is significantly lower in STZ-treated mice versus vehicle controls (**Fig. 5.2C**, unpaired t-test, $p < 0.0001$, n = 188 recordings, mean $R^2 = 0.98$) but not in *db/db* versus *db/+* mice (**Fig. 5.2D**, n = 142 recordings, mean $R^2 = 0.99$). We can also estimate the activity of the DAT by using a Michaelis-Menten curve fit to estimate Vmax against a plot of the maximum decay rate of each transient (**Fig. 5.2E**). We found that the uptake rate was significantly lower in STZ-treated vs vehicle-treated mice (**Fig. 5.2F**, STZ-treated: Vmax = 20.1 ± 2.3 μM/s, $R^2 = 0.88$; vehicle-treated: Vmax = 22.0 ± 2.6 μM/s, $R^2 = 0.83$; comparison of fits: $p < 0.0001$). However, we did not find a significant difference in uptake rate between *db/db* and *db/+* mice (**Fig. 5.2G**, *db/db*: Vmax = 11.97 ± 1.23 μM/s, $R^2 = 0.67$; *db/+*: Vmax = 12.3 ±1.3 μM/s, $R^2 = 0.83$).

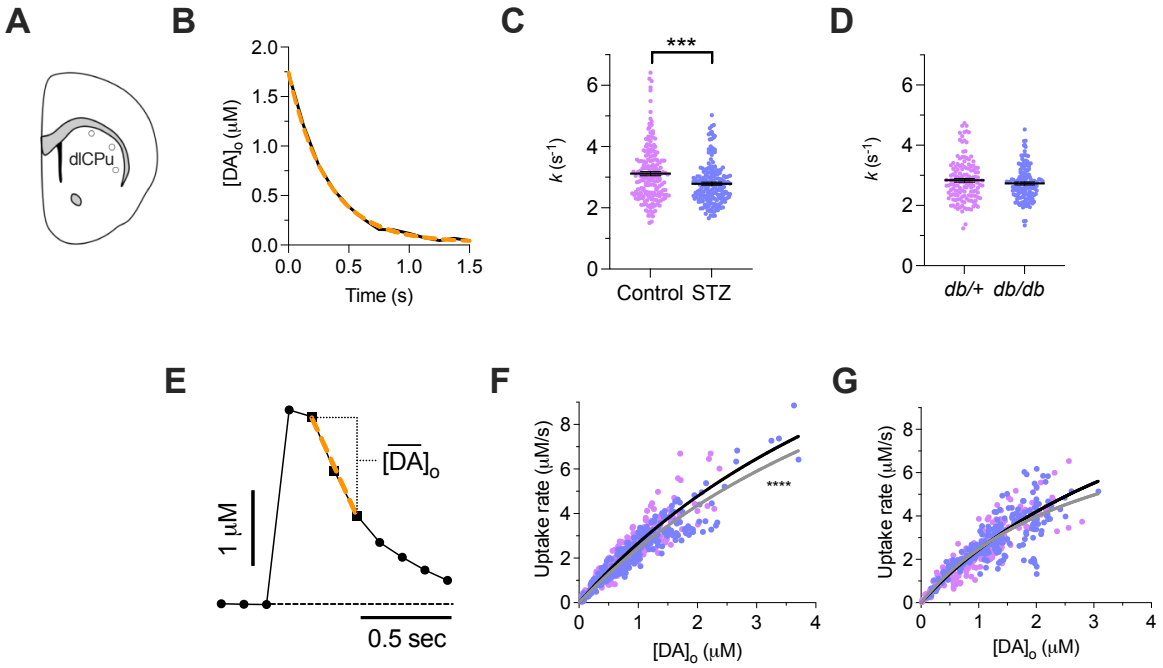

Figure 5.2. Dopamine re-uptake is altered in the STZ-model of diabetes

(A) Diagram showing recording sites used for re-uptake analysis

(B) Representative example of falling phase of evoked extracellular dopamine profile (black line) and fit of a one-phase exponential decay curve to approximate falling phase (orange dashed line). $R^2 = 0.99$.

(C+D) Population data and mean (±SEM) for exponential decay constants (*k*) from approximation to one-phase exponential decay fit calculated for each DA transient in STZ-diabetic vs controls (n = 188; mean $R^2 > 0.98$) or in db/db vs db/+ (n = 142; mean R^2 = 0.99). Unpaired t-test, $p < 0.001$ (***)

(E) Representative example of $[DA]_o$ profile depicting sampling rate and mean $[DA]_o$ recorded at that point, for use in Michaelis-Menten plots in (F+G)

(F) Maximum decay rate of each transient plotted against mean $[DA]_o$ at that rate, with Michaelis-Menten curve fit for STZ-treated diabetic mice (Vmax = 20.1 ± 2.3 μM/s; R^2 = 0.88) vs vehicle-treated control mice (Vmax = 22.0 ± 2.6 μM/s; R^2 = 0.83). Km constrained to equal value of 7.23 μM. Comparison of fits: $P < 0.0001$ (****)

(G) Maximum decay rate of each transient plotted against mean $[DA]_o$ at that rate, with Michaelis-Menten curve fit for *db/db* diabetic mice (Vmax = 11.97 ± 1.23 μM/s; R^2 = 0.67) vs *db/+* control mice (Vmax = 12.3 ± 1.3 μM/s; R^2 = 0.83). Km constrained to equal value of 3.9 μM for each genotype.

Data collected and analysed together with Dr Stefania Vietti-Michelina

5.3.3. The pulse-number dependence of dopamine release is not altered in diabetes

Given previous findings that insulin receptor activity regulates DA release via ChIs, we also investigated the pulse-number dependence of DA release in these diabetes models. This is because the pulse-number dependence of DA release is powerfully regulated by nAChRs, with the pulse-number dependence of DA release increasing as nAChRs on DA axons are either not active or inactivated due to extracellular levels of ACh. We tested this by comparing the ratio of $[DA]_o$ evoked by either 1p or 4p 100 Hz electrical stimulation in each diabetes model, in drug-free aCSF and 1 μM DHβE to block the nAChRs. In either dlCPu or NAc, we did not find a significant effect of treatment for STZ-treated mice versus vehicle-treated control mice (**Fig. 5.3.A+C**, two-way RM ANOVA. (**A**) dlCPU: Main effect of treatment, $F_{(1,10)} = 1.282$, p = 0.3512; (**C**) NAc: Main effect of treatment, $F_{(1,10)} = 1.585$, p = 0.2367). We also did not find a significant effect of genotype for *db/db* vs *db/+* mice (**Fig. 5.3B+D**. Two-way RM ANOVA. (**B**) dlCPU: Main effect of genotype, $F_{(1,8)} = 1.054$, p = 0.3346; (**D**) NAc: Main effect of genotype, $F_{(1,6)} = 1.598$, p = 0.2530). These data suggest that in these models of diabetes, the pulse-number dependence of $[DA]_o$ is not affected.

5.4. Discussion

These experiments show that striatal dopaminergic neurotransmission is altered in both type 1 and type 2 models of diabetes. They also show reduced re-uptake in the type 1 model, but not the type 2 model. Finally, they do not show any change in the pulse-number dependence of DA release in either model. These results suggest that diabetes can alter dopaminergic neurotransmission, perhaps with a difference in mechanism between type 1 and type 2 diabetes.

5.4.1. Alteration of DA release in diabetes models

Our findings that dopamine release is altered in the diabetes models is consistent with the previous findings that DAT expression is reduced in both models. However, the DAT exerts multiple

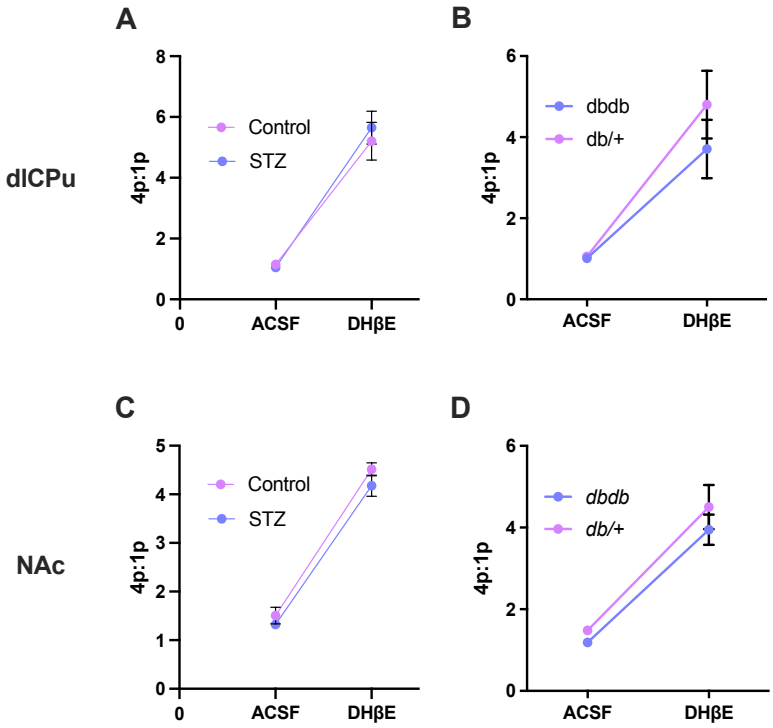

Figure 5.3. Pulse-number dependence of dopamine release is not altered in diabetes

(A+C) Ratio of DA release evoked by 1p and 4p 100 Hz, in the presence and absence of DHβE in STZ-treated diabetic and vehicle-treated non-diabetic mice.

(A) dlCPu: Treatment X DHβE, $F_{(1,10)} = 0.4885$, p = 0.5005 (n.s.). Effect of DHβE, $F_{(1,10)} = 124.3$, p < 0.0001 (****). Effect of Treatment, $F_{(1,10)} = 1.282$, p = 0.3512 (n.s.). Control: n = 6 slices / 5 animals. STZ: n = 6 slices / 5 animals

(C) NAc: Treatment X DHβE, $F_{(1,10)} = 0.5989$, p = 0.4569 (n.s.). Effect of DHβE, $F_{(1,10)} = 853.9$, p < 0.0001 (****). Effect of Treatment, $F_{(1,10)} = 1.585$, p = 0.2367 (n.s.). Control: n = 6 slices / 5 animals, STZ: n = 6 slices / 4 animals

(**B+D**) Ratio of DA release evoked by 1p and 4p 100 Hz, in the presence and absence of DHβE in *db/db* diabetic and *db/+* non-diabetic mice.

(B) dlCPu: 4p:1p in *db/db* and *db/+* mice in the presence or absence of DHβE. dlCPu. DHβE X Genotype: F(1,8) = 0.9096, p = 0.3688 (n.s.). Effect of DHβE: F(1,8) = 34.14, p = 0.0004 (***). Effect of Genotype: F(1,8) = 1.054, p = 0.3346 (n.s.). *db/db* and *db/+*: n = 5 slices / 5 animals

(D) NAc: 4p:1p in *db/db* and *db/+* mice in the presence or absence of DHβE. NAc. DHβE X Genotype: F(1,6) = 0.1567, p = 0.7059 (n.s.). Effect of DHβE: F(1,6) = 78.14, p = 0.0001 (***). Effect of Genotype: F(1,6) = 1.598, p = 0.2530 (n.s.) *db/db* and *db/+*: n = 4 slices / 4 animals

Data collected and analysed together with Dr Stefania Vietti-Michelina

effects not only on DA uptake, but also DA release and re-release (Threlfell, Mohammadi et al. 2021). Therefore, it is difficult to predict the relationship between DAT function and DA release, and this needs to be investigated experimentally.

There is previous evidence that DAT function is altered in neurodegeneration (Threlfell, Mohammadi et al. 2021). Intuitively, neurodegeneration of dopaminergic axons will reduce the overall

expression of functional DAT in the striatum, slowing re-uptake. But this will also reduce the number of DA release sites, reducing the quantity $[DA]_o$. Our results show that the profile of DA release and re-uptake is altered in both type 1 and type 2 models of diabetes (Fig. 5.1**)**, consistent with a reduction in DAT expression and availability of DAT translocation sites. We found an increase in evoked peak $[DA]_o$ in the type 2 model of diabetes but not type 1. This may be due to the reduction in DA content identified by our collaborators in the type 1 but not type 2 model of diabetes, reducing the amount of dopamine available to be released in the type 1 model and not manifesting as greater evoked peak $[DA]_o$ in comparison to vehicle-treated control (Perez-Taboada, Alberquilla et al. 2020). The Slc6a3$^{IRES\text{-}Cre}$ mouse line that expresses Cre-recombinase selectively in DAT-expressing neurons exhibits a ~ 16% decrease in DAT protein levels, with the effect of significantly slower DA transients but no effect on peak $[DA]_o$ (Threlfell, Mohammadi et al. 2021). This is much smaller than the ~ 80% and ~ 70% reductions in DAT expression in the STZ-treated and *db/db* diabetic mice respectively and may explain why an effect on peak evoked $[DA]_o$ is revealed under these conditions.

Further investigation of DA re-uptake kinetics (Fig. 5.2) shows a reduction in both the single-exponential decay constant and V_{max} in the type 1 STZ-treatment diabetes model. This is also consistent with the lower DAT expression reported by our collaborators (Perez-Taboada, Alberquilla et al. 2020). However, we did not find a significant change in DA re-uptake in the type 2 model of diabetes, despite lower DAT expression levels. However, given the much greater reduction in DAT expression in both models compared to Slc6a3$^{IRES\text{-}Cre}$ heterozygous mice, it is surprising that there is only a subtle effect on DA re-uptake in the STZ-treatment model and no effect in the *db/db* model. This may be the result of additional compensatory mechanisms resulting in increased trafficking of DAT to the axon membrane, or perhaps limitations in directly comparing protein content and function. This discrepancy between reported DAT expression level and function in disease states should be further investigated. The differences between the STZ-treated and *db/db* mice may be due to the underlying differences in insulin dysregulation between type 1 and type 2 diabetes.

One aim of this collaboration was to understand if diabetes models showed signs of nigrostriatal degeneration, as a risk-factor for PD. Our results showed that changes in dopaminergic

neurotransmission were region-specific for the dlCPu, with no change in the NAc. This is relevant because DA release in the NAc is spared in the *SNCA-OVX* model of PD (Janezic, Threlfell et al. 2013). In the *SNCA-OVX* mouse model of PD, there is no difference in overall levels of DAT expression, but there is a significant increase in radio-labelled cocaine binding, indicating enhanced DAT availability (Threlfell, Mohammadi et al. 2021). This is reflected in results showing a greater single-exponential decay constant and values for V_{max} and K_m in *SNCA-OVX* vs Snca-null mice. Our results showing a reduction in single-exponential decay constant and V_{max} in the type 1 diabetes model is more similar to the Snca-null animals. There may be an accompanying change not only in the number of DA-translocation sites, but also in the in the dimerization state of the DAT (Zhen and Reith 2018). Shifting from a monomeric to a dimeric (or tetrameric) conformation may reduce the translocation rate, in turn reducing DA re-uptake. Assessment of any difference in the conformation of DAT between the diabetes models and their respective controls would be a valuable subsequent experiment to better understand how the DAT may be changing to give the results shown above.

5.4.2 Insulin receptor regulation of ChIs in diabetes

Although not the primary aim of this collaboration, we also investigated whether there may be a change in the nAChR activation state on DA axons in the diabetes models versus their respective controls. This was because of previous research showing that insulin enhances the excitability of ChIs, increasing the activation of nAChRs on DA axons, increasing evoked DA release (Stouffer, Woods et al. 2015). Furthermore, they also identified that the ability of insulin to mediate this increase is lost in animals that are fed an obesogenic diet and have greater bodyweight than control animals.

We found no significant interaction between the effects of diabetes and pulse-number dependence of DA release, suggesting that the level of nAChR activation is not significantly different between the diabetes models and their respective controls. There are key considerations when comparing these results with those found by Stouffer et al. Firstly, there may species differences since Stouffer et al. performed their experiments in rats rather than mice in the present study. Secondly, the rats fed an obesogenic diet had a higher bodyweight and greater circulating plasma insulin levels than

controls, but at this point were still able to regulate their blood glucose concentrations within normal levels, unlike the diabetic mice used here. The type 2 diabetes mice exhibit insulin resistance which would result in high circulating levels of insulin, but indirect mechanisms of hyperglycaemia may alter the interaction between insulin receptors and dopamine release. Further research could investigate whether the effect of insulin on DA release is altered in these mice, and I would hypothesise that the mechanism of insulin to increase DA release would be reduced or lost due to insulin resistance.

A subsequent study specifically examining the effect of insulin on DAT activity showed that insulin increases V_{max} (Patel, Stouffer et al. 2019). We would hypothesise that the type 2 diabetes model has higher levels of insulin than the type 1 model. This may explain why in the type 1 model with lower DAT expression and lower insulin levels, we observed slower uptake kinetics, but in the type 2 model with higher insulin levels this is offset against lower DAT expression, versus its internal control. Again, diabetes has a number of systemic effects beyond insulin levels, including dysregulated blood-sugar levels, which may also exert an effect of dopaminergic neurotransmission.

In conclusion, we found that DA release is altered in both type 1 and type 2 models of diabetes. Consistent with findings from our collaborators, we identified impaired DAT function in the type 1 model. Although we did not find altered uptake kinetics in our type 2 model, this may be due to the phenotype of high circulating insulin enhancing the activity of residual DAT. Further research is warranted, particularly at later time points to see if a reduction in DA release consistent with neurodegeneration is observed, and evaluating any conformational changes in the DAT which can also be observed in neurodegenerative disease.

Chapter 6: General Discussion

DA has an important function within the striatum of modulating the response of the output MSNs to the afferent inputs from cortex and thalamus. DA release from DA neurons originating in the midbrain is not only regulated by somatodendritic activity but is also controlled at the level of the axon, where local mechanisms can gate and even drive DA release (Sulzer, Cragg et al. 2016). The striatum has a wide range of neurotransmitters and neuromodulators expressed by a diverse range of neurons and astrocytes, which have the potential to locally regulate DA release. A better understanding of the regulatory mechanisms of DA release may also allow us to better understand changes in dopaminergic neurotransmission in diseased states, and identify new targets for treatment.

The aim of my project was to investigate the presynaptic regulation of dopamine. In Chapter 3, I investigate the role of cGlyRs and eGlyRs in local modulation of striatal DA release. We show that both cGlyrs and eGlyRs are able to regulate DA release, an ambient glycine tone is present in striatum, and that eGlyRs act indirectly via nAChRs expressed on DA axons. In Chapter 4, I investigate the role of these receptors to modulate the activity of ChIs and ACh release, as a known indirect mechanism of regulating DA release. We show that both cGlyRs and eGlyRs regulate ACh release, the presence of cGlyR and eGlyR subunits expressed in striatal ChIs, and that eGlyRs regulate the activity of ChIs. An overall schematic of these findings is shown in Figure 6.1. Finally, in Chapter 5, I investigate whether dopaminergic neurotransmission is altered in diabetes, given previous evidence of co-morbidities with Parkinson's disease. We show that dopaminergic neurotransmission is subtly altered, with changes in DA release and DA re-uptake likely due to changes in DAT expression and function. In this chapter, I will discuss my results within the wider context of regulation of dopaminergic neurotransmission in health and disease.

6.1. cGlyRs regulate striatal DA release

Glycinergic neurotransmission and cGlyR function has historically been associated with the caudal CNS, particularly the spinal cord and hindbrain. This was linked to early studies showing low levels of strychnine binding sites and expression of GlyT2, the neuronal glycine transporter that is a marker for presynaptic glycinergic terminals, in the forebrain (Young and Snyder 1973, Zeilhofer,

Studler et al. 2005). Beyond these regions, there has been relatively little investigation of glycinergic neurotransmission, particularly in comparison to GABA, the other fast inhibitory neurotransmitter. Within the striatum, there was previous evidence for the expression of cGlyRs and even a regulatory effect on dopamine levels, even though results were conflicting and mechanism unclear (Yadid, Pacak et al. 1993, Sergeeva and Haas 2001, McCracken, Lowes et al. 2017). In Chapter 3, I revisit this question within the context of indirect modulation of DA release via other mechanisms, such as ChIs and astrocytes. I found that cGlyRs were functional and expressed in striatum, and regulate the release of both DA and ACh, although with the effect on DA not mediated indirectly via ACh.

6.1.1. cGlyRs regulate DA release

I found that strychnine alone was able to reduce evoked DA release in dlCPu and NAc (Chapter 3, Section 3.1.), showing that cGlyRs regulate evoked striatal DA release. This data supports the findings of Yorgasson et al, who also found that strychnine reduced evoked DA release in NAc core (Yorgason, Wadsworth et al. 2022). I also found that strychnine reduced DA release evoked by the selective stimulation of DA axons targeted using optogenetic stimulation (Chapter 3, Section 3.1.). This supports the hypothesis of an ambient glycine tone present in striatum that mediates tonic activation of cGlyRs, rather than glycine being coincidentally evoked via non-specific electrical stimulation. Previous studies observed tonic strychnine-sensitive currents present on striatal MSNs, supporting my results (McCracken, Lowes et al. 2017, Molchanova, Comhair et al. 2017). Experiments using picrotoxin, at low concentrations selective for extrasynaptic cGlyRs, would help to distinguish between the contribution of synaptic and extrasynaptic cGlyRs for this effect.

It is interesting that the effect of intra-striatal strychnine appears to be lower or absent in vivo, with higher concentrations (> 20μM) required to show any effect on DA levels if any is observed (Molander and Soderpalm 2005, Yorgason, Wadsworth et al. 2022). This is true for studies investigating changes in non-evoked extracellular DA levels, and evoked extracellular DA release. This may be due to better perfusion in a slice preparation allowing higher concentrations of strychnine within tissue, or indirect mechanisms mediated via an intact system. Nevertheless, the reduction of evoked DA release

by strychnine (~35%) shows cGlyR control of a similar magnitude to A1 receptors (~50%) that mediate a tonic inhibition of DA release, and shows that cGlyRs powerfully regulate DA release (Roberts, Lambert et al. 2022).

6.1.2. cGlyRs regulate ACh release, but not sufficiently to alter DA release

Although not the primary aim of this project, I also considered where cGlyRs are expressed in the striatum to regulate DA release. In particular, there is evidence for the expression of functional cGlyRs on striatal ChIs (Sergeeva 1998, Darstein, Landwehrmeyer et al. 2000, Sergeeva and Haas 2001). Given their powerful role in regulating DA release, I hypothesised that cGlyRs may regulate DA release (at least partially) indirectly via ChIs acting on nAChRs expressed on DA axons (Rice and Cragg 2004, Threlfell and Cragg 2011). I found that the strychnine mediated reduction in DA release was not dependent on nAChRs, which ruled out any off target effects of strychnine acting as antagonist at nAChRs as previously reported, but also showed that strychnine did not indirectly alter ChI activity (Matsubayashi, Alkodon et al. 1998, Garcia-Colunga and Miledi 1999). I found that strychnine was able to increase evoked ACh release (Chapter 4, Section 4.3.1.). This showed that, similar for DA release, ACh release is under the control of tonic cGlyR activity, but in combination with the FSCV data, this effect is insufficient to alter the activity of downstream nAChRs on DA axons. Strychnine increased ACh release with an effect on the AUC rather than peak evoked ACh. This is consistent with the increase in ACh release mediated by GABA-R antagonists, that also increases AUC rather than peak evoked ACh (Dr Stefania Vietti-Michelina, personal communication).

6.1.3. cGlyRs are also expressed on a sub-population of NPY+ interneurons

Our results using RNAscope not only showed the expression of cGlyR subunits in ChIs, but also showed the α2 subunits expressed in a small subpopulation (~25%) of *Npy*+ cells (Chapter 4, Section 4.3.2.). This has not been described before and suggests the functional expression of cGlyRs on these interneurons. Although use of *Npy*+ expression is a useful contrast against ChIs, both LTSIs and

NGF interneurons express NPY. To investigate expression specifically on LTSIs, co-expression of SST would provide an LTSI-specific marker in striatum (Ibanez-Sandoval, Tecuapetla et al. 2011). Approximately 25% of *Npy*+ cells are NGF interneurons, which may represent the portion of *Npy*+ interneurons expressing α2 cGlyR subunits. LTSIs inhibit DA release via $GABA_BR$ signalling (Holly, Davatolhagh et al. 2021), and a hypothesis would suggest that strychnine application might indirectly regulate DA release via GABAergic signalling. This possible indirect effect on DA release should be tested further, by testing the effects of strychnine in $GABA_BR$ antagonist, but these results also highlight the wide spread of cGlyRs on both ChIs and NPY+ interneurons across the striatum.

6.2. Functional eGlyRs are expressed in striatum and regulate DA release via ChIs

Initially, eGlyRs were only thought to be functional in heterologous expression systems (Chatterton, Awobuluyi et al. 2002), then only in juvenile animals (Grand, Abi Gerges et al. 2018). eGlyRs have now been identified *in vivo* in adult animals, first in adult medial habenula but also in basolateral amygdala and cortical SST+ interneurons (Otsu, Darcq et al. 2019, Bossi, Dhanasobhon et al. 2022). Research into the distribution and function of this receptor is still in its infancy. No previous study had investigated a contribution of eGlyRs for the glycinergic regulation of DA release, having only relatively recently been identified in adult forebrain. However, previous ISH data provided a strong hypothesis for their expression and possible function in striatum (Allen Institute for Brain Science, 2011, Experiment: 73907499). I found that CGP-78608 alone reduces evoked DA release, suggesting that these receptors are tonically active, and the complete dependence of this effect on nAChRs strongly suggests a mechanism mediated via ChIs. This indirect regulatory mechanism highlights the key role that ChIs play in the regulation of DA release. I also found that application of glycine mediates non-evoked ACh release, an excitatory effect likely mediated via eGlyRs.

6.2.1. ChIs express eGlyRs on ChIs

In Chapter 3, I showed that eGlyRs were able to alter DA release, and the that their effect was wholly dependent on nAChRs. This suggests a mechanism where eGlyRs change the activation of nAChRs, likely by modulating ACh release (Threlfell and Cragg 2011). This is supported by previous ISH data showing expression of Grin3A in the striatum, with a distribution indicative of striatal interneurons including ChIs (Allen Institute for Brain Science, 2011, Experiment: 73907499). Our RNAscope data shows the presence of Grin3A in striatal ChIs and *Npy*+ cells, and patch-clamp recordings pharmacologically define eGlyR currents in ChIs. This identifies a mechanism whereby glycine can mediate an excitatory effect on ChIs.

CGP-78608 acts by binding to the GluN1 subunit that mediates eGlyR desensitisation. This mechanism is state-dependent, whereby CGP-78608 cannot bind if the GluN1 subunit already has glycine bound, and the eGlyR is desensitised (Grand, Abi Gerges et al. 2018). Therefore, the receptors must be tonically active, such that they are already in an active conformation, but CGP-78608 binding prevents desensitisation. Therefore, there are a mixed population of eGlyRs in our preparation, of which some are tonically active and others desensitised, because CGP-78608 is able to mediate an effect in the absence of added agonist. This suggests that eGlyRs maintain the excitability of ChIs under the control of ambient striatal glycine, as observed in cortical interneurons (Bossi, Dhanasobhon et al. 2022).

6.2.2. Glycine evokes spontaneous release of ACh

The excitatory effect of glycine on ChIs was observed in non-evoked recordings where glycine evoked spontaneous ACh release, measured using $GRAB_{ACh3.0}$, in a TTX-sensitive manner. A previous study found that glycine mediated TTX-sensitive efflux of radiolabelled ACh from striatal tissue, consistent with my findings (Hernandes, de Magalhaes et al. 2007). However, when measuring ChI firing rate, application of glycine alone only reduced firing rate, with glycine only mediating an increase in firing rate in the presence of CGP-78608 and strychnine (Fig. 4.12.). A key difference

between these two experiments is that the experiment detecting ACh release was performed in the presence of ambenonium, inhibiting the activity of AChE to allow visualisation of the signals. However, this elevates extracellular ACh, and may activate muscarinic autoreceptors on ChIs. This may alter the overall effect of glycine on ChIs, producing a different result between electrophysiology and $GRAB_{ACh3.0}$ recordings. To avoid any confounding effect of ambenonium, the recordings investigating the effect of glycine on ChI firing rate could also be investigated in the presence of ambenonium to allow direct comparison to the $GRAB_{ACh3.0}$ data.

We also found Grin3A expression in *Npy*+ cells. If further experiments identify expression in LTSIs, cortical SST+ interneurons co-express Grin3A, suggesting this may be consistent between brain regions (Bossi, Dhanasobhon et al. 2022). Previous evidence has shown that LTSIs can modulate DA release via GABAergic transmission acting on $GABA_BRs$ (Holly, Davatolhagh et al. 2021). It would be interesting to see if any component of eGlyR regulation of DA release is mediated indirectly via GABA - although this seems unlikely since DHβE occluded the entire effect of CGP-78608.

6.3. The striatum contains an ambient glycine tone, regulated by astrocytic GlyT1

Previous studies found that inhibition of GlyT1 increased tonic currents mediated by cGlyRs in striatum, or the effect of the cGlyR antagonist strychnine (McCracken, Lowes et al. 2017, Molchanova, Comhair et al. 2017). I found that GlyT1 inhibition by sarcosine enhanced the effect of strychnine and enhanced the effect of exogenous application of glycine. This supports previous the previous evidence for functional expression of GlyT1 in striatum. The alternative mechanism of glycine uptake is via GlyT2, which is selectively expressed on neurons. However, there is very little evidence for the expression of GlyT2 in striatum, and GlyT1 is the predominant glycine uptake mechanism in striatum (Zeilhofer, Studler et al. 2005, Munoz, Yevenes et al. 2018).

GlyT2 is also commonly used as a presynaptic marker for glycinergic fibres, so its absence from striatum poses the question of the source of endogenous striatal glycine (Mangin, Guyon et al.

2002, Zeilhofer, Studler et al. 2005). There is only one study suggesting that VGAT-expressing neurons are a neuronal source of glycine, and the predominant hypothesis is that any glycine tone would be astrocytic in source. Glycine release is possible via reversal of the GlyT1 transporter, and similar to ENT1 mediated release and re-uptake of adenosine, glycine may also be released via GlyT1 reversal (Shibasaki, Hosoi et al. 2017, Roberts, Lambert et al. 2022). An *in vivo* study found that intrastriatal fluorocitrate administration, causing the selective ablation of astrocytes, did not alter levels of glycine recorded by microdialysis (Adermark, Lagstrom et al. 2022). This likely demonstrates the complex role of GlyT1 as a regulator of both glycine release and re-uptake, such that loss of GlyT1 function may result in no net change in extracellular glycine levels.

Given the absence of strong evidence for striatal glycinergic innervation, previous studies hypothesised that taurine, a partial agonist at cGlyRs, might be the endogenous agonist. There is good evidence for this: the striatum is particularly enriched in taurine and the taurine transporter (TauT) (Palkovits, Elekes et al. 1986, Sergeeva, Fleischer et al. 2007), taurine is established as a gliotransmitter via release from VRACs on astrocytes, and the taurine tone mediated via its release from VRACs has been shown to mediate tonic inhibition on cGlyRs in another brain region (Mongin, Cai et al. 1999, Choe, Olson et al. 2012). In my experiments, I found that taurine can reduce DA release and ACh release similarly to glycine, suggesting a common mechanism via cGlyRs. This could be tested further by performing experiments in the presence of $GABA_AR$ antagonists to rule out off-target effects (Jia, Yue et al. 2008). However, since GlyT1 also regulates the tonic activity of striatal cGlyRs, it is likely that there is tonic activation of cGlyRs mediated by both ambient glycine and taurine, and these ligands are not mutually exclusive.

We found that the prolonged decline of DA release upon continuous glycine application is blocked by the non-specific adenosine receptor antagonist caffeine, showing that it is mediated via adenosine receptors (Chapter 3, Section 3.3.15). We also found that oxotremorine-M, used to silence ChIs, did not stop the prolonged decline of DA release by glycine. This argues against the co-release of ATP from ChIs and its subsequent hydrolysis as the source of adenosine (Threlfell, Clements et al. 2010). An additional candidate gliotransmitter associated with glycine is adenosine.

ATP and adenosine are both candidate gliotransmitters, that could ultimately act as the source of adenosine observed to mediate the prolonged decline of DA release in our experiments. Adenosine levels in the striatum are at least partly regulated via the ENT1 transporter located on astrocytes (Roberts, Lambert et al. 2022). GlyT1 is electrogenic, resulting in net depolarisation upon inward transport of glycine (Zhang, Uchendu et al. 2021). However, it is not yet clear how this would then alter the activity of astrocytes or stimulate adenosine release from astrocytes.

Astrocytes have an important role as hubs that regulate extrasynaptic tone of neurotransmitters that mediate tonic currents on target neurons, indirectly regulating DA release. Our lab has recently shown their importance in regulating tonic GABA and adenosine regulation of DA release, and my findings show that it also regulates the glycinergic regulation of DA release (Roberts, Doig et al. 2020, Roberts, Lambert et al. 2022). More broadly, this highlights the key role they play in regulating striatal neurotransmission, having been previously overlooked. Reduced expression of GATs in Parkinson's disease contributes to enhanced tonic inhibition of DA release, and it would be interesting to explore if GlyT1 expression is also altered, as a contributing factor to the pathology of Parkinson's disease (Roberts, Lambert et al. 2022). This could be tested using the *SNCA*-OVX mouse model of Parkinson's disease, to investigate whether the cGlyR tone exposed by application of strychnine (Fig. 3.1) is enhanced and secondly whether the effect of inhibition of GlyT1 using sarcosine (Fig. 3.3) on the enhancement of the cGlyR tone is reduced. This would help to identify if there is a common mechanism in Parkinson's disease where there is an increased inhibitory tone on DA release mediated by the lower expression of inhibitory neurotransmitter transporters on astrocytes.

To further refine our understanding of how glycinergic regulation of striatal DA release takes place, subcellular localisation of GlyR proteins would be valuable. Functionally, localisation of cGlyRs to DA axons could be undertaken using electrophysiology, where patch recordings of the DA axon and synaptic isolation using pharmacological blockade could allow the investigation of cGlyR currents on DA axons. This approach has been used recently to demonstrate functional expression of $GABA_A$Rs on DA axons in striatum (Kramer, Twedell et al. 2020). Anatomical localisation of GlyR proteins could also be undertaken using cryogenic electron microscopy, particularly for identification of axonal or somatodendritic expression in interneurons. This may also inform the circumstances under which GlyR

function and glycine as the ligand is released. For example, eGlyRs are located throughout the soma and dendrites of SST+ interneurons in cortex rather than being enriched on dendrites (Bossi, Dhanasobhon et al. 2022). This distribution of eGlyRs across subcellular compartments argues against a role of eGlyRs in these cells receiving synaptic glycinergic transmission (complemented by the paucity of local glycinergic innervation) but supports a role of glycine acting as a volume transmitter, regulating the tonic activity of this interneuron (Bossi, Dhanasobhon et al. 2022).

6.4. $GRAB_{ACh.3.0}$ can record ACh levels, but glycine may cause changes in fluorescence independent of ACh binding

The new $GRAB_{ACh}$ sensors are a powerful tool for the detection of ACh with sub second temporal resolution, similar to FSCV used to detect DA. This allows us to detect ACh release using discrete electrical stimulation, and non-evoked changes in extracellular ACh concentration. However, during application of glycine, I observed a TTX-insensitive reduction of baseline fluorescence that I also observed in a mutant version of the sensor that cannot bind to ACh (Chapter 4, Section 4.3.10) (Jing, Li et al. 2020). This suggests that glycine is interacting with the sensor directly. A recent study for the $GRAB_{Ado1m}$ sensor showed that the cpGFP fluororphore is sensitive to changes in intracellular conditions, such as pH, and reduced its fluorescence independent of ligand-binding (Wu, Cui et al. 2023). Therefore, glycine may be mediating a similar effect, via an indirect mechanism. These findings show the importance of using a ligand-binding mutant control for these sensors, to ensure that changes in fluorescence reflect a true change in agonist concentration. Interestingly, the reduction of baseline fluorescence by glycine appears to vary between sensors, with the reduction of baseline fluorescence appearing to be smaller for $GRAB_{DA2m}$ (Chapter 3, Section 3.3.10). This may reflect different sensitives between sensors to what are putatively similar changes in intracellular conditions (assuming expression on the same groups of cells.

An interesting question is how exogenous application of glycine might mediate widespread changes in intracellular activity, which then alter baseline fluorescence of $GRAB_{ACh}$ sensor. I hypothesise this may be the result of either mGlyR activation (Laboute, Zucca et al. 2023) or

downstream of GlyT1 activation and the putative release of gliotransmitters such as ATP or adenosine, but this requires further investigation.

More broadly, changes observed by myself and others in baseline fluorescence raises questions about the analysis and interpretation of GRAB imaging data (Chapter 4, Section 4.4.3). Normalising evoked fluorescence (ΔF) by the baseline fluorescence (F_0) is used to control for different levels of sensor expression between brain slices and animals. The assumption is that baseline fluorescence should be a function of the number of ligand binding sites, how many of those sites are bound by ambient (non-evoked ACh), and the fluorescence of each activated sensor. In experiments where we expect a change in the ambient levels of ACh (e.g. application of the AChE inhibitor ambenonium), this will change the factor by which ΔF is normalised, altering $\Delta F/F_0$ independent of changes in ΔF. However, I also collected pilot data indicating that the presence of glycine and accompanying reduction in baseline fluorescence did not alter the response to a fixed concentration of ACh, when normalised to the pre-drug condition (Chapter 4, Section 4.3.9). This needs to be investigated more thoroughly, but suggests that an option is to normalise changes in fluorescence to the pre-drug fluorescence, rather than the baseline fluorescence at the time of recording as taken for evoked ACh release. More broadly, this emphasises the importance of understanding the signal components of these new GRAB sensor tools, and how best to interpret them to answer distinct questions about basal and evoked neurotransmitter release.

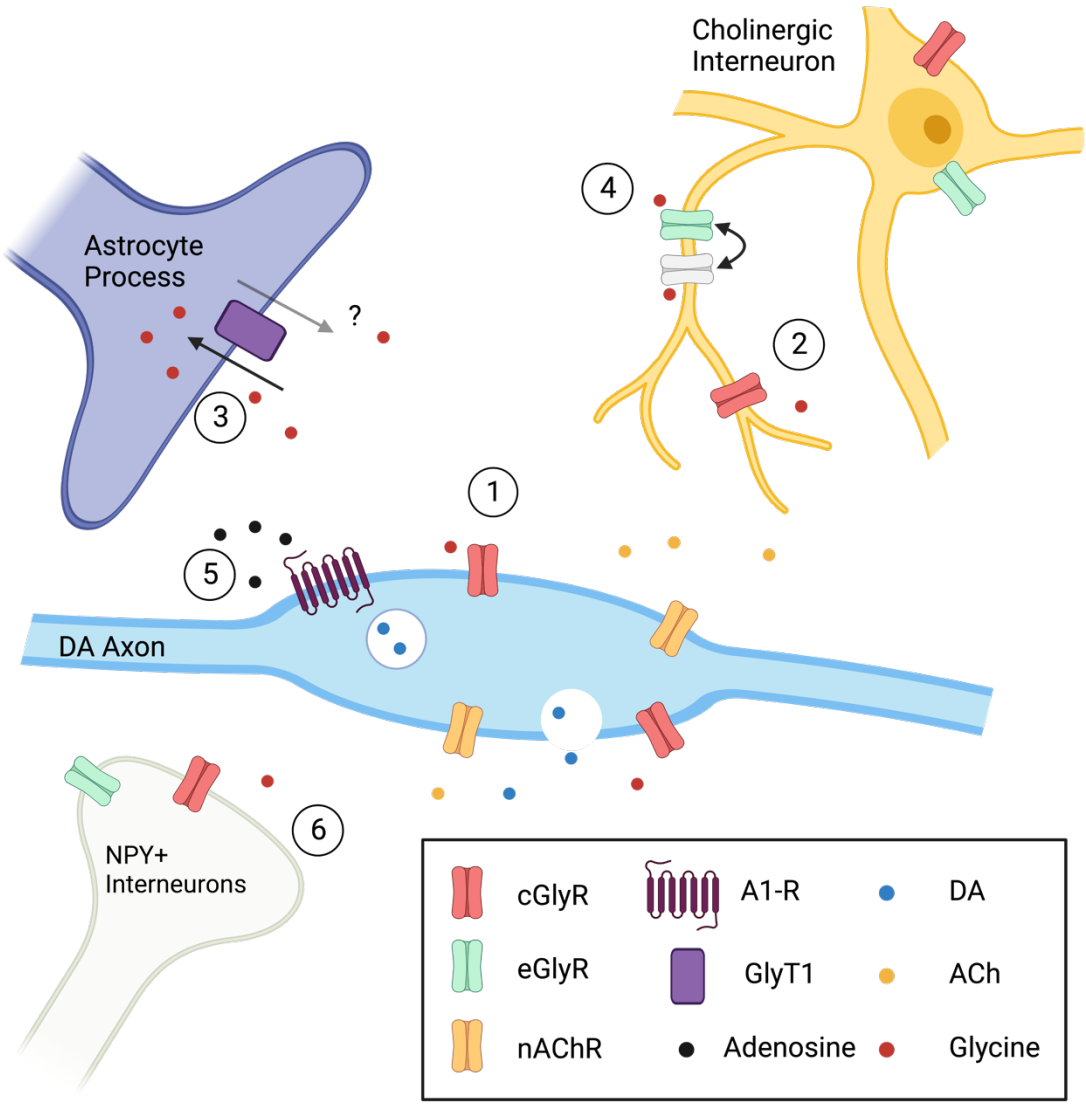

Figure 6.1. Schematic of striatal glycinergic signalling regulating DA release arising from this thesis

1. cGlyRs exhibit tonic activity. Strychnine (cGlyR antagonist) decreases evoked DA release. cGlyRs are putatively expressed on DA axons.
2. cGlyRs on ChIs exhibit tonic activity. Strychnine increases evoked ACh release.
3. GlyT1 mediates glycine uptake. Sarcosine (GlyT1 inhibitor) enhances the reduction of DA release by strychnine and enhances the effect of a lower concentration of glycine. GlyT1 reversal is a putative source of striatal glycine.
4. eGlyRs are expressed on ChIs, in a mixed population of active (green) and desensitised (white) receptors. CGP-78608 (stopping eGlyR desensitisation) reduces evoked ACh release and reduces evoked DA release. Glycine reduces the firing rate of ChIs, facilitation of eGlyRs increases the firing rate. Glycine application can evoke ACh release.
5. Prolonged glycine application increases activation of adenosine receptors (A1-Rs putatively expressed on DA axons), reducing DA release.
6. NPY+ interneurons (LTSIs and/or NGFs) express both cGlyRs and eGlyRs.

6.5. Dopaminergic neurotransmission is altered in diabetes

We investigated whether dopaminergic neurotransmission was altered in diabetes, as part of a collaboration with Profs. Mario Vallejo and Rosario Moratalla. There is evidence for increased co-morbidity between diabetes and Parkinson's disease (Hassan, Sharma Kandel et al. 2020), and our collaborators observed reduced DAT expression in type 1 and type 2 models of diabetes, that we hypothesised would alter DA neurotransmission (Perez-Taboada, Alberquilla et al. 2020). We found that the profile of DA release was altered (Chapter 5, Section 5.1), which would be consistent with altered DAT function. We did not observe a deficit of DA release, consistent with the lack of nigrostriatal degeneration, but actually a subtle increase in DA release of the type 2 diabetes model (Stouffer, Woods et al. 2015). Previous studies have not investigated DA release measured by FSCV in diabetic mice, but have shown regulation of DA release indirectly via insulin receptors expressed on ChIs (Stouffer, Woods et al. 2015, Patel, Stouffer et al. 2019). We did not see any difference in nAChR activity in our experiments (Chapter 5, Section 5.3.3) but this would be interesting to investigate further, especially differences between type 1 and type 2 diabetes that would have differential activation of insulin receptors. As a lab, our focus is on Parkinson's disease, but these findings shows that nigrostriatal vulnerability is present across other diseases and should also be tested. Testing at later timepoints in the disease may reveal neurodegeneration, including a reduction in DA release.

6.6. Conclusion

In this thesis, I have investigated the presynaptic regulation of striatal dopamine release, in health and disease. I have found that glycine regulates dopamine release via classical glycine receptors, and that functional excitatory glycine receptors regulate dopamine release indirectly via cholinergic interneurons. I also show that these receptors are tonically active, with an ambient striatal glycine tone mediated by glycine transporter 1 that is expressed on astrocytes. I also show that dopamine release is altered in type 1 and type 2 models of diabetes, indicative of dysfunctional dopaminergic

neurotransmission. These results contribute to our understanding of the mechanisms that regulate dopamine release under healthy conditions, and dysfunction arising during disease.

References

Adermark, L., O. Lagstrom, A. Loften, V. Licheri, A. Havenang, E. A. Loi, R. Stomberg, B. Soderpalm, A. Domi and M. Ericson (2022). "Astrocytes modulate extracellular neurotransmitter levels and excitatory neurotransmission in dorsolateral striatum via dopamine D2 receptor signaling." Neuropsychopharmacology **47**(8): 1493-1502.

Aosaki, T., H. Tsubokawa, A. Ishida, K. Watanabe, A. M. Graybiel and M. Kimura (1994). "Responses of tonically active neurons in the primate's striatum undergo systematic changes during behavioral sensorimotor conditioning." J Neurosci **14**(6): 3969-3984.

Artasensi, A., A. Pedretti, G. Vistoli and L. Fumagalli (2020). "Type 2 Diabetes Mellitus: A Review of Multi-Target Drugs." Molecules **25**(8).

Ascherio, A. and M. A. Schwarzschild (2016). "The epidemiology of Parkinson's disease: risk factors and prevention." The Lancet Neurology **15**: 1257-1272.

Asri, R., B. O'Neill, J. C. Patel, K. A. Siletti and M. E. Rice (2016). "Detection of evoked acetylcholine release in mouse brain slices." Analyst **141**(23): 6416-6421.

Athauda, D. and T. Foltynie (2016). "Insulin resistance and Parkinson's disease: A new target for disease modification?" Prog Neurobiol **145-146**: 98-120.

Baer, K. (2009). "Localisation of glycine receptors in the human forebrain, brainstem, and cervical spinal cord: an immunohistochemical review." Frontiers in Molecular Neuroscience **2**.

Baker, K. L., F. B. Bolger and J. P. Lowry (2017). "Development of a microelectrochemical biosensor for the real-time detection of choline." Sensors and Actuators B: Chemical **243**: 412-420.

Beccano-Kelly, D. A., M. Cherubini, Y. Mousba, K. M. L. Cramb, S. Giussani, M. C. Caiazza, P. Rai, S. Vingill, N. Bengoa-Vergniory, B. Ng, G. Corda, A. Banerjee, J. Vowles, S. Cowley and R. Wade-Martins (2023). "Calcium dysregulation combined with mitochondrial failure and electrophysiological maturity converge in Parkinson's iPSC-dopamine neurons." iScience **26**(7): 107044.

Bennett, B. D. and J. P. Bolam (1993). "Characterization of calretinin-immunoreactive structures in the striatum of the rat." Brain Res **609**(1-2): 137-148.

Bennett, B. D. and C. J. Wilson (1999). "Spontaneous activity of neostriatal cholinergic interneurons in vitro." J Neurosci **19**(13): 5586-5596.

Bevan, M. D., P. A. Booth, S. A. Eaton and J. P. Bolam (1998). "Selective innervation of neostriatal interneurons by a subclass of neuron in the globus pallidus of the rat." J Neurosci **18**(22): 9438-9452.

Bjorklund, A. and S. B. Dunnett (2007). "Dopamine neuron systems in the brain: an update." Trends Neurosci **30**: 194-202.

Book, A., I. Guella, T. Candido, A. Brice, N. Hattori, B. Jeon, M. J. Farrer and S. M. I. o. t. G. Consortium (2018). "A Meta-Analysis of alpha-Synuclein Multiplication in Familial Parkinsonism." Front Neurol **9**: 1021.

Bosco, D., M. Plastino, D. Cristiano, C. Colica, C. Ermio, M. De Bartolo, P. Mungari, G. Fonte, D. Consoli, A. Consoli and A. Fava (2012). "Dementia is associated with insulin resistance in patients with Parkinson's disease." J Neurol Sci **315**(1-2): 39-43.

Bossi, S., D. Dhanasobhon, G. C. R. Ellis-Davies, J. Frontera, M. de Brito Van Velze, J. Lourenco, A. Murillo, R. Lujan, M. Casado, I. Perez-Otano, A. Bacci, D. Popa, P. Paoletti and N. Rebola (2022). "GluN3A excitatory glycine receptors control adult cortical and amygdalar circuits." Neuron **110**(15): 2438-2454 e2438.

Braak, H., K. D. Tredici, U. Rub, R. A. I. de Vos, E. N. H. Jansen Steur and E. Braak (2003). "Staging of brain pathology related to sporadic Parkinson's disease." Neurobiology of Aging **24**: 197-211.

Brimblecombe, K. R. and S. J. Cragg (2015). "Substance P Weights Striatal Dopamine Transmission Differently within the Striosome-Matrix Axis." J Neurosci **35**: 9017-9023.

Brimblecombe, K. R. and S. J. Cragg (2017). "The Striosome and Matrix Compartments of the Striatum: A Path through the Labyrinth from Neurochemistry toward Function." ACS Chem Neurosci **8**: 235-242.

Brimblecombe, K. R., S. Threlfell, D. Dautan, P. Kosillo, J. Mena-Segovia and S. J. Cragg (2018). "Targeted Activation of Cholinergic Interneurons Accounts for the Modulation of Dopamine by Striatal Nicotinic Receptors." eNeuro **5**.

Cai, Y. and C. P. Ford (2018). "Dopamine Cells Differentially Regulate Striatal Cholinergic Transmission across Regions through Corelease of Dopamine and Glutamate." Cell Rep **25**(11): 3148-3157 e3143.

Castro, D. C. and M. R. Bruchas (2019). "A Motivational and Neuropeptidergic Hub: Anatomical and Functional Diversity within the Nucleus Accumbens Shell." Neuron **102**(3): 529-552.

Cereda, E., M. Barichella, C. Pedrolli, C. Klersy, E. Cassani, R. Caccialanza and G. Pezzoli (2011). "Diabetes and risk of Parkinson's disease: a systematic review and meta-analysis." Diabetes Care **34**(12): 2614-2623.

Chatterton, J. E., M. Awobuluyi, L. S. Premkumar, H. Takahashi, M. Talantova, Y. Shin, J. Cui, S. Tu, K. A. Sevarino, N. Nakanishi, G. Tong, S. A. Lipton and D. Zhang (2002). "Excitatory glycine receptors containing the NR3 family of NMDA receptor subunits." Nature **415**(6873): 793-798.

Chattipakorn, S. C. and L. L. McMahon (2001). "Pharmacological Characterization of Glycine-Gated Chloride Currents Recorded in Rat Hippocampal Slices." J Neurophysiol **87**: 1515-1525.

Chefer, V. I., A. C. Thompson, A. Zapata and T. S. Shippenberg (2009). "Overview of brain microdialysis." Curr Protoc Neurosci **Chapter 7**: Unit7 1.

Chen, H., O. Charlat, L. A. Tartaglia, E. A. Woolf, X. Weng, S. J. Ellis, N. D. Lakey, J. Culpepper, K. J. Moore, R. E. Breitbart, G. M. Duyk, R. I. Tepper and J. P. Morgenstern (1996). "Evidence that the diabetes gene encodes the leptin receptor: identification of a mutation in the leptin receptor gene in db/db mice." Cell **84**(3): 491-495.

Cherubino, F., E. Bossi, A. Miszner, C. Ghezzi and A. Peres (2010). "Transient currents in the glycine cotransporter GlyT1 reveal different steps in transport mechanism." J Mol Neurosci **41**(2): 243-251.

Chesselet, M. F. and A. M. Graybiel (1986). "Striatal neurones expressing somatostatin-like immunoreactivity: evidence for a peptidergic interneuronal system in the cat." Neuroscience **17**: 547-571.

Choe, K. Y., J. E. Olson and C. W. Bourque (2012). "Taurine release by astrocytes modulates osmosensitive glycine receptor tone and excitability in the adult supraoptic nucleus." J Neurosci **32**(36): 12518-12527.

Chuhma, N., K. F. Tanaka, R. Hen and S. Rayport (2011). "Functional connectome of the striatal medium spiny neuron." J Neurosci **31**: 1183-1192.

Chung, W. S., N. J. Allen and C. Eroglu (2015). "Astrocytes Control Synapse Formation, Function, and Elimination." Cold Spring Harb Perspect Biol **7**(9): a020370.

Clarke, D. J., A. D. Smith and J. P. Bolam (1983). "Uptake of [3H]taurine into medium-size neurons and into identified striatonigral neurons in the rat neostriatum." Brain Res **289**(1-2): 342-348.

Clarke, R. B., B. Soderpalm, A. Lotfi, M. Ericson and L. Adermark (2015). "Involvement of Inhibitory Receptors in Modulating Dopamine Signaling and Synaptic Activity Following Acute Ethanol Exposure in Striatal Subregions." Alcohol Clin Exp Res **39**(12): 2364-2374.

Clayton, J. A. and C. Tannenbaum (2016). "Reporting Sex, Gender, or Both in Clinical Research?" JAMA **316**(18): 1863-1864.

Condon, M. D., N. J. Platt, Y. F. Zhang, B. M. Roberts, M. A. Clements, S. Vietti-Michelina, M. Y. Tseu, K. R. Brimblecombe, S. Threlfell, E. O. Mann and S. J. Cragg (2019). "Plasticity in striatal dopamine release is governed by release-independent depression and the dopamine transporter." Nat Commun **10**(1): 4263.

Contant, C., D. Umbriaco, S. Garcia, K. C. Watkins and L. Descarries (1996). "Ultrastructural characterization of the acetylcholine innervation in adult rat neostriatum." Neuroscience **71**: 937-947.

Cragg, S. J. (2003). "Variable dopamine release probability and short-term plasticity between functional domains of the primate striatum." J Neurosci **23**: 4378-4385.

Cragg, S. J. (2006). "Meaningful silences: how dopamine listens to the ACh pause." Trends Neurosci **29**: 125-131.

Cragg, S. J. and M. E. Rice (2004). "DAncing past the DAT at a DA synapse." Trends Neurosci **27**: 270-277.

Crittenden, J. R., I. Cantuti-Castelvetri, E. Saka, C. E. Keller-McGandy, L. F. Hernandez, L. R. Kett, A. B. Young, D. G. Standaert and A. M. Graybiel (2009). "Dysregulation of CalDAG-GEFI and CalDAG-GEFII predicts the severity of motor side-effects induced by anti-parkinsonian therapy." Proceedings of the National Academy of Sciences **106**: 2892-2896.

Crittenden, J. R. and A. M. Graybiel (2011). "Basal Ganglia Disorders Associated with Imbalances in the Striatal Striosome and Matrix Compartments." Frontiers in Neuroanatomy **5**: 1-25.

Crittenden, J. R., P. W. Tillberg, M. H. Riad, Y. Shima, C. R. Gerfen, J. Curry, D. E. Housman, S. B. Nelson, E. S. Boyden and A. M. Graybiel (2016). "Striosome–dendron bouquets highlight a unique striatonigral circuit targeting dopamine-containing neurons." Proceedings of the National Academy of Sciences **113**: 11318-11323.

Cuia, M., R. Arasa, W. V. Christiana, P. M. Rappolda, M. Hatwara, J. Panzaa, V. Jackson-Lewis, J. A. Javitchc, N. Ballatoria, S. Przedborski and K. Tieua (2009). "The organic cation transporter-3 is a pivotal modulator of neurodegeneration in the nigrostriatal dopaminergic pathway." Proc Natl Acad Sci U S A **106**(19): 8043-8048.

Damasceno, D. C., A. O. Netto, I. L. Iessi, F. Q. Gallego, S. B. Corvino, B. Dallaqua, Y. K. Sinzato, A. Bueno, I. M. Calderon and M. V. Rudge (2014). "Streptozotocin-induced diabetes models: pathophysiological mechanisms and fetal outcomes." Biomed Res Int **2014**: 819065.

Dani, J. A. and D. Bertrand (2007). "Nicotinic acetylcholine receptors and nicotinic cholinergic mechanisms of the central nervous system." Annu Rev Pharmacol Toxicol **47**: 699-729.

Darstein, M., G. B. Landwehrmeyer, C. Kling, C.-M. Becker and T. J. Feuerstein (2000). "STRYCHNINE-SENSITIVE GLYCINE RECEPTORS IN RAT CAUDATOPUTAMEN ARE EXPRESSED BY CHOLINERGIC INTERNEURONS." Neuroscience **96**(1): 33-39.

Darstein, M., P. A. Löschmann, R. Knörle and T. J. Feuerstein (1997). "Strychnine-sensitive glycine receptors inducing [3H]-acetylcholine release in rat caudatoputamen: a new site of action of ethanol?" Naunyn-Schmiedeberg's Archives of Pharmacology **356**(6): 738-745.

Darweesh, S. K. L., K. G. Raphael, P. Brundin, H. Matthews, R. K. Wyse, H. Chen and B. R. Bloem (2018). "Parkinson Matters." J Parkinsons Dis **8**(4): 495-498.

De Pablo-Fernandez, E., R. Goldacre, J. Pakpoor, A. J. Noyce and T. T. Warner (2018). "Association between diabetes and subsequent Parkinson disease: A record-linkage cohort study." Neurology **91**(2): e139-e142.

DeFronzo, R. A., E. Ferrannini, L. Groop, R. R. Henry, W. H. Herman, J. J. Holst, F. B. Hu, C. R. Kahn, I. Raz, G. I. Shulman, D. C. Simonson, M. A. Testa and R. Weiss (2015). "Type 2 diabetes mellitus." Nat Rev Dis Primers **1**: 15019.

del Olmo, N., J. Bustamante, R. M. del Rio and J. M. Solis (2000). "Taurine activates GABAA but not GABAB receptors in rat hippocampal CA1 area." Brain Res **864**: 298-307.

Deleuze, C., M. Runquist, H. Orcel, A. Rabie, G. Dayanithi, G. Alonso and N. Hussy (2005). "Structural difference between heteromeric somatic and homomeric axonal glycine receptors in the hypothalamo-neurohypophysial system." Neuroscience **135**(2): 475-483.

Descarries, L., V. Gisiger and M. Steriade (1997). "Diffuse transmission by acetylcholine in the CNS." Prog Neurobiol **53**(5): 603-625.

Devoght, J., J. Comhair, G. Morelli, J.-M. Rigo, R. D'Hooge, C. Touma, R. Palme, I. Dewachter, M. vandeVen, R. J. Harvey, S. Schiffmann, E. Piccart and B. Brône (2022). "Lack of the glycine receptor alpha 2 increases striatal activity and motivated behavior."

Durisic, N., A. G. Godin, C. M. Wever, C. D. Heyes, M. Lakadamyali and J. A. Dent (2012). "Stoichiometry of the human glycine receptor revealed by direct subunit counting." J Neurosci **32**(37): 12915-12920.

Ehmsen, J. T., Y. Liu, Y. Wang, N. Paladugu, A. E. Johnson, J. D. Rothstein, S. du Lac, M. P. Mattson and A. Hoke (2016). "The astrocytic transporter SLC7A10 (Asc-1) mediates glycinergic inhibition of spinal cord motor neurons." Sci Rep **6**: 35592.

Elghaba, R., N. Vautrelle and E. Bracci (2016). "Mutual Control of Cholinergic and Low-Threshold Spike Interneurons in the Striatum." Front Cell Neurosci **10**: 111.

Erdem, F. A., M. Ilic, P. Koppensteiner, J. Golacki, G. Lubec, M. Freissmuth and W. Sandtner (2019). "A comparison of the transport kinetics of glycine transporter 1 and glycine transporter 2." J Gen Physiol **151**(8): 1035-1050.

Ericson, M., A. Molander, R. Stomberg and B. Söderpalm (2006). "Taurine elevates dopamine levels in the rat nucleus accumbens; antagonism by strychnine." European Journal of Neuroscience **23**(12): 3225-3229.

Errasti-Murugarren, E., J. Fort, P. Bartoccioni, L. Diaz, E. Pardon, X. Carpena, M. Espino-Guarch, A. Zorzano, C. Ziegler, J. Steyaert, J. Fernandez-Recio, I. Fita and M. Palacin (2019). "L amino acid transporter structure and molecular bases for the asymmetry of substrate interaction." Nat Commun **10**(1): 1807.

Exley, R., M. A. Clements, H. Hartung, J. M. McIntosh and S. J. Cragg (2008). "Alpha6-containing nicotinic acetylcholine receptors dominate the nicotine control of dopamine neurotransmission in nucleus accumbens." Neuropsychopharmacology **33**: 2158-2166.

Exley, R. and S. J. Cragg (2008). "Presynaptic nicotinic receptors: a dynamic and diverse cholinergic filter of striatal dopamine neurotransmission." Br J Pharmacol **153 Suppl**: S283-297.

Farroni, J. S. and B. A. McCool (2004). "Extrinsic factors regulate partial agonist efficacy of strychnine-sensitive glycine receptors." BMC Pharmacol **4**: 16.

Forstera, B., B. Munoz, M. K. Lobo, R. Chandra, D. M. Lovinger and L. G. Aguayo (2017). "Presence of ethanol-sensitive glycine receptors in medium spiny neurons in the mouse nucleus accumbens." J Physiol **595**(15): 5285-5300.

Foster, N. N., J. Barry, L. Korobkova, L. Garcia, L. Gao, M. Becerra, Y. Sherafat, B. Peng, X. Li, J. H. Choi, L. Gou, B. Zingg, S. Azam, D. Lo, N. Khanjani, B. Zhang, J. Stanis, I. Bowman, K. Cotter, C. Cao, S. Yamashita, A. Tugangui, A. Li, T. Jiang, X. Jia, Z. Feng, S. Aquino, H. S. Mun, M. Zhu, A. Santarelli, N. L. Benavidez, M. Song, G. Dan, M. Fayzullina, S. Ustrell, T. Boesen, D. L. Johnson, H. Xu, M. S. Bienkowski, X. W. Yang, H. Gong, M. S. Levine, I. Wickersham, Q. Luo, J. D. Hahn,

B. K. Lim, L. I. Zhang, C. Cepeda, H. Hintiryan and H. W. Dong (2021). "The mouse cortico-basal ganglia-thalamic network." Nature **598**(7879): 188-194.

Friedman, J. M., R. L. Leibel, D. S. Siegel, J. Walsh and N. Bahary (1991). "Molecular mapping of the mouse ob mutation." Genomics **11**(4): 1054-1062.

Furman, B. L. (2015). "Streptozotocin-Induced Diabetic Models in Mice and Rats." Curr Protoc Pharmacol **70**: 5 47 41-45 47 20.

Gantz, S. C., C. P. Ford, H. Morikawa and J. T. Williams (2018). "The Evolving Understanding of Dopamine Neurons in the Substantia Nigra and Ventral Tegmental Area." Annu Rev Physiol **80**: 219-241.

Garas, F. N., E. Kormann, R. S. Shah, F. Vinciati, Y. Smith, P. J. Magill and A. Sharott (2018). "Structural and molecular heterogeneity of calretinin-expressing interneurons in the rodent and primate striatum." J Comp Neurol **526**(5): 877-898.

Garcia-Colunga, J. and R. Miledi (1999). "Modulation of nicotinic acetylcholine receptors by strychnine." Proceedings of the National Academy of Sciences **96**(7): 4113-4118.

Gentet, L. J. and J. D. Clements (2002). "Binding site stoichiometry and the effects of phosphorylation on human alpha1 homomeric glycine receptors." J Physiol **544**(Pt 1): 97-106.

Gerfen, C. R., K. G. Baimbridge and J. J. Miller (1985). "The neostriatal mosaic: compartmental distribution of calcium-binding protein and parvalbumin in the basal ganglia of the rat and monkey." Proc Natl Acad Sci U S A **82**(24): 8780-8784.

Gerfen, C. R., M. Herkenham and J. Thibault (1987). "The neostriatal mosaic: II. Patch- and matrix-directed mesostriatal dopaminergic and non-dopaminergic systems." The Journal of Neuroscience **7**: 3915-3934.

Gerfen, C. R. and D. J. Surmeier (2011). "Modulation of striatal projection systems by dopamine." Annu Rev Neurosci **34**: 441-466.

Gibbs, E., E. Klemm, D. Seiferth, A. Kumar, S. L. Ilca, P. C. Biggin and S. Chakrapani (2023). "Conformational transitions and allosteric modulation in a heteromeric glycine receptor." Nat Commun **14**(1): 1363.

Giorguieff-Chesselet, M. F., M. L. Kemel, D. Wandscheer and J. Glowinski (1979). "Glycine stimulates the spontaneous release of newly synthesized 3H-dopamine in rat striatal slices." European Journal of Pharmacology **60**(1): 101-104.

Gittis, A. H., D. K. Leventhal, B. A. Fensterheim, J. R. Pettibone, J. D. Berke and A. C. Kreitzer (2011). "Selective inhibition of striatal fast-spiking interneurons causes dyskinesias." J Neurosci **31**(44): 15727-15731.

Gonzales, K. K. and Y. Smith (2015). "Cholinergic interneurons in the dorsal and ventral striatum: anatomical and functional considerations in normal and diseased conditions." Ann N Y Acad Sci **1349**(1): 1-45.

Grand, T., S. Abi Gerges, M. David, M. A. Diana and P. Paoletti (2018). "Unmasking GluN1/GluN3A excitatory glycine NMDA receptors." Nat Commun **9**(1): 4769.

Graybiel, A. M. (1998). "The basal ganglia and chunking of action repertoires." Neurobiol Learn Mem **70**(1-2): 119-136.

Grenningloh, G., I. Pribilla, P. Prior, G. Multhaup, K. Beyreuther, O. Taleb and H. Betz (1990). "Cloning and expression of the 58 kd beta subunit of the inhibitory glycine receptor." Neuron **4**(6): 963-970.

Grudzinska, J., R. Schemm, S. Haeger, A. Nicke, G. Schmalzing, H. Betz and B. Laube (2005). "The beta subunit determines the ligand binding properties of synaptic glycine receptors." Neuron **45**(5): 727-739.

Harsing, L. G., Jr. and P. Matyus (2013). "Mechanisms of glycine release, which build up synaptic and extrasynaptic glycine levels: the role of synaptic and non-synaptic glycine transporters." Brain Res Bull **93**: 110-119.

Hartung, H., S. Threlfell and S. J. Cragg (2011). "Nitric oxide donors enhance the frequency dependence of dopamine release in nucleus accumbens." Neuropsychopharmacology **36**: 1811-1822.

Harvey, R. J. and B. K. Yee (2013). "Glycine transporters as novel therapeutic targets in schizophrenia, alcohol dependence and pain." Nature Reviews Drug Discovery **12**(11): 866-885.

Hassan, A., R. Sharma Kandel, R. Mishra, J. Gautam, A. Alaref and N. Jahan (2020). "Diabetes Mellitus and Parkinson's Disease: Shared Pathophysiological Links and Possible Therapeutic Implications." Cureus **12**(8): e9853.

Häusser, M. A., W. H. Yung and M. G. Lacey (1992). "Taurine and glycine activate the same Cl− conductance in substantia nigra dopamine neurones." Brain Research **571**(1): 103-108.

Hedges, D. M., J. D. Obray, J. T. Yorgason, E. Y. Jang, V. K. Weerasekara, J. D. Uys, F. P. Bellinger and S. C. Steffensen (2018). "Methamphetamine Induces Dopamine Release in the Nucleus Accumbens Through a Sigma Receptor-Mediated Pathway." Neuropsychopharmacology **43**(6): 1405-1414.

Hernandes, M. S., L. de Magalhaes and L. R. Troncone (2007). "Glycine stimulates the release of labeled acetylcholine but not dopamine nor glutamate from superfused rat striatal tissue." Brain Res **1168**: 32-37.

Hirata, Y., H. Suzuno, T. Tsuruta, K. Oh-hashi and K. Kiuchi (2008). "The role of dopamine transporter in selective toxicity of manganese and rotenone." Toxicology **244**(2-3): 249-256.

Holly, E. N., M. F. Davatolhagh, K. Choi, O. O. Alabi, L. Vargas Cifuentes and M. V. Fuccillo (2019). "Striatal Low-Threshold Spiking Interneurons Regulate Goal-Directed Learning." Neuron.

Holly, E. N., M. F. Davatolhagh, R. A. Espana and M. V. Fuccillo (2021). "Striatal low-threshold spiking interneurons locally gate dopamine." Curr Biol **31**(18): 4139-4147 e4136.

Huang, H., L. Barakat, D. Wang and A. Bordey (2004). "Bergmann glial GlyT1 mediates glycine uptake and release in mouse cerebellar slices." J Physiol **560**(Pt 3): 721-736.

Hunnicutt, B. J., B. C. Jongbloets, W. T. Birdsong, K. J. Gertz, H. Zhong and T. Mao (2016). "A comprehensive excitatory input map of the striatum reveals novel functional organization." Elife **5**.

Hussy, N., V. Bres, M. Rochette, A. Duvoid, G. Alonso, G. Dayanithi and F. C. Moos (2001). "Osmoregulation of Vasopressin Secretion via Activation of Neurohypophysial Nerve Terminals Glycine Receptors by Glial Taurine."

Hussy, N., C. Deleuze, A. Pantaloni, M. G. Desarménien and F. C. Moos (1997). "Agonist action of taurine on glycine receptors in rat supraoptic magnocellular." J Physiol **50**(3): 609-621.

Hyland, B. I., J. N. Reynolds, J. Hay, C. G. Perk and R. Miller (2002). "Firing modes of midbrain dopamine cells in the freely moving rat." Neuroscience **114**: 475-492.

Ibanez-Sandoval, O., F. Tecuapetla, B. Unal, F. Shah, T. Koos and J. M. Tepper (2011). "A novel functionally distinct subtype of striatal neuropeptide Y interneuron." J Neurosci **31**(46): 16757-16769.

Ito, R. and A. Hayen (2011). "Opposing roles of nucleus accumbens core and shell dopamine in the modulation of limbic information processing." J Neurosci **31**(16): 6001-6007.

Janezic, S., S. Threlfell, P. D. Dodson, M. J. Dowie, T. N. Taylor, D. Potgieter, L. Parkkinen, S. L. Senior, S. Anwar, B. Ryan, T. Deltheil, P. Kosillo, M. Cioroch, K. Wagner, O. Ansorge, D. M. Bannerman, J. P. Bolam, P. J. Magill, S. J. Cragg and R. Wade-Martins (2013). "Deficits in dopaminergic transmission precede neuron loss and dysfunction in a new Parkinson model." Proc Natl Acad Sci U S A **110**: E4016-4025.

Jankovic, J. and E. K. Tan (2020). "Parkinson's disease: etiopathogenesis and treatment." J Neurol Neurosurg Psychiatry **91**(8): 795-808.

Javitt, D. C., A. Hashim and H. Sershen (2005). "Modulation of striatal dopamine release by glycine transport inhibitors." Neuropsychopharmacology **30**(4): 649-656.

Javitt, D. C., H. Sershen, A. Hashim and A. Lajtha (2000). "Inhibition of dopamine release by glycine and glycyldodecylamide." Brain Res Bull **52**(3): 213-216.

Jentsch, T. J. (2016). "VRACs and other ion channels and transporters in the regulation of cell volume and beyond." Nat Rev Mol Cell Biol **17**(5): 293-307.

Jia, F., M. Yue, D. Chandra, A. Keramidas, P. A. Goldstein, G. E. Homanics and N. L. Harrison (2008). "Taurine is a potent activator of extrasynaptic GABA(A) receptors in the thalamus." J Neurosci **28**(1): 106-115.

Jiang, Z., K. Krnjevic, F. Wang and J. H. Ye (2004). "Taurine activates strychnine-sensitive glycine receptors in neurons freshly isolated from nucleus accumbens of young rats." J Neurophysiol **91**(1): 248-257.

Jiao, R., W. Liu, L. Yin, Z. Qiao, J. Li, L. Zhou, M. Younus, L. Wang, H. Xu and Z. Zhou (2020). "A method for recording the two phases of dopamine release in mammalian brain striatum slices." The Analyst.

Jing, M., Y. Li, J. Zeng, P. Huang, M. Skirzewski, O. Kljakic, W. Peng, T. Qian, K. Tan, J. Zou, S. Trinh, R. Wu, S. Zhang, S. Pan, S. A. Hires, M. Xu, H. Li, L. M. Saksida, V. F. Prado, T. J. Bussey, M. A. M. Prado, L. Chen, H. Cheng and Y. Li (2020). "An optimized acetylcholine sensor for monitoring in vivo cholinergic activity." Nat Methods **17**(11): 1139-1146.

Jing, M., P. Zhang, G. Wang, J. Feng, L. Mesik, J. Zeng, H. Jiang, S. Wang, J. C. Looby, N. A. Guagliardo, L. W. Langma, J. Lu, Y. Zuo, D. A. Talmage, L. W. Role, P. Q. Barrett, L. I. Zhang, M. Luo, Y. Song, J. J. Zhu and Y. Li (2018). "A genetically encoded fluorescent acetylcholine indicator for in vitro and in vivo studies." Nat Biotechnol **36**(8): 726-737.

John, C. E. and S. R. Jones (2007). "Voltammetric characterization of the effect of monoamine uptake inhibitors and releasers on dopamine and serotonin uptake in mouse caudate-putamen and substantia nigra slices." Neuropharmacology **52**(8): 1596-1605.

Jonsson, S., L. Adermark, M. Ericson and B. Soderpalm (2014). "The involvement of accumbal glycine receptors in the dopamine-elevating effects of addictive drugs." Neuropharmacology **82**: 69-75.

Katsarou, A., S. Gudbjornsdottir, A. Rawshani, D. Dabelea, E. Bonifacio, B. J. Anderson, L. M. Jacobsen, D. A. Schatz and A. Lernmark (2017). "Type 1 diabetes mellitus." Nat Rev Dis Primers **3**: 17016.

Kawaguchi, Y., C. J. Wilson, S. J. Augood and P. C. Emson (1995). "Striatal interneurones: chemical, physiological and morphological characterization." Trends Neurosci **18**(12): 527-535.

Kerwin, R. W. and C. J. Pycock (1979). "Specific stimulating effect of glycine on 3H-dopamine efflux from substantia nigra slices of the rat." **54**(1-2): 93-98.

Kocaturk, S., E. B. Guven, F. Shah, J. M. Tepper and M. Assous (2022). "Cholinergic control of striatal GABAergic microcircuits." Cell Rep **41**(4): 111531.

Koos, T., J. M. Tepper and C. J. Wilson (2004). "Comparison of IPSCs evoked by spiny and fast-spiking neurons in the neostriatum." J Neurosci **24**(36): 7916-7922.

Kosillo, P., Y. F. Zhang, S. Threlfell and S. J. Cragg (2016). "Cortical Control of Striatal Dopamine Transmission via Striatal Cholinergic Interneurons." Cereb Cortex.

Kramer, P. F., E. L. Twedell, J. H. Shin, R. Zhang and Z. M. Khaliq (2020). "Axonal mechanisms mediating gamma-aminobutyric acid receptor type A (GABA-A) inhibition of striatal dopamine release." Elife **9**.

Kugler, S., E. Kilic and M. Bahr (2003). "Human synapsin 1 gene promoter confers highly neuron-specific long-term transgene expression from an adenoviral vector in the adult rat brain depending on the transduced area." Gene Ther **10**(4): 337-347.

Laboute, T., S. Zucca, M. Holcomb, D. N. Patil, C. Garza, B. A. Wheatley, R. N. Roy, S. Forli and K. A. Martemyanov (2023). "Orphan receptor GPR158 serves as a metabotropic glycine receptor: mGlyR." Science **379**(6639): 1352-1358.

Lanciego, J. L., N. Luquin and J. A. Obeso (2012). "Functional neuroanatomy of the basal ganglia." Cold Spring Harbor Perspectives in Medicine **2**: 1-20.

Lang, C., K. R. Campbell, B. J. Ryan, P. Carling, M. Attar, J. Vowles, O. V. Perestenko, R. Bowden, F. Baig, M. Kasten, M. T. Hu, S. A. Cowley, C. Webber and R. Wade-Martins (2019). "Single-Cell Sequencing of iPSC-Dopamine Neurons Reconstructs Disease Progression and Identifies HDAC4 as a Regulator of Parkinson Cell Phenotypes." Cell Stem Cell **24**(1): 93-106 e106.

Lape, R., D. Colquhoun and L. G. Sivilotti (2008). "On the nature of partial agonism in the nicotinic receptor superfamily." Nature **454**(7205): 722-727.

Lee, G. H., R. Proenca, J. M. Montez, K. M. Carroll, J. G. Darvishzadeh, J. I. Lee and J. M. Friedman (1996). "Abnormal splicing of the leptin receptor in diabetic mice." Nature **379**(6566): 632-635.

Legendre, P. (1998). "A reluctant gating mode of glycine receptor channels determines the time course of inhibitory miniature synaptic events in zebrafish hindbrain neurons." J Neurosci **18**(8): 2856-2870.

Legendre, P. and H. Korn (1994). "Glycinergic inhibitory synaptic currents and related receptor channels in the zebrafish brain." Eur J Neurosci **6**(10): 1544-1557.

Lemos, J. C., J. H. Shin and V. A. Alvarez (2019). "Striatal cholinergic interneurons are a novel target of corticotropin releasing factor." J Neurosci.

Lewis, T. M., P. R. Schofield and A. M. McClellan (2003). "Kinetic determinants of agonist action at the recombinant human glycine receptor." J Physiol **549**(Pt 2): 361-374.

Lidö, H. H., M. Ericson, H. Marston and B. Söderpalm (2011). "A Role for Accumbal Glycine Receptors in Modulation of Dopamine Release by the Glycine Transporter-1 Inhibitor Org25935." Frontiers in Psychiatry **2**.

Lidö, H. H., R. Stomberg, A. Fagerberg, M. Ericson and B. Söderpalm (2009). "The Glycine Reuptake Inhibitor Org 25935 Interacts With Basal and Ethanol-Induced Dopamine Release in Rat Nucleus Accumbens." **33**(7): 1151-1157.

Like, A. A. and A. A. Rossini (1976). "Streptozotocin-induced pancreatic insulitis: new model of diabetes mellitus." Science **193**(4251): 415-417.

Lim, S. A. O., U. J. Kang and D. S. McGehee (2014). "Striatal cholinergic interneuron regulation and circuit effects." Frontiers in Synaptic Neuroscience **6**: 1-23.

Liu, C., X. Cai, A. Ritzau-Jost, P. F. Kramer, Y. Li, Z. M. Khaliq, S. Hallermann and P. S. Kaeser (2022). "An action potential initiation mechanism in distal axons for the control of dopamine release." Science **375**(6587): 1378-1385.

Lopes, E. F., B. M. Roberts, R. E. Siddorn, M. A. Clements and S. J. Cragg (2019). "Inhibition of Nigrostriatal Dopamine Release by Striatal GABAA and GABAB Receptors." J Neurosci **39**: 1058-1065.

Lynch, J. W. (2004). "Molecular Structure and Function of the Glycine Receptor Chloride Channel." Physiological Reviews **84**(4): 1051-1095.

Madry, C., I. Mesic, I. Bartholomaus, A. Nicke, H. Betz and B. Laube (2007). "Principal role of NR3 subunits in NR1/NR3 excitatory glycine receptor function." Biochem Biophys Res Commun **354**(1): 102-108.

Mallet, N., B. R. Micklem, P. Henny, M. T. Brown, C. Williams, J. P. Bolam, K. C. Nakamura and P. J. Magill (2012). "Dichotomous organization of the external globus pallidus." Neuron **74**(6): 1075-1086.

Mangin, J. M., M. Baloul, L. Prado De Carvalho, B. Rogister, J. M. Rigo and P. Legendre (2003). "Kinetic properties of the alpha2 homo-oligomeric glycine receptor impairs a proper synaptic functioning." J Physiol **553**(Pt 2): 369-386.

Mangin, J. M., A. Guyon, D. Eugene, D. Paupardin-Tritsch and P. Legendre (2002). "Functional glycine receptor maturation in the absence of glycinergic input in dopaminergic neurones of the rat substantia nigra." J Physiol **542**(Pt 3): 685-697.

Marco, S., A. Giralt, M. M. Petrovic, M. A. Pouladi, R. Martinez-Turrillas, J. Martinez-Hernandez, L. S. Kaltenbach, J. Torres-Peraza, R. K. Graham, M. Watanabe, R. Lujan, N. Nakanishi, S. A. Lipton, D. C. Lo, M. R. Hayden, J. Alberch, J. F. Wesseling and I. Perez-Otano (2013). "Suppressing aberrant GluN3A expression rescues synaptic and behavioral impairments in Huntington's disease models." Nat Med **19**(8): 1030-1038.

Martin, G. and G. R. Siggins (2002). "Electrophysiological evidence for expression of glycine receptors in freshly isolated neurons from nucleus accumbens." J Pharmacol Exp Ther **302**(3): 1135-1145.

Martins, I. J., E. Hone, J. K. Foster, S. I. Sunram-Lea, A. Gnjec, S. J. Fuller, D. Nolan, S. E. Gandy and R. N. Martins (2006). "Apolipoprotein E, cholesterol metabolism, diabetes, and the convergence of risk factors for Alzheimer's disease and cardiovascular disease." Mol Psychiatry **11**(8): 721-736.

Matamales, M., J. Gotz and J. Bertran-Gonzalez (2016). "Quantitative Imaging of Cholinergic Interneurons Reveals a Distinctive Spatial Organization and a Functional Gradient across the Mouse Striatum." PLoS One **11**(6): e0157682.

Matsubayashi, H., M. Alkodon, E. F. R. Pereira, K. Swanson and E. X. Albuquerque (1998). "Strychnine: A Potent Competitive Antagonist of ?-Bungarotoxin-Sensitive Nicotinic Acetylcholine Receptors In Rat Hippocampal Neurons." J Pharmacol Exp Ther **284**(3): 904-913.

Matsuda, W., T. Furuta, K. C. Nakamura, H. Hioki, F. Fujiyama, R. Arai and T. Kaneko (2009). "Single nigrostriatal dopaminergic neurons form widely spread and highly dense axonal arborizations in the neostriatum." J Neurosci **29**(2): 444-453.

Maurice, N., J. Mercer, C. S. Chan, S. Hernandez-Lopez, J. Held, T. Tkatch and D. J. Surmeier (2004). "D2 dopamine receptor-mediated modulation of voltage-dependent Na+ channels reduces autonomous activity in striatal cholinergic interneurons." J Neurosci **24**(46): 10289-10301.

McCracken, L. M., D. C. Lowes, M. C. Salling, C. Carreau-Vollmer, N. N. Odean, Y. A. Blednov, H. Betz, R. A. Harris and N. L. Harrison (2017). "Glycine receptor alpha3 and alpha2 subunits mediate tonic and exogenous agonist-induced currents in forebrain." Proc Natl Acad Sci U S A **114**(34): E7179-E7186.

McGregor, M. M. and A. B. Nelson (2019). "Circuit Mechanisms of Parkinson's Disease." Neuron **101**(6): 1042-1056.

Meier, J. C., C. Henneberger, I. Melnick, C. Racca, R. J. Harvey, U. Heinemann, V. Schmieden and R. Grantyn (2005). "RNA editing produces glycine receptor alpha3(P185L), resulting in high agonist potency." Nat Neurosci **8**(6): 736-744.

Mercuri, N. B., P. Calabresi and G. Bernardi (1990). "Effects of Glycine on Neurons in the Rat Substantia Nigra Zona Cornpacta: In Vitro Electrophysiological Study." Synapse **5**: 190-200.

Meredith, G. E. and D. J. Rademacher (2011). "MPTP mouse models of Parkinson's disease: an update." J Parkinsons Dis **1**(1): 19-33.

Meyer, G., J. Kirsch, H. Betz and D. Langosch (1995). "Identification of a gephyrin binding motif on the glycine receptor beta subunit." Neuron **15**(3): 563-572.

Michael, D. J. and R. M. Wightman (1999). "Electrochemical monitoring of biogenic amine neurotransmission in real time." J Pharm Biomed Anal **19**(1-2): 33-46.

Miles, A. R., P. J. Hawrysh, N. Hossein-Javaheri and L. T. Buck (2018). "Taurine activates glycine and GABAA receptor currents in anoxia-tolerant painted turtle pyramidal neurons." J Exp Biol **221**(Pt 21).

Molander, A. and B. Soderpalm (2005). "Glycine Receptors Regulate Dopamine Release in the Rat Nucleus Accumbens." Alcoholism: Clinical & Experimental Research **29**(1): 17-26.

Molchanova, S., S. S. Oja and P. Saransaari (2004). "Characteristics of basal taurine release in the rat striatum measured by microdialysis." **27**(3-4): 261-268.

Molchanova, S. M., J. Comhair, D. Karadurmus, E. Piccart, R. J. Harvey, J. M. Rigo, S. N. Schiffmann, B. Brone and D. Gall (2017). "Tonically Active alpha2 Subunit-Containing Glycine Receptors Regulate the Excitability of Striatal Medium Spiny Neurons." Front Mol Neurosci **10**: 442.

Mongin, A. A., Z. Cai and H. K. Kimelberg (1999). "Volume-dependent taurine release from cultured astrocytes requires permissive [Ca2+]i and calmodulin." Am. J. Physiol. **277**(46): C823–C832.

Mori, M., B. H. Gähwiler and U. Gerber (2002). "b-Alanine and taurine as endogenous agonists at glycine receptors in rat hippocampus in vitro." J Physiol **539**(1): 191-200.

Muddapu, V. R. and V. S. Chakravarthy (2021). "Influence of energy deficiency on the subcellular processes of Substantia Nigra Pars Compacta cell for understanding Parkinsonian neurodegeneration." Sci Rep **11**(1): 1754.

Munoz, B., G. E. Yevenes, B. Forstera, D. M. Lovinger and L. G. Aguayo (2018). "Presence of Inhibitory Glycinergic Transmission in Medium Spiny Neurons in the Nucleus Accumbens." Front Mol Neurosci **11**: 228.

Nagy, K., B. Marko, G. Zsilla, P. Matyus, K. Pallagi, G. Szabo, Z. Juranyi, J. Barkoczy, G. Levay and L. G. Harsing (2010). "Alterations in Brain Extracellular Dopamine and Glycine Levels Following Combined Administration of the Glycine Transporter Type-1 Inhibitor Org-24461 and Risperidone." Neurochemical Research **35**(12): 2096-2106.

Nguyen, T. T., J. P. Bhattarai, S. J. Park and S. K. Han (2013). "Activation of glycine and extrasynaptic GABA(A) receptors by taurine on the substantia gelatinosa neurons of the trigeminal subnucleus caudalis." Neural Plast **2013**: 740581.

Obeso, J. A., M. C. Rodriguez-Oroz, M. Stamelou, K. P. Bhatia and D. J. Burn (2014). "The expanding universe of disorders of the basal ganglia." Lancet **384**(9942): 523-531.

Obeso, J. A., M. Stamelou, C. G. Goetz, W. Poewe, A. E. Lang, D. Weintraub, D. Burn, G. M. Halliday, E. Bezard, S. Przedborski, S. Lehericy, D. J. Brooks, J. C. Rothwell, M. Hallett, M. R. DeLong, C. Marras, C. M. Tanner, G. W. Ross, J. W. Langston, C. Klein, V. Bonifati, J. Jankovic, A. M. Lozano, G. Deuschl, H. Bergman, E. Tolosa, M. Rodriguez-Violante, S. Fahn, R. B. Postuma, D. Berg, K. Marek, D. G. Standaert, D. J. Surmeier, C. W. Olanow, J. H. Kordower, P. Calabresi, A. H. V. Schapira and A. J. Stoessl (2017). "Past, present, and future of Parkinson's disease: A special essay on the 200th Anniversary of the Shaking Palsy." Mov Disord **32**: 1264-1310.

Oldenburg, I. A. and J. B. Ding (2011). "Cholinergic modulation of synaptic integration and dendritic excitability in the striatum." Curr Opin Neurobiol **21**(3): 425-432.

Olsen, R. W. (2006). "Picrotoxin-like channel blockers of GABAA receptors." Proc Natl Acad Sci U S A **103**(16): 6081-6082.

Otsu, Y., E. Darcq, K. Pietrajtis, F. Matyas, E. Schwartz, T. Bessaih, S. Abi Gerges, C. V. Rousseau, T. Grand, S. Dieudonne, P. Paoletti, L. Acsady, C. Agulhon, B. L. Kieffer and M. A. Diana (2019). "Control of aversion by glycine-gated GluN1/GluN3A NMDA receptors in the adult medial habenula." Science **366**(6462): 250-254.

Palkovits, M., I. Elekes, T. Lang and A. Patthy (1986). "Taurine levels in discrete brain nuclei of rats." J Neurochem **47**(5): 1333-1335.

Paoletti, P., C. Bellone and Q. Zhou (2013). "NMDA receptor subunit diversity: impact on receptor properties, synaptic plasticity and disease." Nat Rev Neurosci **14**(6): 383-400.

Pasantes-Morales, H. and A. Schousboe (1989). "Release of Taurine From Astrocytes During Potassium-Evoked Swelling." Glia **2**: 45-50.

Patel, J. C., M. A. Stouffer, M. Mancini, C. Nicholson, K. D. Carr and M. E. Rice (2019). "Interactions between insulin and diet on striatal dopamine uptake kinetics in rodent brain slices." Eur J Neurosci **49**(6): 794-804.

Patyal, R., E. Y. Woo and S. L. Borgland (2012). "Local hypocretin-1 modulates terminal dopamine concentration in the nucleus accumbens shell." Frontiers in Behavioral Neuroscience **6**.

Perea, G., M. Navarrete and A. Araque (2009). "Tripartite synapses: astrocytes process and control synaptic information." Trends Neurosci **32**(8): 421-431.

Perez-Otano, I., R. S. Larsen and J. F. Wesseling (2016). "Emerging roles of GluN3-containing NMDA receptors in the CNS." Nat Rev Neurosci **17**(10): 623-635.

Pérez-Otaño, I., C. T. Schulteis, A. Contractor, S. A. Lipton, J. S. Trimmer, N. J. Sucher and S. F. Heinemann (2001). "Assembly with the NR1 Subunit Is Required for Surface Expression of NR3A-Containing NMDA Receptors." The Journal of Neuroscience **21**(4): 1228-1237.

Perez-Taboada, I., S. Alberquilla, E. D. Martin, R. Anand, S. Vietti-Michelina, N. N. Tebeka, J. Cantley, S. J. Cragg, R. Moratalla and M. Vallejo (2020). "Diabetes Causes Dysfunctional Dopamine Neurotransmission Favoring Nigrostriatal Degeneration in Mice." Mov Disord.

Petersen, M. C. and G. I. Shulman (2018). "Mechanisms of Insulin Action and Insulin Resistance." Physiol Rev **98**(4): 2133-2223.

Pissadaki, E. K. and J. P. Bolam (2013). "The energy cost of action potential propagation in dopamine neurons: clues to susceptibility in Parkinson's disease." Front Comput Neurosci **7**: 13.

Pittolo, S., S. Yokoyama, D. D. Willoughby, C. R. Taylor, M. E. Reitman, V. Tse, Z. Wu, R. Etchenique, Y. Li and K. E. Poskanzer (2022). "Dopamine activates astrocytes in prefrontal cortex via alpha1-adrenergic receptors." Cell Rep **40**(13): 111426.

Poewe, W., K. Seppi, C. M. Tanner, G. M. Halliday, P. Brundin, J. Volkmann, A. E. Schrag and A. E. Lang (2017). "Parkinson disease." Nat Rev Dis Primers **3**: 17013.

Prendergast, B. J., K. G. Onishi and I. Zucker (2014). "Female mice liberated for inclusion in neuroscience and biomedical research." Neurosci Biobehav Rev **40**: 1-5.

Puka, M., K. Sundell, J. W. Lazarewicz and A. Lehmann (1991). "Species differences in cerebral taurine concentrations correlate with brain water content." Brain Res **548**(1-2): 267-272.

Ramanathan, S., J. J. Hanley, J. M. Deniau and J. P. Bolam (2002). "Synaptic convergence of motor and somatosensory cortical afferents onto GABAergic interneurons in the rat striatum." J Neurosci **22**(18): 8158-8169.

Reiner, A., N. M. Hart, W. Lei and Y. Deng (2010). "Corticostriatal projection neurons - dichotomous types and dichotomous functions." Front Neuroanat **4**: 142.

Rice, M. E. and S. J. Cragg (2004). "Nicotine amplifies reward-related dopamine signals in striatum." Nat Neurosci **7**: 583-584.

Rice, M. E., J. C. Patel and S. J. Cragg (2011). "Dopamine release in the basal ganglia." Neuroscience **198**: 112-137.

Richter, F., L. Gabby, K. A. McDowell, C. K. Mulligan, K. De La Rosa, P. C. Sioshansi, F. Mortazavi, I. Cely, L. C. Ackerson, L. Tsan, N. P. Murphy, N. T. Maidment and M. F. Chesselet (2017). "Effects of decreased dopamine transporter levels on nigrostriatal neurons and paraquat/maneb toxicity in mice." Neurobiol Aging **51**: 54-66.

Ring, H. A. and J. Serra-Mestres (2002). "Neuropsychiatry of the basal ganglia." J Neurol Neurosurg Psychiatry(72): 12-21.

Roberts, B. M., N. M. Doig, K. R. Brimblecombe, E. F. Lopes, R. E. Siddorn, S. Threlfell, N. Connor-Robson, N. Bengoa-Vergniory, N. Pasternack, R. Wade-Martins, P. J. Magill and S. J. Cragg (2020). "GABA uptake transporters support dopamine release in dorsal striatum with maladaptive downregulation in a parkinsonism model." Nat Commun **11**(1): 4958.

Roberts, B. M., E. Lambert, J. A. Livesey, Z. Wu, Y. Li and S. J. Cragg (2022). "Dopamine Release in Nucleus Accumbens Is under Tonic Inhibition by Adenosine A(1) Receptors Regulated by Astrocytic ENT1 and Dysregulated by Ethanol." J Neurosci **42**(9): 1738-1751.

Rossi, L. M., I. Reverte, D. Ragozzino, A. Badiani, M. Venniro and D. Caprioli (2020). "Role of nucleus accumbens core but not shell in incubation of methamphetamine craving after voluntary abstinence." Neuropsychopharmacology **45**(2): 256-265.

Ruotsalainen, M. and L. Ahtee (1996). "Intrastriatal taurine increases striatal extracellular dopamine in a tetrodotoxin-sensitive manner in rats." Neurosci Lett **212**(3): 175-178.

Sabatini, B. L. and L. Tian (2020). "Imaging Neurotransmitter and Neuromodulator Dynamics In Vivo with Genetically Encoded Indicators." Neuron **108**(1): 17-32.

Salling, M. C. and N. L. Harrison (2014). "Strychnine-sensitive glycine receptors on pyramidal neurons in layers II/III of the mouse prefrontal cortex are tonically activated." J Neurophysiol **112**(5): 1169-1178.

Saunders, A., A. J. Granger and B. L. Sabatini (2015). "Corelease of acetylcholine and GABA from cholinergic forebrain neurons." Elife **4**.

Savtchouk, I. and A. Volterra (2018). "Gliotransmission: Beyond Black-and-White." J Neurosci **38**(1): 14-25.

Schapira, A. H. (2015). "Glucocerebrosidase and Parkinson disease: Recent advances." Mol Cell Neurosci **66**: 37-42.

Schultz, W. (2016). "Dopamine reward prediction error coding." Dialogues Clin Neurosci **18**(1): 23-32.

Sergeeva, O. A. (1998). "Comparison of glycine- and GABA-evoked currents in two types of neurons isolated from the rat striatum." Neurosci Lett **243**: 9-12.

Sergeeva, O. A., A. N. Chepkova, N. Doreulee, K. S. Eriksson, W. Poelchen, I. Monnighoff, B. Heller-Stilb, U. Warskulat, D. Haussinger and H. L. Haas (2003). "Taurine-induced long-lasting enhancement of synaptic transmission in mice: role of transporters." J Physiol **550**(Pt 3): 911-919.

Sergeeva, O. A., W. Fleischer, A. N. Chepkova, U. Warskulat, D. Haussinger, M. Siebler and H. L. Haas (2007). "GABAA-receptor modification in taurine transporter knockout mice causes striatal disinhibition." J Physiol **585**(Pt 2): 539-548.

Sergeeva, O. A. and H. L. Haas (2001). "Expression and Function of Glycine Receptors in Striatal Cholinergic Interneurones from Rat and Mouse." Neuroscience **104**(4): 1043-1055.

Shibasaki, K., N. Hosoi, R. Kaneko, M. Tominaga and K. Yamada (2017). "Glycine release from astrocytes via functional reversal of GlyT1." J Neurochem **140**(3): 395-403.

Shields, B. C., E. Kahuno, C. Kim, P. F. Apostolides, J. Brown, S. Lindo, B. D. Mensh, J. T. Dudman, L. D. Lavis and M. R. Tadross (2017). "Deconstructing behavioral neuropharmacology with cellular specificity." Science **356**(6333).

Siebler, M., M. Pekel, H. Köller and H.-W. Müller (1993). "Strychnine-sensitive glycine receptors in cultured primary neurons from rat neocortex." **73**(2): 289-292.

Song, J. and J. Kim (2016). "Degeneration of Dopaminergic Neurons Due to Metabolic Alterations and Parkinson's Disease." Front Aging Neurosci **8**: 65.

Specht, C. G. and R. Schoepfer (2001). "Deletion of the alpha-synuclein locus in a subpopulation of C57BL/6J inbred mice." BMC Neurosci **2**: 11.

Storch, A., A. C. Ludolph and J. Schwarz (2004). "Dopamine transporter: involvement in selective dopaminergic neurotoxicity and degeneration." J Neural Transm (Vienna) **111**(10-11): 1267-1286.

Stouffer, M. A., C. A. Woods, J. C. Patel, C. R. Lee, P. Witkovsky, L. Bao, R. P. Machold, K. T. Jones, S. C. de Vaca, M. E. Reith, K. D. Carr and M. E. Rice (2015). "Insulin enhances striatal dopamine release by activating cholinergic interneurons and thereby signals reward." Nat Commun **6**: 8543.

Strange, K., T. Yamada and J. S. Denton (2019). "A 30-year journey from volume-regulated anion currents to molecular structure of the LRRC8 channel." J Gen Physiol **151**(2): 100-117.

Sullivan, M. A., H. Chen and H. Morikawa (2008). "Recurrent inhibitory network among striatal cholinergic interneurons." J Neurosci **28**(35): 8682-8690.

Sulzer, D., S. J. Cragg and M. E. Rice (2016). "Striatal dopamine neurotransmission: regulation of release and uptake." Basal Ganglia **6**: 123-148.

Sun, F., J. Zeng, M. Jing, J. Zhou, J. Feng, S. F. Owen, Y. Luo, F. Li, H. Wang, T. Yamaguchi, Z. Yong, Y. Gao, W. Peng, L. Wang, S. Zhang, J. Du, D. Lin, M. Xu, A. C. Kreitzer, G. Cui and Y. Li (2018). "A Genetically Encoded Fluorescent Sensor Enables Rapid and Specific Detection of Dopamine in Flies, Fish, and Mice." Cell **174**(2): 481-496 e419.

Sun, F., J. Zhou, B. Dai, T. Qian, J. Zeng, X. Li, Y. Zhuo, Y. Zhang, Y. Wang, C. Qian, K. Tan, J. Feng, H. Dong, D. Lin, G. Cui and Y. Li (2020). "Next-generation GRAB sensors for monitoring dopaminergic activity in vivo." Nat Methods **17**(11): 1156-1166.

Surmeier, D. J., J. A. Obeso and G. M. Halliday (2017). "Parkinson's Disease Is Not Simply a Prion Disorder." J Neurosci **37**: 9799-9807.

Sutton, L. P., C. Orlandi, C. Song, W. C. Oh, B. S. Muntean, K. Xie, A. Filippini, X. Xie, R. Satterfield, J. D. W. Yaeger, K. J. Renner, S. M. Young, Jr., B. Xu, H. Kwon and K. A. Martemyanov (2018). "Orphan receptor GPR158 controls stress-induced depression." Elife **7**.

Suzuki, A., S. A. Stern, O. Bozdagi, G. W. Huntley, R. H. Walker, P. J. Magistretti and C. M. Alberini (2011). "Astrocyte-neuron lactate transport is required for long-term memory formation." Cell **144**(5): 810-823.

Szkudelski, T. (2001). "The mechanism of alloxan and streptozotocin action in B cells of the rat pancreas." Physiol Res **50**(6): 537-546.

Taleb, O. and B. Heinrich (1994). "Expression of the human glycine receptor a 1 subunit in Xenopus oocytes: apparent affinities of agonists increase at high receptor density." The EMBO Journal **13**(6): 1318-1324.

Taverna, S., E. Ilijic and D. J. Surmeier (2008). "Recurrent collateral connections of striatal medium spiny neurons are disrupted in models of Parkinson's disease." J Neurosci **28**(21): 5504-5512.

Taylor, C., C. Tsai and J. Lehmann (1988). "Glycine-evoked release of [3H]acetylcholine from rat striatal slices is independent of the NMDA receptor." Naunyn-Schmiedeberg's Archives of Pharmacology **337**(5).

Tepper, J. M., E. D. Abercrombie and J. P. Bolam (2007). Basal ganglia macrocircuits. Gaba and the Basal Ganglia - From Molecules to Systems**:** 3-7.

Tepper, J. M., T. Koos, O. Ibanez-Sandoval, F. Tecuapetla, T. W. Faust and M. Assous (2018). "Heterogeneity and Diversity of Striatal GABAergic Interneurons: Update 2018." Front Neuroanat **12**: 91.

Tepper, J. M., F. Tecuapetla, T. Koos and O. Ibanez-Sandoval (2010). "Heterogeneity and diversity of striatal GABAergic interneurons." Front Neuroanat **4**: 150.

Threlfell, S., M. A. Clements, T. Khodai, I. S. Pienaar, R. Exley, J. Wess and S. J. Cragg (2010). "Striatal muscarinic receptors promote activity dependence of dopamine transmission via distinct receptor subtypes on cholinergic interneurons in ventral versus dorsal striatum." J Neurosci **30**: 3398-3408.

Threlfell, S. and S. J. Cragg (2011). "Dopamine signaling in dorsal versus ventral striatum: the dynamic role of cholinergic interneurons." Front Syst Neurosci **5**: 11.

Threlfell, S., T. Lalic, N. J. Platt, K. A. Jennings, K. Deisseroth and S. J. Cragg (2012). "Striatal dopamine release is triggered by synchronized activity in cholinergic interneurons." Neuron **75**: 58-64.

Threlfell, S., A. S. Mohammadi, B. J. Ryan, N. Connor-Robson, N. J. Platt, R. Anand, F. Serres, T. Sharp, N. Bengoa-Vergniory, R. Wade-Martins, A. Ewing, S. J. Cragg and K. R. Brimblecombe (2021). "Striatal Dopamine Transporter Function Is Facilitated by Converging Biology of alpha-Synuclein and Cholesterol." Front Cell Neurosci **15**: 658244.

Vandenberg, R. J. and K. R. Aubrey (2001). "Glycine transport inhibitors as potential antipsychotic drugs." Expert Opin Ther Targets **5**(4): 507-518.

Voorn, P., L. J. M. J. Vanderschuren, H. J. Groenewegen, T. W. Robbins and C. M. A. Pennartz (2004). "Putting a spin on the dorsal–ventral divide of the striatum." Trends in Neurosciences **27**: 468-474.

Waldvogel, H. J., K. Baer, K. L. Allen, M. I. Rees and R. L. M. Faull (2007). "Glycine receptors in the striatum, globus pallidus, and substantia nigra of the human brain: An immunohistochemical study." The Journal of Comparative Neurology **502**(6): 1012-1029.

Walz, W. and A. F. Allen (1987). "Evaluation of the osmoregulatory function of taurine in brain cells." Exp Brain Res **68**(2): 290-298.

Wang, B., P. C. Chandrasekera and J. J. Pippin (2014). "Leptin- and leptin receptor-deficient rodent models: relevance for human type 2 diabetes." Curr Diabetes Rev **10**(2): 131-145.

Wang, L., Y. Q. Zhai, L. L. Xu, C. Qiao, X. L. Sun, J. H. Ding, M. Lu and G. Hu (2014). "Metabolic inflammation exacerbates dopaminergic neuronal degeneration in response to acute MPTP challenge in type 2 diabetes mice." Exp Neurol **251**: 22-29.

Wichmann, T. and J. O. Dostrovsky (2011). "Pathological basal ganglia activity in movement disorders." Neuroscience **198**: 232-244.

Wojcik, S. M., S. Katsurabayashi, I. Guillemin, E. Friauf, C. Rosenmund, N. Brose and J. S. Rhee (2006). "A shared vesicular carrier allows synaptic corelease of GABA and glycine." Neuron **50**(4): 575-587.

Wu, Y. and A. Parent (2000). "Striatal interneurons expressing calretinin, parvalbumin or NADPH-diaphorase: a comparative study in the rat, monkey and human." Brain Res **863**(1-2): 182-191.

Wu, Z., Y. Cui, H. Wang, H. Wu, Y. Wan, B. Li, L. Wang, S. Pan, W. Peng, A. Dong, Z. Yuan, M. Jing, M. Xu, M. Luo and Y. Li (2023). "Neuronal activity-induced, equilibrative nucleoside transporter-dependent, somatodendritic adenosine release revealed by a GRAB sensor." Proc Natl Acad Sci U S A **120**(14): e2212387120.

Yadid, G., K. Pacak, E. Golomb, J. D. Harvey-White, D. M. Lieberman, I. J. Kopin and D. S. Goldstein (1993). "Glycine stimulates striatal dopamine release in conscious rats." Br J Pharmacol **110**(1): 50-53.

Yang, J., J. Chen, Y. Liu, K. H. Chen, J. M. Baraban and Z. Qiu (2023). "Ventral tegmental area astrocytes modulate cocaine reward by tonically releasing GABA." Neuron.

Yang, Z., B. A. Cromer, R. J. Harvey, M. W. Parker and J. W. Lynch (2007). "A proposed structural basis for picrotoxinin and picrotin binding in the glycine receptor pore." J Neurochem **103**(2): 580-589.

Yao, Y. and M. L. Mayer (2006). "Characterization of a soluble ligand binding domain of the NMDA receptor regulatory subunit NR3A." J Neurosci **26**(17): 4559-4566.

Yorgason, J. T., H. A. Wadsworth, E. J. Anderson, B. M. Williams, J. N. Brundage, D. M. Hedges, A. L. Stockard, S. T. Jones, S. B. Arthur, D. M. Hansen, N. D. Schilaty, E. Y. Jang, A. M. Lee, M. Wallner and S. C. Steffensen (2022). "Modulation of dopamine release by ethanol is mediated by atypical GABAA receptors on cholinergic interneurons in the nucleus accumbens." Addict Biol **27**(1): e13108.

Young, A. B. and S. H. Snyder (1973). "Strychnine Binding Associated with Glycine Receptors of the Central Nervous System." **70**(10): 2832-2836.

Yu, H., X. C. Bai and W. Wang (2021). "Characterization of the subunit composition and structure of adult human glycine receptors." Neuron **109**(17): 2707-2716 e2706.

Yun, S. P., T. I. Kam, N. Panicker, S. Kim, Y. Oh, J. S. Park, S. H. Kwon, Y. J. Park, S. S. Karuppagounder, H. Park, S. Kim, N. Oh, N. A. Kim, S. Lee, S. Brahmachari, X. Mao, J. H. Lee, M. Kumar, D. An, S. U. Kang, Y. Lee, K. C. Lee, D. H. Na, D. Kim, S. H. Lee, V. V. Roschke, S. A. Liddelow, Z. Mari, B. A. Barres, V. L. Dawson, S. Lee, T. M. Dawson and H. S. Ko (2018). "Block of A1 astrocyte conversion by microglia is neuroprotective in models of Parkinson's disease." Nat Med **24**(7): 931-938.

Zafra, F., C. Aragon, L. Olivares, N. C. Danbolt, C. Gimenez and J. Storm-Mathisen (1995). "Glycine transporters are differentially expressed among CNS cells." J Neurosci **15**(5 Pt 2): 3952-3969.

Zampese, E. and D. J. Surmeier (2020). "Calcium, Bioenergetics, and Parkinson's Disease." Cells **9**(9).

Zeilhofer, H. U., B. Studler, D. Arabadzisz, C. Schweizer, S. Ahmadi, B. Layh, M. R. Bösl and J.-M. Fritschy (2005). "Glycinergic neurons expressing enhanced green fluorescent protein in bacterial artificial chromosome transgenic mice." **482**(2): 123-141.

Zhang, W. H., M. K. Herde, J. A. Mitchell, J. H. Whitfield, A. B. Wulff, V. Vongsouthi, I. Sanchez-Romero, P. E. Gulakova, D. Minge, B. Breithausen, S. Schoch, H. Janovjak, C. J. Jackson and C. Henneberger (2018). "Monitoring hippocampal glycine with the computationally designed optical sensor GlyFS." Nat Chem Biol **14**(9): 861-869.

Zhang, Y. W., S. Uchendu, V. Leone, R. T. Bradshaw, N. Sangwa, L. R. Forrest and G. Rudnick (2021). "Chloride-dependent conformational changes in the GlyT1 glycine transporter." Proc Natl Acad Sci U S A **118**(10).

Zhen, J. and M. E. A. Reith (2018). "Functional properties of dopamine transporter oligomers after copper linking." J Neurochem **144**(2): 162-171.

Zheng, Y. and Y. Li (2023). "Past, Present, and Future of Tools for Dopamine Detection." Neuroscience.

Zhou, F. M., Y. Liang and J. A. Dani (2001). "Endogenous nicotinic cholinergic activity regulates dopamine release in the striatum." Nature Neuroscience **4**: 1224-1229.

Zhu, H. and E. Gouaux (2021). "Architecture and assembly mechanism of native glycine receptors." Nature **599**(7885): 513-517.